SYNTHESIS OF NOVEL POLYISOBUTYLENE/POLYSTYRENE AND POLYISOBUTYLENE/MODIFIED SOYBEAN OIL BASED POLYURETHANES AND THEIR CHARACTERIZATIONS

by

Elif Kurnaz

B.S., Chemistry, Boğaziçi University, 2012

M.S., Chemistry, Boğaziçi University, 2015

Submitted to the Institute for Graduate Studies in
Science and Engineering in partial fulfillment of
the requirements for the degree of
Doctor of Philosophy

Graduate Program in Chemistry

Boğaziçi University

2024

To my beloved parents

ACKNOWLEGEMENTS

I am eternally grateful to my supervisor Prof. Turgut Nugay for his endless patience and guidance throughout my PhD study and his invaluable lessons in teaching me scientific inquiry and critical thinking. His kindness, hard work, and passion for science have always been a great source of inspiration for me.

I would like to express my appreciation to my thesis committee members Prof. Nihan Nugay, Prof. Nergis Arsu, Prof. Sinan Şen, and Assist. Prof. Mehmet Fırat İlker for taking their valuable time for reviewing my thesis and for their insightful comments. I am especially grateful to Prof. Nihan Nugay for her most valuable guidance and support in completing this study. I would like to thank Prof. Sinan Şen for his time and effort in training me on DMA and DSC and all his help and encouragement throughout this study.

I would like to acknowledge Dr. Ayla Türkekul and Ali Uzun for NMR and XRD analyses. I wish to thank Recep Koç for his kind visits to our laboratory to fix SEC.

My heartfelt thanks go to my dear Dr. Çimen Özgüç and Ekmel Helvacıoğlu for being genuine friends and most enjoyable labmates. All these years we spent in the laboratory have gifted me with precious memories for a lifetime. I am so much thankful to my dear friends Gamze Bahadır Söylemez, Gül Öncü, Duygu Baykal, Sinem Palantöken, and Ece Çiftçi Vatansever for always bearing with me and encouraging me when I needed it the most. I would like to extend my thanks to all the friends and faculty of the Chemistry Department.

Finally, I owe my innermost gratitude to my beloved parents for their endless love, patience, and support throughout my whole life.

This research has been supported by Boğaziçi University research fund (BAP) with project codes 16B05P4 and 23BD3.

ABSTRACT

SYNTHESIS OF NOVEL POLYISOBUTYLENE/POLYSTYRENE AND POLYISOBUTYLENE/MODIFIED SOYBEAN OIL BASED POLYURETHANES AND THEIR CHARACTERIZATIONS

The research study consists of two parts. In the first part, di-allyl and di-hydroxyl telechelic polyisobutylenes (PIBs) were synthesized with close to 100% chain end functionality. This was achieved by conducting living cationic polymerization of IB and suitable functionalization techniques. Besides, di-hydroxyl telechelic polystyrene (PSt) was synthesized by living anionic polymerization of St, then quenching the living chain ends with ethylene oxide (EO). Furthermore, macroinitiators were obtained by deprotonating the hydroxyl groups of these polymers, then di-oligoethylene oxide (OEO) telechelic PIB and PSt were synthesized by anionic ring-opening oligomerization of EO. Finally, these functionalized polymers, 4,4'-methylene diphenyl diisocyanate (MDI) and 1,4-butanediol were used to synthesize a series of PIB/PSt/OEO based polyurethanes (PUs) in various compositions. The successful synthesis of products was confirmed by using spectroscopic and chromatographic techniques. The mechanical tests of PIB/PSt PUs showed that OEO segment containing samples can achieve high strength, toughness, and creep resistance. All these results indicate that newly synthesized OEO-based PIB/PSt PUs are promising compared to conventional, low-strength, and low-creep-resistant poly(PSt-b-PIB-b-PSt) (SIBS). The second part involves the use of vegetable oil-based polyols to prepare novel cross-linked PUs based on PIB. For this purpose, triglycerides from soybean oil (SBO) were converted into polyols with primary hydroxyl functionalities by adding 2-mercaptoethanol to olefinic double bonds under UV radiation. Then, PIB diol, SBO based polyol, and MDI were reacted at specific mole ratios to produce cross-linked PIB-based PU films. Most importantly, the selective acid catalyzed hydrolysis of the cross-linked materials enabled the synthesis of block copolymers having carboxylic acid functionality. It is possible to use these carboxylic acid functional PIBs as a building block in the development of PIB-based polymer conjugates.

ÖZET

YENİ POLİİZOBÜTİLEN/POLİSTİREN VE POLİİZOBÜTİLEN/MODİFİYE SOYA YAĞI ESASLI POLİÜRETANLARIN SENTEZİ VE KARAKTERİZASYONLARI

Bu araştırma çalışması iki bölümden oluşmaktadır. İlk bölümde izobutilenin di-alil ve di-hidroksi telekelik polimerleri %100'e yakın zincir ucu fonksiyonelliği ile sentezlendi. Bu sentezler izobutilenin canlı katyonik polimerizasyonu ve uygun fonksiyonlandırma teknikleriyle başarıldı. Ayrıca, di-hidroksil telekelik polistiren (PSt) St'in yaşayan anyonik polimerizasyonu takiben zincir uçlarının etilen oksit (EO) ile fonksiyonlandırılmasıyla sentezlenmiştir. Dahası bu polimerlerin hidroksil gruplarının deprotonasyonuyla makro başlatıcılar elde edildi, ardından EO'nun anyonik halka açılımı oligomerizasyonuyla di-oligoEO (OEO) telekelik PIB ve PSt sentezlendi. Son olarak, zincir ucu fonksiyonlanırılmış polimerler, 4,4'-metilen difenil diizosiyanat (MDI) ve 1,4-bütandiol, çeşitli kompozisyonlarda bir dizi PIB/PSt/OEO PU'yu sentezlemek için kullanıldı. Ürünlerin sentezindeki başarı, spekroskopik ve kromatografik teknikler kullanılarak doğrulandı. PIB/PSt PU'ların mekanik testleri, OEO segmenti içeren numunelerin yüksek mukavemet, tokluk ve sürünme direnci elde edebildiğini gösterdi. Tüm bu sonuçlar, yeni sentezlenen OEO bazlı PIB/PS PU'ların bilinen, düşük mukavemetli ve düşük sürünmeye dirençli poli(PSt-b-PIB-b-PSt) (SIBS) kıyasla umut verici olduğunu göstermektedir. İkinci bölüm PIB bazlı yeni çapraz bağlı PU'ların hazırlanmasında bitkisel yağ bazlı poliollerin kullanımını içermektedir. Bu amaçla, soya fasulyesi yağındaki (SBO) trigliseritler UV radyasyonu altında olefinik çift bağlara 2-merkaptoetanol eklenerek birincil hidroksil fonksiyonlu poliollere dönüştürüldü. Daha sonra çapraz bağlı PIB bazlı PU filmler üretmek için PIB diol, SBO bazlı poliol ve MDI belirli mol oranlarında reaksiyona sokuldu. Daha önemlisi, çapraz bağlı malzemelerin seçici asit katalizli hidrolizi, karboksilik asit fonksiyonlu blok kopolimerlerin sentezlenmesini sağladı. Karboksilik asit fonksiyonel PIB'lerin PIB bazlı polimer konjugatların geliştirilmesinde yapı taşı olarak kullanılması mümkündür.

TABLE OF CONTENTS

LIST OF FIGURES

LIST OF TABLES

LIST OF SYMBOLS

-b-	-block-
g	Gram
h	Hour
ml	Milliliter
mmHg	Millimeter of Mercury
M_n	Number Average Molecular Weight
M_p	Peak Molecular Weight
M_w	Weight Average Molecular Weight
M_w/M_n	Polydispersity Index
MPa	Megapascal
mW	Milliwatt
nm	Nanometer
Tg	Glass Transition Temperature
Tm	Melting Temperature
δ	Chemical shift
µL	Microliter

LIST OF ACRONYMS/ABBREVIATION

9-BBN	9-Borabicyclo[3.3.1]nonane
A-PIB-A	di-allyl telechelic polyisobutylene
Ar	Argon
ATMS	Allyltrimethylsilane
ATRP	Atom transfer radical polymerization
BCl_3	Boron thrichloride
BDO	1,4-butanediol
$CaCl_2$	Calcium chloride
CaH_2	Calcium hydride
$CDCl_3$	Deuterated chloroform
CH_3Cl	Chloromethane
CH_3OH	Methanol
Cl-PIB-Cl	di-tert-chloride telechelic polyisobutylene
$CoCl_2$	Cobalt(II) chloride
Cs	Cesium
DMTBIP	Dimethyl 5-tert-butyl isophthalate
DBTDL	Dibutyltin dilaurate
DCM	Dichloromethane
DiCumOMe	1,4-bis(2-methoxyisopropyl) benzene
DMA	Dynamic mechanical analysis
DMD	Dimethyldioxirane
DMPA	2,2-dimethoxy-2-phenylacetophenone
DPM	Diphenylmethane
DPMK	Diphenylmethylpotassium
DSC	Differential scanning calorimetry
DtBP	di-tert-butylpyridine
EO	Ethylene oxide
$EtAlCl_2$	Ethylaluminum dichloride
Equiv.	Equivalent
FTIR	Fourier transform infrared spectroscopy

HACE	Hydrogen bond accepting chain extender
HCl	Hydrogen chloride
HDO	1,6-Hexanediol
HMDI	4,4′-Methylenebis(cyclohexyl isocyanate)
HNO_3	Nitric acid
H_2O_2	Hydrogen peroxide
HO-PIB-OH	di-hydroxyl telechelic polyisobutylene
HO-PSt-OH	di-hydroxyl telechelic polystyrene
HS	Hard segment
H_2SO_4	Sulfuric acid
IB	Isobutylene
K	Potassium
KOH	Potassium hydroxide
Li	Lithium
$LiAlH_4$	Lithium aluminum hydride
MDI	4,4′-Methylene diphenyl diisocyanate
MeMgBr	Methylmagnesium bromide
$MgSO_4$	Magnesium sulfate
MWD	Molecular weight distribution
N_2	Nitrogen
Na	Sodium
NaCl	Sodium chloride
$NaHCO_3$	Sodium bicarbonate
NaN_3	Sodium azide
Na_2SO_4	Sodium chloride
NMP	1-Methyl-2-pyrrolidone
NMR	Nuclear magnetic resonance spectroscopy
OEO-b-PIB-b-OEO	di-oligoethylene oxide telechelic polyisobutylene
OEO-b-PSt-b-OEO	di-oligoethylene oxide telechelic polystyrene
PC	Polycarbonate
p-DCC	p-dicumyl chloride
PDI	Polydispersity index
PEO	Poly(ethylene oxide)

PEO-b-PSt-b-PEO	poly(ethylene oxide)-b-polystyrene-b-poly(ethylene oxide)
PIB	Polyisobutylene
P_2O_5	di-phosphorous pentoxide
PSt	Polystyrene
PStLi	Polystyryl lithium
PStK	Polystyryl potassium
PTMO	Polytetramethyleneoxide
PU	Polyurethane
RAFT	Reversible addition fragmentation chain transfer
SBO	Soybean oil
SBS	poly(styrene-b-butadiene-b-styrene)
SEBS	poly(styrene-b-ethylene-butylene-b-styrene)
SEC	Size exclusion chromatography
sec-BuLi	sec-butyllithium
SIBS	poly(styrene-b-isobutylene-b-styrene)
SIS	poly(styrene-b-isoprene-b-styrene)
TBAH	Tetrabutylammonium hydroxide
TBDCA	5-tert-butyl-1,3-dicumyl alcohol
TBDCC	5-tert-butyl-1,3-dicumyl chloride
TBIPA	5-tert-butyl isophthalic acid
t-BuCl	tert-butyl chloride
t-Bu-m-DiCumOMe	5-tert-butyl-1,3-bis(2-methoxyisopropyl) benzene
t-Bu-OK	Potassium tert-butoxide
TCC	Tricumyl chloride
TDI	2,4-toluene diisocyanate
TGA	Thermogravimetric analysis
THF	Tetrahydrofuran
$TiCl_4$	Titanium tetrachloride
TMEDA	Tetramethylethylenediamine
TPE	Thermoplastic elastomer
UV	Ultraviolet
XRD	X-ray diffraction
$ZnBr_2$	Zinc (II) bromide

1. INTRODUCTION

1.1. Polyisobutylene

Isobutylene is an olefinic hydrocarbon of industrial and scientific importance. Cationic polymerization of isobutylene enables commercial production of various polyisobutylene (PIB) grades ranging from low molecular weight viscous liquids to high molecular weight rubbery solids [1-3]. Such PIB grades along with butyl rubber, a copolymer of isobutylene with ~2% isoprene, are important industrial scale applications of cationic polymerization [3-8]. The interest in PIB based products stems from the unparalleled features of PIB namely gas and moisture impermeability, thermal and oxidative stability, high tack and damping, chemical inertness and biocompatibility [8,9]. This special set of characteristics makes PIBs versatile polymers used in a variety of applications such as viscosity modifiers, lubricant additives, adhesives, sealants [4-8] and medical devices [9-15]. For example, low molecular weight PIBs with high exo terminal unsaturation (e.g., BASF's Glissopal®) are used as intermediates in the production of additives for fuels and lubricants [5]. The molecular structure of PIB (Figure 1.1) tells us a lot about its exceptional inertness. The repeating unit of PIB, consisting of alternating secondary and quaternary main chain carbon atoms with two methyl side groups, is incapable of undergoing oxidation [12]. The presence of the inert pendant methyl groups tightly dominating the surface of the polymer as well as the absence of cleavable functional groups render PIB biologically and chemically inert [14].

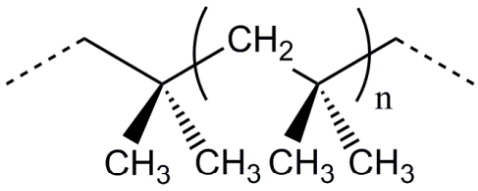

Figure 1.1. Repeating unit of PIB.

Living cationic polymerization enables the development of well defined end functional PIBs and PIB based block copolymers [10]. Commercially successful isobutylene based products obtained from living polymerization include di-allyl telechelic

PIB based architectural sealant (EPION®, Kaneka Co.), Polystyrene-b-Polyisobutylene-b-Polystyrene (SIBS) thermoplastic elastomer (SIBSTAR®, Kaneka Co.), and biomedical grade SIBSs used in medicine as a drug-eluting coating on TAXUS® coronary stent (Boston Scientific Co.) [10], and as a microshunt to treat glaucoma (PRESERFLO®, Santen Pharmaceutical Co.) [15].

1.2. Living Cationic Polymerization of Isobutylene

Living cationic polymerization remains the sole technique that allows control over molecular weight, chain end functionalization, and the polymer achitecture of PIB. This can be explained by the nucleophilicity of isobutylene and the stability of the active center [8]. Two methyl substituents, being the electron releasing groups, increase the electron density of the double bond and facilitate its nucleophilic attact on the positively charged active center (carbenium ion). Besides, these substituents inductively stabilize the resulting tertiary carbocation and hence favor propagation over chain breaking reactions [2,3]. Among other monomers active in cationic polymerization such as vinyl ethers and styrene derivatives, isobutylene is considered to have the ideal combination of nucleophilicity, carbocation stability as well as steric hindrace [8]. In terms of anionic polymerization, isobutylene is not reactive because of the inherent unstability of the forming carbanion. Stabilization of the forming negative charge by the electron withdrawing substituents (e.g., cyano, carbonyl and phenyl) is required for a monomer to be polymerizable by anionic mechanism [3]. Radical polymerization of isobutylene, on the other hand, results in oligomerization. In general, radical polymerization of alpha-olefins are challenging due to the participation of easily abstractable allylic Hs in chain transfer reaction, which is especially the case for isobutylene as it has six allylic Hs [16]. Volkis et al. studied Li^+ catalyzed radical polymerization of isobutylene [17-19]. However, these studies lead to highly branched PIB of low molecular weight that has found no practical application and remain as an academic interest only [16]. Consequently, it is not possible to synthetize a high molecular weight PIB via a radical process.

The road to living cationic polymerization of isobutylene was paved by Kennedy and coworkers [20]. Initial efforts resulted in the development of the inifer technique in the 1980s [21-25]. The term inifer signifies the dual role of the reagent as both initiator and

chain transfer agent. This technique allowed the synthesis of first examples of di-tert-chloride telechelic PIB, Cl-PIB-Cl, using p-dicumyl chloride (p-DCC, initiator-transfer agent)/BCl_3 initiating system in DCM [19]. Although this technique proved its value in terms of absence of chain transfer to monomer at -80 °C, intramolecular cycloalkylation after one isobutylene unit addition was shown to lead to five membered indanyl ring at higher temperatures (Figure 1.2a) [22]. Indeed it was realized that indanyl formation was inevitable for an unhindered dicumyl chloride/BCl_3 induced polymerization unless the temperature and the polarity of the reaction medium were decreased (e.g., in DCM/n-hexane mixture below -40 °C) [22]. Furthermore, with tricumyl chloride (TCC)/BCl_3 initiating system, tri-tert-chloride telechelic PIB was obtained without indane formation even at ~-30 °C. This suggested that the hindered nature of TCC inhibited intramolecular alkylation [23]. Therefore, Santos et al. synthetised 5-tert-butyl-1,3-dicumyl chloride, (TBDCC), a sterically hindered initiator with a bulky tert-butyl group on the meta position (Figure 1.2b). By the use of TBDCC/BCl_3 initiating system, the synthesis of Cl-PIB-Cl free of indanyl groups became feasible in CH_3Cl/n-hexane mixture in the range from -30 to -80 °C [24,25].

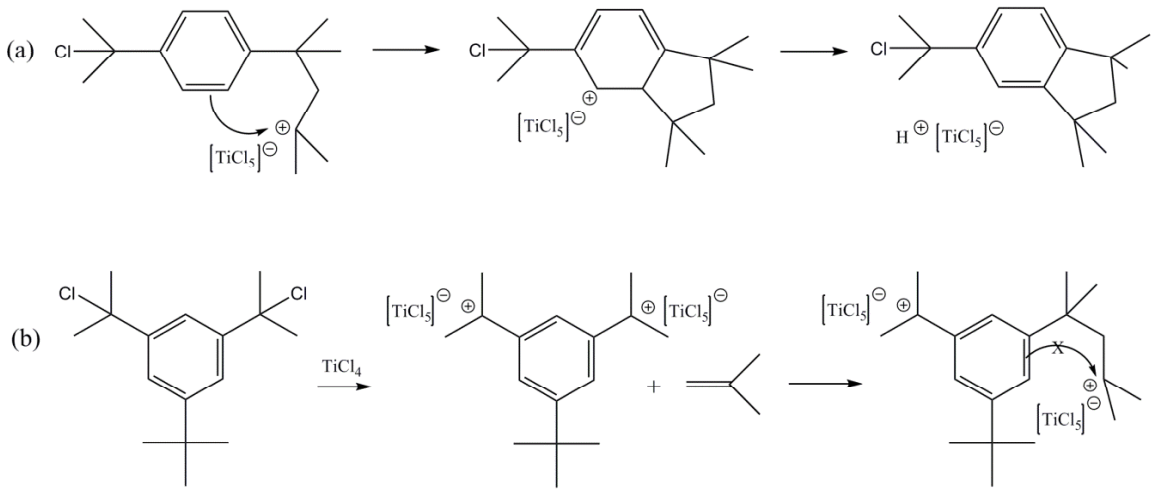

Figure 1.2. (a) Formation of indanyl ring for p-DCC (Adapted with permission from [22], Springer Nature, Copyright (1969)), (b) sterically hindered dicumyl chloride [24].

Besides cumyl chlorides, various cumyl type initiators including esters and ethers were investigated in the course toward living isobutylene polymerization [26]. diCumyl acetate (DiCumOAc) [27] and 1,4-bis(2-methoxyisopropyl) benzene (DiCumOMe) [28] in conjuction with BCl_3 were reported to be efficient initiating systems for the preparation of

Cl-PIB-Cl. Similar to DCC/BCl_3 inifer system, the polymerizations were carried out in the CH_3Cl/n-hexane mixtures at -70 °C to avoid indanyl ring formation. Wang et al. showed that the synthesis of Cl-PIB-Cl can be achieved at higher temperatures (-30 °C) by a living process using a dicumyl ether with steric hindrance. 5-tert-butyl-1,3-bis(2-methoxyisopropyl) benzene (t-Bu-m-DiCumOMe)/BCl_3 initiating system induced living polymerization characteristics, i.e., the linear increase of Mn with monomer conversion while the number of polymer chains is constant [29]. Furthermore, $TiCl_4$ was found to exhibit higher counter anion stability and solubility compared to BCl_3. Cumyl esters and ethers co-initiated with $TiCl_4$ induced living polymerization of isobutylene [30,31]. Kaszas et al. successfully employed DiCumOMe/$TiCl_4$ initiating system for the synthesis of Cl-PIB-Cl in CH_3Cl/n-hexane mixture at -80 °C [31].

Above mentioned living processes inherently yielded chain ends with tert-chloride groups. PIBs with various end functionalities were obtained through modifications of these tert-chloride groups or by in situ quenching of living chains. Primary di-hydroxyl telechelic PIB (HO-PIB-OH) is particularly important as it is the precursor for the synthesis of chemically and biologically stable polyurethanes (PUs) [32]. Kennedy et al. prepared the first well defined di-hydroxyl telechelic PIB through pDCC/BCl_3 initiated inifer technique followed by chain end functionalization [33]. First, tert-chloride terminals were dehydrochlorinated with potassium tert-butoxide (t-Bu-OK) in THF under reflux conditions to obtain exo-olefin telechelic intermeadiate. Then, exo-olefin terminals were converted into primary hydroxyl groups via hydroboration reaction with 9-BBN and subsequent alkaline oxidation. It was noted that during the oxidation step 1,5-cyclooctanediol byproduct was also formed.

Keki et al. synthesized di-hydroxyl telechelic PIB through exo-olefin and epoxide telechelic PIB intermediates [34]. Terminal tert-chloride groups obtained from the inifer technique was converted to the exo-olefin groups by dehydrochlorination reaction with t-Bu-OK. Following that exo-olefin groups were subjected to dimethyldioxirane (DMD) oxidation reagent to introduce epoxy end groups, which were then isomerized into aldehydes with $ZnBr_2$ catalyst. In the final step, the reduction of aldehyde groups with $LiAlH_4$ resulted in primary hydroxyl end groups. This strategy offers an alternative route that involves more steps than the previous one. Moreover, although the exo-olefin chain

ends are useful as they can be quantitatively converted into hydroxyl groups, the dehydrochlorination process by which they are obtained has limitations [35,36]. Feldthusen et al. investigated the effect of reaction conditions on the dehydrochlorination reaction of tert-chloride telechelic PIB with t-Bu-OK. They showed that thermally induced HCl loss under reflux conditions led to 3% endo-olefin chain ends. These unreactive internal olefins jeopardize the success of further derivatizations, e.g., hydroboration, epoxidation, etc [36].

On the other hand, allyl end group was a better intermediate for the preparation of hydroxyl functionalized PIB as it is more reactive than the exo-olefin group [37]. Wilczek and Kennedy reported quantitative allylation of tert-chloride terminated PIB by allyltrimethylsilane (ATMS) in the presence of excess $TiCl_4$ [38]. They noticed that in the presence of BCl_3, competing side reactions with ATMS occurred. Later, Ivan and Kennedy accomplished the first end quenching of living isobutylene polymerization initiated by DiCumOMe/$TiCl_4$ in CH_3Cl/n-hexane mixture (40/60 v/v) with ATMS. Primary di-hydroxyl telechelic PIB was then obtained by hydroboration/oxidation reaction of the allyl groups as shown in Figure 1.3 [37]. Since then, in situ quenching with ATMS has been used as an efficient synthetic route for obtaining allyl chain ends.

Ummadisetty and Kennedy developed a methodology for quantitative synthesis of PIBs with various functional groups including primary hydroxyl [39]. The route for hydroxyl terminated PIB involves end-quenching living chains with ATMS, followed by anti-Markovnikov hydrobromination and subsequent alkaline hydrolysis as depicted in Figure 1.4. The substitution reaction of primary bromide to hydroxyl without undesired HBr elimination could be achieved by refluxing the polymer dissolved in a 75/25 mixture of THF/1-Methyl-2-pyrrolidone (NMP) in the presence of low concentrations of water. Exo-olefin chain end of Glissopal was also subjected to the same experimental procedure. However, the terminal β-CH_3 group reduced the efficiency of conversion. This required the conversion of Br to the benzoate in a refluxing mixture of THF/NMP before the alkaline hydrolysis step.

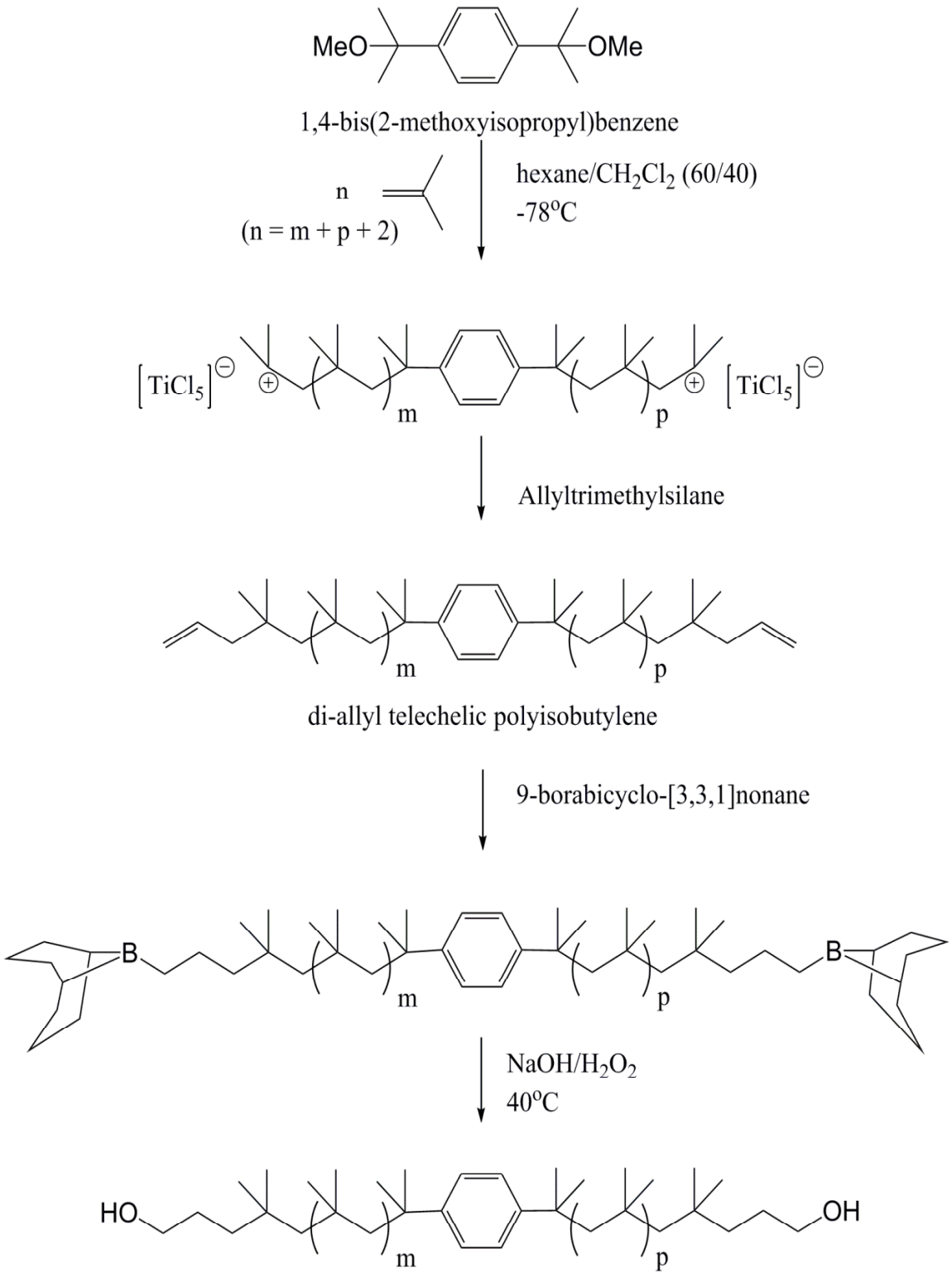

Figure 1.3. Synthesis of di-allyl telechelic PIB and further modifications [37]. Adapted with permission from [37], Springer Nature, Copyright (2003).

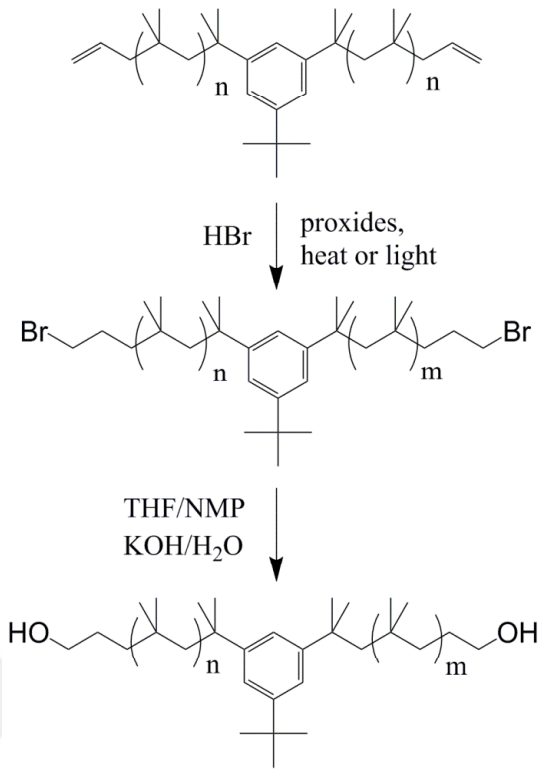

Figure 1.4. Synthesis of di-hydroxyl telechelic PIB via hydrobromination and alkaline hydrolysis [39]. Adapted with permission from [39], John Wiley and Sons, Copyright (2008).

Ojha et al. introduced a range of functional groups into PIB, including hydroxyl group, through nucleophilic substitution of allyl chloride end group [40]. Allyl chloride capped PIB was obtained by 1,4-trans-addition of butadiene to living chains coinitiated with $TiCl_4$ in hexane/CH_3Cl (60/40) mixture at -80 °C. Mono and di-hydroxy telechelic PIB were obtained by post-polymerization hydrolysis reaction with KOH at 130 °C (Figure 1.5). This approached utilizes the increased reactivity of allyl chloride in the hydrolysis reaction compared to the alkyl chloride counterpart but still requires an additional halide exchange reaction, yielding the more reactive allyl bromide.

In situ end-capping with a protected N-(ω-Hydroxyalkyl) pyrrole was investigated as a more direct route to obtain primary hydroxyl functional PIBs. Morgan and Storey reported single pot two step synthesis of mono and di-hydroxy terminated PIBs by using N-(2-tert-Butoxyethyl) pyrrole as quenching agent (Figure 1.6 a) [41]. First, N-(2-tert-Butoxyethyl) pyrrole capped polymers were prepared by $TiCl_4$ assisted alkylation of the pyrrole ring with living chain ends in 60/40 mixture of hexane/CH_3Cl at -60 °C.

Afterwards, in the deprotection step, in situ cleavage of tert-butyl ether was achieved by charging the reactor with $EtAlCl_2$ and H_2SO_4 mixture at 0 °C. It was observed that dihydroxy functional PIB was contaminated with ~2% coupling product as a result of double alkylated pyrrole rings. Morgan et al. demonstrated that alkoxybenzene compounds such as (3-bromopropoxy) benzene can be effectively used in end capping of TBDCC/$TiCl_4$ initiated living PIB chains [42]. The alkylation reaction was shown to occur at para position without chain coupling due to multiple alkylations. The primary bromide terminals were then replaced by benzyl ester groups in refluxing potassium benzoate (C_6H_5COOK) solution. Alkaline hydrolysis of the resulting polymer incorporated primary hydroxyl groups into the chain ends (Figure 1.6 b).

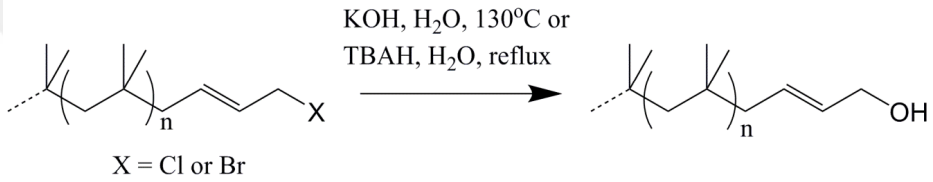

Figure 1.5. Conversion of allyl halide telechelic PIB to hydroxy telechelic PIB [40]. Adapted with permission from [40], American Chemical Society, Copyright (2008).

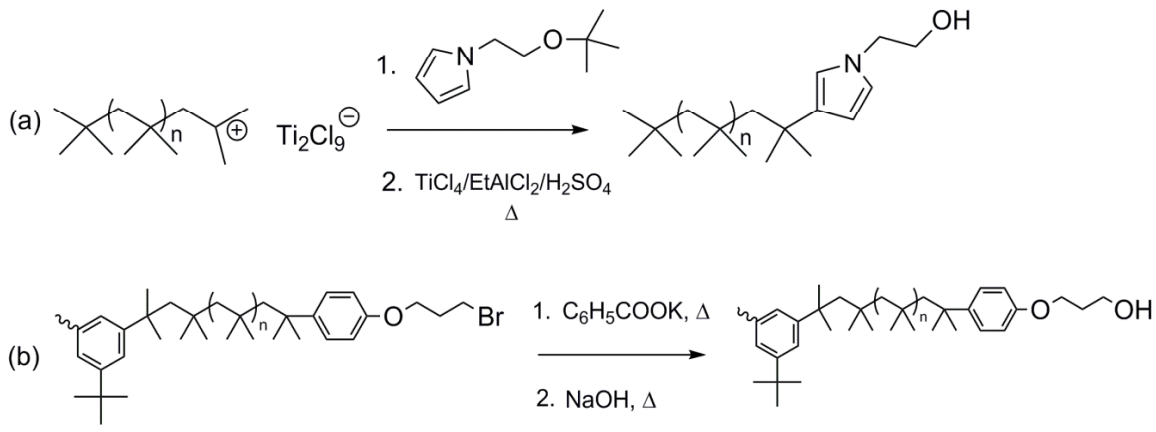

Figure 1.6. Syntheses of hydroxyl telechelic PIBs via in-situ end-capping with (a) N-(2-tert-Butoxyethyl) pyrrole (Adapted with permission from [41], American Chemical Society, Copyright (2010)), and (b) (3-bromopropoxy) benzene (Adapted with permission from [42], American Chemical Society, Copyright (2010)).

Furthermore, Storey group developed synthetic strategies that combine in situ quenching techniques with click chemistry to place a range of functional groups at the

chain ends [43,44]. Martinez-Castro et al. synthesized terminal azide functional PIB via a 1-(ω-haloalkyl)pyrrolyl capped intermediate or via direct quenching of living chain ends with a 1-(ω-azidoalkyl)pyrrole. Hydroxyl functionality was then introduced into the polymer via copper(I) catalyzed cycloaddition of the terminal azide and propargyl alcohol (Figure 1.7 a). Magenau et al. used photo-initiated thiol-ene click chemistry for an efficient synthesis of primary hydroxyl functional PIBs from exo-olefin terminated PIB intermediates. UV initiated radical addition of 5-mercapto-1-pentanol to exo-olefin terminals, obtained from quenching of living chain ends with a hindered amine, was achieved in the presence of dimethoxy-2-phenylacetophenone (DMPA, photo-initiator) in less than 10 minutes (Figure 1.7 b).

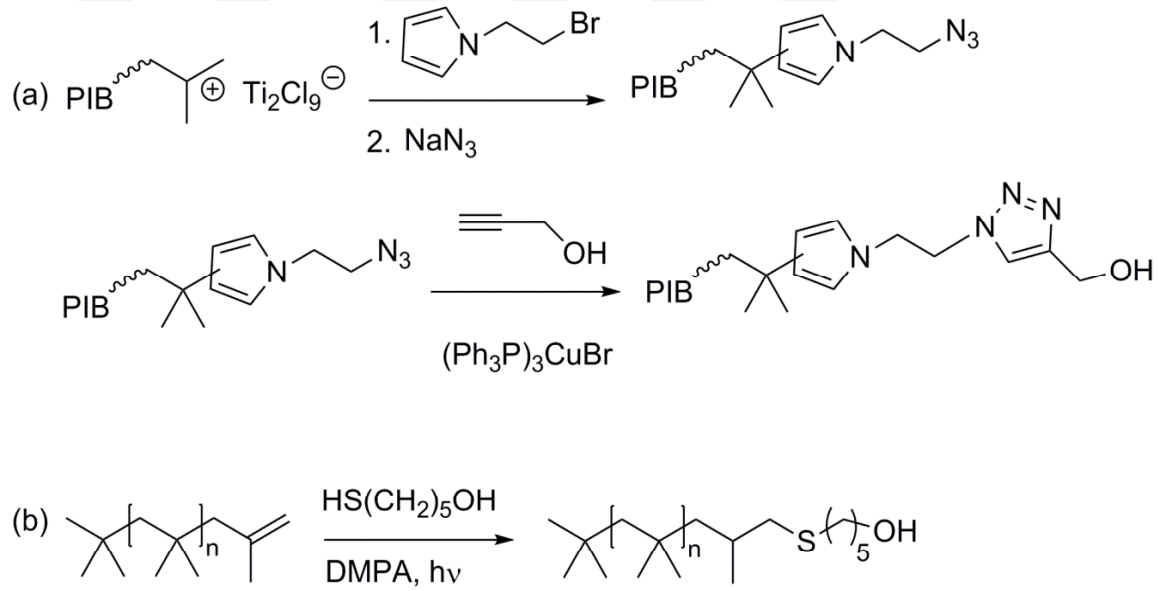

Figure 1.7. Syntheses of hydroxyl telechelic PIBs via (a) in-situ quenching with 1-(2-bromoethyl) pyrrole and subsequent azide-alkyne cycloaddition (Adapted with permission from [43], John Wiley and Sons, Copyright (2010)), (b) thiol-ene click chemistry (Adapted with permission from [44], Royal Society of Chemistry, Copyright (2010)).

In a patent issued in 2014, Nugay et al. reported a rapid and quantitative synthesis of well defined primary di-hydroxy telechelic PIBs containing sulfur atoms at each chain end (-SCH_2CH_2OH) [45]. The proposed method involved UV initiated thiol-ene addition reaction of allyl, endo-, and exo-olefin end groups of PIB with mercapto alcohols and hence lowered the cost of polymer modification. Toth et al. also synthesized -SCH_2CH_2OH telechelic PIB via photo-initiated radical thiol-ene addition reaction of 2-mercaptoethanol

onto di-allyl telechelic PIB (Figure 1.8) [46]. This sulfur containing PIB diol was used in the preparation of PUs as a cost effective alternative to HO-PIB-OH obtained from hydroboration/oxidation. Hydrolytic-oxidative resistance, thermal and mechanical properties of -S- containing PIB based PU were investigated and compared with PU prepared from HO-PIB-OH and with a commercial PU.

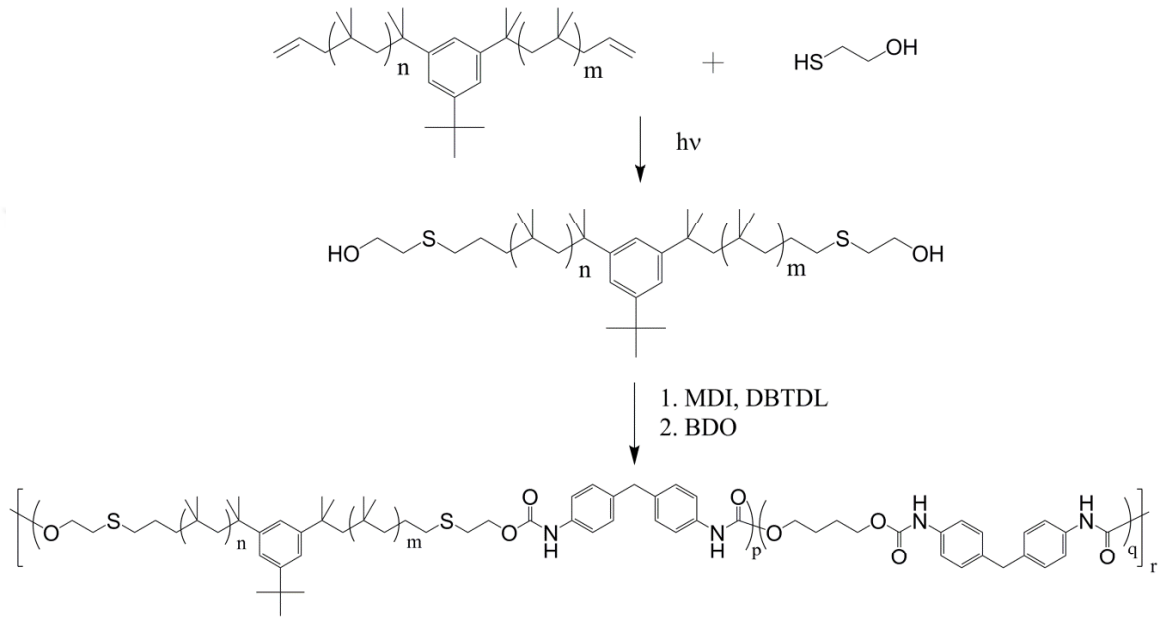

Figure 1.8. Synthesis of -SCH_2CH_2OH telechelic PIB via thiol-ene click chemistry and PIB based PU. Adapted with permission from [46], John Wiley and Sons, Copyright (2015).

Considering the previous research, hydroboration/oxidation of allyl functional chain ends emerged as a pereferred and feasible method for the synthesis of HO-PIB-OH initiated by TBDCC/$TiCl_4$. As stated in a recent review of the multifunctional initiators employed in the living isobutylene synthesis, TBDCC/$TiCl_4$ is used as the most suitable initiating system especially for obtaining low molecular weight difunctional PIBs [26].

1.3. Polystyrene

Styrene is a nonpolar vinyl monomer with a phenyl substituent. It can be polymerized by anionic, cationic and radical chain polymerization mechanisms because the phenyl substituent can delocalize the propagating charge or radical over the aromatic ring

[3]. Free radical polymerization of styrene by radical initiators such as peroxides is extensively used in the production of commercial polystyrenes (PSts), which are amorphous plastics [3]. Compared to ionic polymerization techniques, radical polymerization is easy to implement on an industrial scale and available for bulk, solution, and emulsion processes [47]. However, because of uncontrolled chain transfer and termination reactions, control over the molecular weight, polydispersity index, and macromolecular engineering is limited [47]. These challenges can be overcome by using controlled/living radical polymerization techniques (ATRP, RAFT) and well defined molecular structures can be achieved. Nevertheless, even for these controlled radical techniques, some degree of chain breaking reactions is inevitable. This leads to relatively high dispersities, especially at high molecular weights [47]. Moreover, the challenges regarding to the use of costly controlling agents and their removal through multipurification steps limit industrial scale utilization of these techniques [47]. On the other hand, in living anionic polymerization, chain growth proceeds without chain breaking reactions. This feature enables the preparation of polymers with a low polydispersity (<1.1), controlled molecular weights, and precise chain end functionality, thus allowing the syhthesis of block copolymers [47]. Anionic living polymerization is highly valued as the most reliable technique for the preparation of block copolymers. This is because the living character of propagating species facilitates the sequential addition of various monomers [47].

Pure PSt has a relatively brittle nature with rigid polymer chains [3]. On the other hand, styrenic block copolymers obtained by copolymerization of styrene with diene monomers such as butadiene or isoprene, are thermoplastic elastomers (TPEs). Styrenic block copolymers constitute a significant portion of TPEs in volume [47,48]. The first commercial styrenic TPEs with polydiene elastomeric segments, poly(styrene-b-butadiene-b-styrene) (SBS) and poly(styrene-b-isoprene-b-styrene) (SIS), were developed by Shell in the early 1960s [47,48]. These triblock copolymers, which contain high cis-isomers of 1,4-PB and 1,4-PI, are industrially produced using alkyllithium initiated anionic polymerization in a hydrocarbon solvent [49]. The unsaturated midblocks render these polymers susceptible to thermal and UV induced degradation. The hydrogenation of the polybutadiene segment transforms SBS into poly(styrene-b-ethylene-butylene-b-styrene) (SEBS), the saturated analog with improved oxidation resistance [50]. Although styrenic

TPEs are widely used for various applications, including packaging, sealant and adhesive, their gas barrier properties are poor [50]. SIBS is another type of styrenic block copolymer, that exhibits superior gas impermeability, oxidative stability, and vibration dampening characteristics compared to conventional styrenic TPEs [50]. This TPE contains PIB elastomeric segments that can only be achieved through living cationic polymerization, initiated by di-, tri-, and tetra-functional initiators [51].

1.4. Living Anionic Polymerization of Styrene

In a seminal paper published in 1956, Szwarc and coworkers reported the first living anionic polymerization of styrene induced by sodium (Na) naphthalenide in THF [52]. They revealed the mechanism of the initiation and proved the existence of living chain ends. Importantly, it was shown that the Na naphthalenide initiator can be used to synthesize block copolymer, e.g. A-B-A. The reaction of naphthalene, an aromatic hydrocarbon, with metallic Na in THF gives the green colored Na naphthalenide complex [52,53]. When added to the styrene solution in THF, the naphthalenide radical anion initiates the polymerization of styrene via an electron transfer process. The process results in the formation of styryl radical anion which dimerizes into styryl dianions as shown in Figure 1.9.

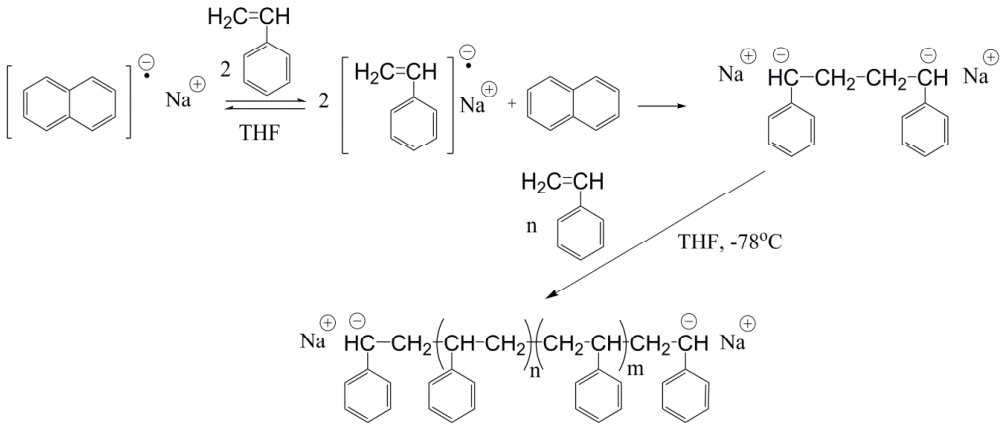

Figure 1.9. Na-naphthalenide initiated anionic polymerization of styrene [49]. Adapted with permission from [49], John Wiley and Sons, Copyright (2010).

Since the green color of the initiator turns into the orange-red color of the benzyl anion, the formation of styryl anions can be confirmed visually. The polystyryl chains

grow uniformly and the solution remains orange-red throughout the polymerization under conditions free of oxygen and moisture [52,53]. The living character of the polystyryl chains was proven by introducing a second portion of styrene by keeping the ratio of styrene to THF unchanged. The increase in the viscosity of the solution as well as the quantitative conversion of both portions of styrene showed that the chain ends remained active and capable of adding further monomer.

The term living polymers was introduced by Szwarc and used for the polymers like polystyryl sodium that propagate without the occurrence of chain transfer and termination reactions, and have the ability to grow if more monomer is charged to the system [52-54]. Given that the carbanions are highly reactive species, they cannot keep their integrity for the long term. Later, the definition of livingness was modified by Szwarc such that a polymer was called living if its chain ends remain active long enough required for the completion of a synthetic task [54]. The polymerization requires the complete elimination of moisture, oxygen and other electrophilic impurities from the reaction medium. This is because the highly nucleophilic carbanionic chain ends react rapidly with such impurities, resulting in the loss of their living character [49]. For example, in the presence of oxygen, it is well known that the chain ends undergo an undesired chain coupling reaction [53]. When the polymerization is run in an inert nitrogen or argon atmosphere and the solvents and reagents are properly purified, chain growth occurs through the addition of monomer to the propagating carbanions, while undesired chain breaking reactions like chain transfer and termination do not occur. As the active chain ends keep their integrity during polymerization, it becomes possible to synthesize various macromolecular structures such as well-defined block-graft copolymers, stars, and dendrimers, and to investigate their morphology-property relationships [55].

Anionic polymerization of styrene can be induced by electron transfer mechanism or by nucleophilic addition of carbanions [49], [56]. As mentioned above, styrene can be efficiently initiated using Na naphthalenide radical anion. This radical anion is obtained from the reaction of naphthalene, an electron deficient aromatic hydrocarbon, with Na metal through an electron transfer from the surface of Na to naphthalene. When introduced into the monomer solution, Na naphthalenide transfers an electron to styrene, resulting in the formation of a styryl radical anion, which is in equilibrium with the aromatic radical

anion. This equilibrium favors the aromatic radical anion on account of the low electron affinity of styrene. Nevertheless, the equilibrium shifts to the right as the resulting styryl radical anions rapidly dimerize to form bifunctional styryl dianions that initiate chain growth at both anionic ends (Figure 1.9) [49], [56]. This method is still used to obtain bifunctional PSts. Apart from Na naphthalenide, lithium (Li) and potassium (K) naphthalenides are also frequently used as efficient electron transfer initiators. Another type of initiation mechanism involves the nucleophilic addition of carbanions such as alkyllithiums. It is well known that alkyllithium compounds exist as dimers, tetramers, and hexamers in hydrocarbon solvents, depending on the alkyl group [49], [56]. The degree of intermolecular association of alkyllithiums determines the efficiency of the initiation. Therefore, the use of an appropriate initiator is important. For example, n-butyllithium (hexameric) initiated styrene polymerization in cyclohexane resulted in incomplete initiation with 30% unreacted initiator, while the less associated sec-butyllithium (sec-BuLi) enabled fast initiation [49].

1.5. Living Anionic Polymerization of Ethylene Oxide

Ethylene oxide (EO) is a three membered cyclic ether, which is also known as the simplest epoxide or oxirane [3]. Because of the high ring strain, the anionic polymerization of EO can be readily induced by hydroxides, alkoxides, alkyl and aryl compounds of Na, K and Cs [3], [57]. Figure 1.10 shows the polymerization of EO through anionic ring-opening mechanism. The initiation and subsequent chain growth involve nucleophilic attack of alkoxide anions on the monomer. When the polymerization is carried out in a polar aprotic solvent such as THF, the resulting poly(ethylene oxide) (PEO) exhibits the characteristics of a living polymer with a Poisson distribution [58].

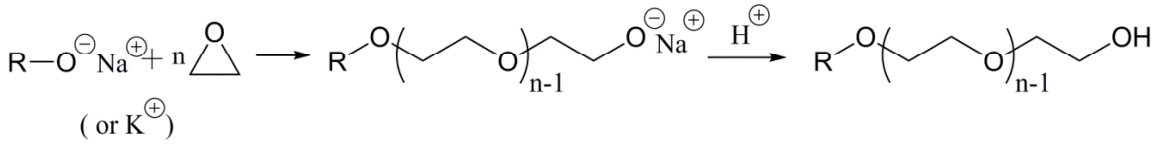

Figure 1.10. Anionic ring-opening polymerization of EO [58]. Adapted with permission from [58] licensed under CC BY 4.0.

Association of the alkoxide chain ends is a characteristic feature of the anionic polymerization of EO [56], [57]. The strength of this association highly influenced by the type of counterion. Unlike Na, K or cesium (Cs) counterions, Li does not promote propagation because of the very strong association of Li alkoxides [59-62]. For the same reason, butyllithium or Li naphthalenide initiation of EO does not also result in further propagation [60]. The fact that of Li alkoxides are incapable of polymerizing EO is extensively utilized as an efficient method to synthesize hydroxyl functionalized polymers [61-64]. Quirk and Ma end capped polystyryl lithium (PStLi) with excess EO in benzene to give hydroxyethyl functionalized PSt in quantitative yields. ^{13}C NMR analysis of the product revealed the addition of only one EO unit at each chain end (Figure 1.11) [61].

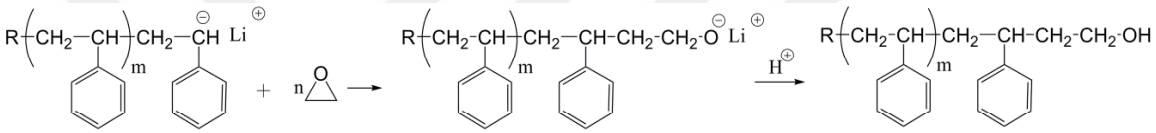

Figure 1.11. Functionalization of polystyryl lithium with EO [61]. Adapted with permission from [61], John Wiley and Sons, Copyright (2003).

Block copolymers of PSt and PEO are of interest due to their amphiphilic nature. These amphiphilic polymers containing incompatible hydrophilic PEO and hydrophobic PSt segments exhibit self association behavior [65]. Living anionic polymerization is the most reliable route to obtain triblock copolymers of styrene and EO. Szwarc synthesized PEO-b-PSt-b-PEO triblock copolymer in THF via sequential anionic polymerization of styrene and EO using α-methyl styrene tetrameric dianion sodium initiator [66]. Xie and Zhou used K naphthalenide initiator in a sequential polymerization of styrene and EO in toluene [67]. It was noted that, the polymerization rate of EO in block copolymerization was significantly lower than in homopolymerization. Therefore, extraction of homopolymers of styrene and EO from the triblock copolymer was necessary. Wilhelm et al. prepared PEO-b-PSt-b-PEO triblock copolymers to study the critical micelle concentration values in water using fluorescence and light scattering techniques [68]. Polymerizations were initiated by using K naphthalenide. Following the polymerization of styrene in THF at -78 °C, EO was introduced to the living polystyryl solution, and then polymerization was continued at room temperature for 40 h. SEC characterization, using

UV absorbance and RI detectors, indicated that the obtained copolymers were free of PSt and PEO homopolymers.

Another successful synthetic method to produce block copolymers of PEO involves the use of diphenylmethylpotassium (DPMK) as deprotonating agent. Zhang et al. synthesized PEO-b-PSt-b-PEO (PDI<1.1) from di-hydroxy telechelic PSt precursor using DPMK as shown in Figure 1.12 [69]. The precursor was obtained through Li naphthalenide initiated styrene polymerization in cyclohexane, followed by quenching of living polymer chains with EO. Subsequently, the hydroxyl groups were partially deprotonated in the presence of DPMK in THF. The resulting polymeric dianion with K counterions was utilized as a macroinitiator in anionic ring opening polymerization of EO at 50 °C for 48 h. Angot et al. combined anionic polymerization of EO with ATRP of styrene to prepare tri- and tetraarmed star PEO_n-b-PSt_n block copolymers. In this strategy, PEO tri- and tetraarmed stars were produced from 1,3-propanediol and pentaerythritol precursors, respectively, after partial deprotonation by DPMK and subsequent polymerization of EO [70].

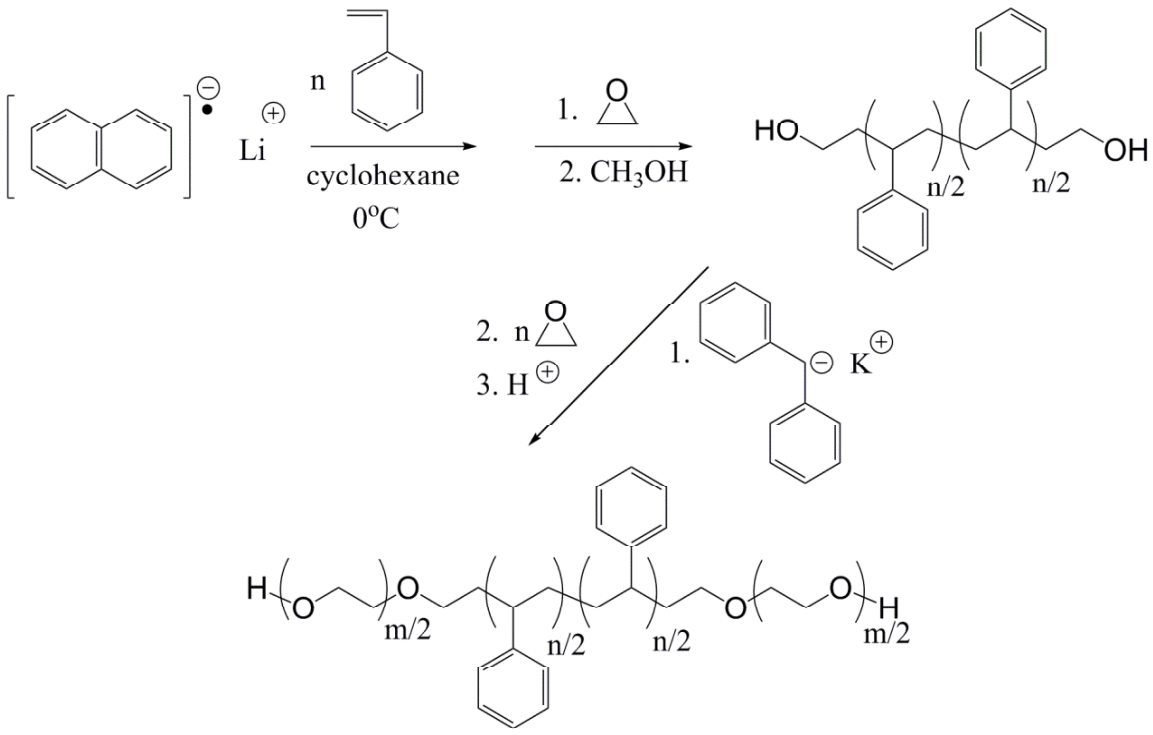

Figure 1.12. Synthesis of PEO-b-PSt-b-PEO triblock copolymer [69]. Adapted with permission from [69], John Wiley and Sons, Copyright (2011).

1.6. SIBS

Pure PIB is not an elastomer suitable for applications requiring shape retention by itself; rather it resembles gum [71,72]. However, PIB can be transformed into an elastomer either through chemical crosslinking, as in the case of butyl rubber, or through meltable physical crosslinks, as in the case of SIBS [72]. SIBS is a triblock copolymer consisting of PIB midblocks covalently bonded to PSt end segments. The incompatibility between the covalently bonded segments results in a self assembled structure in which hard PSt domains physically crosslink the soft PIB matrix. Being physically crosslinked, it can be processed by dissolving in nonpolar solvents (spray coating, solvent casting), or by injection and compression molding [71].

SIBS is synthesized by living cationic polymerization using a sterically hindered dicumyl initiator through the sequential addition of isobutylene and styrene as illustrated in Figure 1.13 [71]. In the first stage, PIB midblock is polymerized by t-Bu-m-DiCumOMe/$TiCl_4$ bifunctional initiator in hexane/methyl chloride solvent mixture at -80 °C until the targeted molecular weight is reached. Upon the introduction of styrene, the living PIB chains initiate styrene polymerization at both ends to produce PSt end segments.

SIBS is especially useful as a biomaterial due to its excellent biostability and biocompatibility [71]. This polymer is degradation resistant, as it does not contain any labile functional groups susceptible to cleavage by oxidative or enzymatic processes [71]. The first biomedical grade SIBS was utilized in cardiology as paclitaxel eluting polymeric coating on TAXUS coronary stent to prevent restenosis of arteries. Another noteworthy application of SIBS is in ophthalmology as a glaucoma drainage tube, PRESERFLO, to control intraocular pressure [15]. Moreover, its use as a synthetic heart valve was investigated. However, its poor creep and mechanical properties were known to limit its clinical use [71], [73].

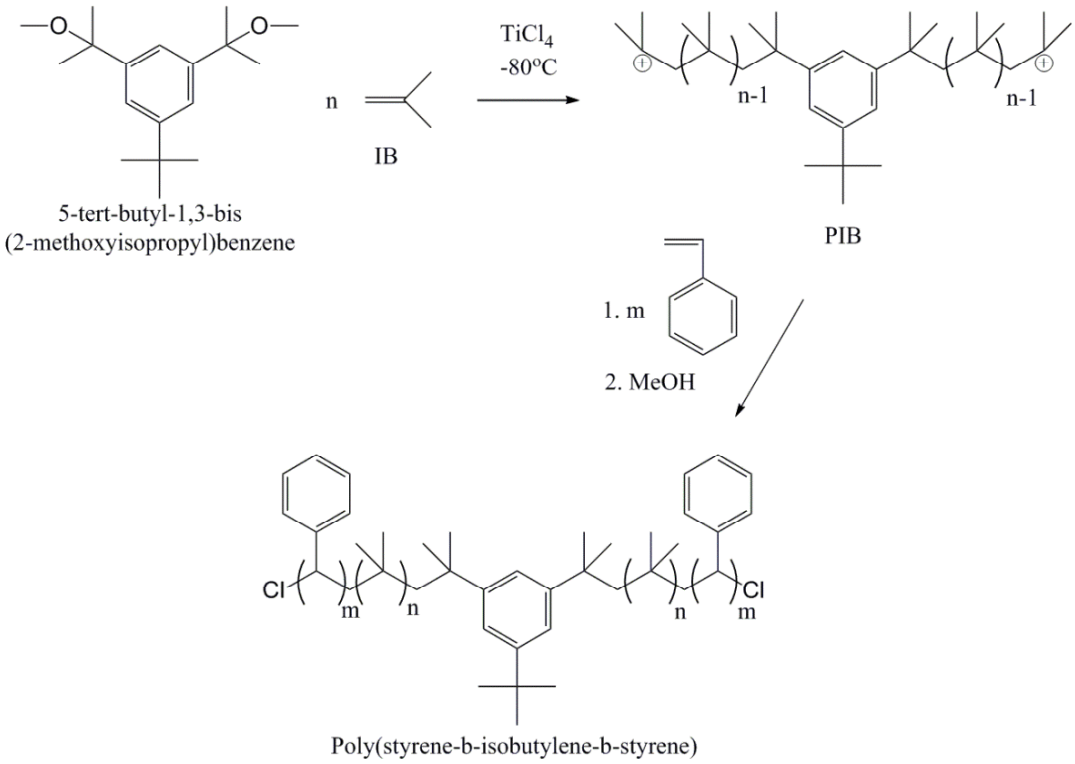

Figure 1.13. Synthesis of SIBS [71]. Adapted with permission from [71], Elsevier, Copyright (2008).

1.7. Polyurethanes

Polyurethanes (PUs) are desirable materials with a broad spectrum of properties ranging from flexible elastomers to rigid plastics. Interest in PU materials is because they can be designed for numerous industrial applications, including foams, coatings, adhesives, sealants, and fibers, by optimizing the key parameters such as stoichiometry and the chemistry of building blocks [74,75]. In addition to commercial commodities of PUs for everyday applications, biomedical grade PUs have also found widespread use in biomaterial applications since the late 1950s. Their outstanding mechanical properties and biocompatibility make PUs one of the most preferred polymers for medical devices such as wound dressing, pacemakers, artificial hearts valves, vascular stents, and catheters [76].

PUs are prominent polymeric materials with their unique segmented block copolymer structure resulting from the coexistence of alternating hard urethane and soft polyol segments [76]. The constituents of these blocks are chosen so that the hard segment has a glassy or crystalline nature at use temperature, whereas the soft segment has a

rubbery nature [76]. PUs are typically formulated using a macrodiol, a diisocyanate, and a chain extender. Soft segments are composed of macrodiols with aliphatic structures and low intermolecular forces, thus giving flexibility to PU [77]. The most commonly used examples are polyester and polyether diols. The hard segments, on the other hand, are generally formed from the diisocyanate and chain extender, and are responsible for the mechanical strength of PUs. To achieve this structure, both aromatic and aliphatic diisocyanates are utilized, such as TDI (2,4-toluene diisocyanate), MDI (4,4′-Methylene diphenyl diisocyanate), and HMDI, which is the hydrogenated version of MDI (4,4′-Methylenebis(cyclohexyl isocyanate)). Besides, chain extenders, such as small molecule diols or diamines are used to increase the molecular weight of the polymer by enlarging the hard segments [77]. Diisocyanates react with macrodiols and chain extenders to give urethane bonds. Urethane bonds being polar, are incompatible with the relatively nonpolar soft segments, and consequently, a phase separated structure unique to PUs occurs [77]. In this structure, due to the structural rigidity of hard segments and hydrogen bonding interactions (Figure 1.14), nanometer sized hard segment domains form in a matrix of flexible soft segments and act as physical crosslinks providing elastomeric behavior to PUs [74].

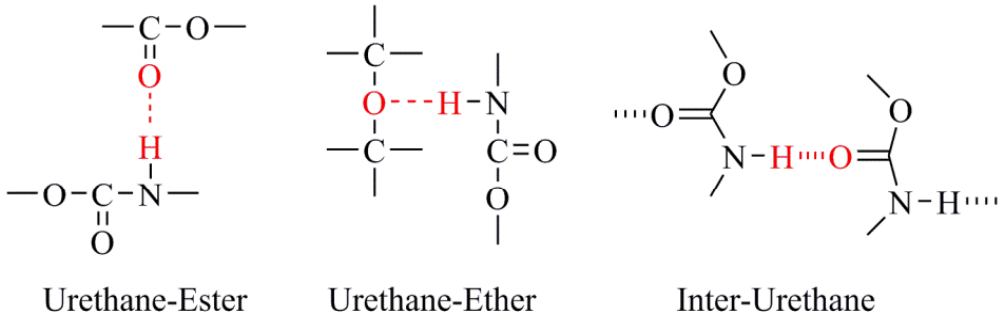

Figure 1.14. Hydrogen bonding in PUs [74]. Adapted with permission from [74], Springer Nature, Copyright (2011).

Synthesis of PUs is usually done through a prepolymer route in two steps. First, a diisocyanate terminal prepolymer is aimed by reacting a stoichiometric excess of diisocyanate and macrodiol in the presence of a catalyst. Then, the prepolymer is extended to higher molecular weights upon addition of the chain extender, as shown in Figure 1.15 [74], [77].

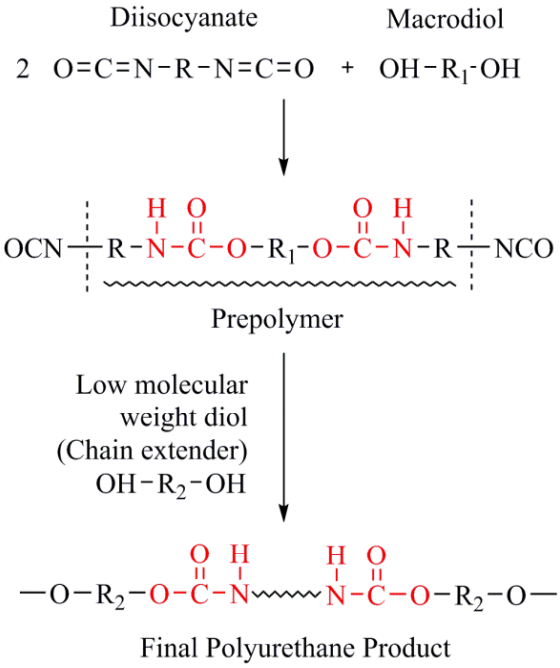

Figure 1.15. Two-step polymerization synthesis route to PUs [74]. Adapted with permission from [74], Springer Nature, Copyright (2011).

1.8. PIB based Polyurethanes

The inherent urethane linkages of PUs are known to be labile to undergo hydrolysis and oxidation. This severely limits the performances of PU based materials and poses a major handicap. Additionally, the commonly used polyester and polyether soft segments are also susceptible to hydrolytic and oxidative deterioration. Consequently, the mechanical properties of PUs are not sustained for long-term medical applications [78-81]. Achieving biostability without compromising mechanical durability is a big challenge to overcome.

PIB, however, is a polymer of industrial importance which exhibits exceptional oxidative-hydrolytic-chemical stability, biocompatibility, and gas impermeability [75]. PIB is widely utilized in various areas necessiating high damping properties, gas impermeability, as well as environmental and chemical stability. These areas include tire inner liners (chlorobutyl and bromobutyl rubbers), tank liners, vibration-proof materials, engine mounts, pharmaceutical stoppers, and others [3]. Besides, PIB has been utilized in biomaterial science. Specifically, the triblock copolymer of isobutylene with styrene

(SIBS) is utilized as paclitaxel releasing polymeric coating on the TAXUS coronary stent. The absence of polar groups renders these TPEs results in exceptional biostability and biocompatibility [71].

In this particular context, PIB based PUs have been developed as distinctive materials that combine the superior properties of PIB, such as exceptional inertness, chemical, and biostability with the high strength of segmented thermoplastic PUs [75]. Although the early PIB based PUs demonstrated superior hydrolytic-oxidative-thermal and barrier properties compared to conventional TPUs [82], their mechanical performances were relatively poor [83-84]. This outcome can be attributed to the high incompatibility between the nonpolar completely hydrocarbon PIB soft segments and the polar urethane hard segments, as well as the absence of reinforcing hydrogen bonds, resulting in poor stress transfer between phases [75].

In order to enhance the mechanical properties and overcome the incompatibility issue between hard and soft phases of PIB based PUs, some sophisticated approaches have been recently reported by the Kennedy group [75]. One of them is the utilization of compatibilizing soft cosegments such as polytetramethyleneoxide diols (PTMO diol). In the first two articles of the research, they discussed the preparation of PIB based polyurea and polyurethane urea elastomers exhibiting hydrolytic-oxidative stabilities. They showed that the mechanical properties were improved upon the incorporation of PTMO co-soft segments [85,86].

In subsequent articles [87-89], the effects of PTMO soft segments on mechanical properties, resistance to oxidation and hydrolysis, morphology, and biocompatibility of PIB based PUs were examined. The addition of 20% PTMO by weight was reported to improve both tensile strengths and elongations. The elastomeric properties of hybrid PIB/PTMO PUs were reported to be similar to commercially available biomedical PUs (50% PIB, 20% PTMO, and 30 % HDO = tensile strength >30 MPa and elongation 700%) [87].

Figure 1.16 outlines the synthesis strategy and suggested micromorphology of PIB/PTMO based PUs. In the presence of the catalyst, HMDI reacts with PIB diol and

PTMO diol cosegment to give prepolymer, which is chain-extended with HDO [88]. In the scheme, the solid red lines represent PIB soft segments. The dotted red lines are PTMO or PC co-soft segments. The long blue lines correspond to the hard segments. The short blue lines that connect two soft segments signify the dispersed hard segments. This model (Figure 1.16) was proposed according to the results of structural, thermal, and mechanical characterizations [89]. It emphasizes the presence of H bonding (thin black lines) within the urethane hard domains, and between the PTMO soft segments and urethane hard domains. Besides, according to the model, inert PIB segments envelope and protect the vulnerable groups of PU [88,89].

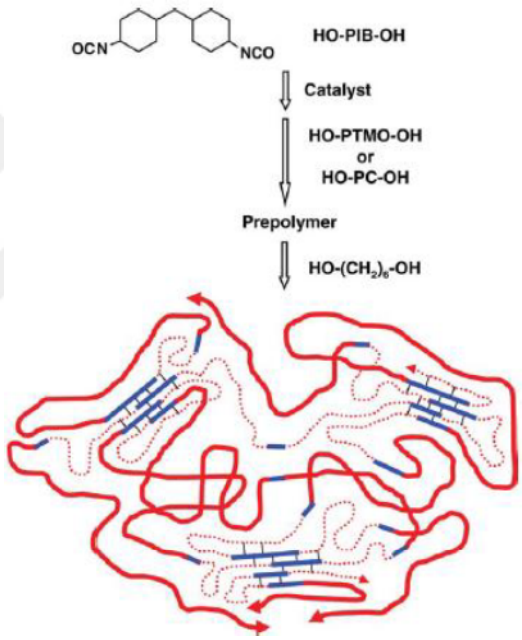

Figure 1.16. Synthesis strategy and idealized micromorphology of a PIB/PTMO (or PIB/PC) based PU. Reproduced from [88] with permission from John Wiley and Sons, Copyright (2010).

As shown in Figure 1.17 (a), highly nonpolar PIB soft segments and polar urethane hard segments are incompatible and form strongly segregated phases with sharp interfaces. As a result of the distinct interfaces and non-existence of H bonding interactions between the rigid and flexible phases, insufficient stress transfer between phases occurs. This situation is believed to be the reason for the poor mechanical characteristics observed in prior PIB based PUs. On the other hand, H bonds that arise between ether groups of PTMO and urethane bonds of hard segments (Figure 1.17 (b)) enhance compatibility between the

PIB matrix and rigid hard segments, and hence improve mechanical properties [89]. In the scheme, HS^{cr} and HS^{am} signify the crystalline and amorphous hard segments. HS^{d} represents dispersed hard segments that connect two soft segments.

The fifth article of the research investigated the amount of PIB (wt %) required for oxidative and hydrolytic resistance [88]. Tensile strengths and elongations of various PIB based PUs differing in PIB/PTMO/HDO content were measured after they were exposed to 35% HNO_3 and $H_2O_2/CoCl_2$ solutions. According to the results, 60-70 wt% PIB provides the most protection againts oxidative-hydrolytic deterioration (93% and 72% retention of tensile strengths for samples with 70 wt% and 60 wt% PIB, respectively). In addition, the commercial biomedical PUs, Carbothane and Elast-Eon, were severely degraded upon exposure to HNO_3 [88].

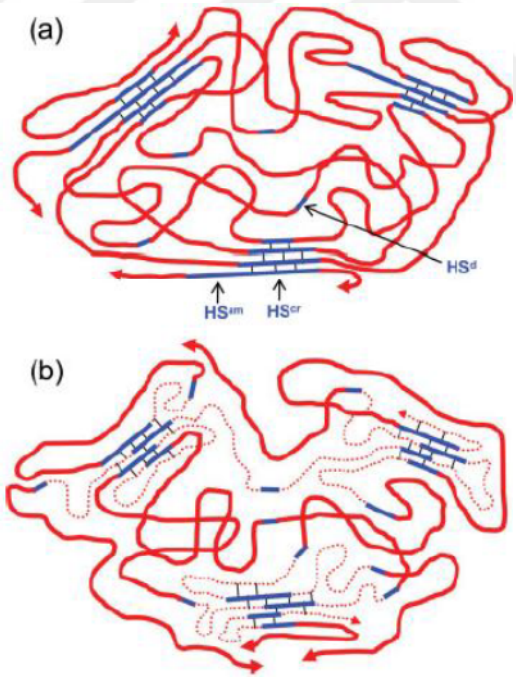

Figure 1.17. Idealized micromorphologies (a) a PIB based PU containing 70 wt% PIB and 30 wt% HS, and (b) a PIB/PTMO based PU with 50 wt% PIB, 20 wt% PTMO, and 30 wt% HS. Reproduced from [89] with permission from John Wiley and Sons, Copyright (2009).

Another approach considers the utilization of flexible H bond accepting chain extenders (HACEs) together with conventional chain extenders [75]. In the sixth article of

the research, the mechanism of reinforcement in PIB based PUs formulated with HACE was investigated [90]. Figure 1.18 shows the structures of HACEs studied in this research. They are thought to increase the molecular weight of the hard segments via terminal –OH or $–NH_2$ groups and provide a number of functional groups with H bonding capability (e.g., –O- and $–N(CH_3)$-) within hard segments, which in turn increase flexibility (toughen) the hard segments (improved mechanical properties). Figure 1.19 shows the synthesis strategy of PIB based PUs prepared using both conventional chain extenders and HACEs. Figure 1.20 emphasizes the extended hard segments that are formed by linking chain extender-diisocyanate units and HACEs together through covalent and H bonds. Improved mechanical properties (20-30 MPa tensile strength and 600-700% elongation) were attributed to the additional H bonding that arises from incorporating HACEs into hard segment and the increased flexibility of hard segments under stress [90].

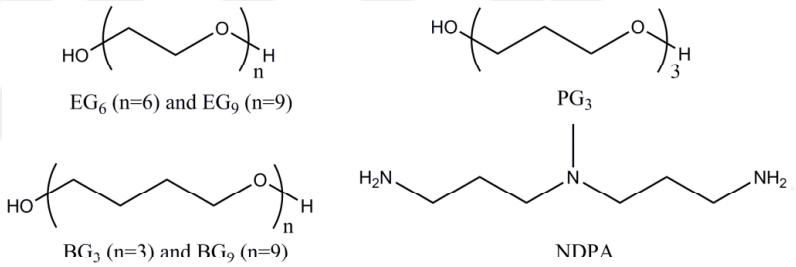

Figure 1.18. Structures of HACEs investigated [90]. Adapted with permission from [90], John Wiley and Sons, Copyright (2010).

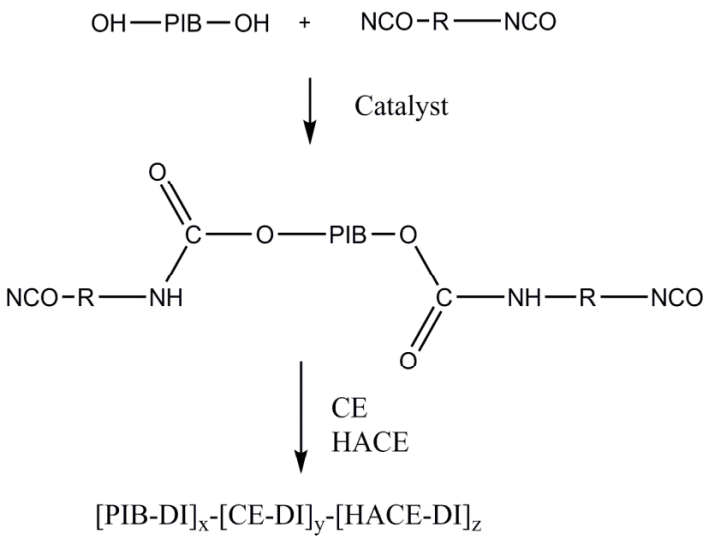

Figure 1.19. Synthesis strategy PIB based PU reinforced with HACE [90]. Adapted with permission from [90], John Wiley and Sons, Copyright (2010).

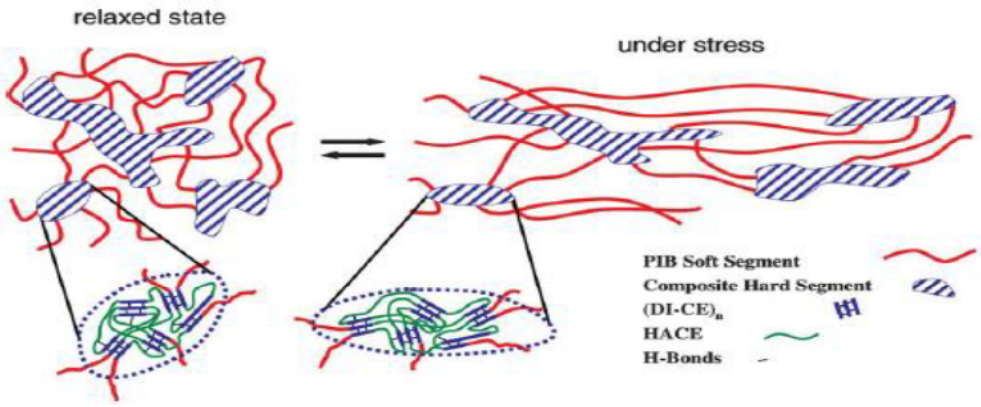

Figure 1.20. An idealized microstructural illustration of PIB based PUs reinforced with HACE in the relaxed state and under stress. Reproduced from [90] with permission from John Wiley and Sons, Copyright (2010).

1.9. Vegetable Oil Based Polyols and Polyurethanes

In recent years, vegetable oils have become sustainable alternatives to petrochemicals derived from limited petroleum resources. They are widely used as biobased platform chemicals in surfactants, cosmetic products, and lubricants [91,92] They are also used in preparation of various polymers including PUs, polyesters, polyamides, and resins (e.g., acrylic, epoxy) [93]. The synthesis of vegetable oil based polyols and PUs obtained therefrom is an area of active research [94].

Vegetable oils consist of triglycerides formed from the esterification of glycerol and three fatty acids. The fatty acid composition of each vegetable oil varies. For example, the main constituents of soybean oil are linoleic acid (C18:2) and oleic acid (C18:1) [95]. The structure of soybean oil and its fatty acid composition are given in Figure 1.21 and Figure Table 1.1.

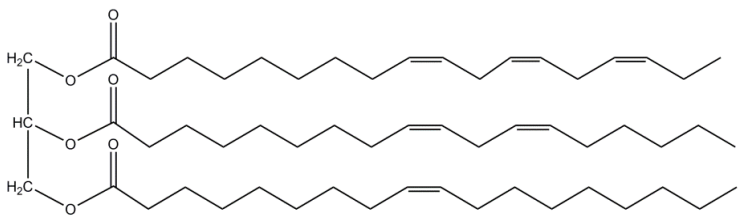

Figure 1.21. Structure of soybean oil [96]. Adapted with permission from [96], licensed under CC BY-NC-SA 3.0.

Table 1.1. Fatty acid composition of soybean oil [96]. Adapted with permission from [96], licensed under CC BY-NC-SA 3.0.

Fatty acid	Percentage in soybean oil, %	Number of C atoms: Number of double bonds	Structure of fatty acid
Palmitic acid	10-11	C16:0	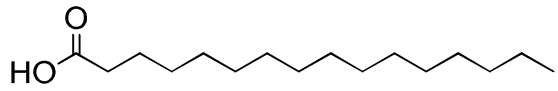
Stearic acid	4-6	C18:0	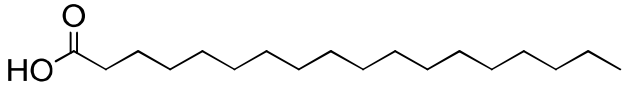
Oleic acid	23-25	C18:1	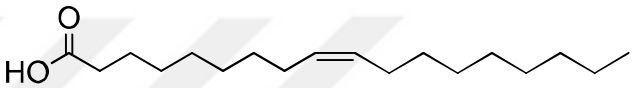
Linoleic acid	50-55	C18:2	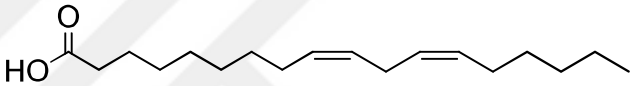
Linolenic acid	6-9	C18:3	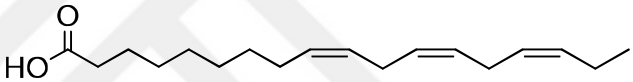

The potential of vegetable oils as abundant renewable bioresources with modifiable functionalities has long been explored as a platform for novel functional monomers and various polymers for the chemical industry, which is largely dominated by petrochemicals derived from limited petroleum resources [92], [97-100]. Most commonly, the synthesis of vegetable oil based polymers is done either through the polymerization of double bonds in pristine or modified triglycerides via several polymerization techniques (e.g., free radical and metathesis polymerizations, cationic copolymerization) or through conversion of fatty acid derivatives into monomers with multiple functionalities for PUs, polyesters, and polyamides [91]. Double bonds and ester groups, which are common to all triglycerides, provide the opportunity to introduce new functionalities such as epoxy, amine, isocyanate, vinyl moieties, and hydroxyl groups [101,102]. Given that the polyol is the main constituent of PUs, a significant amount of research has been conducted to modify vegetable oil fatty chains with hydroxyl groups to increase the bio-content of PUs [99,100].

Double bonds and ester groups are the most prominent active sites of triglycerides. They can be modified to introduce hydroxyl functionality into triglyceride, which then

serves as the polyol in PU synthesis. Methods used in the preparation of polyols from vegetable oils can be listed as follows: 1) Epoxidation of double bonds and subsequent ring-opening of the epoxide by a nucleophile, which is the most common method; 2) transesterification of ester group with an alcohol (e.g., polyol) or amidation with amines; 3) hydroformylation of double bond in the presence of Rh catalyst followed by reduction to alcohol (hydrogenation); 4) ozonolysis of double bond followed by reduction to alcohol (through an aldehyde intermediate); 5) radical addition of hydroxyl functional thiols to double bond (thiol-ene reaction) (Figure 1.22) [95].

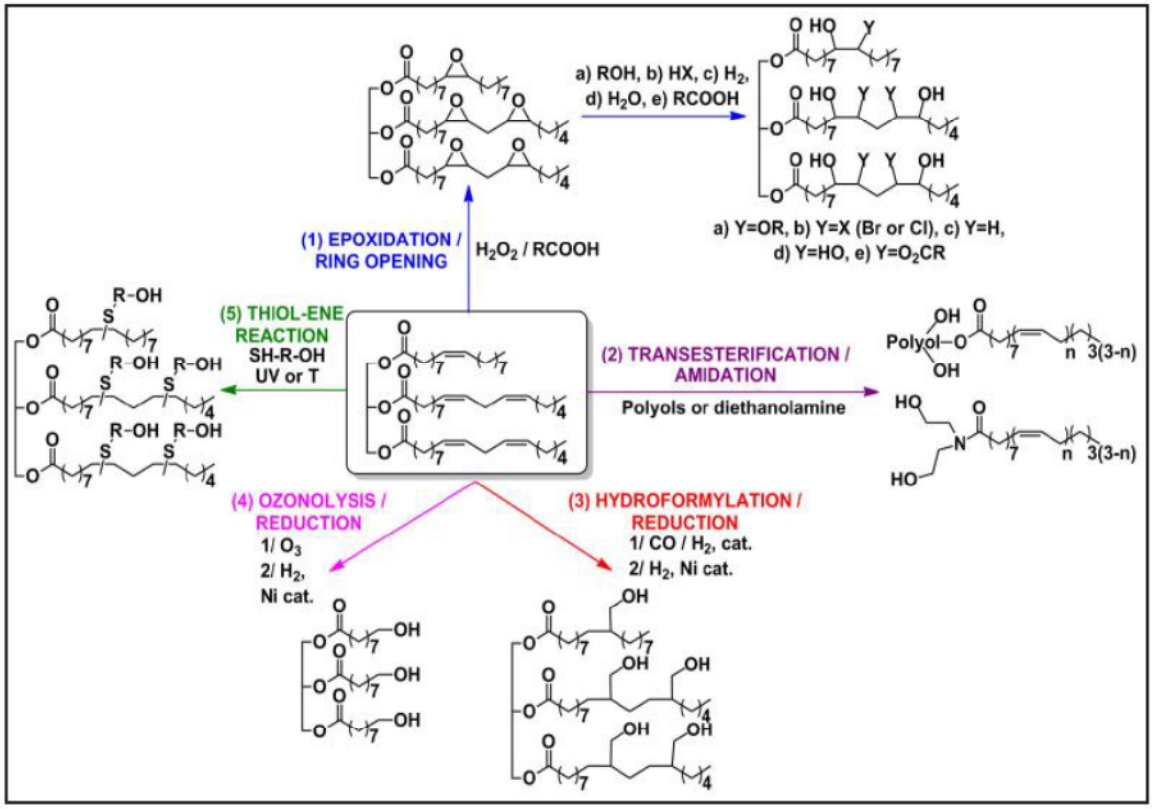

Figure 1.22. Common strategies for incorporating OH groups into triglycerides. Reproduced with permission from [95] licensed under CC BY 4.0.

The production of commercial polyols highly relies on the epoxidation-ring opening strategy [103]. Although this strategy benefits from a wide variety of nucleophiles such as alcohols, amines, thiols, inorganic and carboxylic acids used in the ring-opening of oxirane, the resulting polyols typically have secondary hydroxyl groups unless a polyfunctional nucleophile like ethane-1,2-diol and diethanolamine is used [103]. It is possible to functionalize the double bonds of fatty acid chains with primary hydroxyl

groups using the Hydroformylation and ozonolysis reactions. These reactions proceed through the intermediacy of an aldehyde. Although the hydroformylation strategy is effective in generating polyols with multiple hydroxyl groups, it requires the use of an expensive Rh catalyst for quantitative conversion [103,104]. Compared with the hydroformylation, the ozonolysis strategy yields lower molecular weight polyol with a maximum of three terminal hydroxyl groups [103,104]. In addition, the aforementioned strategies follow a mechanism consisting of two steps. Consequently, the thiol-ene reaction stands out among others as it enables the synthesis of polyols with primary hydroxyl functionalities in a one-step reaction under mild reaction conditions [101], [105-108].

Thiol-ene reaction is a powerful technique characterized by high reaction rates, quantitative conversions with known regioselectivity, and simple reaction setup, i.e., tolerance to oxygen. Figure 1.23 illustrates UV initiated radical Thiol-ene addition process [109].

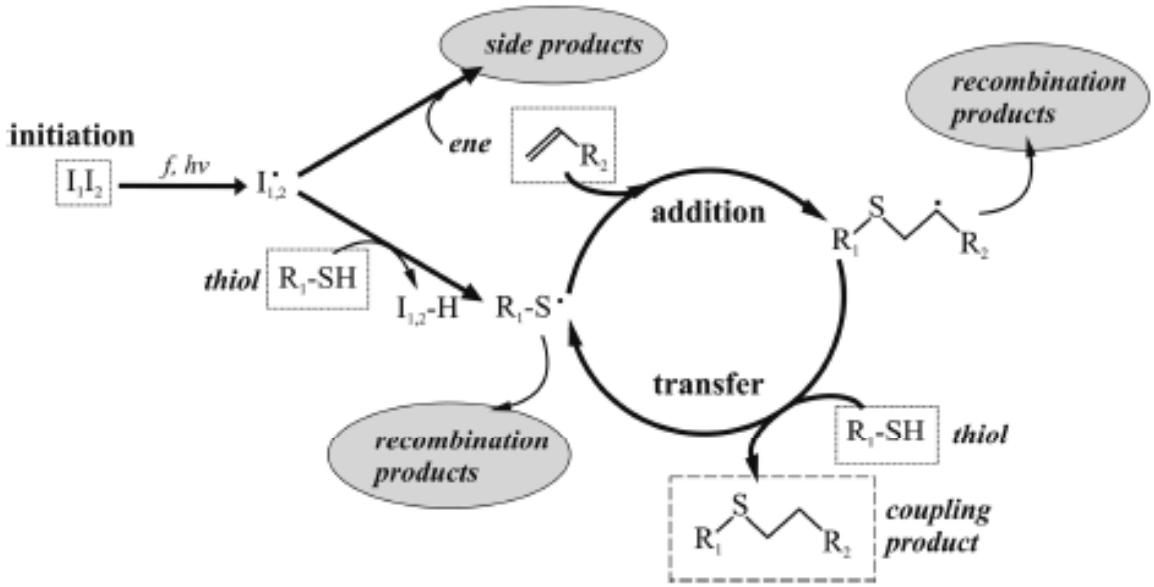

Figure 1.23. Principle of UV-Initiated Thiol−Ene “Click” Chemistry. Reproduced from [109] with permission from American Chemical Society, Copyright (2013).

Radical mediated addition of thiols to enes can be induced either by UV light typically combined with a photoinitiator or by a thermal initiator. The UV initiated process starts with the generation of initiator-derived radicals upon irradiation of a photoinitiator. These radicals remove hydrogen from a thiol molecule generating thiyl radicals, which in

turn add to a double bond in an anti-Markovnikov fashion. The thio-ether coupling product is formed when the forming carbon radicals remove hydrogen from another thiol molecule [109].

Thiol-ene reaction is widely utilized in the synthesis of networks, dendrimers, star, and hyperbranched polymers, or polymer chain modifications because of its benefits, including high reaction rates, quantitative conversions with known regioselectivity, and simple reaction setup, i.e., tolerance to oxygen [110]. In oleochemistry, one of the major applications of Thiol-ene reaction is the synthesis of polyols starting from a fatty acid derivative, e.g., 10-undecenoic acid, [111-115] or directly from triglycerides [105-108].

Desroches et al. reported the synthesis of polyols from rapeseed oil with primary hydroxyl groups via UV-initiated addition of 2-mercaptoethanol onto olefinic double bonds, and PU obtained therefrom [105]. In a model study, the photoaddition of the mercapto compound onto oleic acid was studied in terms of optimum reaction conditions and byproducts. Thiol/double bond ratio was found to be the major parameter governing the reaction kinetics, the extent of side reactions as well as thiol grafting. Under optimized conditions, i.e., bulk reaction for a thiol/ene ratio of 3/1 at 15 W/cm^2 without the use of a photoinitiator, only 65% of double bonds were reported to be grafted with the mercapto compound because of disulfide formation and intermolecular coupling of carbon-centered radicals (Figure 1.24).

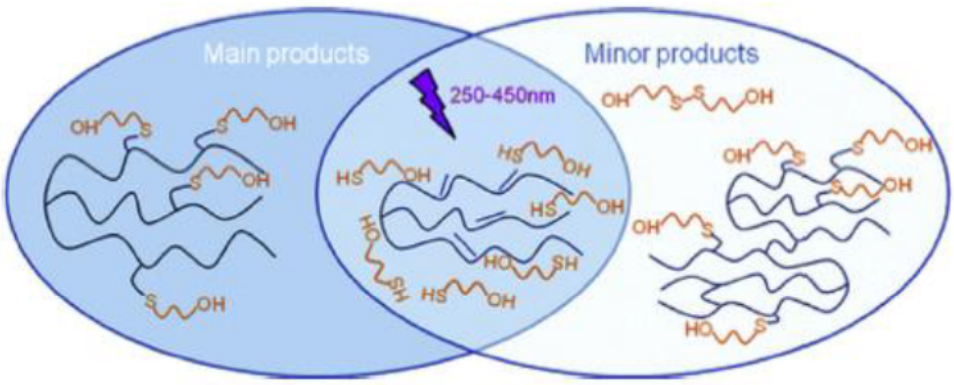

Figure 1.24. Main product and side reactions that may form during thiol-ene reactions of 2-mercaptoethanol and rapeseed oil. Reproduced from [105] with permission from American Chemical Society, Copyright (2011).

Caillol et al. converted soybean oil into polyol by thermal thiol-ene addition of 2-mercaptoethanol using azobisisobutyronitrile at 80 ºC [105]. The polyol or its mixture with Desmophen 1150 was copolymerized with a prepolymer of MDI to synthesize soft and ductile PU elastomers. Tensile strength at break and maximum elongation (%) values for the PU obtained solely from soybean oil based polyol were 1.3 MPa and 20%, respectively.

Alagi et al. reported the synthesis of quantitative functionalization of soybean and castor oils with primary hydroxyl groups via UV-induced 2-mercaptoethanol addition at low temperatures in the presence of a photoinitiator [107]. Quantitative functionalization of soybean oil was achieved at -20 °C for 24 h under a nitrogen atmosphere when the thiol to ene ratio is 4. In an analogous study, Alagi et al. demonstrated the usefulness of photoinitiated thiol-ene reaction for synthesizing vegetable oils with predetermined hydroxyl functionalities [108]. Soybean oil polyols with average hydroxyl functionality ranging between 2 and 4 were achieved by adjusting the irradiation time and the extent of double bond conversion. The resulting polyols, together with polytetramethylene ether glycol (PTMEG), were used in synthesis of hyperbranched TPUs exhibiting hard and tough elastomer behavior.

2. OBJECTIVES OF RESEARCH

The first part aims to enhance the low creep properties of SIBS by introducing crystallizable polyurethane sequences and, hence, hydrogen bonds. Telechelic polymers consisting of di-hydroxy or di-amine groups are commonly used to synthesize polyurethanes. Therefore, HO-PIB-OH and HO-PSt-OH were first planned to be synthesized using cationic or anionic polymerization techniques to achieve these structures. Moreover, to overcome the possible phase separation between these two incompatible polymers during polyurethane synthesis, we designed the synthesis of OEO-b-PIB-b-OEO and OEO-b-PSt-b-OEO which contain oligo-ethylene oxide blocks that could act as a compatibilizer. Finally, it was decided to synthesize polystyrene and polyisobutylene-based polyurethane materials by reacting the abovementioned macrodiols with aromatic diisocyanates like MDI and chain extenders such as 1,4-butanediol at different weight percentages.

The second part aims to develop a synthetic methodology for the synthesis of a novel bio-based PIB PU with a soybean oil derivative. Three stages of the methodology are (a) conversion of SBO triglycerides to a polyol with primary hydroxyl functionalities via UV activated thiole-ene chemistry, (b) optimization of the grafting efficiency, (c) synthesis of novel SBO and PIB based PU network. In order to show the reprocessability of the obtained network, selective hydrolysis of network moieties which can be resulting in a soybean oil based PIB PU having valuable polar sites for their further blends and composites forms was also studied.

Molecular structure and molecular weight of the obtained PUs are characterized by ^{1}H NMR, FTIR and SEC. Thermal and mechanical properties are studied with DSC, TGA and DMA techniques, and stress-strain test.

3. SYNTHESIS AND CHARACTERIZATION OF A NOVEL DIHYDROXY TELECHELIC POLYISOBUTYLENE/POLYSTYRENE BASED POLYURETHANE THERMOPLASTIC ELASTOMER

3.1. Experimental

3.1.1. Materials

Titanium tetrachloride ($TiCl_4$), calcium hydride (CaH_2), diphenylmethane (DPM), di-phosphorous pentoxide (P_2O_5), dibutyltin dilaurate (DBTDL), benzophenone, fluorene, methanol, magnesium sulfate ($MgSO_4$), hydrochloric acid (HCl), sodium hydroxide (NaOH) and sodium chloride (NaCl), from Merck, were used without further purification. Sodium (Na) and potassium (K) from Alfa Aesar and sec-butyllithium (sec-BuLi, 1.3 M solution in cyclohexane) from Sigma Aldrich were used as received. Lithium (Li) was purchased from Sigma Aldrich. Styrene (St), 1,4-butanediol (BDO), tetramethylethylenediamine (TMEDA), tetrahydrofuran (THF), cyclohexane, n-hexane, dichloromethane (DCM) were purchased from Merck.

3.1.2. Purifications of Solvents and Reagents

Styrene was distilled from fluorenyl Li prior to use. BDO dried over Na metal and TMEDA dried over CaH_2 were vacuum distilled and stored under N_2. THF was freshly distilled from the violet-colored Na benzophenone complex and Li naphthalenide solution. Cyclohexane was purified by distilling first from sec-BuLi/α-methyl styrene solution, then over a fresh Na mirror. DCM and n-hexane were refluxed and distilled over CaH_2, and DCM was further dried by distilling over P_2O_5. EO and ATMS from Sigma Aldrich were dried over CaH_2 and vacuum distilled just before use. 4,4′-Methylene diphenyl diisocyanate (MDI) from Across was vacuum distilled ($2x10^{-2}$ mbar, ~135 °C) and stored in the refrigerator under N_2. Isobutylene (IB, Scot Speciality Gases) was dried by passing through a column packed with anhydrous calcium sulfate, cobalt chloride, and silica gel and condensed into a dry graduated cylinder cooled to -40 °C in an acetone-dry ice bath.

Lithium (Li) naphthalenide was prepared according to the literature [116]. The granular Li was treated with a solution of benzophenone in THF to clean the metal surface. Then, the THF solution of Na benzophenone was removed from the medium by successive filtration-back distillation (THF). The remaining THF was removed from the flask containing the Li granules via evaporation at reduced pressure, and the Li granules were stored under a dry argon atmosphere.

3.1.3. Synthesis of di-Hydroxy Telechelic Polyisobutylene (HO-PIB-OH)

3.1.3.1. Synthesis of 5-tert-Butyl-1,3-dicumyl chloride (TBDCC). A sterically hindered di-functional cationic initiator was synthesized from 5-tert-butyl isophthalic acid (TBIPA) via esterification, Grignard reactions and chlorination reaction as previously described by Wang et al. [29]. In this context, first TBIPA was refluxed in MeOH in the presence of H_2SO_4 to yield the corresponding diester, dimethyl 5-tert-butyl isophthalate (DMTBIP). Subsequently, the obtained product was subjected to a Grignard reaction with MeMgBr, resulting in 5-tert-butyl-1,3-dicumyl alcohol (TBDCA). Finally, TBDCA was chlorinated with gaseous HCl to obtain the desired product, TBDCC [25], [117].

In the 3rd step, TBDCA (7.5 g, 0.03 mol), stored in deep freeze under N_2 atmosphere, was weighed into a flame dried reactor containing $CaCl_2$. The reactor was connected to the high vacuum line, degassed, and purged with N_2. In a separate flask equipped with a dropper, HCl (g) was generated by the dropwise addition of H_2SO_4 onto NaCl. The produced gas was fed into the reactor through PTFE cannula under continuous N_2 flush and bubbled through the alcohol dissolved in dry DCM (100 ml) at 0 °C for six hours (Figure 3.1). Excess HCl was neutralized by bubbling it through a NaOH solution. After the solution was warmed to room temperature, it was filtered through a fine sintered glass. DCM was removed using the rotary evaporator, and the initiator was further dried on the high vacuum line. It was then dissolved in dry hexane (14 ml) and recrystallized in the deep freeze. Afterward, the hexane was removed using the rotary evaporator, and the initiator was further dried on the high vacuum line (Figure 3.2). It was kept under N_2 atmosphere at - 20 °C.

^{1}H NMR (400 MHz, $CDCl_3$, δ): 1.35 (s, 9H, $C(CH_3)_3$), 2.01 (s, 12H, $C(CH_3)_2$), 7.52–7.62 (3H, –C_6H_3 aromatic)

3.1.3.2. Synthesis of di-Allyl Telechelic PIB by Carbocationic Polymerization (A-PIB-A).

The polymerization was conducted in a freshly distilled n-hexane/DCM (60:40 %) solvent mixture using TBDCC/$TiCl_4$ initiating system and TMEDA proton trap at -80 ºC under N_2 (Figure 3.3) TBDCC (1.7907 g, 6.234 mmol) was weighed into a 1L flame-dried reactor and dissolved in n-hexane (400 ml) and DCM (267 ml) solvent mixture. TMEDA (1.422 ml, 9.482 mmol) was injected into the reactor using a syringe with a steel capillary, and the reactor was subsequently cooled to -80 ºC. Isobutylene (24.60 ml, 334 mmol) was condensed into a dry graduated cylinder at -40 ºC and transferred into the reactor via a steel capillary. Finally, $TiCl_4$ (8.886 ml, 81 mmol) dissolved in DCM (20 ml) was equilibrated to -80 ºC and transferred into the reactor to initiate the polymerization. After 1 h, the polymerization was quenched by the dropwise addition of ATMS (19.81 ml, 124.7 mmol) at – 80 °C for 30 min (Figure 3.4). Following the in situ end quenching, the reaction was terminated with methanol. The polymer solution was concentrated and precipitated into methanol. The precipitated polymer was dissolved in hexane (180 ml) and washed successively with 5% $NaHCO_3$ solution and water. The organic layer was dried over Na_2SO_4, filtered through a fine sintered glass, and the solvent was removed using the rotary evaporator. The obtained polymer was dried on the high vacuum line at 60 ºC.
^{1}H NMR (400 MHz, $CDCl_3$, δ): 1.03–1.22 (6 H, –CH_3 methyl protons of PIB), 1.35–1.46 (2 H, –CH_2– methylene protons of PIB), 4.75–5.20 (4 H, –CH=CH_2), 5.6–6 (2 H, –CH=CH_2), 7.16 (3 H, –C_6H_3 aromatic)

3.1.3.3. Hydroboration Reaction of A-PIB-A. In a flame-dried flask equipped with a dropping funnel, A-PIB-A (18 g, 5.343 mmol) was dissolved in dry THF (90 ml). 9-BBN (53,56 ml, 0.5 M, 26.7 mmol, 5 equiv. per chain) was added dropwise, and the reaction was carried out at room temperature for 5 h. Then, KOH (4.5 g, 80.1 mol, 15 equiv. per chain) in MeOH (29.8 ml) was transferred into the dropper via a steel capillary under an N_2 atmosphere and added dropwise at room temperature. Subsequently, aqueous H_2O_2 (50%, 5.439 ml, 80.1 mmol, 15 equiv. per chain) was added dropwise over the ice bath, and the mixture was allowed to stir overnight at room temperature.

After an overnight reaction, hexane (180 ml) and water (51 ml) were added to the mixture, and then the organic phase was washed with 5% aqueous $NaHCO_3$ (51 ml). The organic layer was dried over $MgSO_4$, and following the filtration through a fine sintered

glass, the solvent was evaporated on the rotary evaporator. The polymer was dissolved in hexane and precipitated in MeOH three times to get rid of the impurities like cyclooctane-1,5-diol. The polymer was dried on the high vacuum line at 60 ºC [33], [118,119].
^{1}H NMR (400 MHz, $CDCl_3$, δ): 1.03–1.22 (6 H, –CH_3 methyl protons of PIB), 1.35–1.46 (2 H, –CH_2– methylene protons of PIB), 3.55–3.66 (4 H –CH_2CH_2OH), 7.17 (3 H, –C_6H_3 aromatic)

3.1.4. Synthesis of OEO-b-PIB-b-OEO

The synthesis of OEO-b-PIB-b-OEO was done in accordance with papers authored by Francis et al. [120] and Zhang et al. [69], that is by partial deprotonation of HO-PIB-OH in the presence of freshly prepared diphenylmethylpotassium (DPMK), followed by anionic ring-opening oligomerization of EO.

In a 500 ml flame-dried flask, HO-PIB-OH (8.1236 g, 2.4113 mmol) was weighed and dissolved in dry THF (100 ml) under Ar atmosphere. DPMK (2.455 ml, 0.58 M) was injected into the polymer solution over an ice bath. Upon completion of the injection, the ice bath was removed, and the reaction mixture was stirred for an hour. Subsequently, the reactor was immersed in the ice bath, and EO (2.38 ml, 48.2 mmol) was transferred via a steel capillary under Ar flush. Then, the reactor was kept on stirring for about two days at room temperature. Following that, the reaction mixture was stirred at 50 ºC for 10 h and at room temperature for two more days. After termination with acidic methanol, the solvent was evaporated to dryness. The polymer was dissolved in hexane, dried over $MgSO_4$, filtered, and precipitated into methanol twice. Finally, it was dried on the high vacuum line at 60 ºC.
^{1}H NMR (400 MHz, $CDCl_3$, δ): 1.03–1.22 (6 H, –CH_3 methyl protons of PIB), 1.35–1.46 (2 H, –CH_2– methylene protons of PIB), 3.3–3.84 (4 H –CH_2CH_2O– EO units), 7.17 (3 H, –C_6H_3 aromatic)

3.1.5. Synthesis of di-Hydroxy Telechelic Polystyrene (HO-PSt-OH)

Li naphthalenide was prepared according to the reference [116]. Li (0.156 g, 21 mmol) and naphthalene (3.204 g, 25 mmol) were weighed into a flame-dried round bottom

flask, degassed by freeze-pump-thaw cycles, and charged with Ar. Freshly distilled THF (100 ml) was transferred into the reaction flask in an ice bath through a steel capillary under Ar pressure. The reaction mixture was then stirred at room temperature until the dissolution of the metal before filtering through a sintered glass in an Ar atmosphere (Figure 3.5). The concentration of the initiator solution was found to be 0.2162 M by titrating against standardized HCl solution using phenolphthalein as an indicator.

The polymerization was carried out using the Li naphthalenide initiator in freshly distilled cyclohexane (150 ml) under an Ar atmosphere (Figure 3.6) [61], [63]. The initiator was injected into the reaction flask dropwise until the green color of the radical anion persisted. Then, the required amount (30.8 ml, 6.67 mmol, 0.21625 M in radical anion) was injected, and the reactor was placed in an ice bath. The polymerization was started by transferring distilled St (11 ml, 10 g, 96 mmol) to the reactor under continuous stirring. After 45 min., EO (1.66 ml, 33.3 mmol, 5 equiv. of chain end) was transferred to the living PStLi solution, and the reaction mixture was stirred overnight at room temperature. Following termination with acidic methanol, the polymer was precipitated in methanol and dried in a vacuum oven (white powder).
^{1}H NMR (400 MHz, $CDCl_3$, δ): 1.2–2.6 (3H, –CH_2CH– PSt main chain), 3.17–3.42 (4H, –CH_2CH_2OH), 6.05–7.25 (5H, –C_6H_5– aromatic)

3.1.6. Synthesis of OEO-b-PSt-b-OEO

Diphenylmethylpotassium (DPMK) was synthesized according to the reference [120]. K (1 g, 25.6 mmol) was weighed into a flame dried 500 ml two-neck round bottom flask in a dry box. The flask was connected to the vacuum line and placed in an ice bath. Naphthalene (1.64 g, 12.8 mmol) in dry THF (29 ml) was prepared and transferred to the flask containing K via a steel capillary under Ar flush. The color of the solution turned dark green in minutes (Figure 3.7). The reaction mixture was allowed to stirr overnight for a complete dissolution of K. To the K naphthalenide solution at 0 ºC, DPM (4.307 g, 25.6 mmol) in THF (15 ml) was transferred via a steel capillary under Ar. Brown-red color became visible in an hour. The reaction mixture was kept on stirring for 1 week at room temperature. The brown-red colored DPMK solution was filtered through a sintered glass using Ar overpressure and kept under an Ar atmosphere in the refrigerator (Figure 3.8).

Polymerization was done according to a previously reported procedure [69]. HO-PSt-OH (5 g, 1.261 mmol) was weighed in a 500 ml flame-dried flask and dissolved in dry THF (100 ml). DPMK (1,4 ml, 0.58 M) was injected into the reaction flask in an ice bath. After one hour, distilled EO (1.4 ml, 0.0283 mol) was transferred to the flask in the ice bath via a steel capillary under Ar flush and kept on stirring at room temperature for a while. The reaction mixture was then stirred at 50 ºC for 2 days. After termination with acidic methanol, the polymer solution was concentrated on the rotary evaporator, precipitated two times in cold petroleum ether, and stored in the refrigerator. The polymer was dried in a vacuum oven at room temperature for 18 h and on the high vacuum line for 16 h.

^{1}H NMR (400 MHz, $CDCl_3$, δ): 1.22–2.6 (3H, –CH_2CH– PSt main chain), 3.9–3.44 (4H, –CH_2CH_2O– EO units), 6.27–7.24 (5H, –C_6H_5– aromatic)

3.1.7. Synthesis of PIB PU

HO-PIB-OH (1.0087 g, 0.29 mmol) and MDI (0.3348 g, 1.33 mmol) were weighed into a flame-dried reactor equipped with a condenser. The mixture was dissolved in dry THF (3 ml) and heated to 65 °C under N_2 atmosphere. DBTDL catalyst (0.83 mg, 0.0013 mmol, 0.1 ml of 8.3 mg/ml THF solution) was injected into the solution, and the prepolymerization reaction was carried out at 65 ºC for 1 h. BDO (0.0939 g, 1.04 mmol) dissolved in dry THF (3 ml) was transferred to the reactor via a steel capillary under N_2 pressure. Following the chain extension reaction for 3 h at 65 ºC, the polymer was cast into a 7x7 cm glass mold. THF was evaporated slowly at room temperature for 5 days. The obtained film was further dried in the vacuum oven at 60 ºC for 19 h. The same casting method was applied to all other PU films.

3.1.8. Synthesis of OEO-b-PIB-b-OEO PU

OEO-b-PIB-b-OEO (1.00 g, 0.27 mmol) and MDI (0.3330 g, 1.33 mmol) were weighed into a flame-dried reactor equipped with a condenser. The mixture was dissolved in dry THF (4 ml) and heated to 65 °C under N_2 atmosphere. DBTDL catalyst (0.85 mg, 0.0013 mmol, 0.5 ml of 1.70 mg/ml THF solution) was injected into the solution, and the prepolymerization reaction was carried out at 65 ºC for 1 h. BDO (0.0955 g, 1.06 mmol)

dissolved in dry THF (3 ml) was transferred to the reactor via a steel capillary under N_2 pressure. Following the chain extension reaction for 3 h at 65 ºC, the polymer was cast into a 7x7 cm glass mold.

3.1.9. Synthesis of PSt PU

HO-PSt-OH (1.0013 g, 0.25 mmol) and MDI (0.3320 g, 1.33 mmol) were weighed into a flame-dried reactor equipped with a condenser. The mixture was dissolved in dry THF (4 ml) and heated to 65 °C under N_2 atmosphere. DBTDL catalyst (0.86 mg, 0.0014 mmol, 0.54 ml of 1.6 mg/ml THF solution) was injected at 65 ºC, and the polymer solution was refluxed in THF for 1 h. Following the transfer of BDO (0.0971 g, 1.08 mmol) dissolved in dry THF (3.5 ml) via a steel capillary under N_2 atmosphere, the mixture was refluxed in THF for 3 h. After 3h chain extension reaction, the polymer solution was cast into a 7x7 cm glass mold.

3.1.10. Synthesis of OEO-b-PSt-b-OEO PU

OEO-b-PSt-b-OEO (0.8815 g, 0.20 mmol) and MDI (0.2914 g, 1.16 mmol) were weighed in a flame-dried reactor equipped with a condenser. The mixture was dissolved in dry THF (4 ml) and heated to 65 °C under N_2 atmosphere. DBTDL catalyst (0.75 mg, 0.0012 mmol, 0.47 ml of 1.6 mg/ml THF solution) was injected at 65 ºC, and the polymer solution was refluxed in THF for 1 h. Following the transfer of BDO (0.0867 g, 0.96 mmol) dissolved in dry THF (3.5 ml) via a steel capillary under N_2 atmosphere, the mixture was refluxed in THF for 3 h. After 3h chain extension reaction, the polymer solution was cast into a 7x7 cm glass mold.

3.1.11. Synthesis of PIB/PSt PU

HO-PIB-OH (1.0030 g, 0.29 mmol), HO-PSt-OH (0.26 g, 0.065 mmol), and MDI (0.1515 g, 0.60 mmol) were weighed into a flame-dried reactor equipped with a condenser. The mixture was dissolved in dry THF (4 ml) and heated to 65 °C under N_2 atmosphere. DBTDL catalyst (0.38 mg, 0.0006 mmol, 0.045 ml of 8.3 mg/ml THF solution) was injected into the solution, and the prepolymerization reaction was carried out at 65 ºC for 1

h. BDO (0.0209 g, 0.23 mmol) dissolved in dry THF (3 ml) was transferred into the reactor via a steel capillary under N2 pressure. Following the chain extension reaction for 3 h at 65 ºC, the polymer solution was cast into a 7x7 cm glass mold.

3.1.12. Synthesis of PIB/OEO-b-PSt-b-OEO PU

HO-PIB-OH (0.9993 g, 0.29 mmol), OEO-b-PSt-b-OEO (0.26 g, 0.057 mmol), and MDI (0.1485 g, 0.59 mmol) were weighed into a flame-dried reactor equipped with a condenser. The mixture was dissolved in dry THF (4 ml) and heated to 65 °C under N_2 atmosphere. DBTDL catalyst (0.38 mg, 0.0006 mmol, 0.045 ml of 8.3 mg/ml THF solution) was injected into the solution, and the prepolymerization reaction was carried out at 65 ºC for 1 h. BDO (0.0213 g, 0.24 mmol) dissolved in dry THF (3 ml) was transferred into the reactor via a steel capillary under N_2 pressure. Following the chain extension reaction for 3 h at 65 ºC, the polymer solution was cast into a 7x7 cm glass mold.

3.1.13. Synthesis of OEO-b-PIB-b-OEO/PSt PU

OEO-b-PIB-b-OEO (1.00 g, 0.27 mmol), HO-PSt-OH (0.26 g, 0.065 mmol), and MDI (0.1451 g, 0.58 mmol) were weighed into a flame-dried reactor equipped with a condenser. The mixture was dissolved in dry THF (4 ml) and heated to 65 °C under N_2 atmosphere. DBTDL catalyst (0.43 mg, 0.0007 mmol, 0.25 ml of 1.7 mg/ml THF solution) was injected into the solution, and the prepolymerization reaction was carried out at 65 ºC for 1 h. BDO (0.0219 g, 0.24 mmol) dissolved in dry THF (3 ml) was transferred into the reactor via a steel capillary under N_2 pressure. Following the chain extension reaction for 3 h at 65 ºC, the polymer solution was cast into a 7x7 cm glass mold.

3.1.14. Synthesis of OEO-b-PIB-b-OEO/OEO-b-PSt-b-OEO PU

OEO-b-PIB-b-OEO (1.00 g, 0.27 mmol), OEO-b-PSt-b-OEO (0.26 g, 0.057 mmol), and MDI (0.1456 g, 0.58 mmol) were weighed into a flame-dried reactor equipped with a condenser. The mixture was dissolved in dry THF (4 ml) and heated to 65 °C under N_2 atmosphere. DBTDL catalyst (0.35 mg, 0.0006 mmol, 0.2 ml of 1.76 mg/ml THF solution) was injected into the solution, and the prepolymerization reaction was carried out

at 65 ºC for 1 h. BDO (0.0232 g, 0.26 mmol) dissolved in dry THF (3 ml) was transferred into the reactor via a steel capillary under N_2 pressure. Following the chain extension reaction for 3 h at 65 ºC, the polymer solution was cast into a 7x7 cm glass mold.

3.1.15. Characterization of Samples

Size Exclusion Chromatography (SEC) data were obtained using Waters Isocratic HPLC Pump with Waters 2414 Refractive Index Detector and four Waters 4.6×300 mm Styragel columns HR 3, HR 4, HR 4E, and HR 5E. Distilled THF was used as the mobile phase at a flow rate of 0.35 mL/min. The number average molecular weights (M_n) and the molecular weight distributions (M_w/M_n) of the polymers were calculated using PSt calibration standards ranging from 400 to 2.5×10^6 g/mol.

FT-IR spectra were collected using a Thermo Scientific Nicolet 380 FT-IR spectrometer with a smart orbit diamond ATR accessory. 32 scans for each sample were taken at a resolution of 2 cm^{-1} in the frequency range of 400–4000 cm^{-1}. Spectral analysis was done using EZ-Omnic software.

^1H NMR spectra were recorded on a Varian Gemini 400 MHz spectrometer in deuterated chloroform (δ $CDCl_3$: 7.26 ppm) or deuterated pyridine (δ pyridine-d5: 7.22, 7.58 and 8.74 ppm).

Differential Scanning Calorimetric (DSC) measurements were done with TA Instruments Q200 under N_2. The samples of the solvent cast films were heated from 25 °C to 220 °C at a rate of 50 °C min^{-1} to erase the thermal history and kept at these temperatures for a minute. Next, they were cooled to -90 °C at a rate of 10 °C min^{-1} and then reheated to 220 ºC at 10 °C min^{-1} heating rate.

Thermogravimetric analyses (TGA) of the samples were performed with a Seiko TG/DTA 6300 instrument in a temperature range of 20–600 °C at a heating rate of 10 °C min^{-1} under N_2.

Stress-strain traces were recorded on a Zwick/Roell Universal Testing Instrument with a 1 kN load cell. Three dumbbell shaped samples (50 × 4 × 0.25 mm^3) were cut from the solvent cast films and tested to failure at a drawing rate of 50 mm min^{-1} at room temperature.

Dynamic mechanical analysis of the rectangular strips of the cast films (20 × 5 × 0.25 mm^3) were performed using a TA Instruments DMA-Q800 in film tension mode. The samples were tested at a constant static force of 0.01 N, an oscillating amplitude of 3 μm, and a heating rate of 5 °C/min in the range of -100 to 210 °C under N_2.

Creep strain of the samples (20 × 5 × 0.25 mm^3) was also obtained in film tension mode at a constant stress of 1 MPa for 15 min at 30 °C, followed by a creep recovery for 15 min after removal of the load.

X-ray diffraction (XRD) analyses of the cast films (1.5×1.5 cm^2) were conducted on Rigaku D/Max-Ultimat diffractometer using CuKα radiation (λ=1.54 Å) as the X-ray source, operating at 40 kV and 40 mA. XRD patterns were recorded from 3° to 70° (2θ) with a scanning rate of 2° min^{-1}.

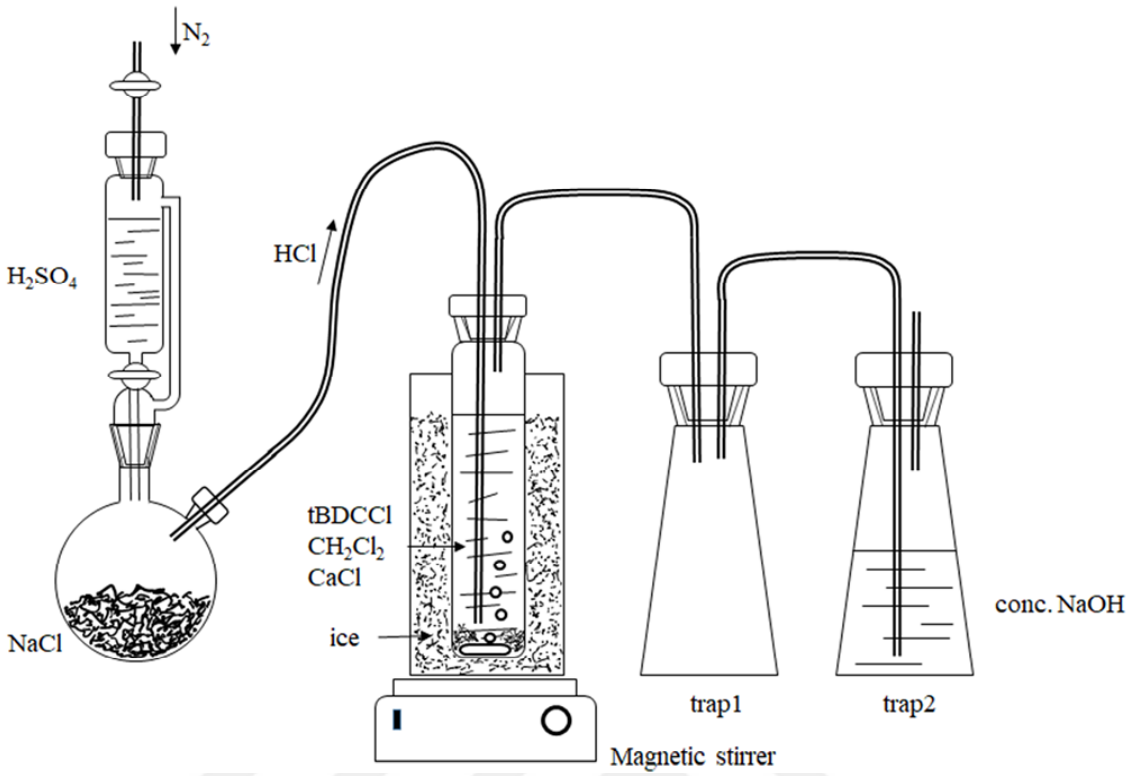

Figure 3.1. Hydrochlorination set up.

Figure 3.2. 5-tert-butyl-1,3-dicumyl chloride (TBDCC) cationic initiator.

Figure 3.3. High vacuum line used in cationic polymerizations.

Figure 3.4. In situ quenching of living PIB chains with ATMS.

Figure 3.5. Lithium naphthalenide anionic initiator.

Figure 3.6. High vacuum line used in anionic polymerizations.

Figure 3.7. Preparation of potassium naphthalenide.

Figure 3.8. Diphenylmethylpotassium (DPMK).

3.2. Results and Discussion

3.2.1. Syntheses and Molecular Characterization of Hydroxyl Telechelic PIB and PSt

3.2.1.1. Synthesis of Carbocationic Initiator (TBDCC). The sterically hindered difunctional initiator, 5-tert-butyl-1,3-dicumyl chloride (TBDCC), was synthesized following the procedure described in the literature (Figure 3.9) [29], [117]. The hydrochlorination of the previously synthesized 5-tert-butyl-1,3-dicumyl alcohol (TBDCA) was carried out by bubbling HCl (g) into the ice-cooled solution of TBDCA in DCM.

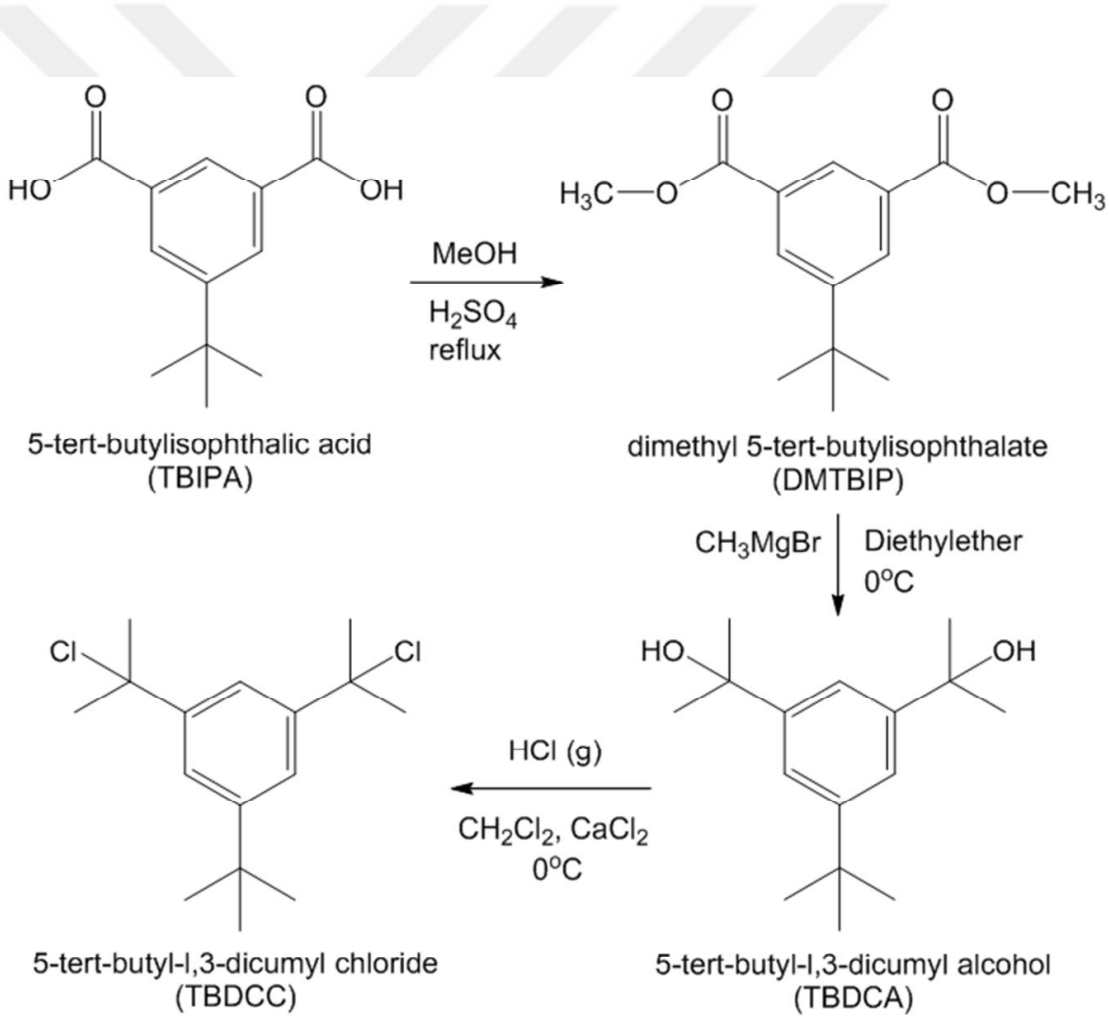

Figure 3.9. Synthesis of 5-tert-butyl-1,3-dicumyl chloride (TBDCC).

Figure 3.10 shows the ^{1}H NMR spectrum of TBDCC with the structure assignments. Resonances at 1.35 and 2 ppm are due to the methyl protons of the t-butyl and isopropyl groups, and those at 7.52-7.62 ppm are due to the aromatic protons.

The hydrochlorination of the cumyl alcohol using HCl follows a substitution process (SN1). However, the formation of undesired exo-olefin products, resulting from dehydration of the cumyl alcohol through an elimination reaction (E1), may lead to contamination of the desired dicumyl chloride and hinder its use in polymerization. In the spectrum, a 4:3 integration ratio for the methyl protons of isopropyl and t-butyl groups, along with the absence of resonances centered at 5 and 5.35 ppm corresponding to the protons of the exo-olefin groups, confirms that quantitative conversion was achieved. TBDCC was obtained with high purity and yield.

TBDCC, in conjuction with $TiCl_4$ coinitiator, is known as an excellent initiating system for living isobutylene polymerization [26]. Due to its sterically hindered aromatic nature, TBDCC allows for initiation without intermolecular alkylation (indanyl rings) and exhibits very high initiation efficiencies. However, it is important to note that the prolonged storage of the initiator should be avoided, even in deep freeze conditions, as dehydrohalogenation of the cumyl halide through an elimination reaction may result in the formation of exo-olefin groups.

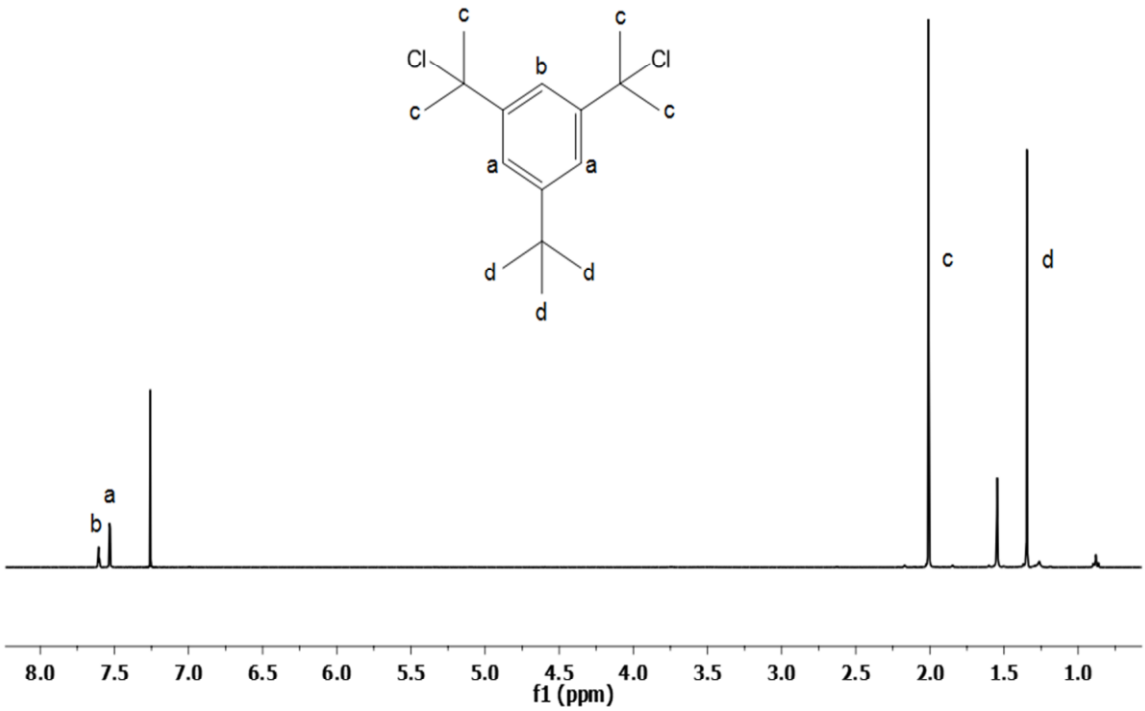

Figure 3.10. ^{1}H NMR spectrum of 5-tert-butyl-1,3-dicumyl chloride (TBDCC).

3.2.1.2. di-Hydroxyl Telechelic PIB (HO-PIB-OH). di-Allyl telechelic PIB (A-PIB-A) was synthesized with a very high allyl functionality (>99%) using the TBDCC/$TiCl_4$ initiating system, followed by quenching the living chain ends with ATMS. Next, regioselective hydroboration of the allyl functional chain ends with 9-BBN followed by alkaline hydrogen peroxide cleavage of carbon-boron bonds yields di-hydroxyl telechelic PIB (OH-PIB-OH).as illustrated in Figure 3.11.

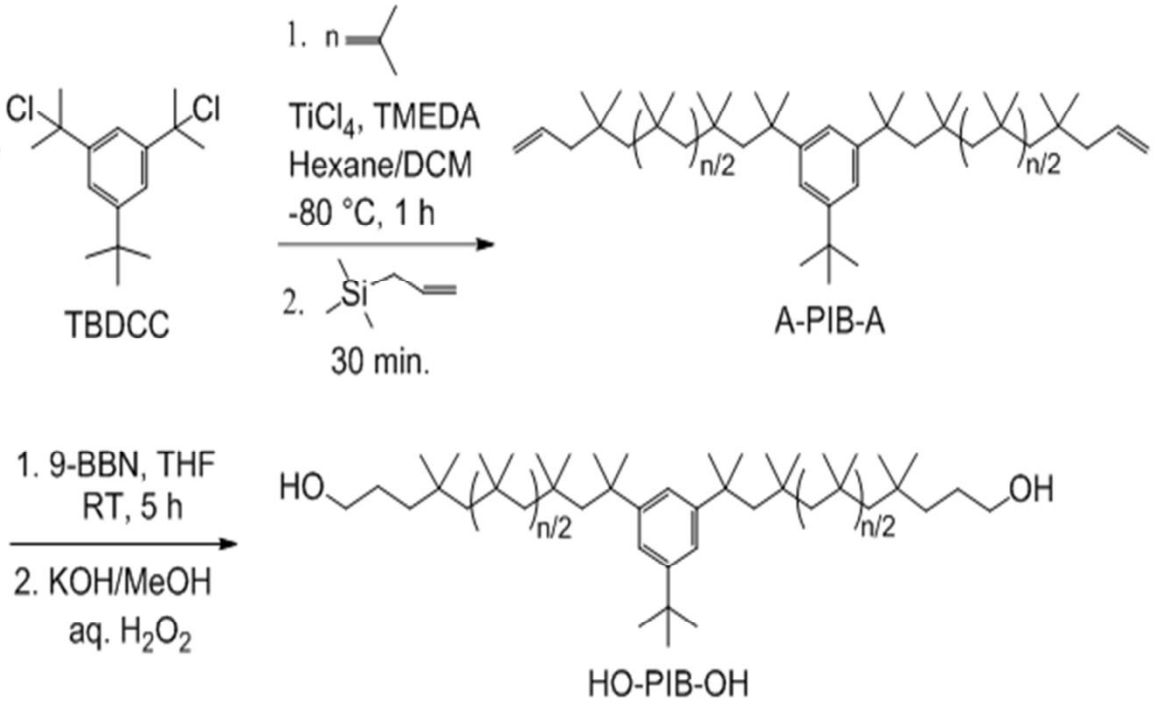

Figure 3.11. Synthesis of A-PIB-A and HO-PIB-OH.

Figure 3.12 shows the ^1H NMR spectrum of A-PIB-A with the structure assignments. The peaks between 1.03–1.22 ppm (peak e) and 1.35–1.46 ppm (peak d) belong to the methyl and methylene protons characteristic of the PIB backbone, respectively. The peak at 7.15 ppm (peak a, singlet) is due to the aromatic hydrogens of the initiator. The protons of the allyl group appear at 5.6–6.0 ppm (–CH_2–CH=CH_2, peak g, multiplet), 4.75–5.20 ppm (–CH_2–CH=CH_2, peak h, triplet), and 2.00 ppm (–CH_2–CH=CH_2, peak f, doublet). The integrated areas of the aromatic protons and the olefinic protons indicate quantitative chain end functionalization. The peak integrals of methyl protons of the PIB backbone and the aromatic protons were used to determine the number average molecular weight (M_n).

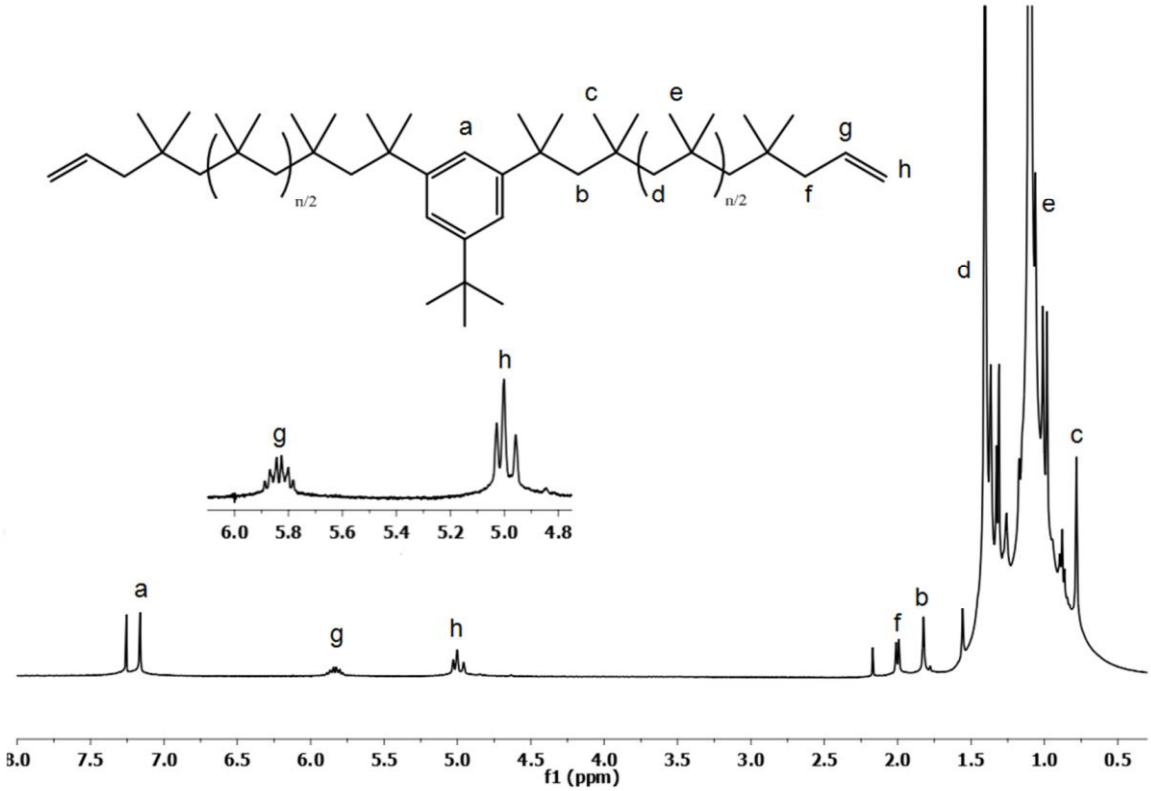

Figure 3.12. ^{1}H NMR spectrum of A-PIB-A.

Table 3.1 displays the molecular weight values determined from the ^{1}H NMR spectrum and SEC. The Mn value obtained from the ^{1}H NMR spectrum is consistent with the targeted molecular weight determined based on the monomer to initiator ratio. Since the average molecular weights and the PDI were determined using the calibration curve constructed with PSt anionic standards, the SEC values may deviate from the theoretical molecular weights. The synthesized polymer exhibits a monomodal molecular weight distribution with PDI=1.13 (Figure 3.13).

Table 3.1. Molecular weight data of di-allyl telechelic PIB.

Sample	$M_{n,NMR}$ (g/mol)	$M_{n,SEC}$ (g/mol)	$M_{p,SEC}$ (g/mol)	PDI_{SEC} (M_w/M_n)
A-PIB-A	3000[1]	3369[2]	3475	1.13

[1] calculated by ^{1}H NMR using the formula $[(A_e/6)/(A_a/3)] \times 56 + 133 + 82$, where A_e and A_a denote the integrated areas of the peaks e and a (Figure 3.12). The ratio gives the number of isobutylene repeating unit and 56 is the molecular weight of isobutylene. 133 and 82 are the masses added due to the initiator and the end groups (–$CH_2CH{=}CH_2$).

[2] used in the calculation for the synthesis of HO-PIB-OH.

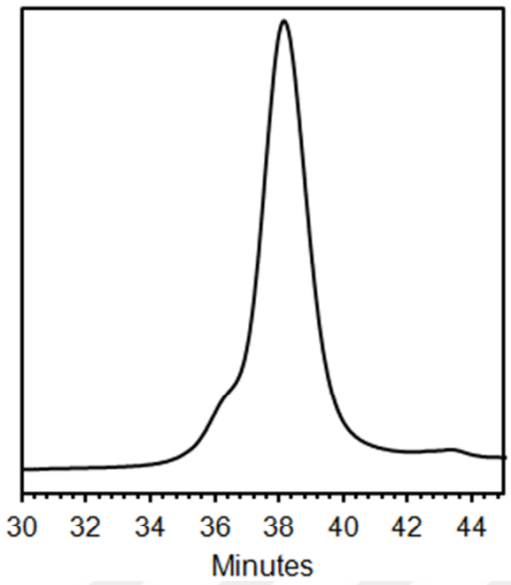

Figure 3.13. SEC trace of A-PIB-A.

The hydroboration-oxidation reaction is a powerful synthetic method that allows for the quantitative conversion of terminal olefins to primary alcohols [121]. The hydroboration of terminal alkenes using 9-BBN, a bicyclic dialkylborane, yields to terminal trialkylborane intermediate through a regioselective anti-Markovnikov addition. The trialkylboranes are known to be reactive toward oxygen and free radicals. In order to prevent side reactions, the reaction is carried out under an inert atmosphere. Subsequent alkaline oxidation of the trialkylborane intermediate cleaves the carbon-boron bonds, resulting in the corresponding primary alcohol and byproducts such as cyclooctane-1,5-diol and boric acid [122].

In the PU synthesis, the presence of these byproducts may have a detrimental effect as they alter the stoichiometry of the reactants. If not completely removed, the residual boric acid can act as a crosslinker. Chung et al. reported the presence of a high molecular weight shoulder in the SEC trace of the hydroxylated polymer after the hydroboration-oxidation reaction of 1,2-polybutadiene due to the formation of branching in the presence of boric acid [123]. In our experiments, poorly purified di-hydroxyl telechelic PIBs resulted in network formation during the prepolymerization step. This gelation can be explained by the presence of the residual boric acid. However, boric acid can be eliminated by complexation with methanol [123,124]. Additionally, cyclooctane-1,5-diol could not be entirely removed by washing with water and filtration, as it was observed to sublime under

reduced pressure (60 °C, $2x10^{-2}$ mmHg) during drying on the high vacuum line. Therefore, after the hydroxylation of A-PIB-A was carried out as described by Pasztoi et al. [119], the product was further purified by dissolving in hexane and precipitating three times into excess methanol.

The ^{1}H NMR spectrum of HO-PIB-OH, shown in Figure 3.14, provides the structure assignments. After the hydroboration-oxidation reaction, the peaks belonging to the protons of the allyl group (peak g,h, and f in Figure 3.12) completely disappear, while a new peak at 3.6 ppm (peak f, triplet) appears due to methylene protons adjacent to the newly formed hydroxyl group. The conversion of the allyl end groups, calculated from the integrals of the aromatic protons (peak a) and the methylene protons of –CH_2OH (peak f), is 97.3%. Complete conversion of the vinyl groups is crucial for successful chain extension with a diisocyanate to high molecular weight PUs. HO-PIB-OH, with such high hydroxyl functionality, serves as a good candidate for the synthesis of the PIB based PUs.

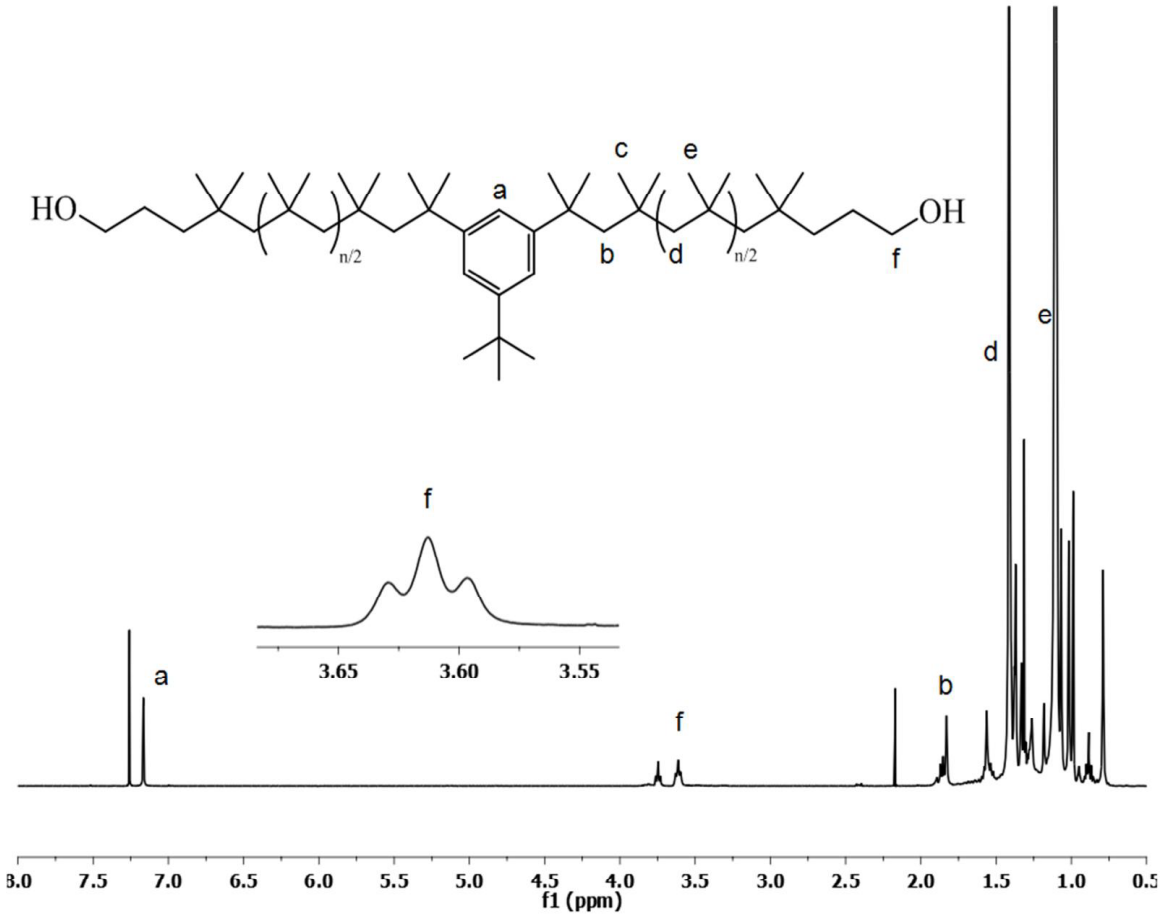

Figure 3.14. ^{1}H NMR spectrum of HO-PIB-OH.

Figure 3.15 shows the FTIR spectrum of HO-PIB-OH. The spectrum exhibits stretching vibrations of O–H and C–O at 3304 and 1058 cm^{-1}, respectively, while no absorptions at 3070, 1636, 993, and 911 are observed due to vinyl groups (–CH=CH_2), confirming the complete conversion of the vinyl end groups. Moreover, the characteristic absorption bands of the PIB backbone appear at 2949 and 2892 cm^{-1} corresponding to C–H stretching vibrations, and at 1470 and 1229 cm^{-1} corresponding to C–H bending vibrations. The peaks at 1388 and 1365 cm^{-1} are assigned to the swing of the two CH_3 groups, which are typical of PIB [125,126].

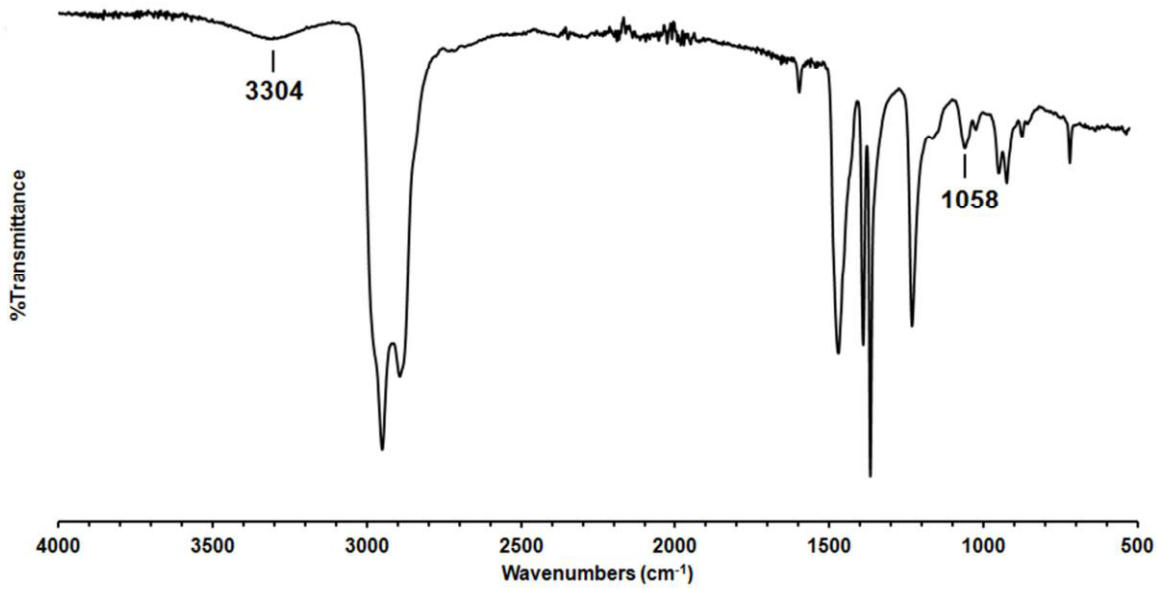

Figure 3.15. FTIR spectrum of HO-PIB-OH.

3.2.1.3. di-Hydroxyl Telechelic PSt (HO-PSt-OH). HO-PSt-OH was synthesized by anionic polymerization of styrene initiated by Li naphthalenide, and followed by quenching of the living chain ends with EO, as illustrated in Figure 3.16.

For this purpose, the Li naphthalenide, a dark green colored negatively charged radical anion formed via electron transfer in THF, was synthesized by reacting metallic Li with a slight excess of naphthalene at 0 °C under an Ar atmosphere [116]. The prepared Li naphthalenide was then used after filtration. The polymerization of styrene was carried out in cyclohexane at 0 °C using the Li naphthalenide initiator, resulting in bifunctional PStLi living chain ends. These living chain ends were subsequently reacted with EO over an ice bath. Since the ring-opening of EO in the presence of a Li counterion cannot propagate, the

overnight reaction at room temperature led to the addition of only one EO unit [61], [63]. The resulting product, HO-PSt-OH, was obtained after protonation with acidic methanol.

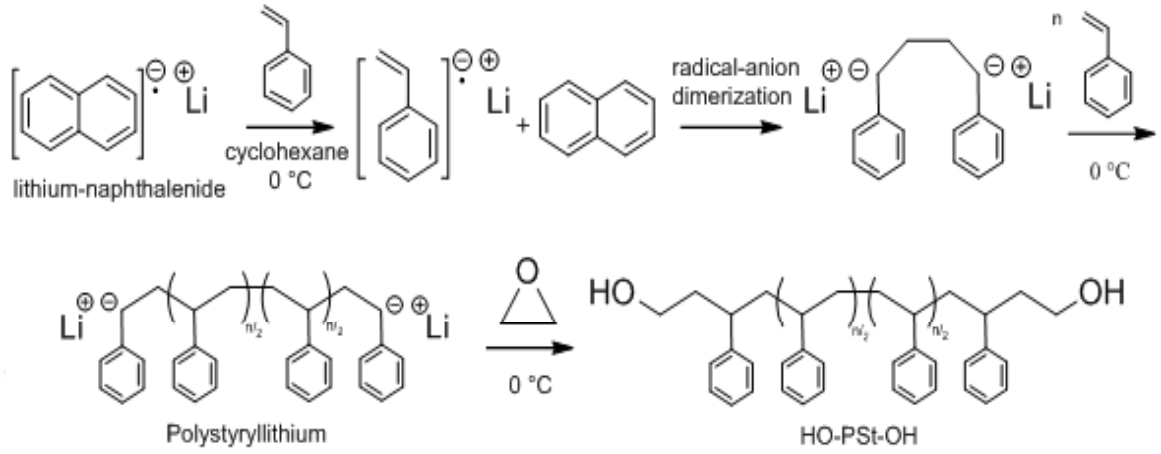

Figure 3.16. Synthesis of HO-PSt-OH.

Figure 3.17 shows the ^{1}H NMR spectrum of HO-PSt-OH with the structure assignments. In the spectrum, the signals corresponding to the aromatic protons (peak a and b) of the PSt appear between 6.2–7.25 ppm, while those for the methylene and methine protons of the backbone (peak c and d, respectively) appear between 1.2–2.6 ppm.

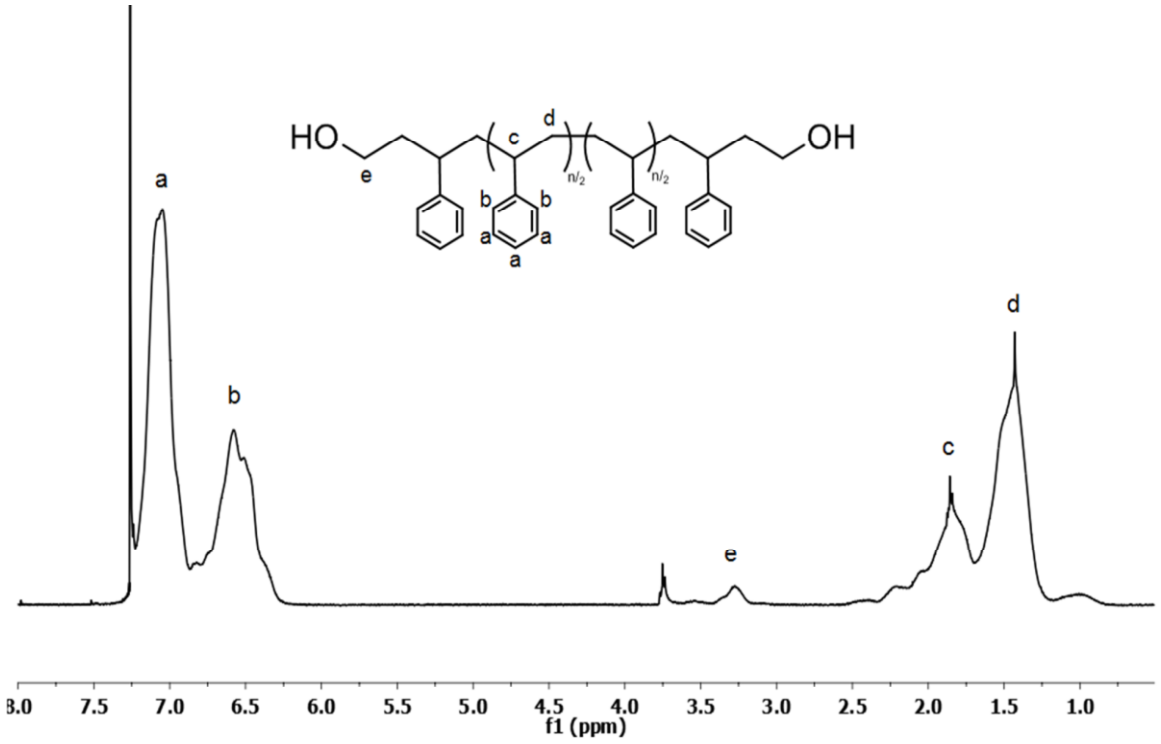

Figure 3.17. ^{1}H NMR spectrum of HO-PSt-OH.

The methylene protons (peak e, $-CH_2CH_2OH$) adjacent to the hydroxyl group are clearly observed between 3.17–3.42 ppm, indicating the successful end functionalization of the chain ends with EO. The number average molecular weight was determined based on the integrated areas of these protons in the alpha position to hydroxyl and the aromatic protons.

Table 3.2 shows the molecular weight values of HO-PSt-OH obtained from ^{1}H NMR and SEC analyses. The Mn value calculated by SEC calibrated against PSt standards was used as the actual molar mass. The SEC trace of the polymer exhibits a narrow monomodal molecular weight distribution with a PDI of 1.15, indicating that the polymerization and the chain end functionalization proceeded without significant side reactions (Figure 3.18).

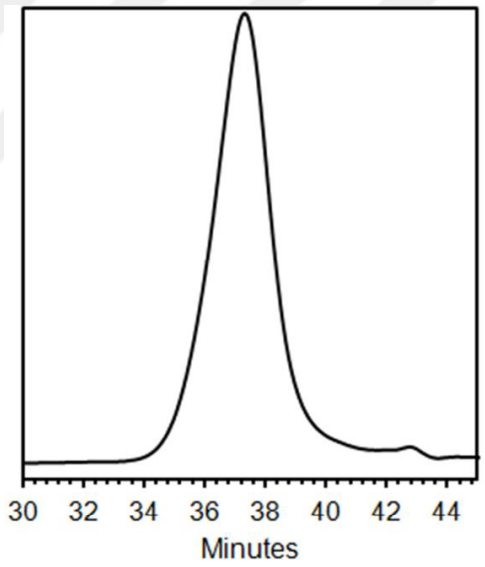

Figure 3.18. SEC trace of HO-PSt-OH.

Table 3. 2. Molecular weight data for HO-PSt-OH.

Sample	$M_{n,NMR}$ (g/mol)	$M_{n,SEC}$ (g/mol)	$M_{p,SEC}$ (g/mol)	PDI_{SEC} (M_w/M_n)
HO-PSt-OH	3436[1]	3965[2]	4073	1.15

[1] determined from ^{1}H NMR using the formula $M_n = [(A_{a+b}/5)/(A_e/4)] \times 104.15 + 90$, where A_{a+b} and A_e are the integrated areas of the protons assigned in Figure 3.17, and the ratio gives the number of styrene (104.15 g/mol) repeating unit. The mass of the end groups is 90 for an average functionality of 2.

[2] used in the calculation for the synthesis of the PSt PU.

3.2.2. Syntheses and Molecular Characterizations of OEO-b-PIB-b-OEO and OEO-b-PSt-b-OEO

3.2.2.1. Synthesis of OEO-b-PIB-b-OEO. OEO-b-PIB-b-OEO was synthesized following a method similar to the previously described for synthesizing PEO-b-PSt-b-PEO triblock copolymer by Zhang et al. [69]. For this purpose, the hydroxyl terminals of HO-PIB-OH were converted to the corresponding K alkoxides by deprotonation with DPMK. These alkoxides then served as a macroinitiator in the anionic ring-opening oligomerization of EO (Figure 3.19).

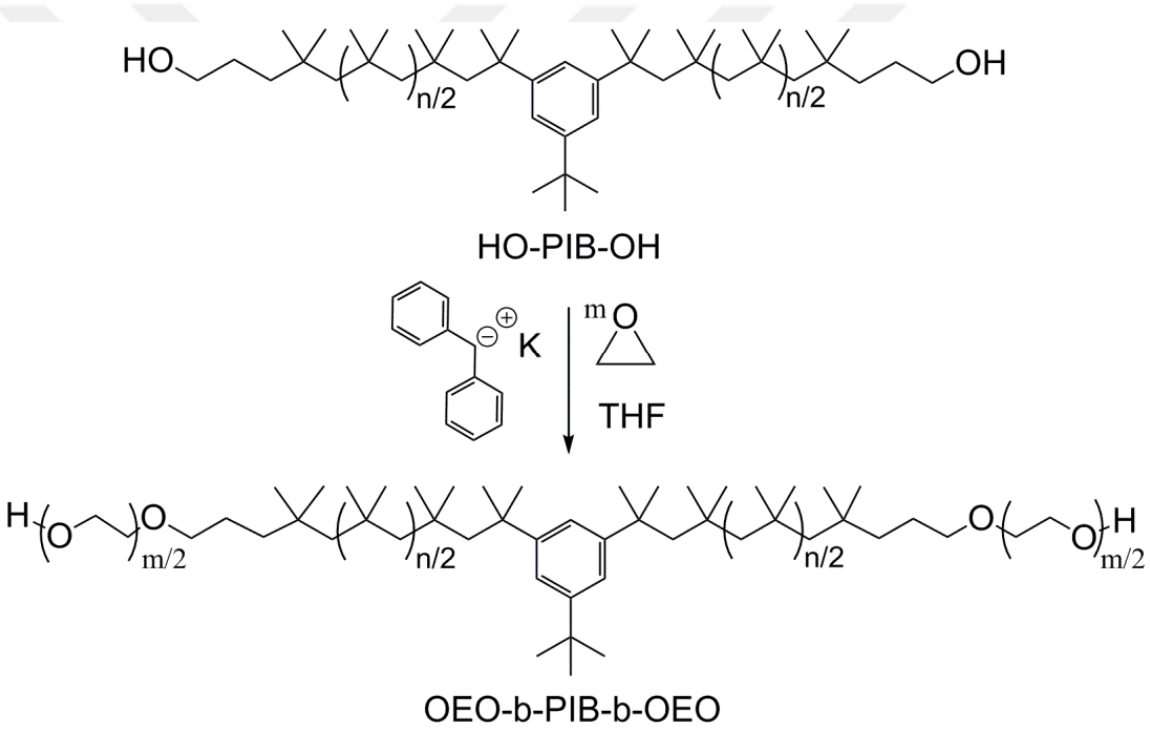

Figure 3.19. Synthesis of OEO-b-PIB-b-OEO.

DPMK was prepared as described in the literature [120] and used after filtration. To prepare DPMK, a glassware setup consisting of two flasks, flask A and B, connected by a bridge with a sintered glass filter in the middle, was assembled. In flask A, K-naphthalenide radical anions were allowed to react with DPM in THF at room temperature for a week. The resulting brown-red colored DPMK solution was then filtered through the sintered glass by applying overpressure of Ar on the flask A side and controlled vacuum on the flask B side. Upon the reaction with DPMK in THF, the color of the polymer solution turned yellow, which then faded to pale yellow after adding EO. The polymer was purified

by redissolving in hexane and precipitating in methanol twice to remove impurities such as DPM, naphthalene, and PEO.

Figure 3.20 shows the ^{1}H NMR spectrum of OEO-b-PIB-b-OEO with the structure assignments. In addition to the characteristic resonances of the PIB backbone (peaks a-e), the resonances observed at 3.3–3.8 ppm arise from the methylene protons of the EO repeating units (–CH_2CH_2O–, peak f). This indicates the successful formation of EO oligomeric block initiated by the K alkoxide terminals.

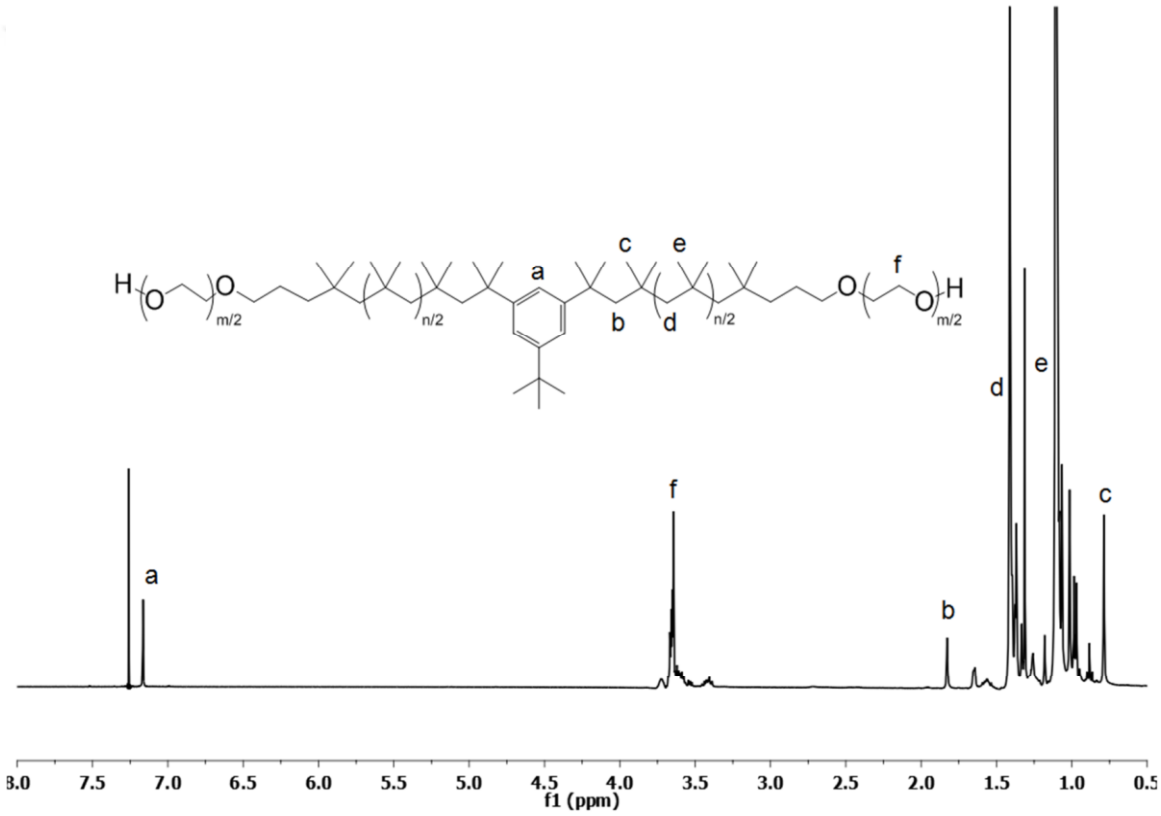

Figure 3.20. ^{1}H NMR spectrum of OEO-b-PIB-b-OEO.

Table 3.3 summarizes the molecular weight data obtained from the SEC characterization using THF as the eluent and ^{1}H NMR. It is a well-known phenomenon that when amphiphilic copolymers are dissolved in a solvent selective for one block, the association of the molecules into micellar structures occurs [127,128]. Therefore, the molecular weight data obtained from SEC in THF, which selectively dissolves the PIB block, cannot represent the actual weight of OEO-b-PIB-b-OEO. However, as the weight of the PIB block ($M_{n,SEC}$) was known, the actual weight of the EO block was calculated

from the integrated areas of the peaks f and e (Figure 3.20) according to the equation given in Table 3.3. The weight of the EO block was found to be 327 g/mol, indicating that an average of 7.4 EO units were added per chain. Consequently, the actual molecular weight of OEO-b-PIB-b-OEO was calculated by summing up the weights of the A-PIB-A precursor and EO block. Figure 3.21 presents the SEC chromatograms of OEO-b-PIB-b-OEO and the starting polymer. After modification, the increase in molecular weight of OEO-b-PIB-b-OEO compared to that of A-PIB-A and a narrow monomodal molecular weight distribution (PDI = 1.15) prove that the precursor efficiently initiates the anionic ring-opening reaction of EO.

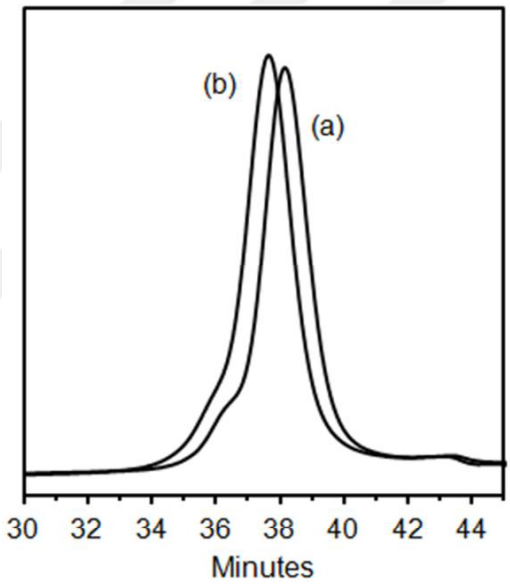

Figure 3.21. SEC traces of starting polymer (a) A-PIB-A and (b) OEO-b-PIB-b-OEO.

Table 3.3. Molecular weight data for OEO-b-PIB-b-OEO.

Sample	$M_{n,SEC}$ (g/mol)	$M_{p,SEC}$ (g/mol)	PDI_{SEC} (M_w/M_n)	$M_{n,SEC}$ PIB block (g/mol)	$M_{n,NMR}$ EO block (g/mol)	M_n (g/mol)
OEO-b-PIB-b-OEO	4045	4211	1.15	3369	327[1]	3696[2]

[1] determined from ^{1}H NMR using the equation:

M_n(EO block) = [(A_f/4) x (3369/56)] / (A_e/6) × 44 = 327 g/mol, where A_f and A_e, respectively, are the integrated areas of the methylene protons of the EO and the methyl protons of the isobutylene repeating units. 44 is the molecular weight of EO.

[2] calculated by using the formula M_n(OEO-b-PIB-b-OEO) = $M_{n,SEC}$ (A-PIB-A) + $M_{n,NMR}$(EO block) and used in the calculations for the synthesis of the corresponding PUs.

FTIR characterization provides further evidence for the addition of EO units. Figure 3.22 presents the FTIR spectra of HO-PIB-OH and OEO-b-PIB-b-OEO. Besides, the vibrations typical of the PIB backbone at 2951 and 2887 cm^{-1} for C–H stretching, at 1462 and 1230 cm^{-1} for C–H bending, and at 1388 and 1365 cm^{-1} for CH_3 swing, the stretching vibrations of O–H and C–O–C ascribed to the EO moieties can be observed at 3406 and 1065 cm^{-1}, respectively.

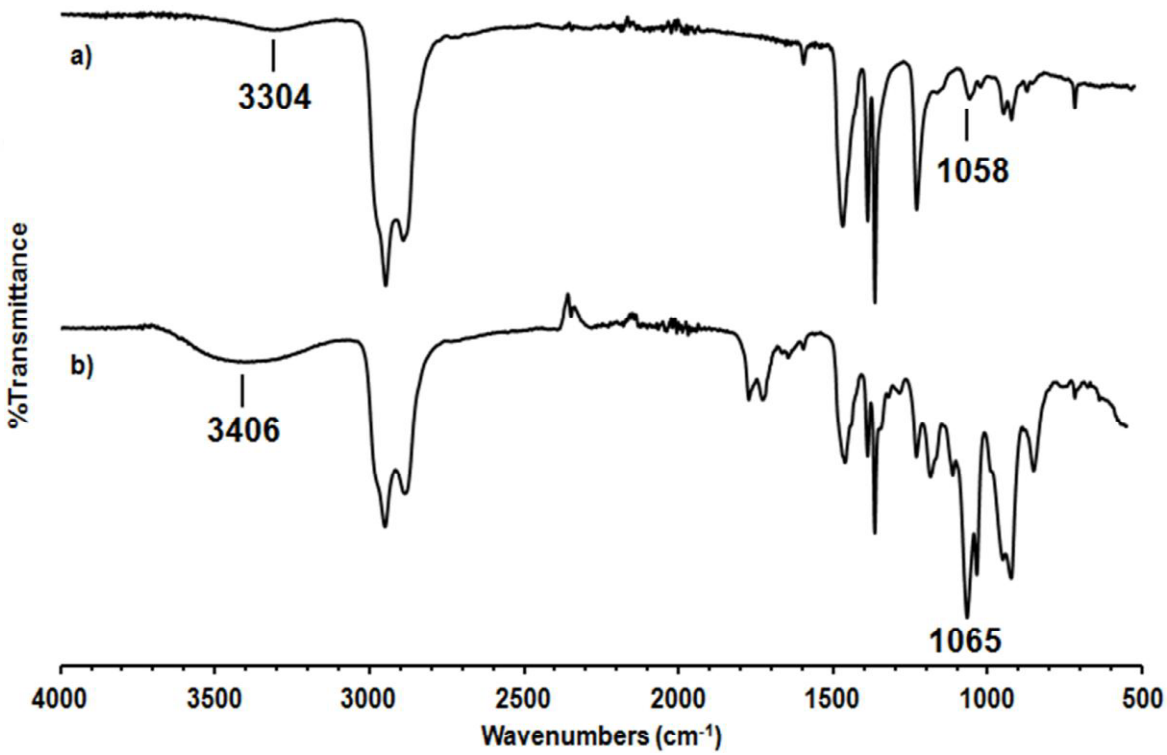

Figure 3.22. FTIR spectra of (a) HO-PIB-OH and (b) OEO-b-PIB-b-OEO.

3.2.2.2. Synthesis of OEO-b-PSt-b-OEO. For the synthesis of OEO-b-PSt-b-OEO, two initial trials were carried out using the K naphthalenide initiated sequential anionic polymerizations of St and EO in cyclohexane and toluene at 0 °C. The initiator was prepared in THF and filtered prior to the polymerizations to remove unreacted K metal. However, these reactions yielded ill-defined products with molecular weights higher than predicted and broad molecular weight distributions.

In the first trial, two remarkable phenomena were observed. Firstly, during the growth of the PSt block in cyclohexane, an efficient stirring of the solution at 0 °C could not be achieved. Therefore, the reactor was removed from the ice bath and stirred at room

temperature for 3h. Apparently, at the studied concentration of K naphthalenide (5×10^{-3} mol in 7 ml THF / 140 ml cyclohexane), PStK (3.5×10^{-2} M chain end) was not soluble in cyclohexane at 0 °C and precipitation took place. Upon heating to room temperature, however, the precipitate was dissolved. This observation is in line with previous studies. Roovers and Bywater studied the effects of counter ions (K, Rb, and Cs) in the anionic polymerization of styrene in cyclohexane at 40 °C [129]. For Rb and Cs counter ions, the solubility of polystyryl chain ends was found to be limited to 7×10^{-4} M and 1.5×10^{-4} M, respectively. For K, the propagation rate was reported to be first order in PStK at low concentrations ($2\text{-}5\times10^{-5}$ M), but the order decreased due to the association of active centers to dimer at higher concentrations [129]. Therefore, the precipitation we observed at 0 °C could be attributed to the association phenomena in hydrocarbons resulting from high active center concentrations. Furthermore, THF from the initiator solution might have also changed the polarity of the medium and decreased the propagation rate.

Secondly, the viscosity of the solution changed dramatically upon the addition of EO, and a gel formation was observed, which immediately ceased the magnetic stirring bar. Therefore, the reaction proceeded for 4 days in a heterogenous reaction medium. The associates break down upon introduction of acidic MeOH, as reported in the literature. This significant increase in the viscosity can be explained by the fact that alcoholate chain ends tend to associate ($–CH_2O^-$, Mt^+) due to high charge density on the anion [59], [130]. SEC characterization of the product revealed a bimodal molecular weight distribution with a PDI of 1.65 ($M_{n\ targeted}$ = 5200 g/mol, $M_{n\ SEC}$ = 20300 g/mol).

The second trial was performed in toluene. Compared to the first trial, no precipitation was observed during the growth of the PSt block at 0 °C for 1 h. Interestingly, no increase in the viscosity after the addition of EO was observed either, suggesting that the ring opening polymerization of EO by the polystyryl chain ends was unsuccessful. The Mn values for the final product and the PSt block were determined from SEC as 11700 and 11400 g/mol, respectively, indicating the addition of about 7 EO units per chain. However, ^{1}H NMR, which is more reliable than SEC for characterizing the EO block, indicated the addition of only two EO units per chain. The discrepancy between the targeted and experimental values of the PSt block, which are 4000 and 11400 g/mol, respectively, could be attributed to incomplete initiation by K naphthalenide in toluene.

Consequently, we decided to carry out the synthesis in two steps utilizing the DPMK deprotonating agent guided by the fact that the rate of proton exchange between the OH group and the alkoxide is rapid compared to the rate of EO polymerization, enabling an efficient initiation [120], [131]. Partial deprotonation of OH-PSt-OH dissolved in THF transformed the hydroxyl terminals into polystyryl alkoxides, which initiated the anionic ring-opening oligomerization of EO, as shown in Figure 3.23. The reaction proceeded in a homogenous solution without any gel formation.

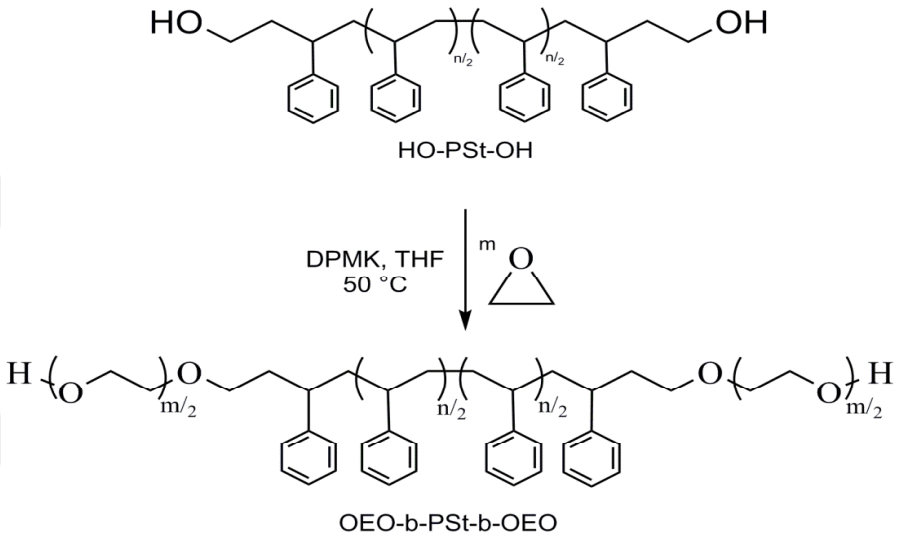

Figure 3.23. Synthesis of OEO-b-PSt-b-OEO.

Figure 3.24 shows the ^{1}H NMR spectrum of OEO-b-PSt-b-OEO with the structure assignments. Besides the characteristic aliphatic and aromatic proton resonances of PSt observed between 1.2–2.6 ppm (peaks c and d) and 6.2–7.25 ppm (peaks a and b), respectively, the resonances appeared at 3–3.8 ppm are attributed to the methylene protons of the EO repeating units (—CH_2CH_2O—, peak f). This indicates a successful ring-opening oligomerization of EO initiated by the polystyryl alkoxide macroinitiator.

The formation of the EO block was also confirmed by the FTIR analysis. In the spectrum of OEO-b-PSt-b-OEO (Figure 3.25 b), the peak appeared at 1105 cm^{-1} is due to the C—O—C stretching vibrations of the EO units. The absorption peaks of the PSt block appeared at 3000–3100 and 1600–1430 cm^{-1} belong to =C—H and C=C aromatic stretching vibrations, respectively. The peaks at 2800-3000 cm^{-1} are due to C—H aliphatic stretching vibrations [126].

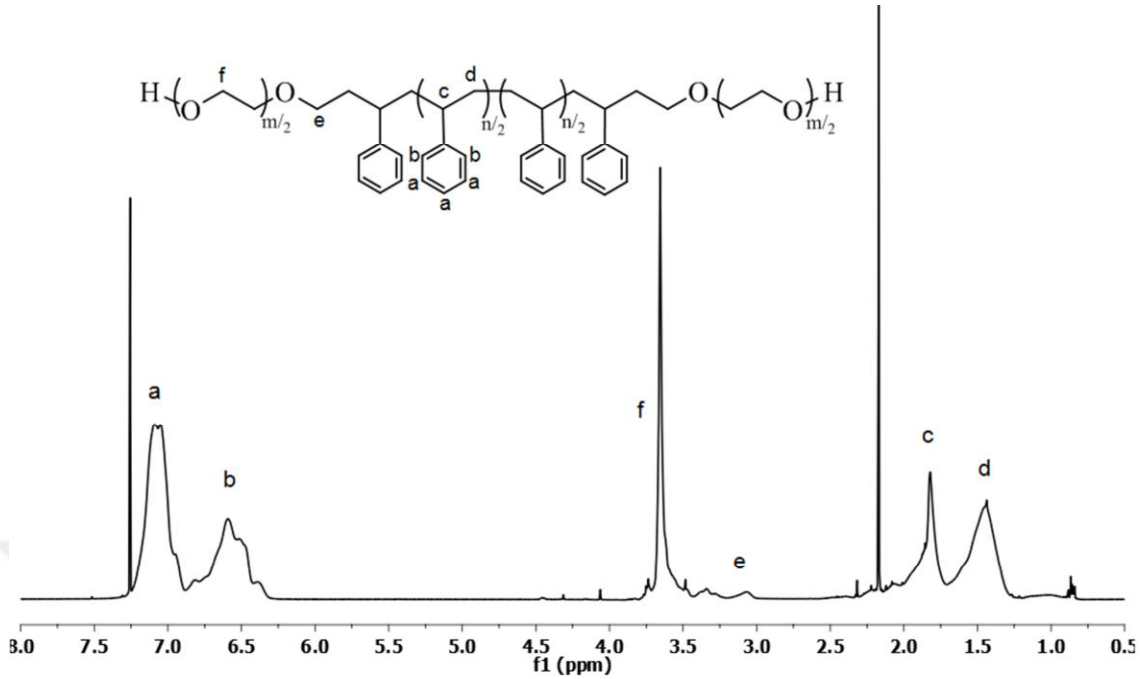

Figure 3. 24. ^{1}H NMR spectrum of OEO-b-PSt-b-OEO.

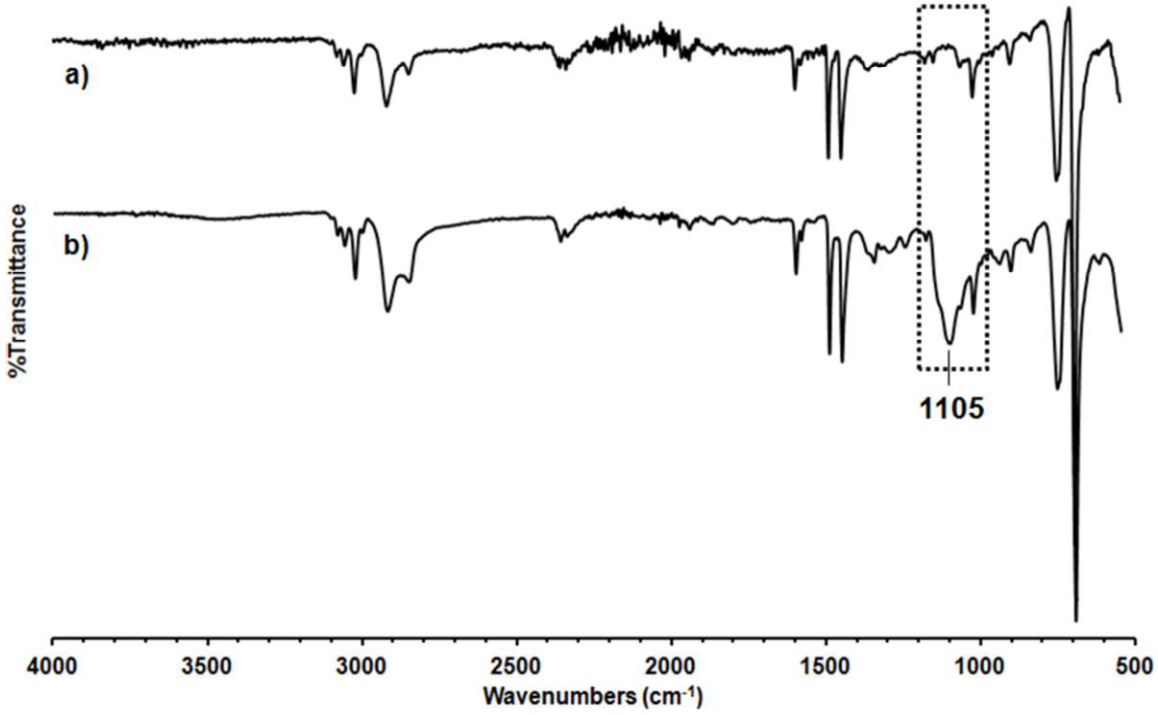

Figure 3. 25. FTIR spectra of (a) HO-PSt-OH and (b) OEO-b-PSt-b-OEO.

Table 3.4 presents the molecular weight data of OEO-b-PSt-b-OEO determined from SEC and ^{1}H NMR, as well as the SEC data of the precursor HO-PSt-OH. The SEC chromatogram of OEO-b-PSt-b-OEO exhibits a narrow monomodal peak with a PDI of

1.15 (Figure 3.26). Compared to the precursor, the peak appears at a lower elution time without any trace of the precursor. However, THF is a selective solvent for the PSt block and hence, OEO-b-PSt-b-OEO would be expected to form micelles in THF given it's amphiphilic nature. Therefore, the Mn obtained from SEC using THF as the eluent may deviate from the actual value [69], [131]. The Mn of the EO block was determined from ^{1}H NMR using the integrated areas of the peaks a, b, and f, and the Mn of the PSt precursor from SEC, according to the formula given in Table 3.4. The Mn of the EO block was found to be 608 g/mol meaning that about 14 EO units were added per chains. Consequently, the actual Mn of OEO-b-PSt-b-OEO was found to be 4573 g/mol by summing up the Mn values of the PS and EO blocks.

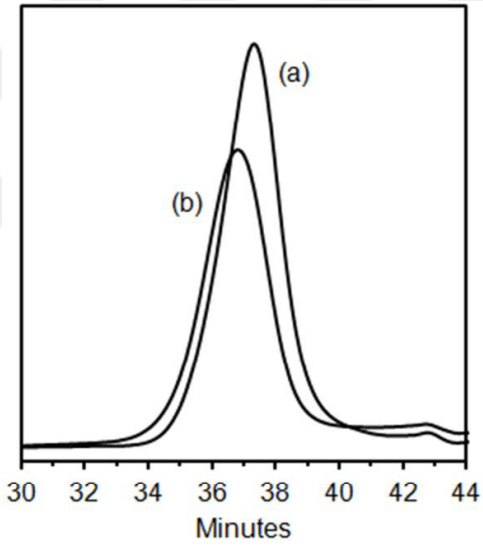

Figure 3.26. SEC traces of (a) HO-PSt-OH and (b) OEO-b-PSt-b-OEO.

Table 3.4. Molecular weight data of OEO-b-PSt-b-OEO.

Sample	$M_{n,SEC}$ (g/mol)	$M_{p,SEC}$ (g/mol)	PDI_{SEC} (M_w/M_n)	$M_{n,SEC}$ PS block (g/mol)	$M_{n,NMR}$ EO block (g/mol)	M_n (g/mol)
HO-PSt-OH	3965	4073	1.15			
OEO-b-PSt-b-OEO	4813	4938	1.14	3965	608[1]	4573[2]

[a] determined from ^{1}H NMR using the equation:

M_n(EO block) = [(A_f/4) x (3965/104.15)] / (A_{a+b}/5) × 44 = 608 g/mol, where Af and Aa+b, respectively, are the integrated areas of the methylene protons of the EO and the aromatic protons of the styrene repeating units. 104.15 and 44 are the molecular weights of St and EO, respectively.

[b] calculated by using the formula M_n(eoPSteo) = $M_{n,SEC}$ (HO-PSt-OH) + $M_{n,NMR}$(EO block) and used in the calculations for the synthesis of the corresponding PUs.

3.2.3. Syntheses and Characterizations of PIB Based PUs

3.2.3.1. PIB PU. In a recent study, Deodhar et al. reported the synthesis of PIB PU with the molecular weight (Mn>100000 Da) and mechanical properties (32 MPa ultimate strength, 630% elongation) that could not be achieved before for the PIB based PUs [132]. The study highlighted the importance of the use of highly purified reagents, particularly isocyanates. Isocyanates, being very reactive functional groups, were shown to contain dimeric, oligomeric and polymeric ureas depending on their shelf life. ^{1}H NMR spectra of the as-received and distilled MDI after weeks of storage at -12 °C revealed the presence of peaks between 7.42-7.52 ppm due to the aromatic protons ortho and meta positions to the urea impurities. A comparison of the properties of PUs synthesized using as-received and pretreated MDI showed that the impurities change the stoichiometric balance, leading to PUs with lesser properties [132]. Considering the polymerization proceeds through a step growth manner, achieving a precise stoichiometry of the reagents is crucial for obtaining high molecular weight PUs.

In our work, the purifications of the reagents were precisely accomplished to get well-defined PUs. MDI was vacuum distilled (at $2x10^{-2}$ mbar and ~135 °C) and kept under N_2 atmosphere. Its ^{1}H NMR spectrum (Appendix A.1) exhibited practically negligible peaks at 7.42-7.52 ppm due to the urea impurities. PIB PU was prepared using the two-step synthesis route. The synthesis strategy was shown in Figure 3.27. First, the prepolymer with terminal isocyanates was synthesized by reacting HO-PIB-OH with stoichiometric excess of MDI using DBTDL catalyst (0.1 mol% with respect to MDI) in THF. Then, the prepolymer was chain extended to higher molecular weights upon the addition of BDO. Generally, the soft and hard segments of PUs and polyureas widely differ in solubility parameter. Therefore, finding a good solvent is a determining factor in obtaining PUs with optimum properties [133]. This solubility difference is more profound for the PUs based on the highly nonpolar PIB soft segments whose solubility parameter is ~16.3 $(MPa)^{1/2}$ [84]. THF, with a solubility parameter of 18.6 MPa, was known to be a good solvent for polyureas based on the PDMS soft segment, which has a solubility parameter similar to that of PIB [133]. THF is also a good solvent for MDI/BDO based hard segments [134]. Therefore, we carried out all PU syntheses in THF at 65 °C.

The amounts of reagents were calculated using the equations

$$\frac{wt_{HO\text{-}PIB\text{-}OH}}{wt_{HO\text{-}PIB\text{-}OH} + wt_{MDI} + wt_{BDO}} = 0.7, \quad (3.1)$$

$$n_{HO\text{-}PIB\text{-}OH} + n_{BDO} = n_{MDI}, \quad (3.2)$$

where the wt% of PIB soft segment in PIB PU was 70% and n represented the number of moles. In all PU syntheses 70:30 wt ratio of soft to hard segment was maintained as 70% PIB renders the PU biostable and calcification resistant [132].

PIB PU was characterized by ^{1}H NMR and FTIR spectroscopy for structural analysis. Figure 3.28 presents the ^{1}H NMR spectrum and the corresponding assignments. The resonances at 8.74, 7.58 and 7.22 ppm were associated with pyridine-d5. The peaks confirming the formation of urethane bonds appeared at 4.35 and 4.23 ppm due to methylene protons (CH_2OCONH) coming from the soft segment (peak d) and BDO (peak h), and at 10.56 ppm due to NH proton (CH_2OCONH, peak p). The peaks at 7.87, 7.31, and 3.95 ppm were assigned to the aromatic protons (peak f and e) and methylene protons (peak g) of MDI, respectively. Besides, PIB related methylene and methyl protons (peak b and c) appeared between 1 and 2 ppm.

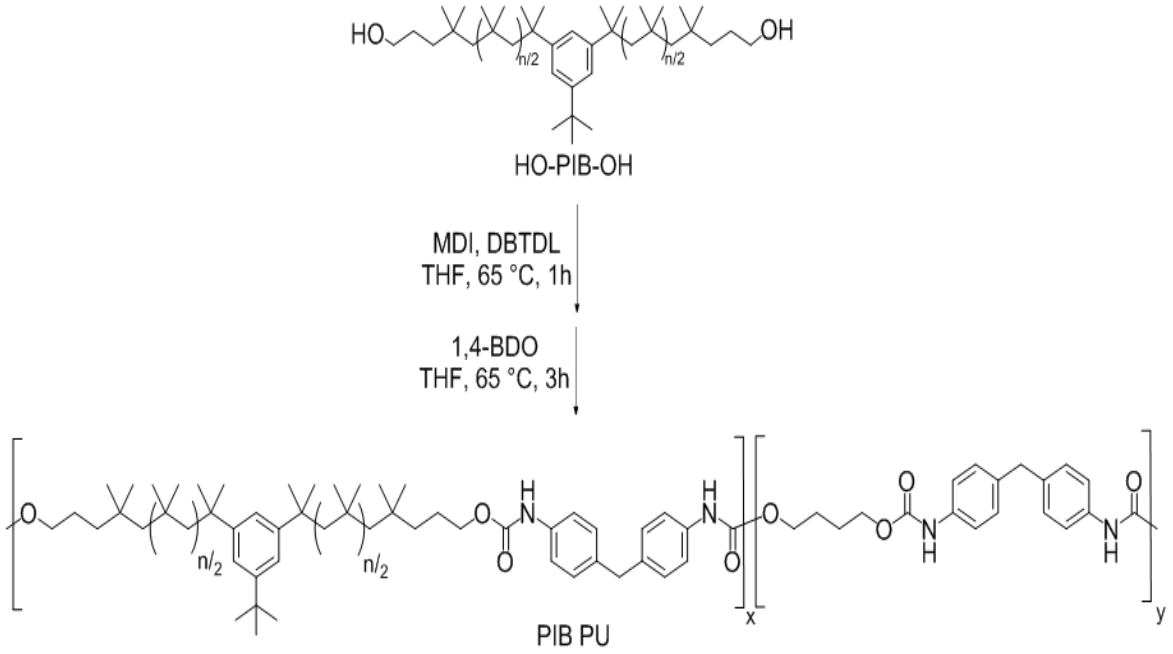

Figure 3.27. Synthesis of PIB PU.

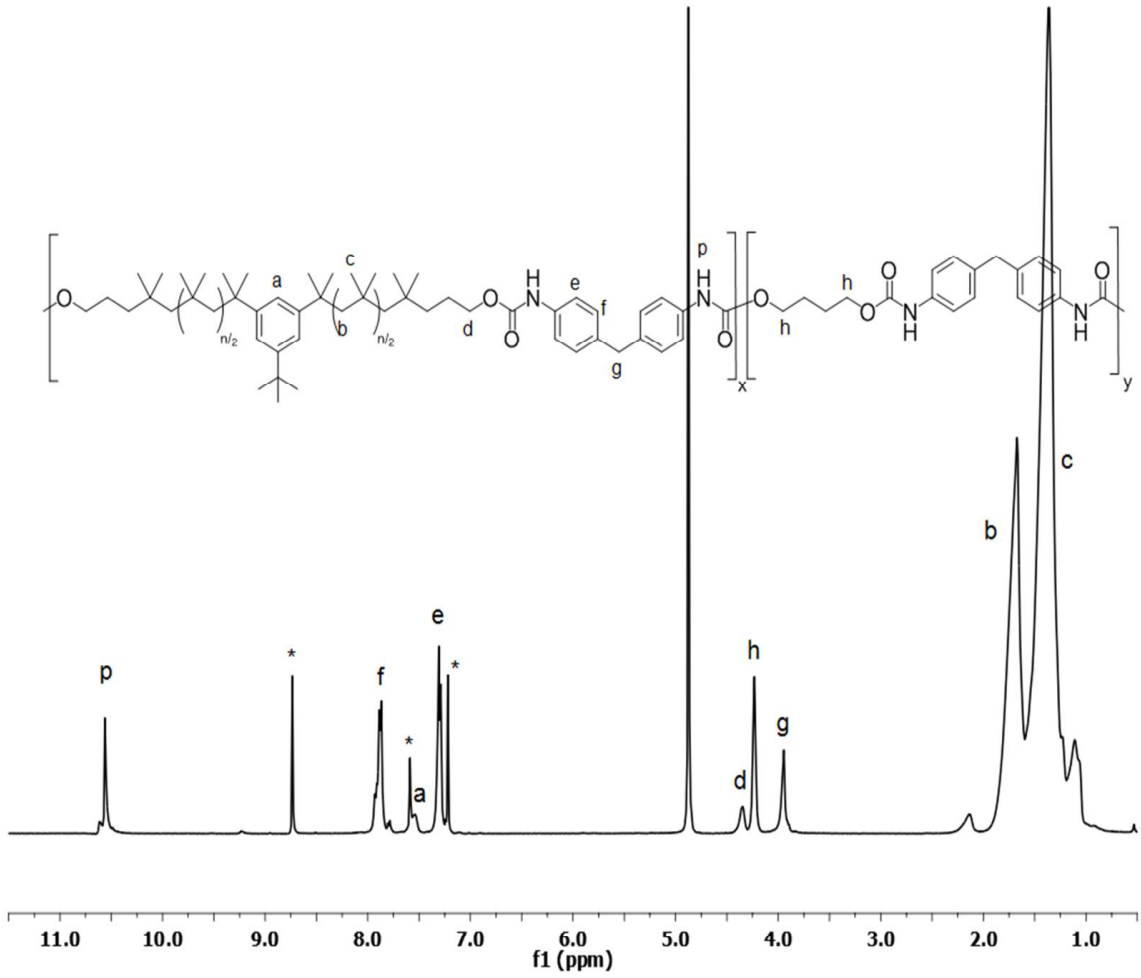

Figure 3.28. ^{1}H NMR spectrum of PIB PU in pyridine-d5. (*pyridine-d5)

Consistent with the ^{1}H NMR results, the FTIR spectrum of PIB PU (Figure 3.29), revealed the characteristic peaks of urethane linkage, i.e. stretching vibrations of C=O and NH groups. The band observed at 1700 cm^{-1} together with a higher frequency shoulder at 1735 cm^{-1} were assigned to H bonded and free C=O stretching vibrations, respectively. These results are in line with those of Toth et al. who showed that the C=O stretch in PIB based PU composed of overlapping bands of free (~1733 cm^{-1}) and H bonded (~1701 cm^{-1}) stretching vibrations [135]. This splitting phenomenon is not uncommon in PU chemistry, and especially for the polyether urethanes two distinct peaks can be detected for the bonded and free C=O groups [136]. In the spectrum, as reported also by Toth et al. [135], the H bonded NH absorption exhibited a prominent peak at 3326 cm^{-1}, while the free NH absorption was appeared as a weak peak at 3441 cm^{-1}. Other bands related to the hard segment included C=C stretching of the aromating rings at 1595 cm^{-1}, and overlaping NH bending and CN stretching at 1526 cm^{-1}, and COC stretching at 1080 cm^{-1}[136].

Furthermore, the bands related to the PIB soft segment were C–H stretching at 2950 and 2893 cm^{-1}, C–H bending at 1471 cm^{-1} and swing of the two CH_3 groups at 1388 and 1365 cm^{-1} [125,126].

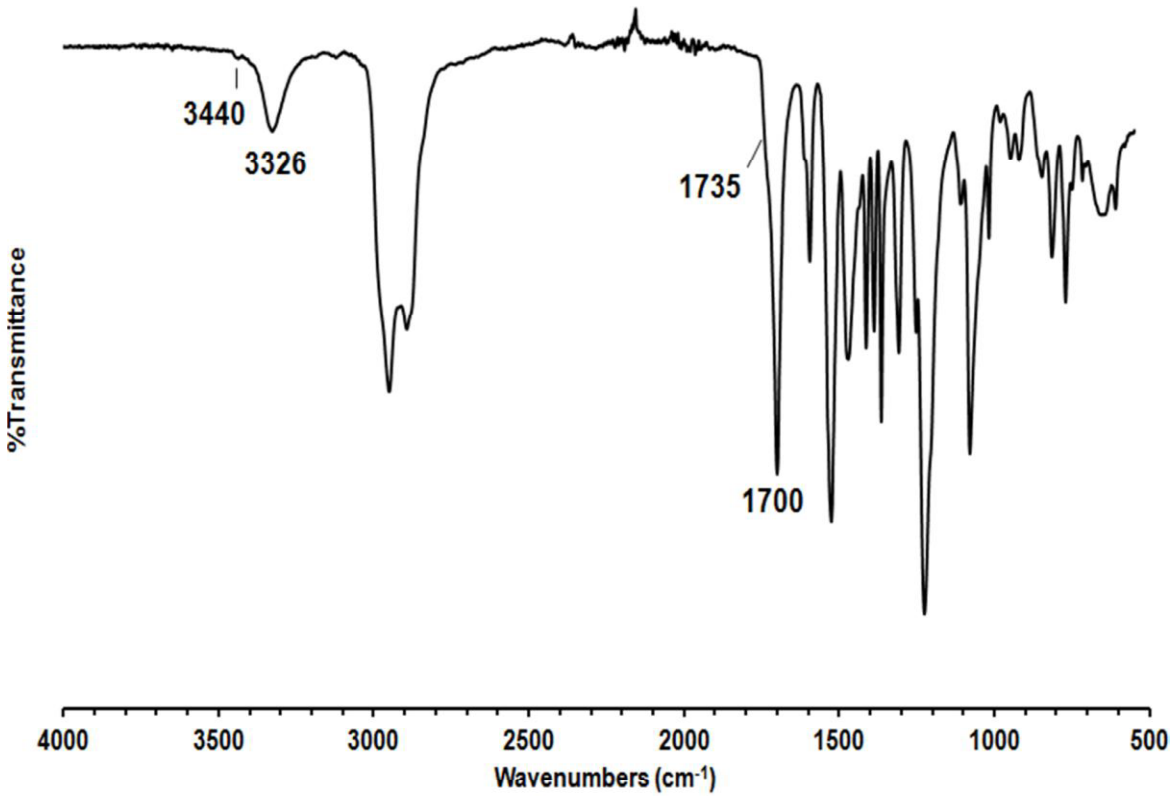

Figure 3.29. FTIR spectrum of PIB PU.

Table 3.5 presents the molecular weight data of PIB PU obtained from SEC. Compared to the starting polymer, HO-PIB-OH (Mn ~3369 g/mol), the Mn value for PIB PU (Mn 76029 g/mol) increased approximately 22 times. As evident in the SEC chromatograms (Figure 3.30), the peak maximum of PIB PU was located in the higher molecular weight region, while the peak originating from the unreacted starting polymer was negligible.

Table 3.5. Molecular weight data of PIB PU.

Sample	$M_{n,SEC}$ (g/mol)	$M_{p,SEC}$ (g/mol)	PDI_{SEC} (M_w/M_n)
PIB PU	76029	133989	1.99

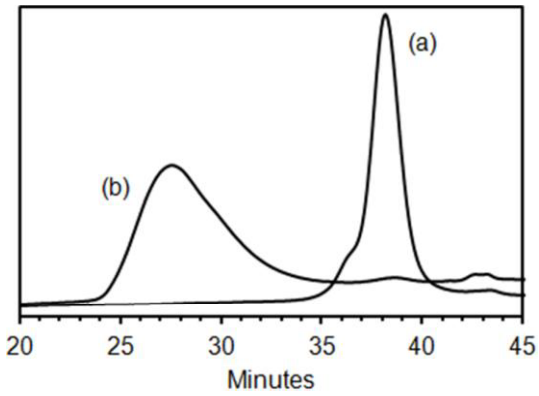

Figure 3.30. SEC traces of (a) A-PIB-A and (b) PIB PU.

3.2.3.2. OEO-b-PIB-b-OEO PU. Figure 3.31 outlines the synthesis strategy of OEO-b-PIB-b-OEO PU. It is a two-step synthesis involving the preparation of the prepolymer and the chain extension. In the first stage, the prepolymer was obtained from the reaction of OEO-b-PIB-b-OEO soft segment with a stoichiometric excess of MDI using DBTDL catalyst (0.1 mol% with respect to MDI). In the second stage, the prepolymer was allowed to react with BDO chain extender which resulted in an increase in the viscosity.

OEO-b-PIB-b-OEO PU was synthesized with the 70:30 wt ratio of soft to hard segment (MDI+BDO). Similar to PIB PU, the amounts of reagents were calculated using the equations

$$\frac{wt_{OEO\text{-}b\text{-}PIB\text{-}b\text{-}OEO}}{wt_{OEO\text{-}b\text{-}PIB\text{-}b\text{-}OEO} + wt_{MDI} + wt_{BDO}} = 0.7, \quad (3.3)$$

$$n_{OEO\text{-}b\text{-}PIB\text{-}b\text{-}OEO} + n_{BDO} = n_{MDI}, \quad (3.4)$$

where the wt% of OEO-b-PIB-b-OEO soft segment was 70% and the mole ratio of NCO to the total OH groups was one.

The ^{1}HNMR spectrum of OEO-b-PIB-b-OEO PU in pyridine-d5 is shown in Figure 3.32. The spectrum resembles to that of PIB PU with an additional peak at 3.66 ppm (peak m) due to EO units. The peaks associated with urethane linkages are observed at 4.34 ppm and 4.23 ppm, which can be attributed to the methylene protons (CH_2OCONH) originating from the soft segment (peak d) and BDO (peak h). The peak at 10.64 ppm (peak p) is due to NH proton of urethane groups (CH_2OCONH). The aromatic protons (peak f and e) and methylene protons (peak g) of MDI appear at 7.89, 7.32, and 3.95 ppm, respectively. The peaks observed between 1 and 2 ppm are the characterisctics methylene and methyl

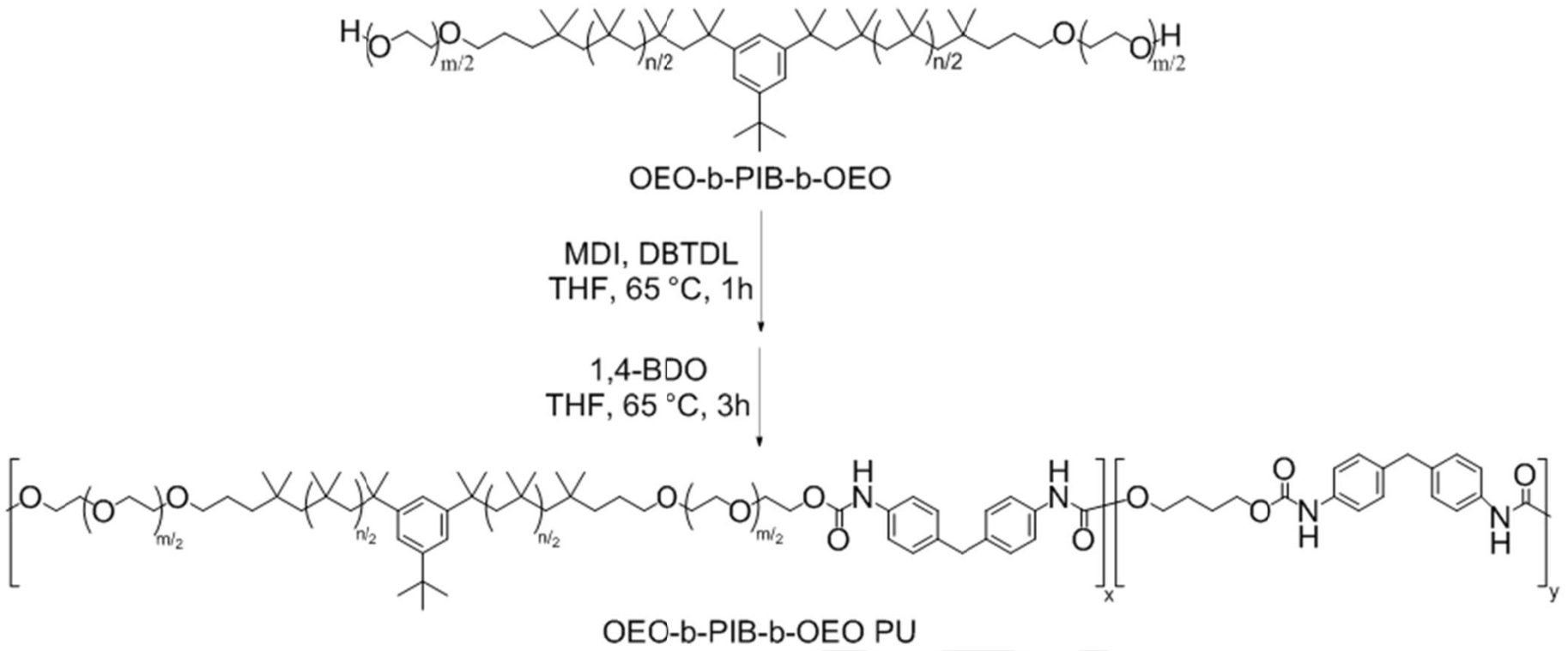

Figure 3.31. Synthesis of OEO-b-PIB-b-OEO PU.

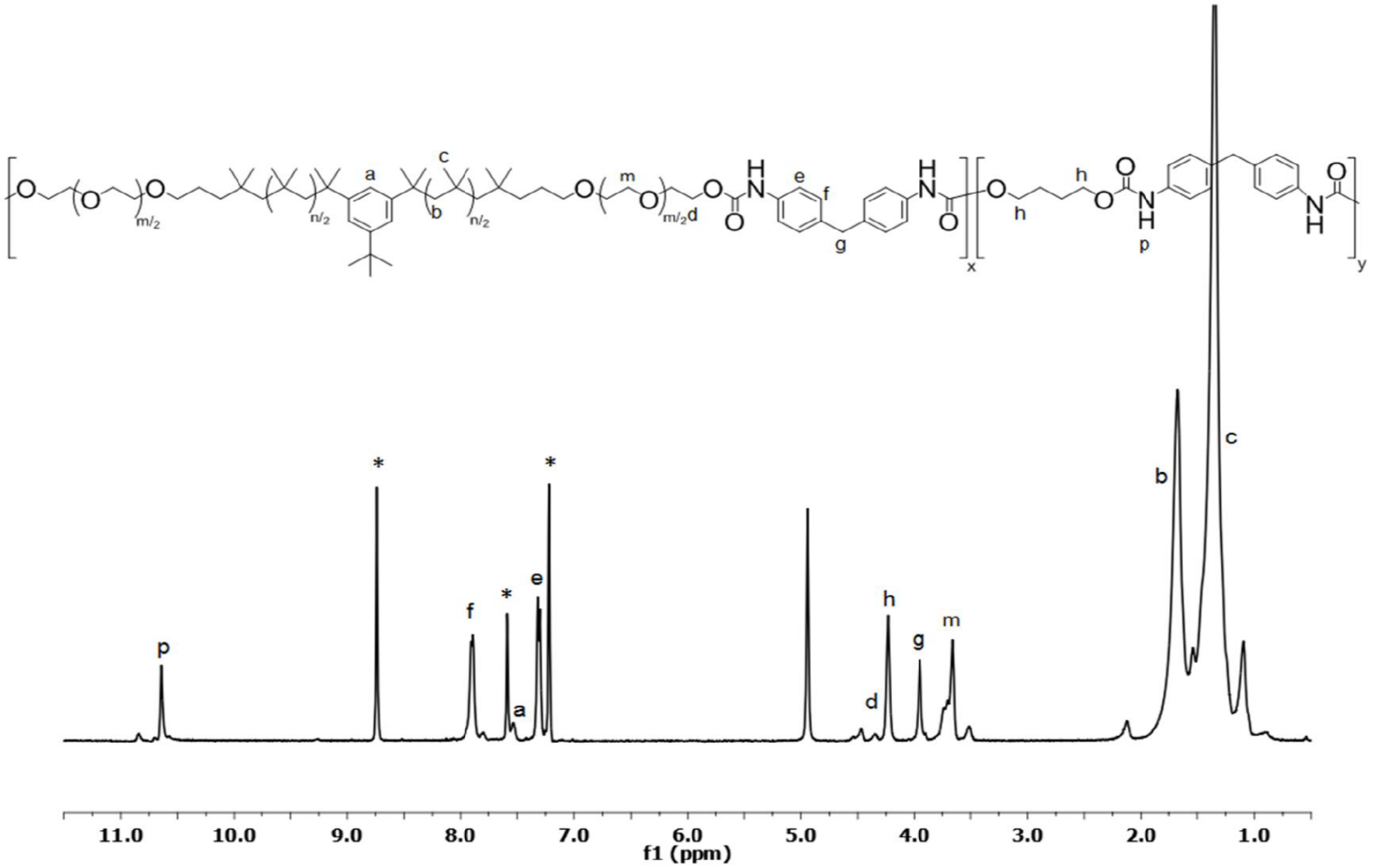

Figure 3.32. ^{1}H NMR spectrum of OEO-b-PIB-b-OEO PU in pyridine-d5. (*pyridine-d5)

protons (peak b and c) of the PIB. The peaks indicated with asterisk at 8.74, 7.58 and 7.22 ppm are associated with pyridine-d5.

Figure 3.33 presents the FTIR spectrum of OEO-b-PIB-b-OEO PU. The insert compares the spectra of PIB PU and OEO-b-PIB-b-OEO PU in the 800-1200 cm^{-1} range. For OEO-b-PIB-b-OEO PU, the band appearing at 1140 cm^{-1} can be ascribed to C–O–C stretching vibrations of EO units, as the aliphatic polyethers are known to absorb at 1150-1060 cm^{-1} region [126]. The peak at 1700 cm^{-1} and a higher frequency shoulder at 1730 cm^{-1} correspond to H bonded and free C=O stretching vibrations. In the NH stretching region, no band at 3440 cm^{-1} associated with free NH is observed, while the H bonded NH absorption peak is observed at 3324 cm^{-1}. The rest of the spectral features are the same with PIB PU as expected. These peaks can be listed as overlaping NH bending and CN stretching, and C–O–C stretching in urethane linkages at 1528 and 1080 cm^{-1}, respectively, and C=C stretching of the aromating rings at 1596 cm^{-1}. The bands associated with the soft segment are C–H stretching at 2950 and 2892 cm^{-1}, C–H bending at 1471 cm^{-1} and swing of the two CH_3 groups at 1388 and 1365 cm^{-1} [125,126].

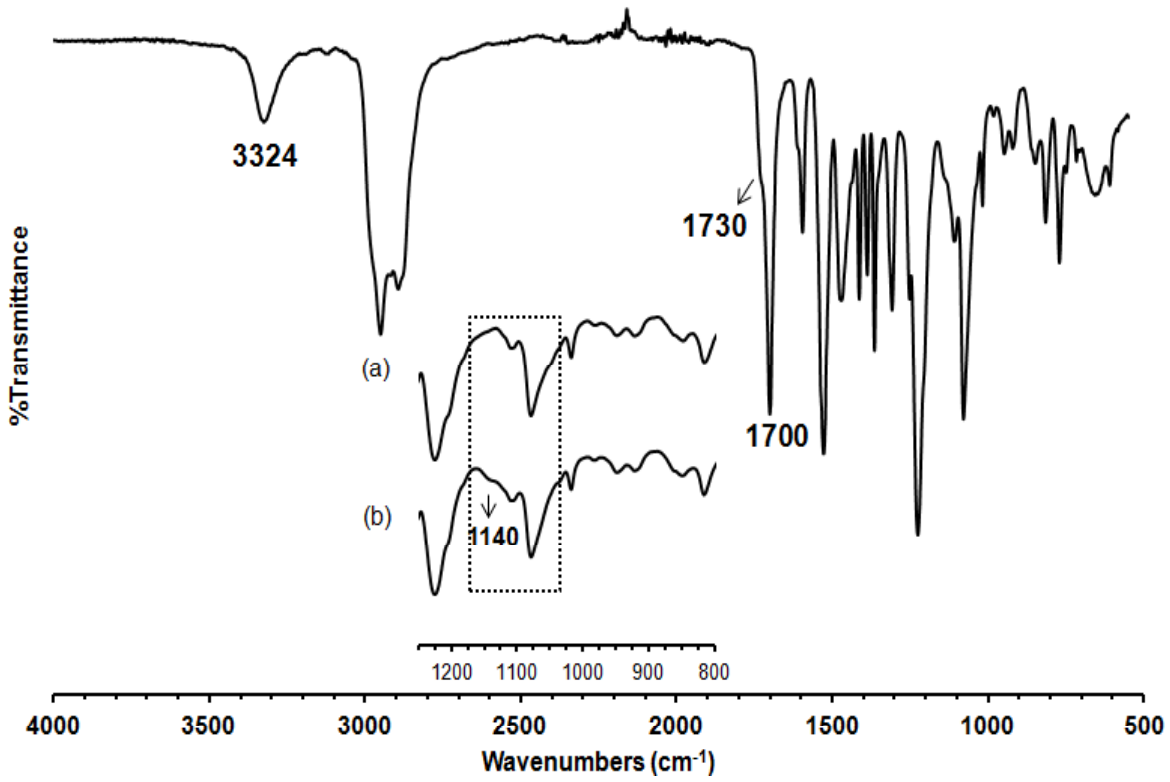

Figure 3.33. FTIR spectrum of OEO-b-PIB-b-OEO PU. Insert: Expanded 800-1200 cm^{-1} range for (a) PIB PU and (b) OEO-b-PIB-b-OEO PU.

The molecular weight data of OEO-b-PIB-b-OEO PU obtained from SEC is given in Table 3.6. Compared to the starting polymer, OEO-b-PIB-b-OEO (Mn 3696 g/mol), the Mn value for OEO-b-PIB-b-OEO PU (Mn 93013 g/mol) increased approximately 25 times. As evident in the SEC chromatograms (Figure 3.34), the peak maximum of PIB PU was located in the higher molecular weight region, while the peak originating from the unreacted starting polymer was negligible.

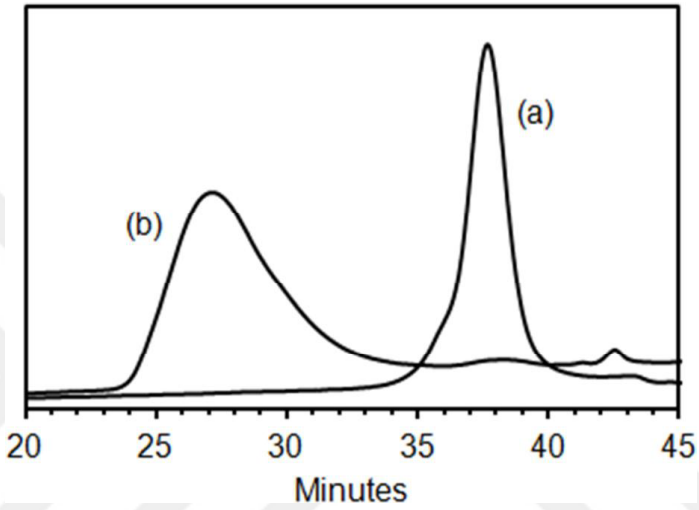

Figure 3.34. SEC traces of (a) OEO-b-PIB-b-OEO and (b) OEO-b-PIB-b-OEO PU.

Table 3.6. Molecular weight analysis data of OEO-b-PIB-b-OEO PU.

Sample	$M_{n,SEC}$ (g/mol)	$M_{p,SEC}$ (g/mol)	PDI_{SEC} (M_w/M_n)
OEO-b-PIB-b-OEO PU	93013	167150	2.02

3.2.4. Syntheses and Characterizations of PSt Based PUs

3.2.4.1. PSt PU. The synthesis strategy was shown in Figure 3.35. First, the prepolymer with terminal isocyanates was synthesized by reacting HO-PSt-OH with a stoichiometric excess of MDI in the presence of DBTDL catalyst (0.1 mol% with respect to MDI) in THF. Then, the prepolymer was chain extended to higher molecular weights upon the addition of BDO.

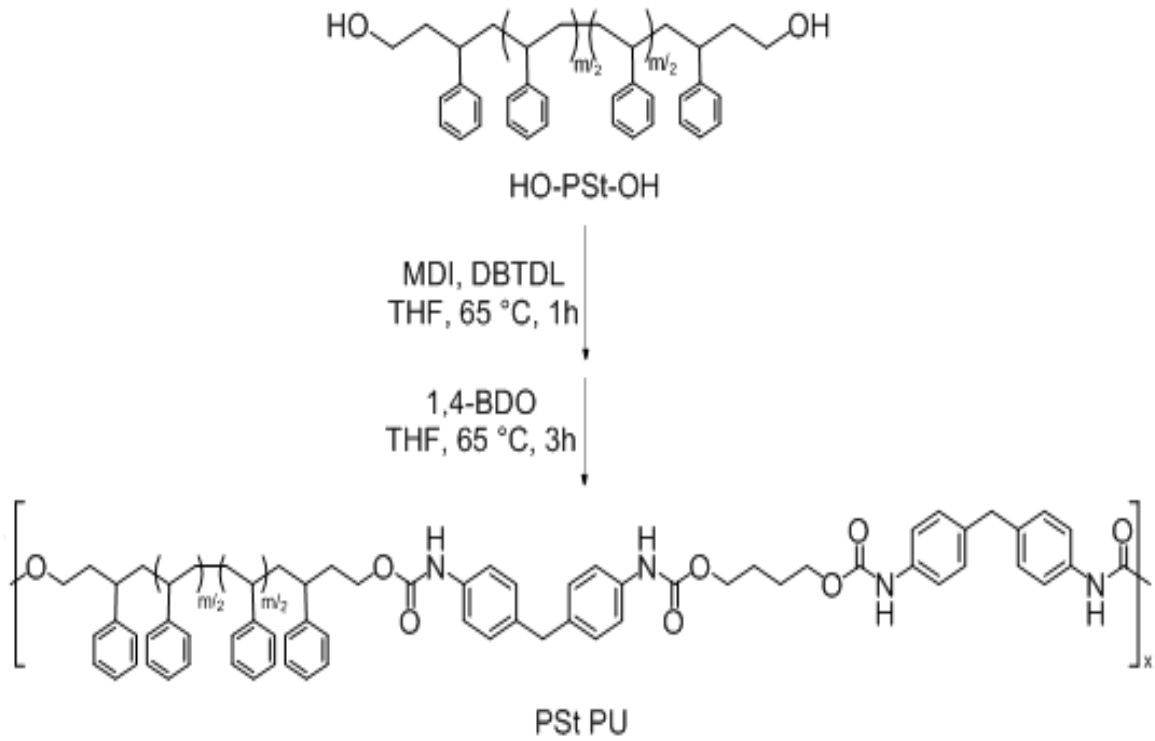

Figure 3.35. Synthesis of PSt PU.

The amounts of reagents were calculated using the equations

$$\frac{wt_{HO\text{-}PSt\text{-}OH}}{wt_{HO\text{-}PSt\text{-}OH} + wt_{MDI} + wt_{BDO}} = 0.7, \quad (3.5)$$

$$n_{HO\text{-}PSt\text{-}OH} + n_{BDO} = n_{MDI}, \quad (3.6)$$

where the wt% of HO-PSt-OH was 70% and the mole ratio of NCO to the total OH groups was one.

Figure 3.36 exhibits the ^{1}H NMR soectrum of PSt PU in pyridine-d5. In the spectrum the methine and methylene protons of PSt backbone (peaks k and l) and the aromatic protons (peaks i and j) are observed between 1.5-2.6 and 6.5-7.5 ppm, respectively. The peaks at 3.67 and 4.23 ppm are due to OCH_2 of PSt (peak d) and BDO (peak h) attached to urethane group. The peak at 10.65 ppm (peak p) is due to NH proton of urethane groups (CH_2OCONH). The aromatic protons of MDI appear at 7.89 (peak f) and 7.30 ppm. The peak at 7.30 merges with the peak of aromatic protons of PSt (peaks e and i). The methylene protons of MDI appear at 3.95 ppm (peak g). The peaks indicated with asterisk at 8.74, 7.58 and 7.22 ppm originate from pyridine-d5.

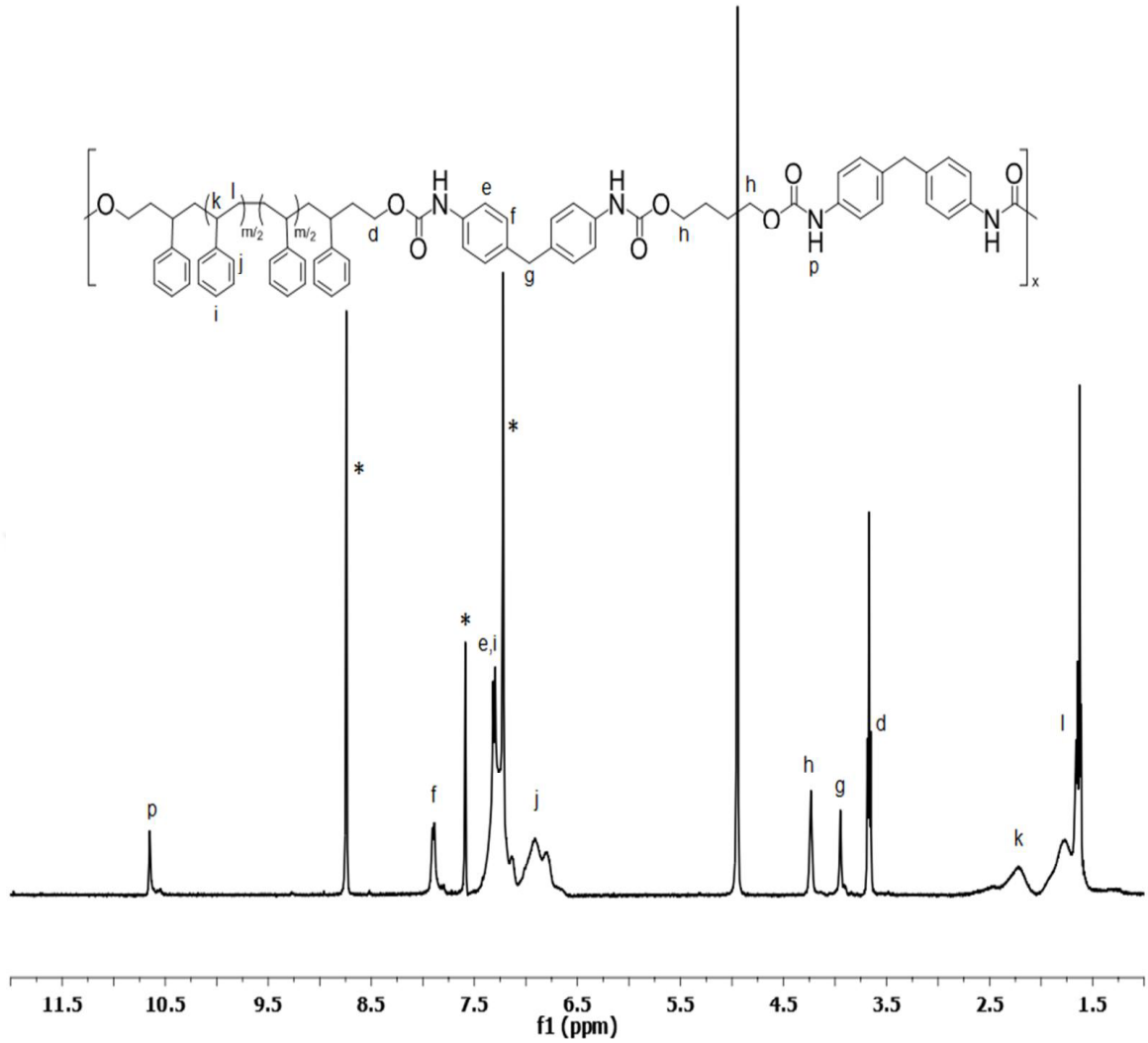

Figure 3.36. ^{1}H NMR spectrum of PSt PU in pyridine-d5. (*pyridine-d5)

In the FTIR spectrum of PSt PU (Figure 3.37), the absorption bands at 2800-3100 cm^{-1} region correspond to aromatic (=C—H) and aliphatic C—H stretching vibrations. Aromatic ring stretching vibrations of PSt are observed at 1492 and 1451 cm^{-1} [126]. In the C=O stretching region, the absorption at 1699 cm^{-1} together with a higher frequency shoulder at 1732 cm^{-1} are attributed to H bonded and free C=O groups, respectively. In the NH stretching region, the absorption for H bonded NH appears at 3318 cm^{-1}, while no noticeable absorption arises from free NH groups. Other bands associated with the urethane groups are overlaping NH bending and CN stretching at 1523 cm^{-1}, and stretching of C–O–C at 1064 cm^{-1}.

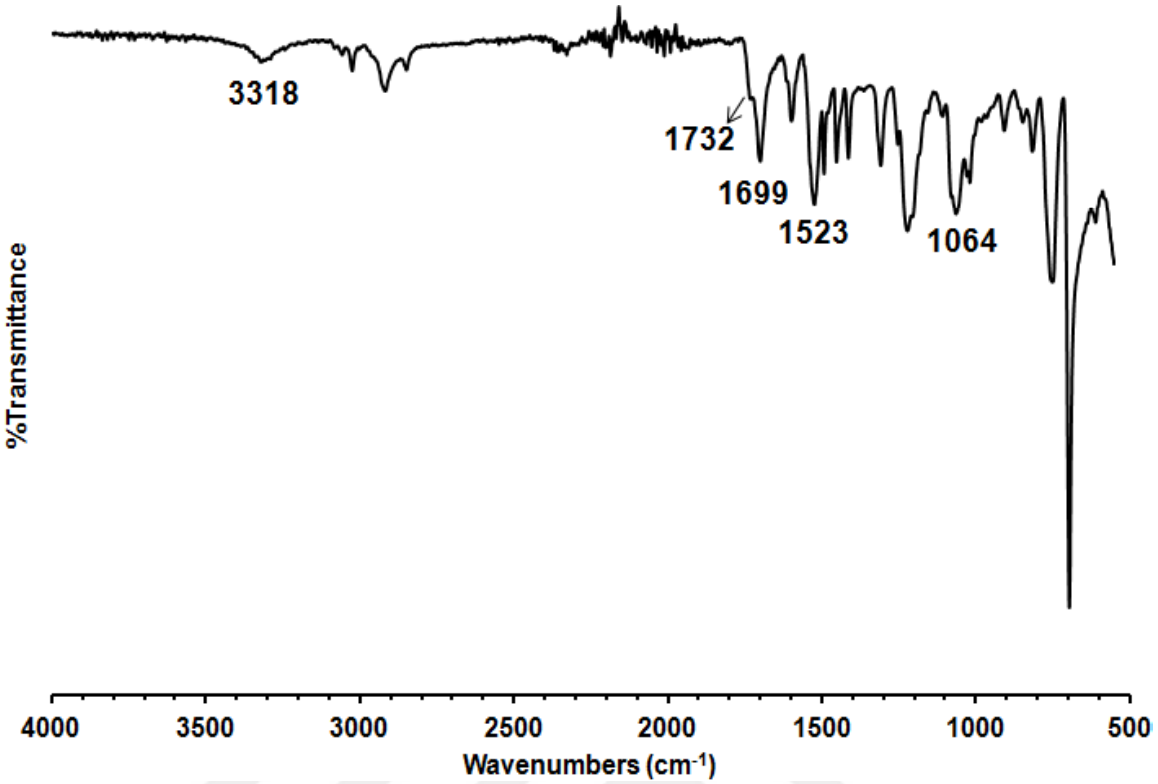

Figure 3.37. FTIR spectrum of PSt PU.

The molecular weight data of PSt PU obtained from SEC is given in Table 3.7. Compared to the starting polymer, HO-PSt-OH (Mn 3965 g/mol), the Mn value for PSt PU (Mn 64603 g/mol) increased approximately 16 times. As evident in the SEC chromatograms (Figure 3.38), the peak maximum of PIB PU was located in the higher molecular weight region, while the peak originating from the unreacted starting polymer was negligible.

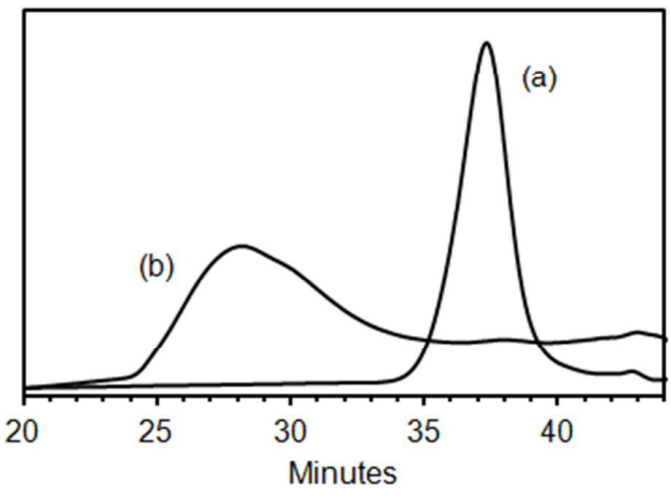

Figure 3.38. SEC traces of (a) HO-PSt-OH and (b) PSt PU.

Table 3.7. Molecular weight analysis data of PSt PU.

Sample	$M_{n,SEC}$ (g/mol)	$M_{p,SEC}$ (g/mol)	PDI_{SEC} (M_w/M_n)
PSt PU	64603	113129	2.12

3.2.4.2. OEO-b-PSt-b-OEO PU. The synthesis strategy was shown in Figure 3.39. First, the prepolymer with terminal isocyanates was synthesized by reacting OEO-b-PSt-b-OEO with a stoichiometric excess of MDI in the presence of DBTDL catalyst (0.1 mol% with respect to MDI) in THF. Then, the prepolymer was chain extended to higher molecular weights upon the addition of BDO.

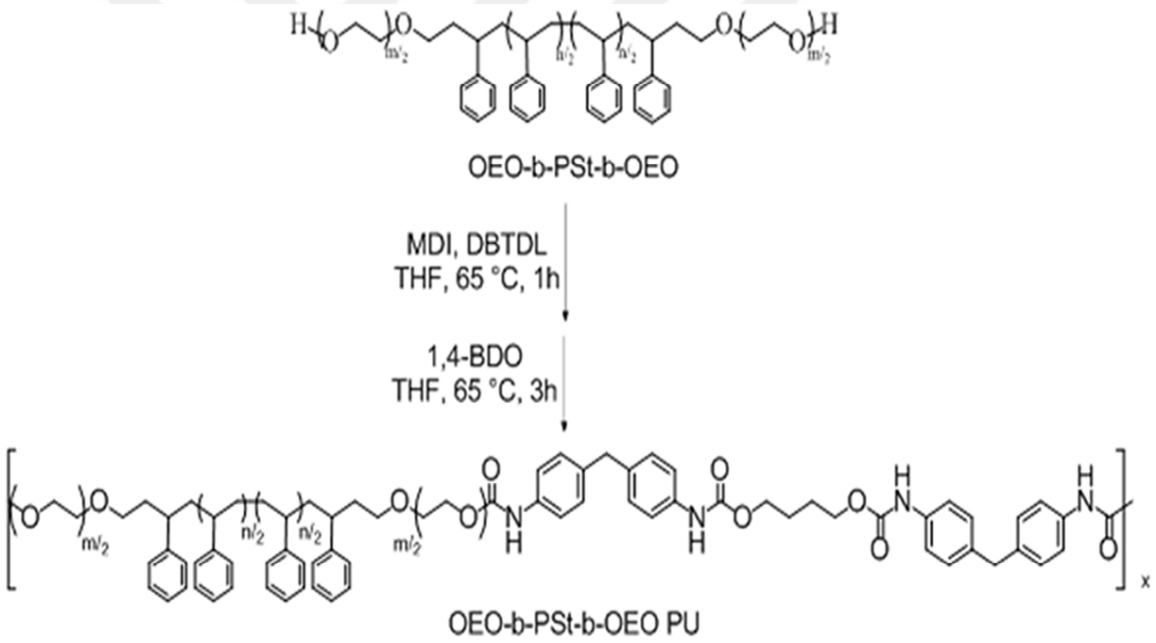

Figure 3.39. Synthesis of OEO-b-PSt-b-OEO PU.

The amounts of reagents were calculated using the equations

$$\frac{wt_{OEO\text{-}b\text{-}PSt\text{-}b\text{-}OEO}}{wt_{OEO\text{-}b\text{-}PSt\text{-}b\text{-}OEO} + wt_{MDI} + wt_{BDO}} = 0.7, \quad (3.7)$$

$$n_{OEO\text{-}b\text{-}PSt\text{-}b\text{-}OEO} + n_{BDO} = n_{MDI}, \quad (3.8)$$

where the wt% of OEO-b-PSt-b-OEO was 70% and the mole ratio of NCO to the total OH groups was one.

Figure 3.40 presents the ^{1}H NMR spectrum of OEO-b-PSt-b-OEO PU in pyridine-d5. The phenyl protons (peaks i and j) and the CH and CH_2 protons of PSt backbone (peaks k and l) resonate between 6.5-7.5 and 1.5-2.6 ppm, respectively. The peaks at 3.65 and 4.23 ppm are assigned to protons of EO block (peak m) and OCH_2 protons of BDO (peak h) attached to the urethane groups, respectively. NH proton of urethane groups (CH_2OCONH) resonate at 10.65 ppm (peak p). Additionally, the resonances associated with MDI are the aromatic protons at 7.89 (peak f) and 7.30 ppm, and the CH_2 protons at 3.95 ppm (peak g). The peak at 7.30 overlaps with the peak of aromatic protons of PSt (peaks e and i). The signals indicated with asterisk at 8.74, 7.58 and 7.22 ppm are attributed to pyridine-d5.

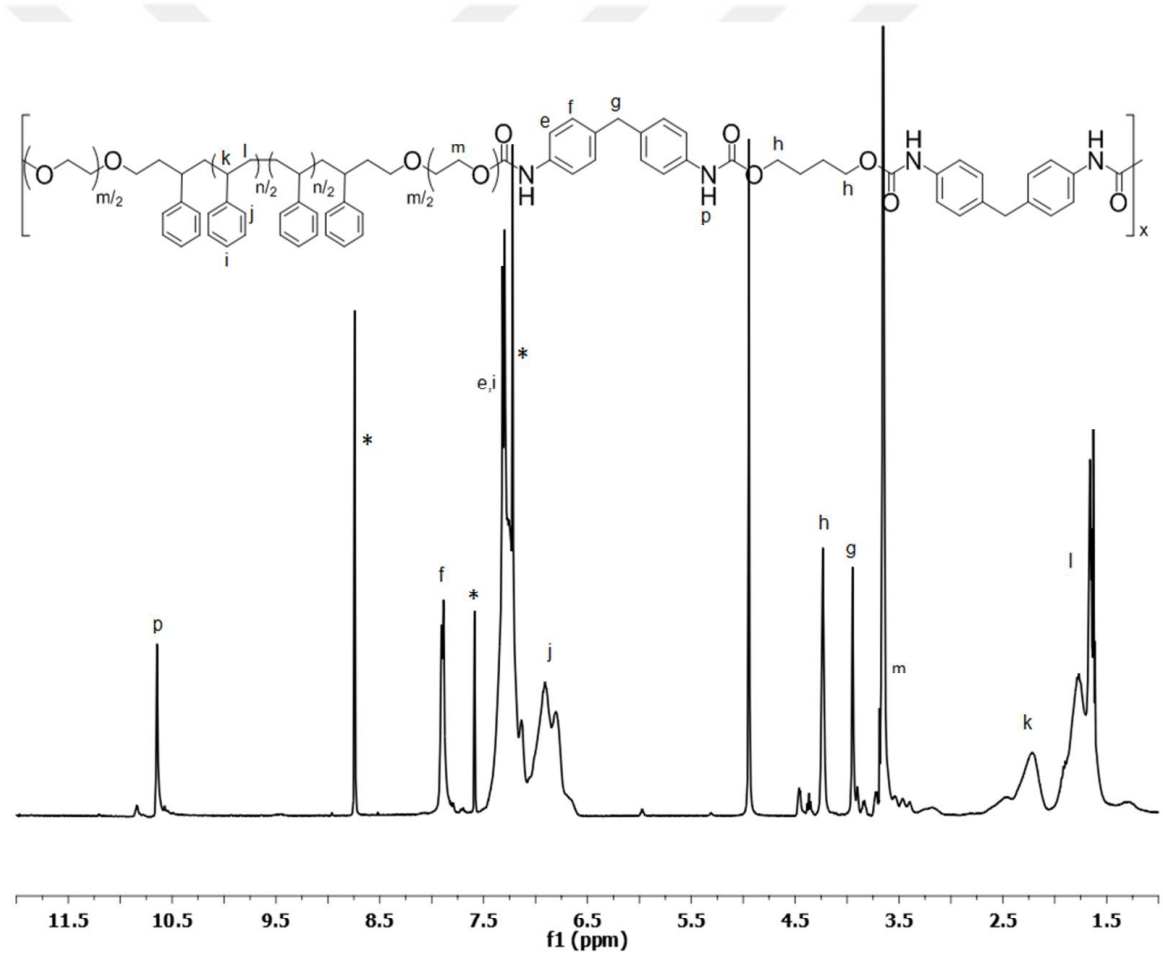

Figure 3.40. ^{1}H NMR spectrum of OEO-b-PSt-b-OEO PU in pyridine-d5. (*pyridine-d5)

Figure 3.41 exhibits the FTIR spectrum of OEO-b-PSt-b-OEO PU. The insert shows the spectra of PSt PU and OEO-b-PSt-b-OEO PU in the 800-1400 cm^{-1} region for comparison. For OEO-b-PSt-b-OEO PU, the breadth of the peak at 1105 cm^{-1} increases and a shoulder at 1140 cm^{-1} appears. This can be attributed to C–O–C stretching vibrations

of EO units, as the aliphatic polyethers are known to absorb at 1150-1060 cm^{-1} region [126]. As expected, the rest of the spectral features are very similar to those of PSt PU, i.e. aromatic and aliphatic C—H stretching (2800-3100 cm^{-1}), aromatic ring stretching of PSt (1492 and 1451 cm^{-1}), H bonded NH stretching (3316 cm^{-1}), overlaping NH bending and CN stretching (1527 cm^{-1}), and C–O–C stretching (1068 cm^{-1}). Similar to PSt PU, the H bonded C=O stretching band appears at 1700 cm^{-1}, while the high frequency shoulder appearing at 1732 cm^{-1} in PSt PU shifts to 1725 cm^{-1} in OEO-b-PSt-b-OEO PU.

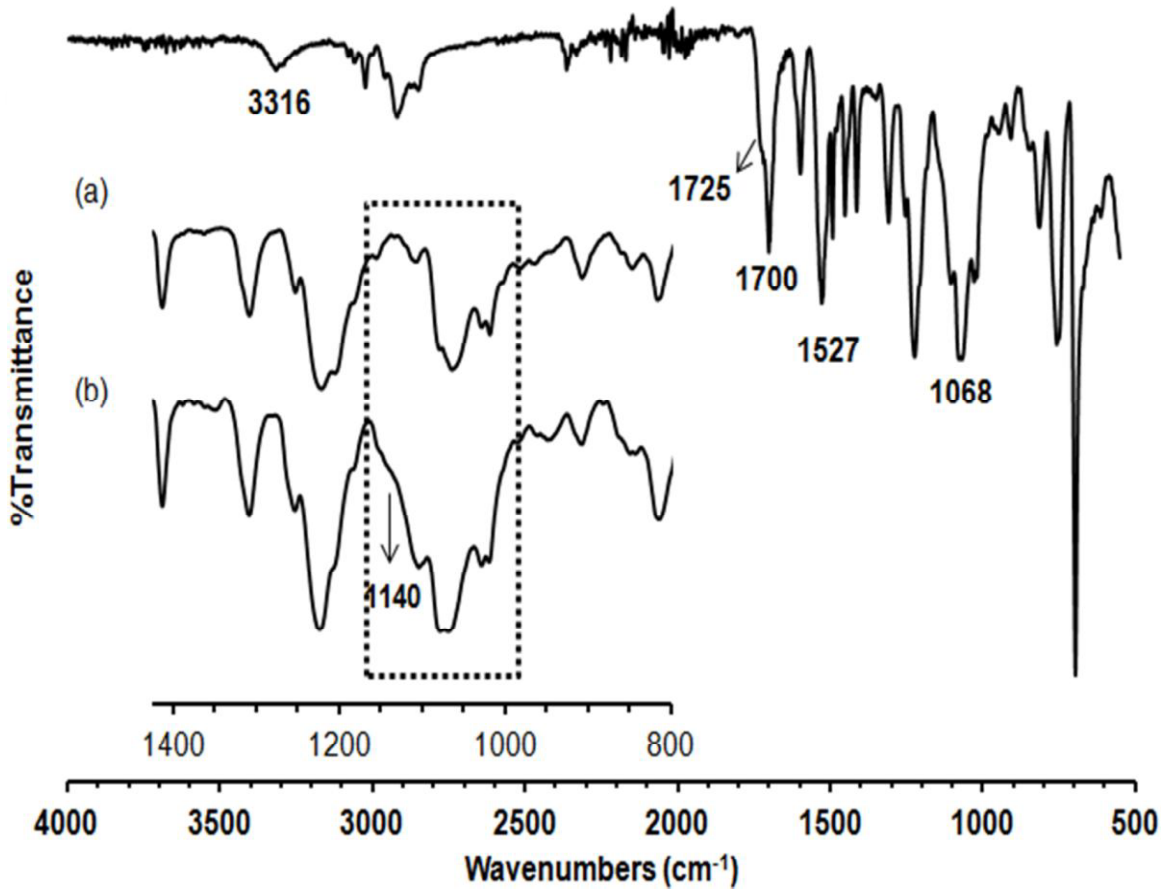

Figure 3.41. FTIR spectrum of OEO-b-PSt-b-OEO PU. Insert: Expanded 800-1400 cm-1 range for (a) PSt PU and (b) OEO-b-PSt-b-OEO PU.

The molecular weight data of OEO-b-PSt-b-OEO PU obtained from SEC is given in Table 3.8. Compared to the starting polymer, OEO-b-PSt-b-OEO (Mn 4573 g/mol), the Mn value for OEO-b-PSt-b-OEO PU (Mn 31877 g/mol) increased approximately 7 times. As evident in the SEC chromatograms (Figure 3.42), the peak maximum of PIB PU was located in the higher molecular weight region, while the peak originating from the unreacted starting polymer was negligible.

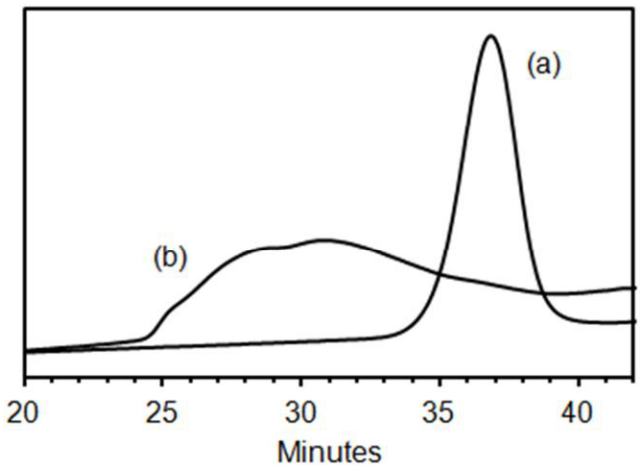

Figure 3.42. SEC traces of (a) OEO-b-PSt-b-OEO and (b) OEO-b-PSt-b-OEO PU.

Table 3.8. Molecular weight analysis data of OEO-b-PSt-b-OEO PU.

Sample	$M_{n,SEC}$ (g/mol)	$M_{p,SEC}$ (g/mol)	PDI_{SEC} (M_w/M_n)
OEO-b-PSt-b-OEO PU	31877	49487	3.02

3.2.5. Syntheses and Characterizations of PIB/PSt Based PUs

3.2.5.1. PIB/PSt PU. Figure 3.43 outlines the synthesis strategy of PIB/PSt PU. It is a two-step synthesis involving the preparation of the prepolymer and the chain extension. In the first stage, the prepolymer was obtained from the reaction of a mixture of HO-PIB-OH soft segment and HO-PSt-OH with a stoichiometric excess of MDI using DBTDL catalyst (0.1 mol% with respect to MDI). In the second stage, the prepolymer was allowed to react with BDO chain extender which resulted in an increase in the viscosity.

PIB/PSt PU was synthesized with the 70:30 wt ratio of soft to hard segment (PSt+MDI+BDO). The amounts of reagents were calculated using the equations

$$\frac{wt_{HO\text{-}PIB\text{-}OH}}{wt_{HO\text{-}PIB\text{-}OH} + wt_{HO\text{-}PSt\text{-}OH} + wt_{MDI} + wt_{BDO}} - 0.7, \quad (3.9)$$

$$n_{HO\text{-}PIB\text{-}OH} + n_{HO\text{-}PSt\text{-}OH} + n_{BDO} = n_{MDI}, \quad (3.10)$$

where the wt% of HO-PIB-OH soft segment was 70% and the mole ratio of NCO to the total OH groups was one.

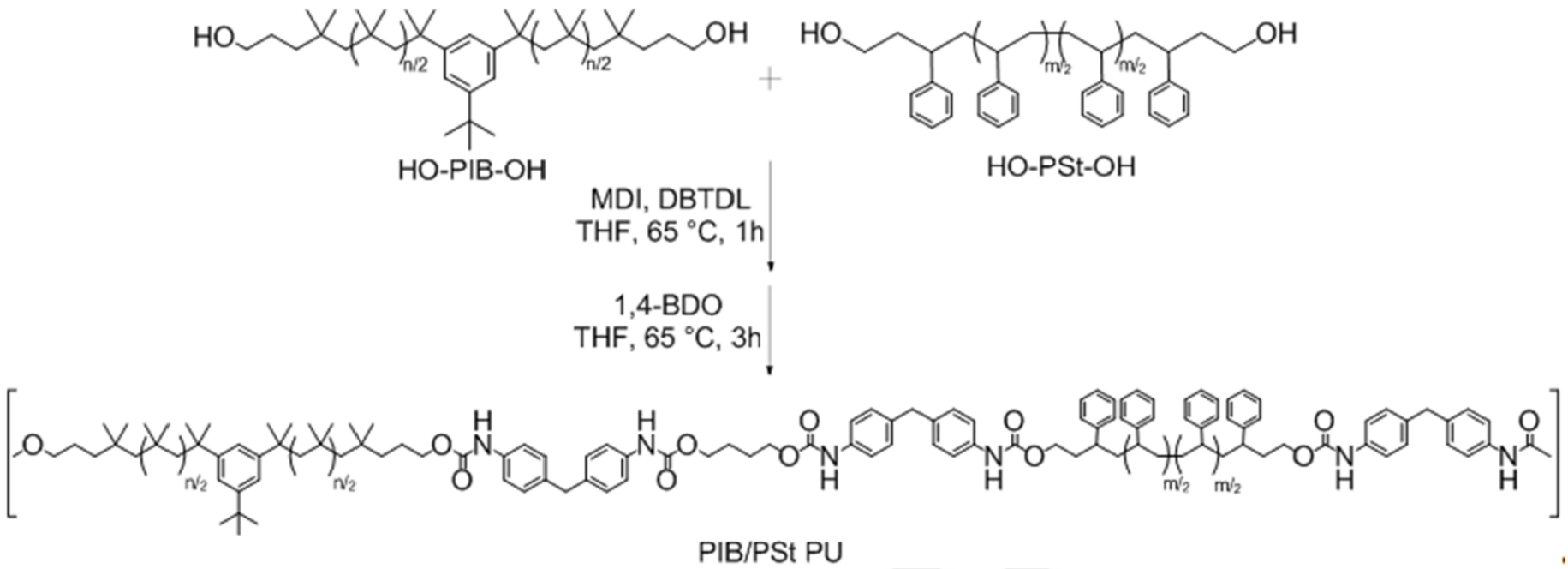

Figure 3. 43. Synthesis of PIB/PSt PU.

The FTIR spectrum of PIB/PSt PU reveals the absorptions typical of PIB and PSt segments, as well as urethane groups (Figure 3.44). Namely, aromatic (=C—H) and aliphatic C—H stretching (2800-3100 cm^{-1}), H bonded NH stretching (3323 cm^{-1}) (free NH stretching is barely visible at 3441), H bonded and free C=O stretching (1702 and 1734 cm^{-1}, respectively), overlapping NH bending and CN stretching (1524 cm^{-1}), C–O–C stretching (1078 cm^{-1}), and swing of the CH_3 groups in the PIB backbone (1388 and 1365 cm^{-1}). Aromatic ring stretching vibrations of PSt overlap with CH bending vibrations of PIB at 1420-1500 cm^{-1} region.

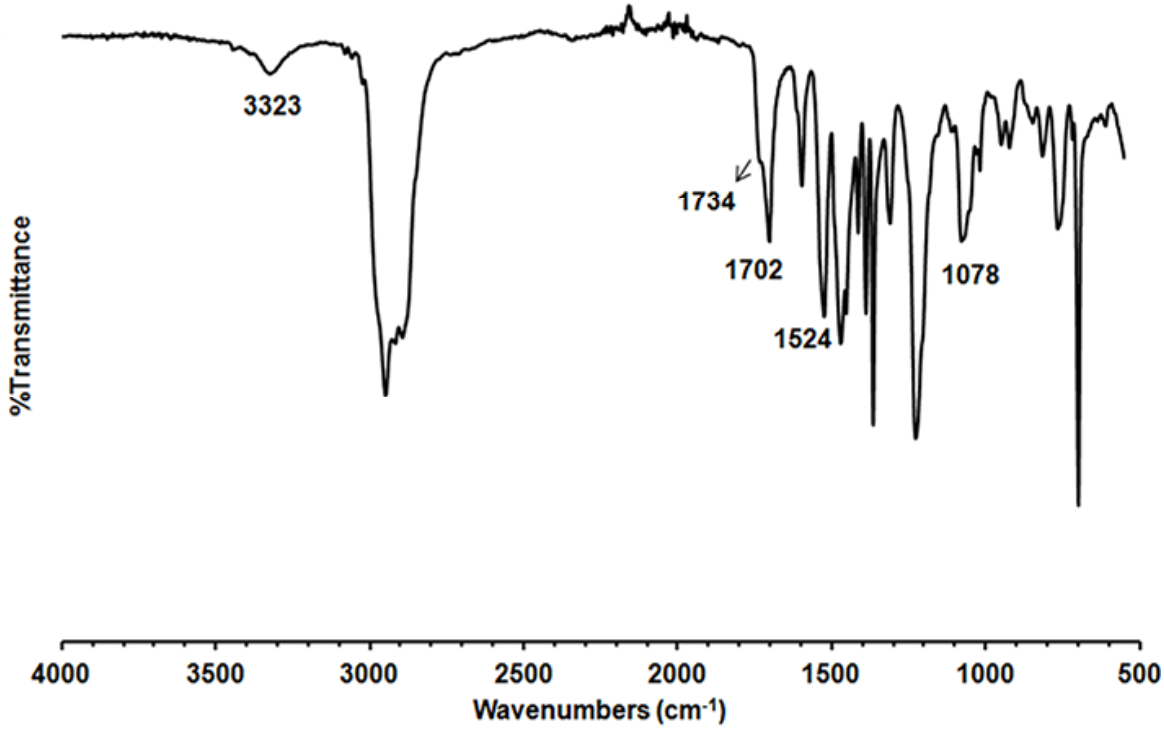

Figure 3. 44. FTIR spectrum of PIB/PSt PU.

In the ^1H NMR spectrum of PIB/PSt PU in $CDCl_3$ (Figure 3.45), in addition to the peaks accountable to PIB and PSt segments, those associated with the urethane groups are visible. The aliphatic main chain protons of PSt and methylene protons of PIB overlap in the region of 1.2-2.0 ppm (Peak k,l,b). Besides, the aromatic protons of PSt that fall within the range of 6.8-7.4 ppm overlap with the aromatic protons of MDI (Peak a,e,f,i). The methylene protons of MDI arise at 3.90 ppm (peak g). The partially overlapping peaks that fall to the region of 4.0-4.3 ppm correspond to OCH_2 groups of PIB, PSt and BDO attached to urethane groups (peak d,h).

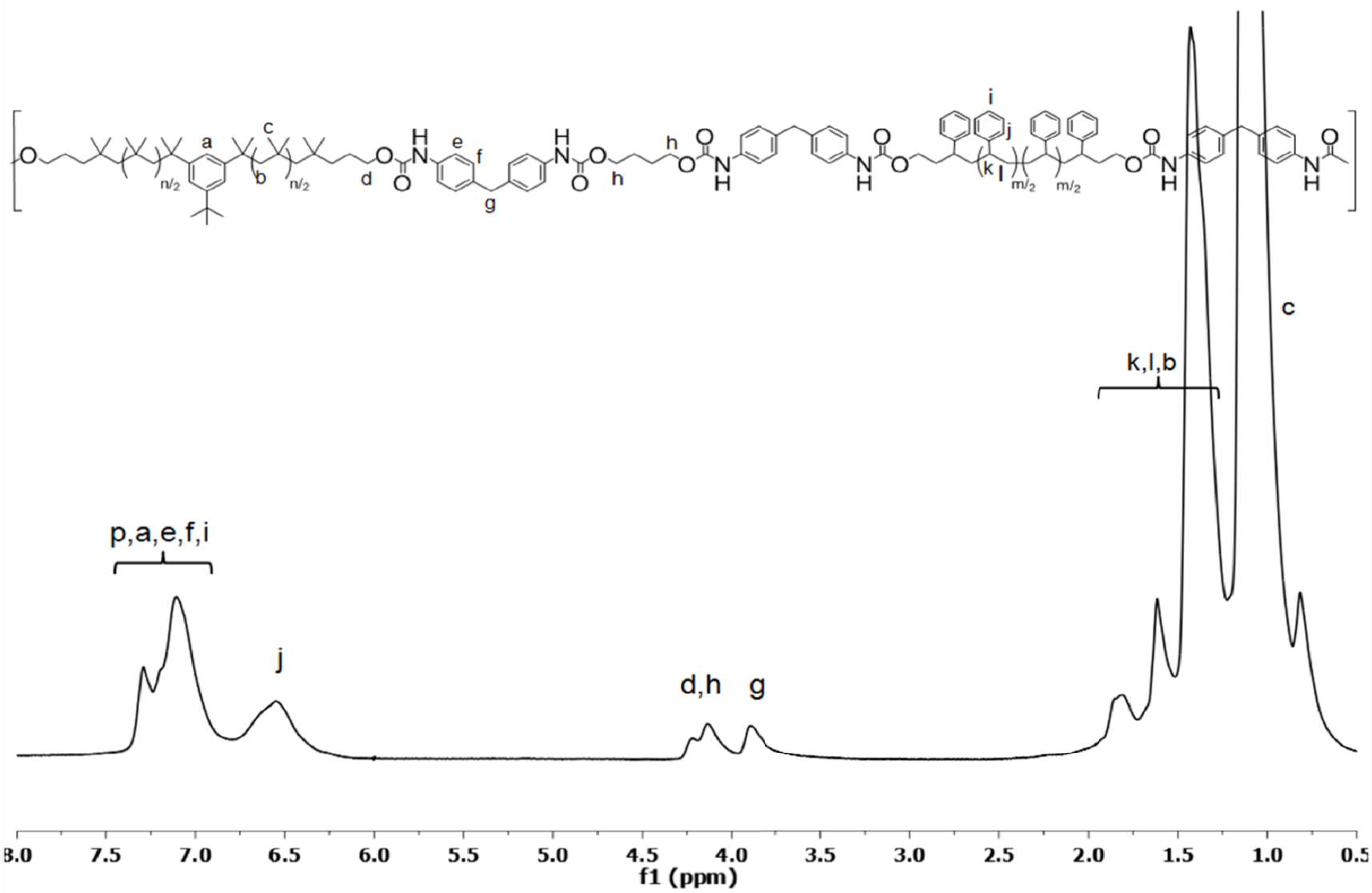

Figure 3.45. ^{1}H NMR spectrum of PIB/PSt PU in $CDCl_3$

The molecular weight data of PIB/PSt PU obtained from SEC is given in Table 3.9. As evident in the SEC chromatograms (Figure 3.46), the peak maximum of PIB/PSt PU was located in the higher molecular weight region, while the peaks originating from the unreacted starting polymers, HO-PIB-OH and HO-PSt-OH, were negligible.

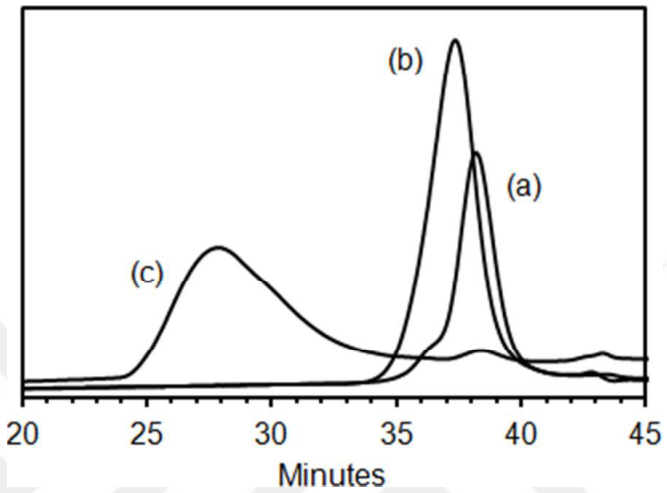

Figure 3.46. SEC traces of (a) A-PIB-A, (b) HO-PSt-OH and (c) PIB/PSt PU.

Table 3.9. Molecular weight analysis data of OEO-b-PSt-b-OEO PU.

Sample	$M_{n,SEC}$ (g/mol)	$M_{p,SEC}$ (g/mol)	PDI_{SEC} (M_w/M_n)
PIB/PSt PU	66092	120910	1.98

3.2.5.2. PIB/OEO-b-PSt-b-OEO PU. The idealized micromorphology and the synthesis strategy of PIB/OEO-b-PSt-b-OEO PU are shown in Figure 3.47 and 3.48, respectively. In the model, the solid black lines represent PIB soft segments. The solid blue and the dotted green lines are PSt and EO blocks of OEO-b-PSt-b-OEO. The solid red lines correspond to the hard segments. The thin yellow lines represent H bonding within the urethane hard segments.

The prepolymer with terminal isocyanates was synthesized by reacting a mixture of HO-PIB-OH and OEO-b-PSt-b-OEO with a stoichiometric excess of MDI in the presence of DBTDL catalyst (0.1 mol% with respect to MDI) in THF. Then, the prepolymer was chain extended to higher molecular weights upon the addition of BDO (Figure 3.48).

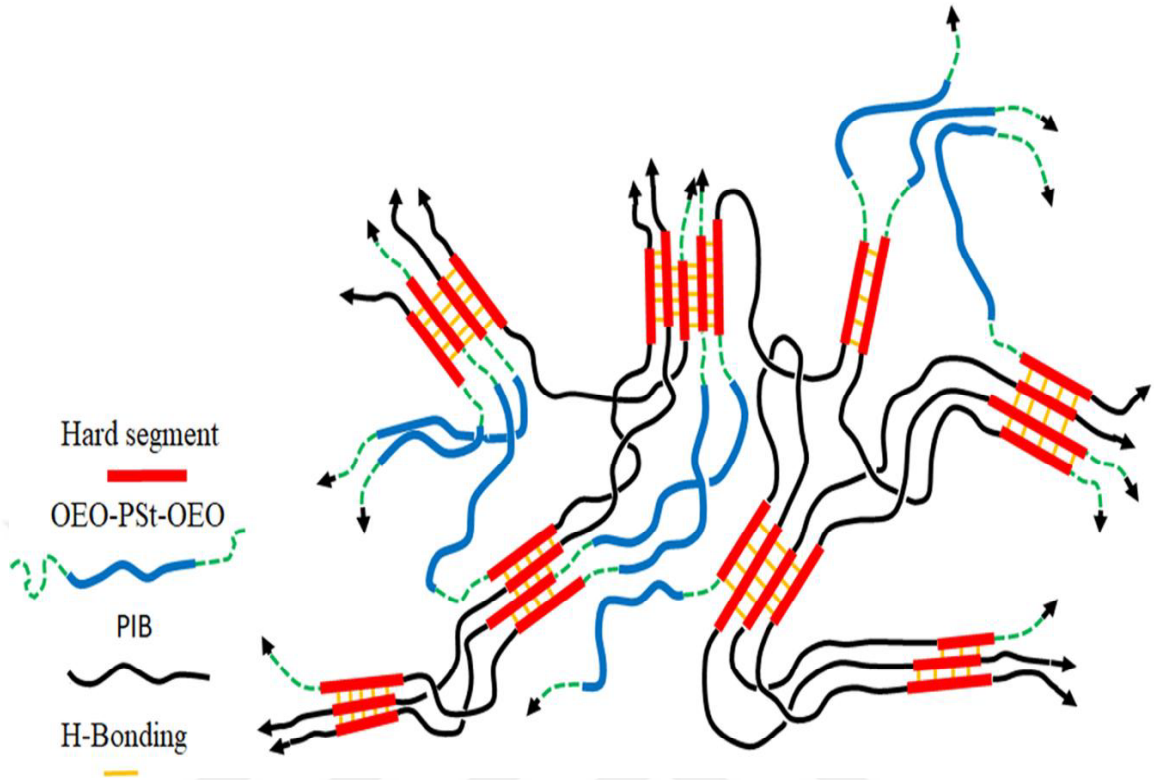

Figure 3.47. The idealized micromorphology of PIB/OEO-b-PSt-b-OEO PU.

The amounts of reagents were calculated using the equations

$$\frac{wt_{HO\text{-}PIB\text{-}OH}}{wt_{HO\text{-}PIB\text{-}OH} + wt_{OEO\text{-}b\text{-}PSt\text{-}b\text{-}OEO} + wt_{MDI} + wt_{BDO}} = 0.7, \quad (3.11)$$

$$n_{HO\text{-}PIB\text{-}OH} + wt_{OEO\text{-}b\text{-}PSt\text{-}b\text{-}OEO} + n_{BDO} = n_{MDI}, \quad (3.12)$$

where the wt% of HO-PIB-OH was 70% and the mole ratio of NCO to the total OH groups was one.

Figure 3.49 exhibits the ^{1}H NMR spectrum of PIB/OEO-b-PSt-b-OEO PU in $CDCl_3$. Although the spectral features are very similar to those of PIB/PSt PU, a new peak at 3.64 ppm originating from the EO blocks confirms the incorporation of OEO-b-PSt-b-OEO segments in the PU structure. Other peaks typical of PIB and PSt segments, and urethane groups can be listed as following: Overlapping CH_2 protons of PIB and aliphatic main chain protons of PSt at 1.2-2.0 ppm (Peak k,l,b), overlapping aromatic protons of PSt and MDI at 6.8-7.4 ppm (Peak a,e,f,i), CH_2 protons of MDI at 3.89 ppm (peak g) and OCH_2 protons of PIB and BDO attached to urethane groups at 4.21 and 4.12 ppm (peaks d and h respectively).

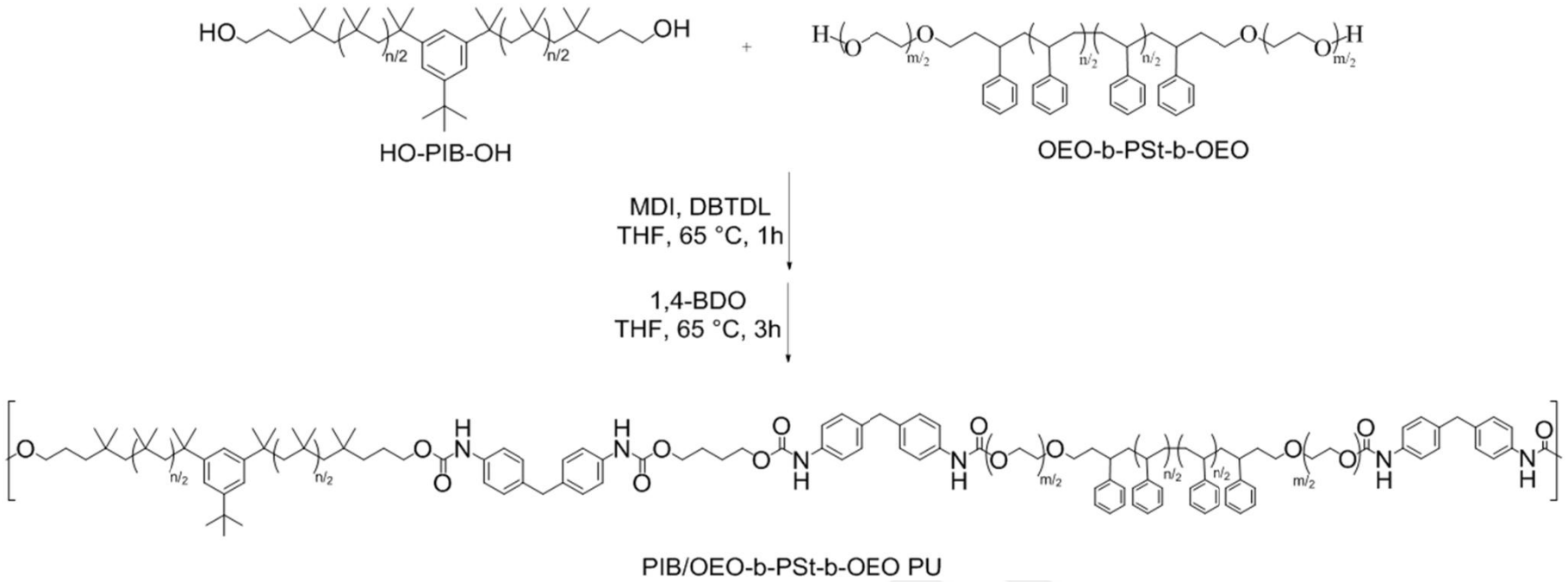

Figure 3.48. Synthesis of PIB/OEO-b-PSt-b-OEO PU.

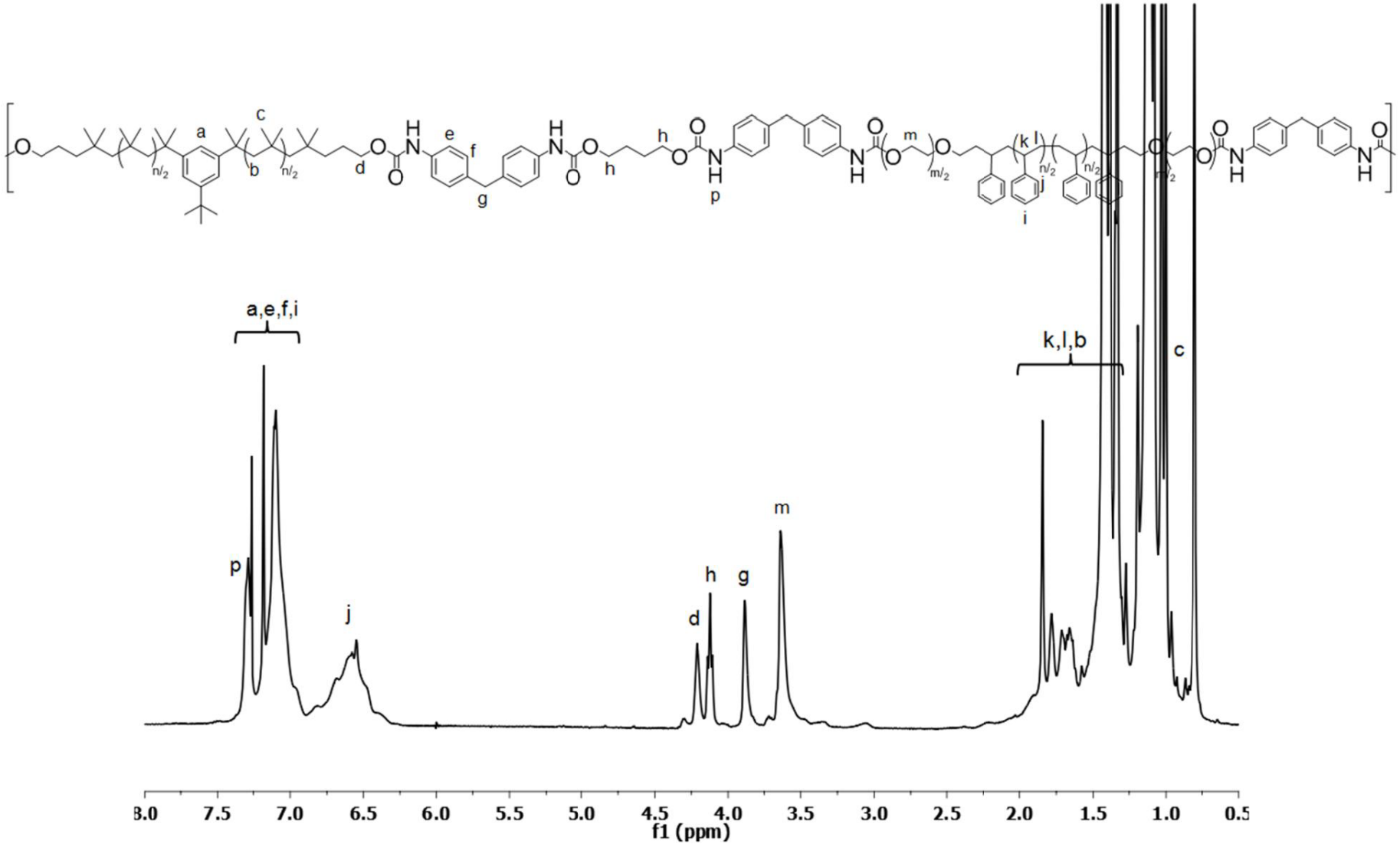

Figure 3.49. ^{1}H NMR spectrum of PIB/OEO-b-PSt-b-OEO PU in $CDCl_3$.

Figure 3.50 shows the FTIR spectrum of PIB/OEO-b-PSt-b-OEO PU. The insert compares the spectra of PIB/PSt PU and PIB/OEO-b-PSt-b-OEO PU in the 900-1300 cm^{-1} region. As discussed in the comparison of PSt PU and OEO-b-PSt-b-OEO PU, the breadth of the peak at 1109 cm^{-1} increases, which can be attributed to C–O–C stretching vibrations of EO units in OEO-b-PSt-b-OEO PU. The rest of the spectral features are very similar to those of PIB/PSt PU, i.e. aromatic (=C—H) and aliphatic C—H stretching (2800-3100 cm^{-1}), H bonded NH stretching (3323 cm^{-1}) (free NH stretching is barely visible at 3441), H bonded and free C=O strecthing (1702 and 1730 cm^{-1}, respectively), overlaping NH bending and CN stretching (1526 cm^{-1}), and C–O–C stretching (1078 cm^{-1}), and swing of the CH_3 groups in the PIB backbone (1388 and 1365 cm^{-1}). Aromatic ring stretching vibrations of PSt overlap with CH bending vibrations of PIB at 1420-1500 cm^{-1} region.

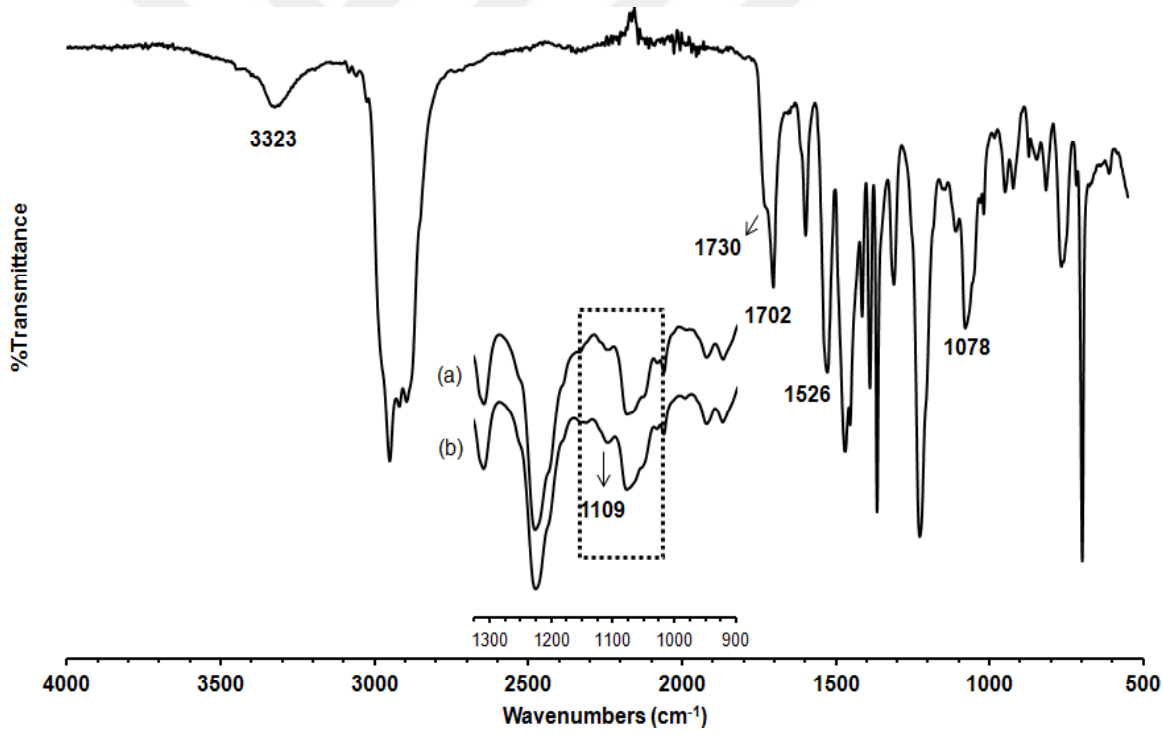

Figure 3.50. FTIR spectrum of PIB/OEO-b-PSt-b-OEO PU. Insert: Expanded 900-1300 cm-1 range for (a) PIB/PSt PU and (b) PIB/OEO-b-PSt-b-OEO PU.

The molecular weight data of PIB/OEO-b-PSt-b-OEO PU obtained from SEC is given in Table 3.10. As evident in the SEC chromatograms (Figure 3.51), the peak maximum of PIB/OEO-b-PSt-b-OEO PU was located in the higher molecular weight region, while the peaks originating from the unreacted starting polymers, HO-PIB-OH and OEO-b-PSt-b-OEO, were negligible.

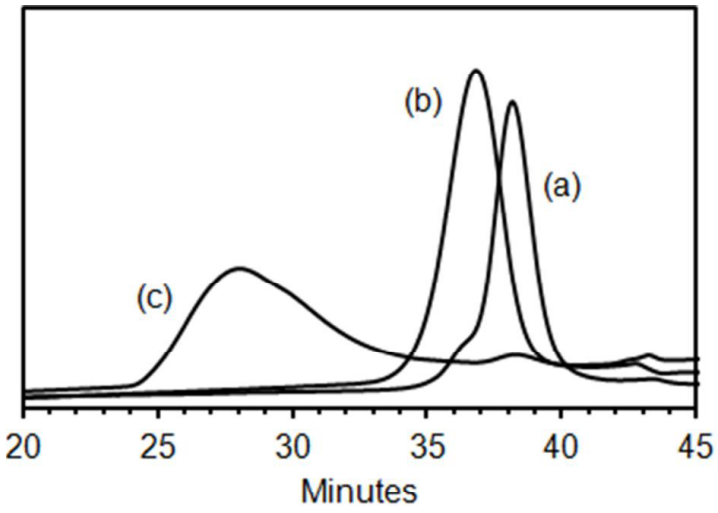

Figure 3.51. SEC traces of (a) A-PIB-A, (b) OEO-b-PSt-b-OEO and (c) PIB/OEO-b-PSt-b-OEO PU.

Table 3.10. Molecular weight analysis data of PIB/OEO-b-PSt-b-OEO PU.

Sample	$M_{n,SEC}$ (g/mol)	$M_{p,SEC}$ (g/mol)	PDI_{SEC} (M_w/M_n)
PIB/OEO-b-PSt-b-OEO PU	61597	111729	2.01

3.2.5.3. OEO-b-PIB-b-OEO/PSt PU. The idealized micromorphology and the synthesis strategy of OEO-b-PIB-b-OEO/PSt PU are shown in Figure 3.52 and 3.53, respectively. In the model, the solid black and the dotted green lines are PIB and EO blocks of OEO-b-PIB-b-OEO. The solid blue lines represent PSt segments. The solid red lines correspond to the hard segments. The thin yellow lines represent H bonding within the urethane hard segments.

The prepolymer with terminal isocyanates was synthesized by reacting a mixture of OEO-b-PIB-b-OEO and HO-PSt-OH with a stoichiometric excess of MDI in the presence of DBTDL catalyst (0.1 mol% with respect to MDI) in THF. Then, the prepolymer was chain extended to higher molecular weights upon the addition of BDO (Figure 3.53).

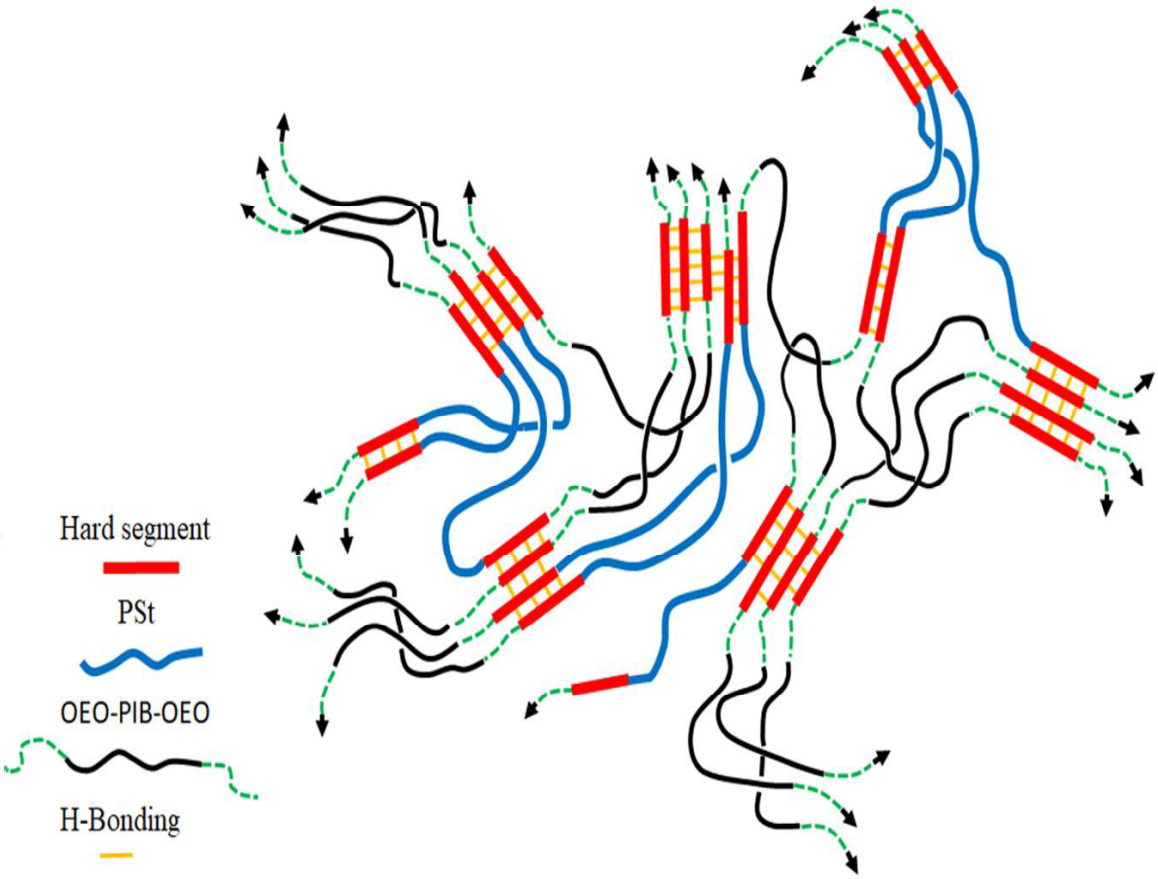

Figure 3.52. The idealized micromorphology of OEO-b-PIB-b-OEO/PSt PU.

The amounts of reagents were calculated using the equations

$$\frac{wt_{OEO\text{-}b\text{-}PIB\text{-}b\text{-}OEO}}{wt_{OEO\text{-}b\text{-}PIB\text{-}b\text{-}OEO} + wt_{HO\text{-}PSt\text{-}OH} + wt_{MDI} + wt_{BDO}} = 0.7, \quad (3.13)$$

$$n_{OEO\text{-}b\text{-}PIB\text{-}b\text{-}OEO} + wt_{HO\text{-}PSt\text{-}OH} + n_{BDO} = n_{MDI}, \quad (3.14)$$

where the wt% of OEO-b-PIB-b-OEO was 70% and the mole ratio of NCO to the total OH groups was one.

Figure 3.54 shows the ^{1}H NMR spectrum of OEO-b-PIB-b-OEO/PSt PU in $CDCl_3$. The peak at 3.64 ppm originates from the EO blocks confirm the incorporation of OEO-b-PIB-b-OEO segments in the PU structure. The peaks at 4.21 (peak d) and 4.10 ppm (peak h) are assigned to OCH_2 protons of OEO-b-PIB-b-OEO soft segment and BDO attached to urethane, respectively. Other peaks typical of PIB and PSt segments include overlapping CH_2 protons of PIB and aliphatic main chain protons of PSt at 1.2-2.0 ppm (Peak k,l,b), overlapping aromatic protons of PSt and MDI at 6.8-7.4 ppm (Peak a,e,f,i), CH_2 protons of MDI at 3.88 ppm (peak g).

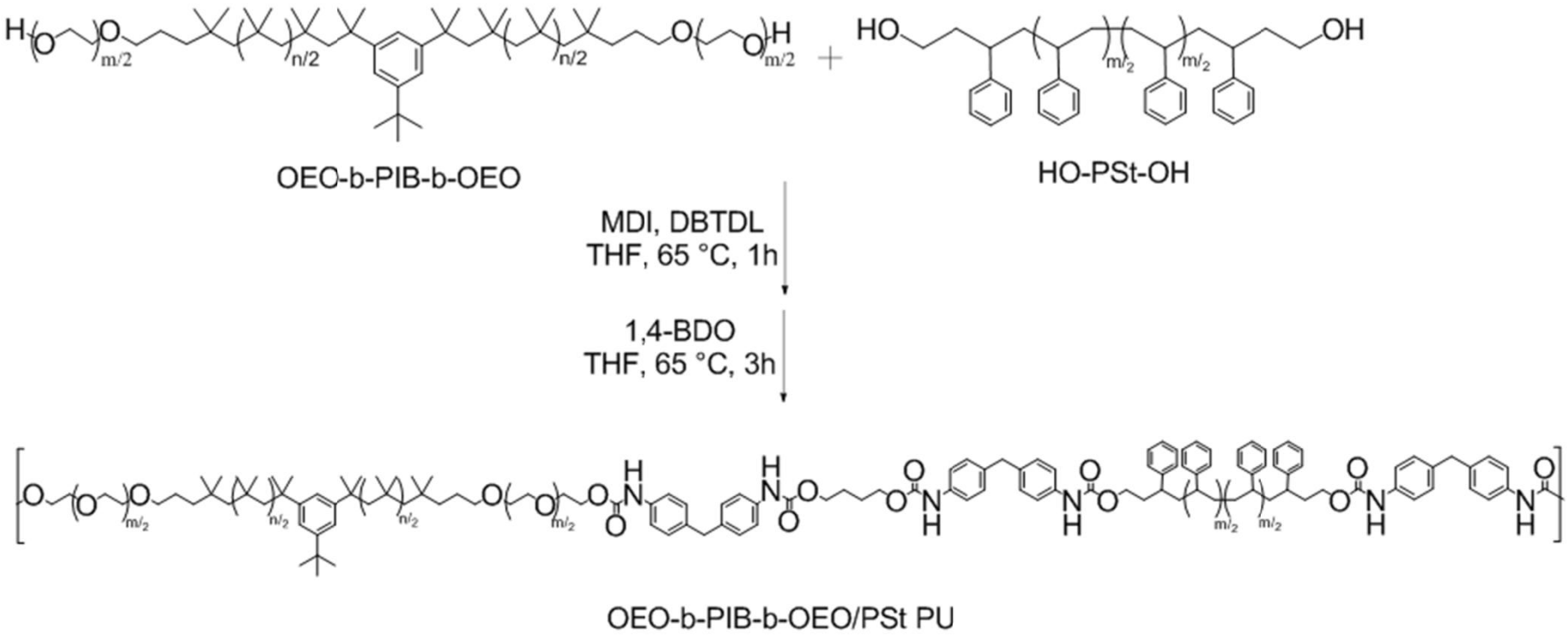

Figure 3.53. Synthesis of OEO-b-PIB-b-OEO/PSt PU.

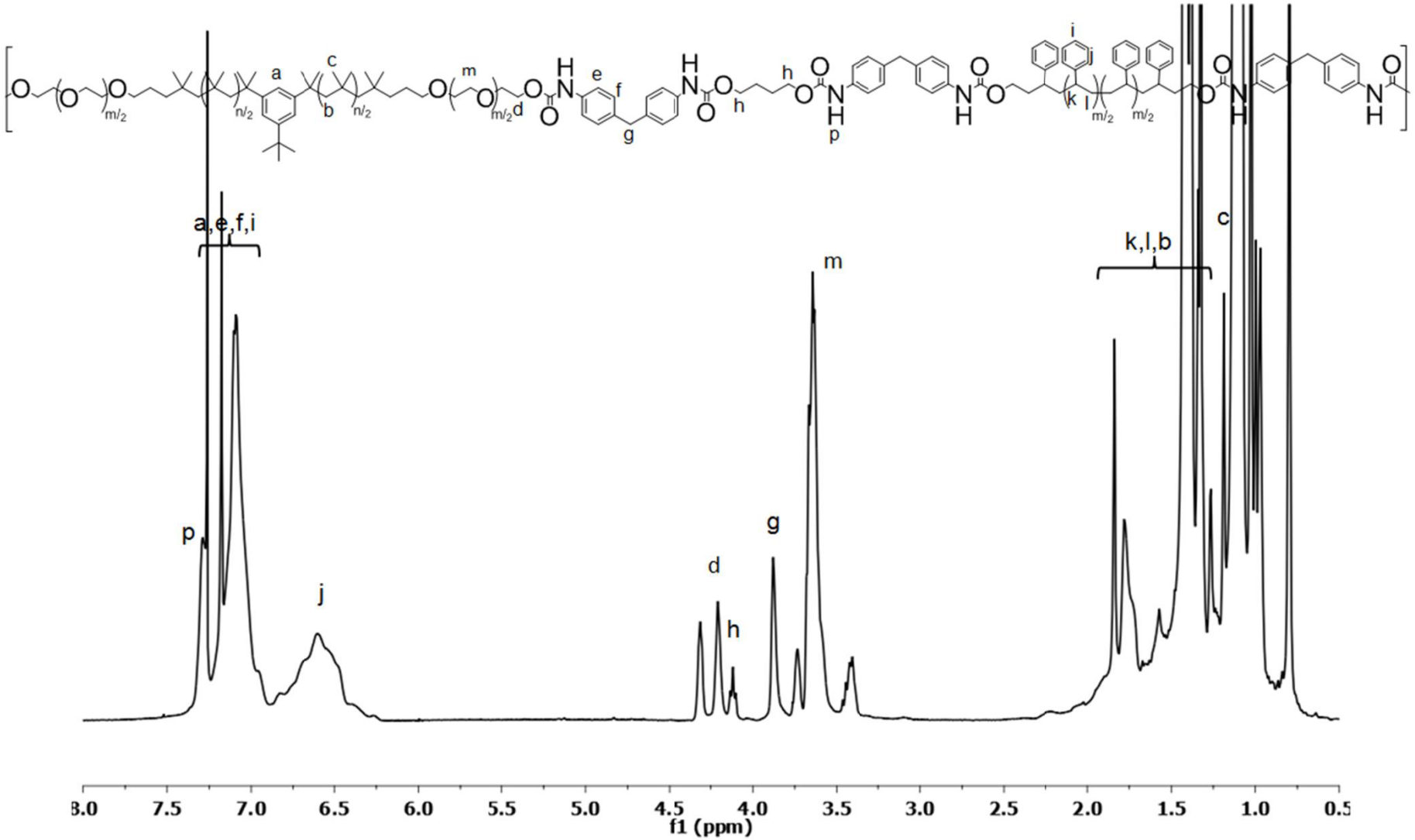

Figure 3.54. ^{1}H NMR spectrum of OEO-b-PIB-b-OEO/PSt PU in $CDCl_3$.

Figure 3.55 displays the FTIR spectrum of OEO-b-PIB-b-OEO/PSt PU. The inserts zoom in the region 900-1300 and 3100-3700 cm^{-1} of PIB/PSt PU and OEO-b-PIB-b-OEO/PSt PU. As discussed in the comparison of PIB PU and OEO-b-PIB-b-OEO PU, in the spectrum of OEO-b-PIB-b-OEO/PSt PU, the increase in the breadth of the peak at 1109 cm^{-1} and the emergence of a broad shoulder at ~1140 cm^{-1} can be assigned to C–O–C stretching vibrations of EO units, indicating the incorporation of OEO-b-PIB-b-OEO in the PU structure. Unlike PIB/PSt PU, the C=O strecthing band is observed to split into two distinct peaks at 1731 and 1703 cm^{-1}, which are due to free and H bonded C=O groups. Furthermore, the comparison of the NH absorption region for PIB/PSt and OEO-b-PIB-b-OEO/PSt PU shows that in the latter the breadth of the band increases and the peak maxima shifts from 3323 to 3314 cm^{-1}. The rest of the spectral features are very similar in the two spectra. That is, aromatic (=C—H) and aliphatic C—H stretching (2800-3100 cm^{-1}), overlaping NH bending and CN stretching (1533 cm^{-1}), and C–O–C stretching (1072 cm^{-1}), and swing of the CH_3 groups in the PIB backbone (1388 and 1365 cm^{-1}). Aromatic ring stretching vibrations of PSt overlap with CH bending vibrations of PIB at 1420-1500 cm^{-1} region.

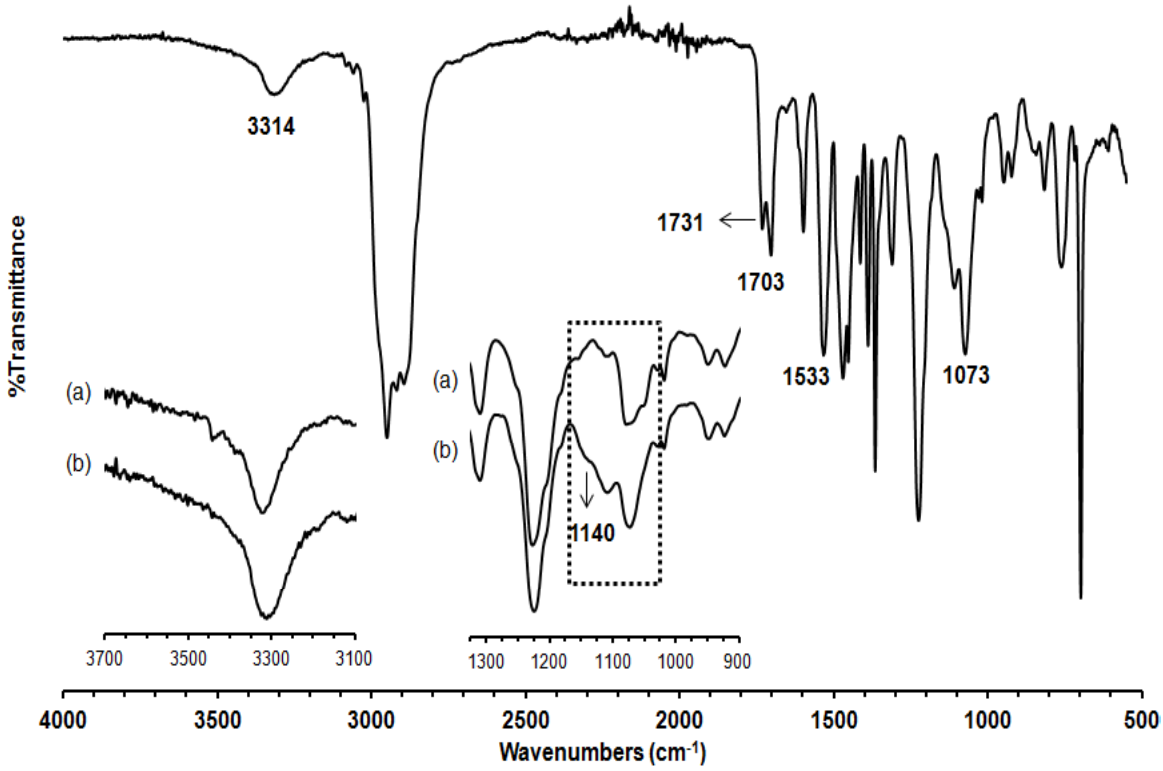

Figure 3.55. FTIR spectrum of OEO-b-PIB-b-OEO/PSt PU. Inserts: Expanded 900-1300 and 3100-3700 cm-1 ranges for (a) PIB/PSt PU and (b) OEO-b-PIB-b-OEO/PSt PU

The molecular weight data of OEO-b-PIB-b-OEO/PSt PU obtained from SEC is given in Table 3.11. As evident in the SEC chromatograms (Figure 3.56), the peak maximum of OEO-b-PIB-b-OEO/PSt PU was located in the higher molecular weight region, while the peak originating from the unreacted starting polymers, OEO-b-PIB-b-OEO and HO-PSt-OH, were negligible.

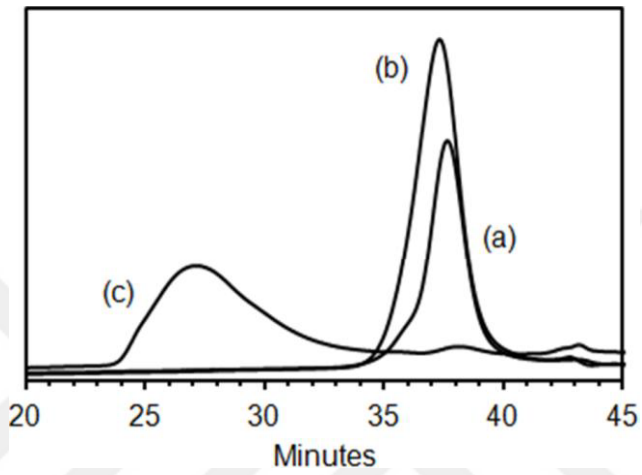

Figure 3.56. SEC traces of (a) OEO-b-PIB-b-OEO, (b) HO-PSt-OH and (c) OEO-b-PIB-b-OEO/PSt PU.

Table 3.11. Molecular weight analysis data of OEO-b-PIB-b-OEO/PSt PU.

Sample	$M_{n,SEC}$ (g/mol)	$M_{p,SEC}$ (g/mol)	PDI_{SEC} (M_w/M_n)
OEO-b-PIB-b-OEO/PSt PU	92418	165859	2.13

3.2.5.4. OEO-b-PSt-b-OEO/OEO-b-PSt-b-OEO PU. The idealized micromorphology and the synthesis strategy of OEO-b-PIB-b-OEO/ OEO-b-PSt-b-OEO PU are shown in Figure 3.57 and 3.58, respectively. In the model, the solid black and the dotted green lines are PIB and EO blocks of OEO-b-PIB-b-OEO. The solid blue and the dotted green lines are PSt and EO blocks of OEO-b-PSt-b-OEO. The solid red lines correspond to the hard segments. The thin yellow lines represent H bonding within the urethane hard segments.

The prepolymer with terminal isocyanates was synthesized by reacting a mixture of OEO-b-PIB-b-OEO and OEO-b-PSt-b-OEO with a stoichiometric excess of MDI in the presence of DBTDL catalyst (0.1 mol% with respect to MDI) in THF. Then, the

prepolymer was chain extended to higher molecular weights upon the addition of BDO (Figure 3.58).

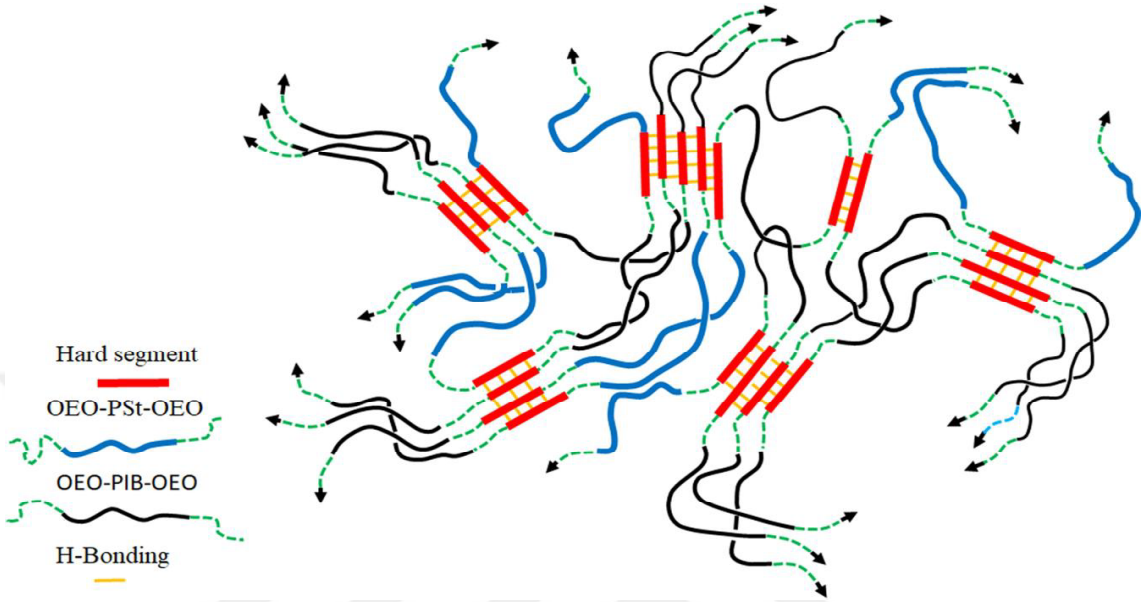

Figure 3.57. The idealized micromorphology of OEO-b-PIB-b-OEO/OEO-b-PSt-b-OEO PU.

The amounts of reagents were calculated using the equations

$$\frac{wt_{OEO\text{-}b\text{-}PIB\text{-}b\text{-}OEO}}{wt_{OEO\text{-}b\text{-}PIB\text{-}b\text{-}OEO} + wt_{OEO\text{-}b\text{-}PSt\text{-}b\text{-}OEO} + wt_{MDI} + wt_{BDO}} - 0.7, \quad (3.15)$$

$$n_{OEO\text{-}b\text{-}PIB\text{-}b\text{-}OEO} + wt_{OEO\text{-}b\text{-}PSt\text{-}b\text{-}OEO} + n_{BDO} = n_{MDI}, \quad (3.16)$$

where the wt% of OEO-b-PIB-b-OEO was 70% and the mole ratio of NCO to the total OH groups was one.

Figure 3.59 presents the ^{1}H NMR spectrum of OEO-b-PIB-b-OEO/OEO-b-PSt-b-OEO PU in $CDCl_3$. The peak at 3.63 ppm originates from the EO blocks attached to PIB and PSt. The spectra of OEO-b-PIB-b-OEO/PSt PU and OEO-b-PIB-b-OEO/OEO-b-PSt-b-OEO PU are very similar. The peaks at 4.21 (peak d) and 4.12 ppm (peak h) are assigned to OCH_2 protons of OEO-b-PIB-b-OEO soft segment and BDO attached to urethane, respectively. Other peaks typical of PIB and PSt segments can be listed as overlapping CH_2 protons of PIB and aliphatic main chain protons of PSt at 1.2-2.0 ppm (Peak k,l,b), overlapping aromatic protons of PSt and MDI at 6.8-7.4 ppm (Peak a,e,f,i), and CH_2 protons of MDI at 3.88 ppm (peak g).

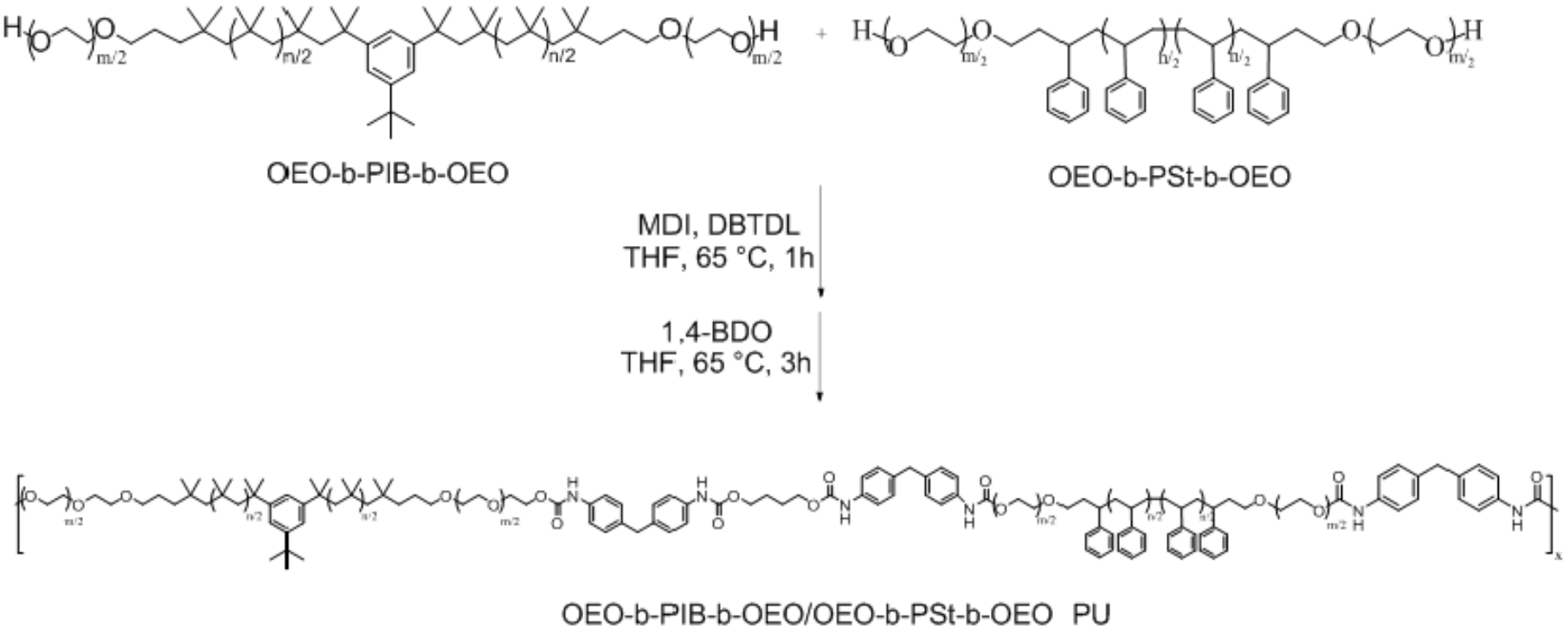

Figure 3.58. Synthesis of OEO-b-PIB-b-OEO/OEO-b-PSt-b-OEO PU

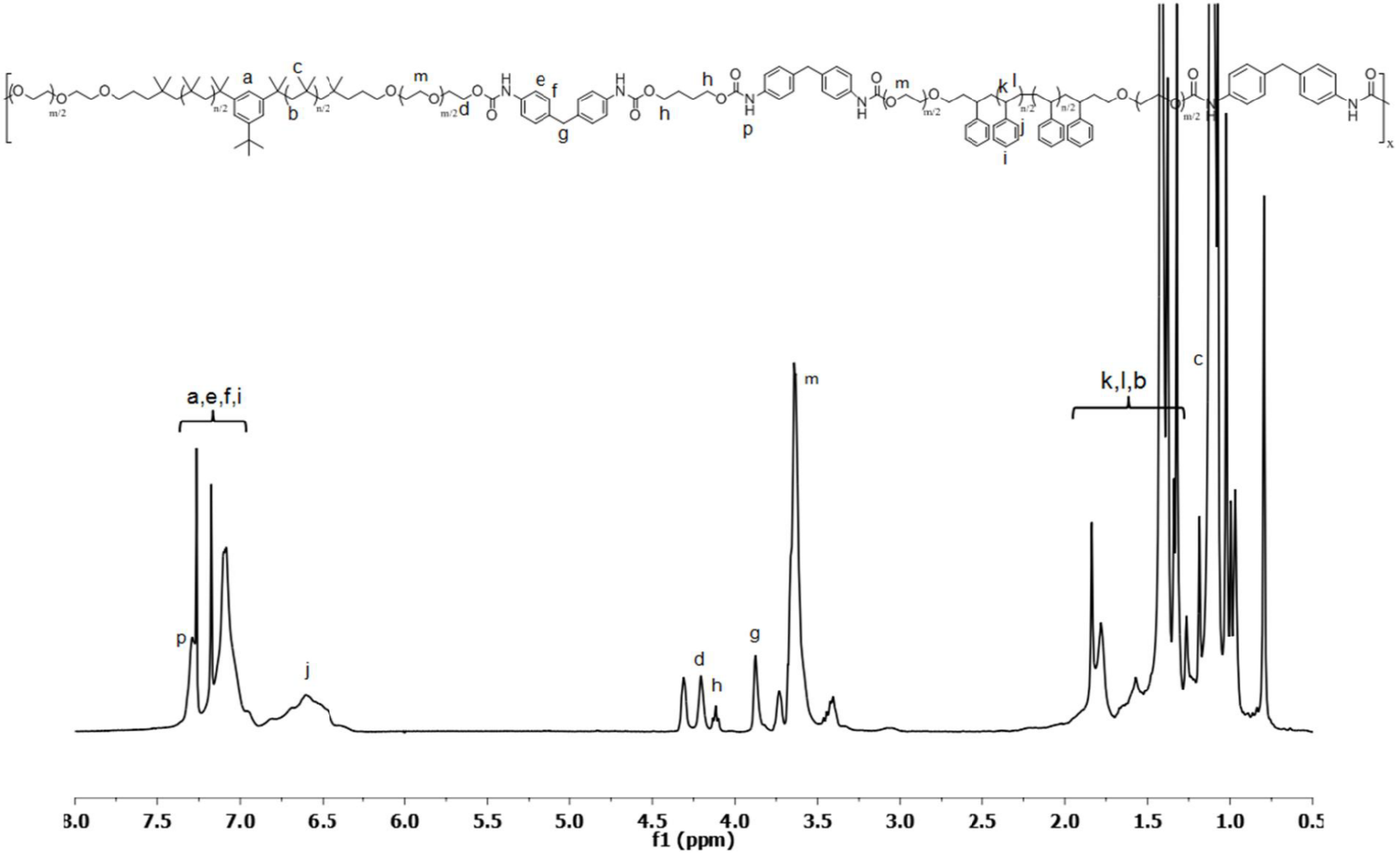

Figure 3.59. ^{1}H NMR spectrum of OEO-b-PIB-b-OEO/OEO-b-PSt-b-OEO PU in $CDCl_3$.

Figure 3.60 shows the FTIR spectrum of OEO-b-PIB-b-OEO/OEO-b-PSt-b-OEO PU. The inserts zoom in the region 900-1300 and 3100-3700 cm^{-1} of PIB/PSt PU and OEO-b-PIB-b-OEO/OEO-b-PSt-b-OEO PU. In the spectrum of OEO-b-PIB-b-OEO/OEO-b-PSt-b-OEO PU, the increase in the breadth of the peak at 1109 cm^{-1} and the emergence of a broad shoulder at ~1140 cm^{-1} can be assigned to C–O–C stretching vibrations of EO units originating from OEO-b-PIB-b-OEO and OEO-b-PSt-b-OEO PU. Unlike PIB/PSt PU, the C=O strecthing band shows two distinct peaks at 1730 and 1703 cm^{-1}, which are assigned to free and H bonded C=O groups, respectively. Besides, the comparison of the NH absorption region for PIB/PSt and OEO-b-PIB-b-OEO/OEO-b-PSt-b-OEO PU shows that in the latter the breadth of the band increases and the peak maxima shifts from 3323 to 3308 cm^{-1}. The rest of the spectral features are very similar in the two spectra. Those can be listed as aromatic (=C—H) and aliphatic C—H stretching (2800-3100 cm^{-1}), overlaping NH bending and CN stretching (1533 cm^{-1}), and C–O–C stretching (1073 cm^{-1}), and swing of the CH_3 groups in the PIB backbone (1388 and 1365 cm^{-1}). Aromatic ring stretching vibrations of PSt overlap with CH bending vibrations of PIB at 1420-1500 cm^{-1} region.

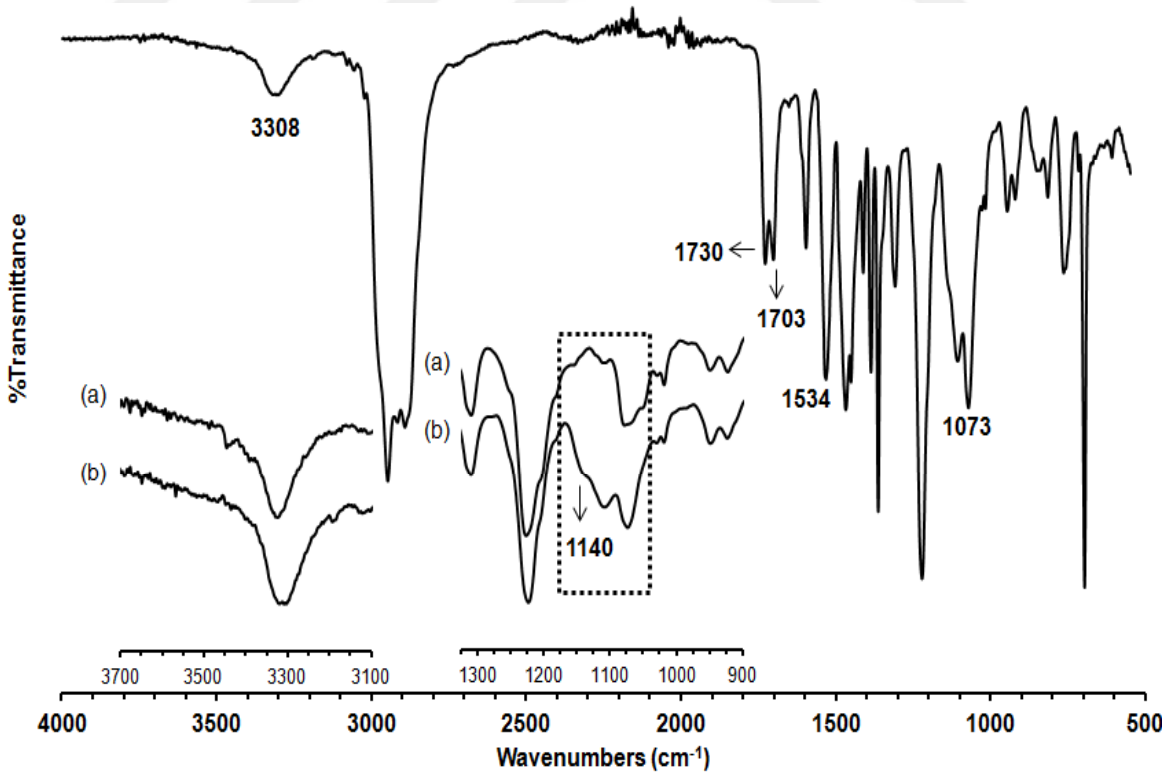

Figure 3.60. FTIR spectrum of OEO-b-PIB-b-OEO/OEO-b-PSt-b-OEO PU. Inserts: Expanded 900-1300 and 3100-3700 cm^{-1} ranges for (a) PIB/PSt PU and (b) OEO-b-PIB-b-OEO/OEO-b-PSt-b-OEO PU.

The molecular weight data of OEO-b-PIB-b-OEO/OEO-b-PSt-b-OEO PU obtained from SEC is given in Table 3.12. As evident in the SEC chromatograms (Figure 3.61), the peak maximum of OEO-b-PIB-b-OEO/OEO-b-PSt-b-OEO PU was located in the higher molecular weight region, while the peak originating from the unreacted starting polymers, OEO-b-PIB-b-OEO and OEO-b-PSt-b-OEO, were negligible.

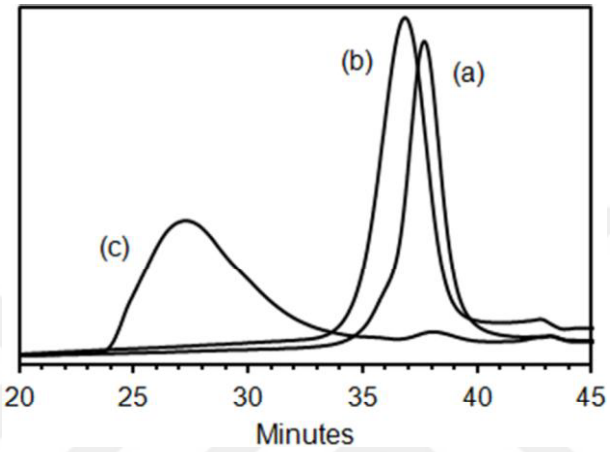

Figure 3.61. SEC traces of (a) OEO-b-PIB-b-OEO, (b) OEO-b-PSt-b-OEO, and (c) OEO-b-PIB-b-OEO/OEO-b-PSt-b-OEO PU.

Table 3.12. Molecular weight analysis data of OEO-b-PIB-b-OEO/OEO-b-PSt-b-OEO PU.

Sample	$M_{n,SEC}$ (g/mol)	$M_{p,SEC}$ (g/mol)	PDI_{SEC} (M_w/M_n)
OEO-b-PIB-b-OEO/OEO-b-PSt-b-OEO PU	88547	154876	2.17

3.2.6. Static and Dynamic Mechanical Properties of PIB/PSt Based PUs

Figure 3.62 displays the stress-strain curves of PUs based on PIB/PSt with or without oligoethyleneoxide (OEO) moieties in their structure. Besides, the creep and tensile creep compliance versus time traces and DMA thermograms for the same series of samples are shown in Figure 3.63 and Figure 3.64 respectively. Table 3.13 provides a summary of characteristic static and dynamic data including tensile stress, strain, tan delta, creep strain/ recovery and permanent deformation values for all PSt/PIB based PUs.

PIB PUs are thermoplastic elastomers that contain both PIB soft domains and crystalline hard domains, which include hydrogen bonding between PU chains. The inclusion of PSt as an additional hard domain in PIB-based PU leads to a reduction in both tensile strength and elongation at break values. This is probably due to the destruction of the typical ordered hard domain morphology in PU, resulting in decreased toughness and lower creep resistance. As a result, very high levels of creep strain and permanent set values are observed. All these negative results indicate that PSt as a very rigid and incompatible domain with PIB, disturbs the crystalline order in PIB-PU. Creep strain, as a time dependent deformation under load, of PIB/PSt PU seems ~% 500 higher than that of PIB PU (Table 3.13), suggesting that lack of considerable chain entanglements and diffuse interphases between hard and soft segments. In spite of this, DMA results indicate a higher tan delta values for PSt containing PUs, which shows the plastic contribution of PSt in the polymer matrix.

Usage of oligomeric EO telechelic units instead of OH, on the other hand, will cause formation of third oligomeric EO phase carrying PIB and PSt phases together with suitable hydrogen bonding sites, leading to a kind of compatibilization and urethane formation (Figure 3.47, 52 and 57). It has been found that by utilizing an OEO-assisted phase mixing method, which involves combining continuous and flexible stress distribution in OEO-b-PIB-b-OEO/OEO-b-PSt-b-OEO PU, there is a significant increase in tensile strength by almost four times and in elongation at break values by two times compared to PIB/PSt PU. Moreover, this technique leads to higher toughness, as demonstrated by higher tan delta values (Table 3.13). It is worth the say that special morphology reached exhibits higher creep resistancy -almost 50 % decrease- as well as recoverability than PIB/PS PU structure. At this point PIB chains tethered to cohesive PSt domains are able to recover their orginal configurations after force removal by leaving quite low permanent deformation. Moreover location, either in PIB or PSt or both seems to affect the phase mixing degree. It can be safely concluded that high strength, tough and creep resistant PIB/PSt PUs can be prepared with oligomeric di-EO telecelicity in both phase. All these results make newly synthesized EO based PIB/PS PUs quite promising against conventional low strength (2-14 MPa, less damping (0.55 tan delta) and low creep resistantancy (60 % creep strain) SIBS (Mn (SIBS) = 59300g/mol, 29 wt% St) [51], [137,138].

It is well known that PIB-PUs with 70% soft segment have an inert array of PIB soft segments that protects the urethane (-NHCOO-) hard segments from environmental vulnerability, resulting in increased oxidative hydrolytic resistance [14]. However, in the case of PSt PU, which reached a very high stress at break value (50 MPa), property changes such as brittleness were observed after a while, and dynamic mechanical analysis could not be performed.

Table 3.13. Static/Dynamic Mechanical data for PIB/PSt based PUs and SIBS [51], [137].

SAMPLE	**Stress (MPa)**	**Elongation (%)**	**Creep Strain (%)**	**Permanent Deformation (%)**	**Creep/Strain Recovery (%)**	**Tan delta**
PIB PU	16.34	223.61	5.08	0.66	87.10	0.70
OEO-b-PIB-b-OEO PU	20.9-25.7	253.5-269.8	9.42	1.45	84.62	0.84
PSt PU	43.6-49.6	1.82	-	-	-	-
OEO-b-PSt-b-OEO PU	3.9-5.9	0.42	-	-	-	-
PIB/PS PU	4.9-6.7	63.4-224.9	27.42	2.41	91.22	0.95
PIB/OEO-b-PSt-b-OEO PU	10.69	259.82	43.12	3.83	91.13	0.96
OEO-b-PIB-b-OEO/PSt PU	18.4-20.9	253.4-282.9	28.31	2.56	90.95	0.85
OEO-b-PIB-b-OEO/OEO-b-PSt-b-OEO PU	16.9-24.8	280.9-299.6	27.92	1.99	92.84	1.35
SIBS	14.2	507	~60[1]	~5[1]	~92[1]	0.55

[1] reference [137]

Additionally, the brittleness feature appeared in OEO-b-PSt-b-OEO immediately after the film was prepared. We attribute this negative feature observed in PSt-based PUs to the fact that PSt does not provide sufficient protection to the urethane hard segment, which causes an increase in oxygen and moisture permeability, leading to a decrease in oxidative and hydrolytic resistance of the material.

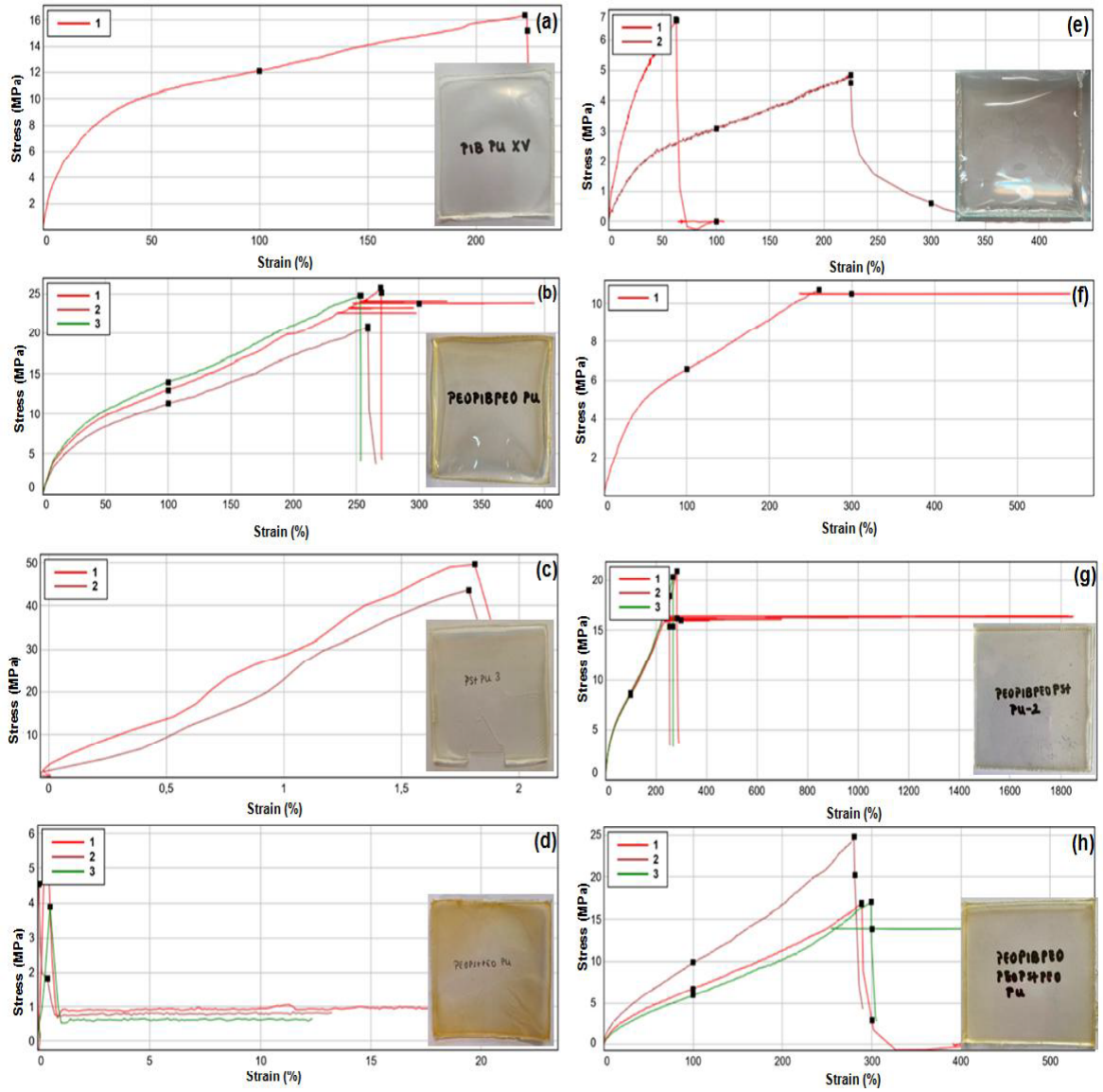

Figure 3.62. Stress-strain traces of (a) PIB PU, (b) OEO-b-PIB-b-OEO PU, (c) PSt PU, (d) OEO-b-PSt-b-OEO PU, (e) PIB/PS PU, (f) PIB/OEO-b-PSt-b-OEO PU, (g) OEO-b-PIB-b-OEO/PSt PU, (h) OEO-b-PIB-b-OEO/OEO-b-PSt-b-OEO PU.

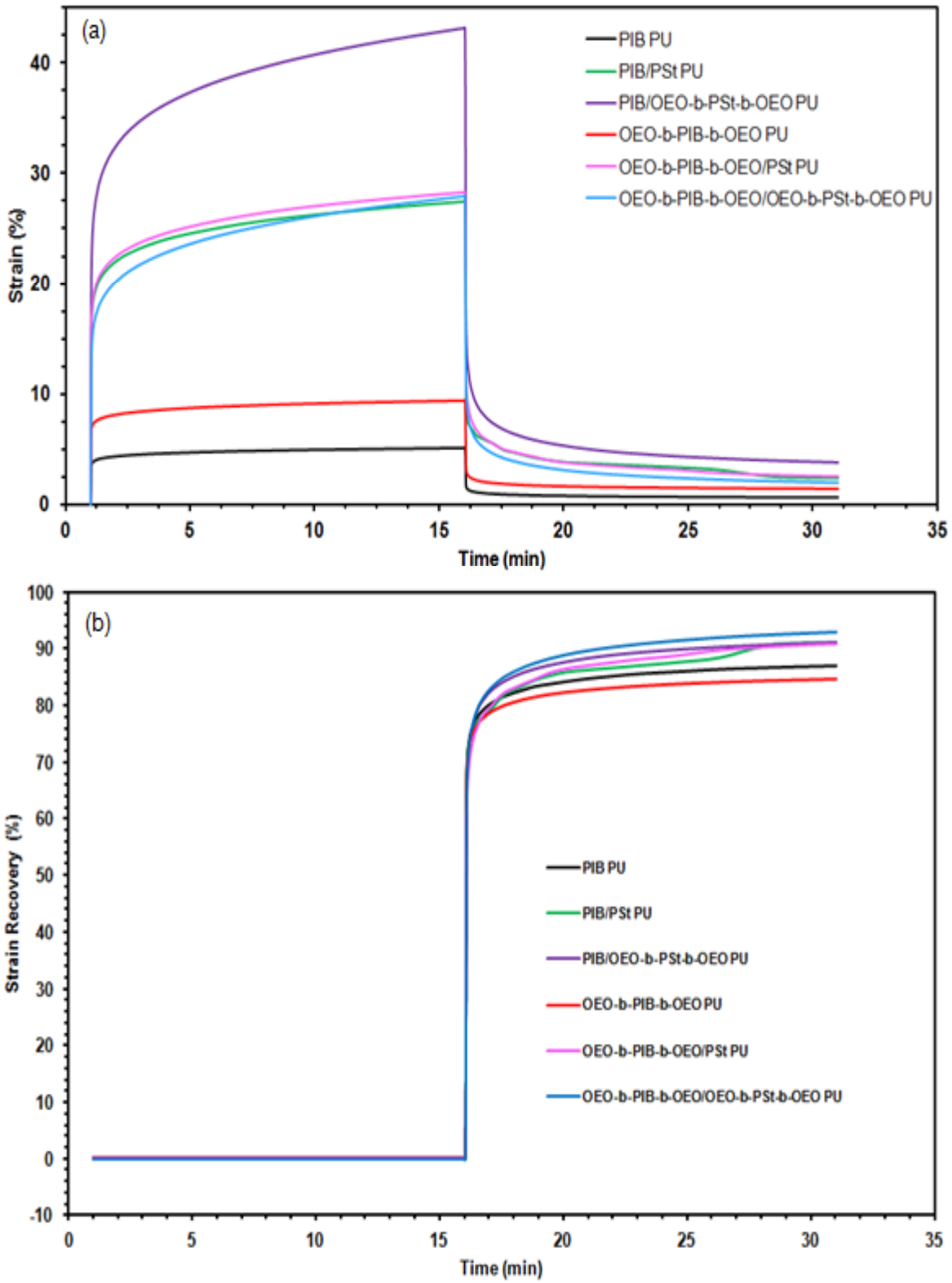

Figure 3.63. (a) Creep versus time and (b) tensile creep compliance versus time of PIB PU, OEO-b-PIB-b-OEO PU, PIB/PS PU, PIB/OEO-b-PSt-b-OEO PU, OEO-b-PIB-b-OEO/PSt PU and OEO-b-PIB-b-OEO/OEO-b-PSt-b-OEO PU.

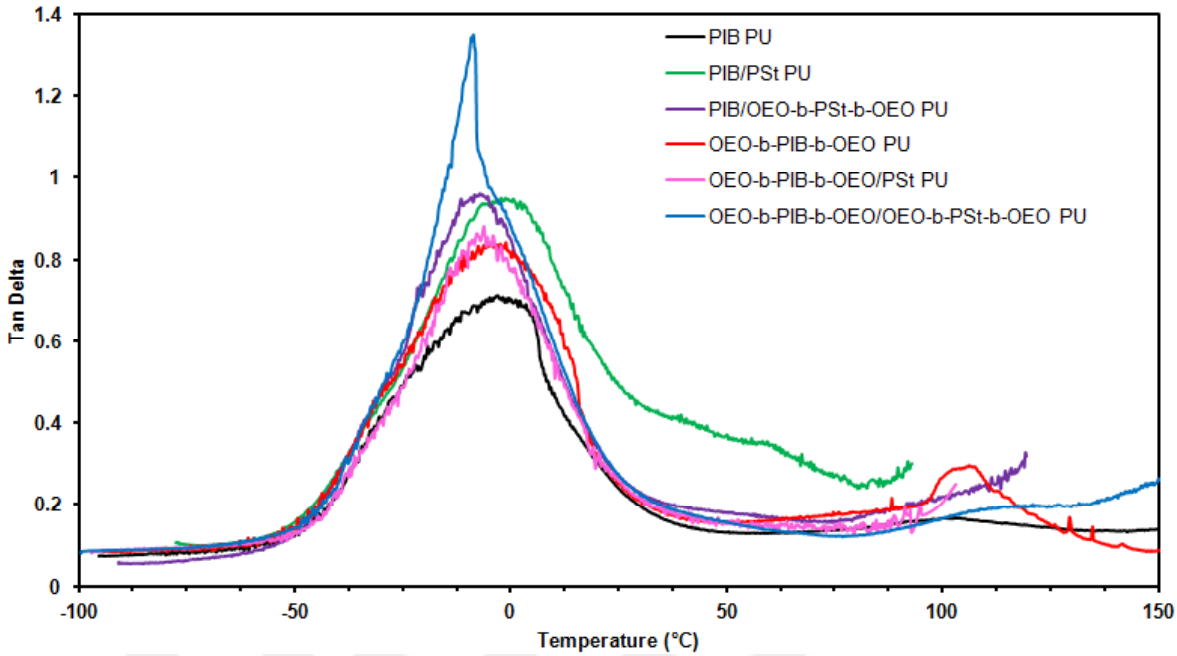

Figure 3. 64. DMA thermograms of PIB PU, OEO-b-PIB-b-OEO PU, PIB/PS PU, PIB/OEO-b-PSt-b-OEO PU, OEO-b-PIB-b-OEO/PSt PU and OEO-b-PIB-b-OEO/OEO-b-PSt-b-OEO PU.

3.2.7. Thermal Properties of PIB/PSt Based PUs

Thermal transitions of PIB/PSt PUs with and without OEO moieties are shown in Figure 3.65-66. Table 3.14 summarizes thermal transition data, including glass transition and melting temperatures.

The soft PIB phase transition in PIB/PSt PU appears around the same temperature, ~ -55 °C with PIB PU. On the other hand, the characteristic hard phase transition arising from amorphous PU segments has shifted from almost 75 °C to a higher temperature of around 110 °C with the additional rigid PSt domains having a Tg of about 100 °C [139]. Besides, disappearence of typical melting endotherm at 189 °C as a signature of highly ordered hard phase in PIB/PSt PU can be attributed to possible destruction of the order in this phase. Based on this observation, we can confirm the conclusions we drew from analyzing the mechanical test results.

When we compare the thermal transitions of PSt PU and OEO-b-PSt-b-OEO PU, we have observed some differences. In the case of PSt-PU, there are two transitions present at

103.13 °C and 116.75 °C, which originate from the PSt segments. As we predicted and mentioned above, there is no hard phase-induced melting point for this example, which could be due to the PSt segments preventing crystallization in the PU domain. It is likely that the addition of H-bonds through urethane segments on the polymer chain causes the observation of a second Tg at a temperature higher than the Tg value of pure PSt.

In the OEO-b-PSt-b-OEO PU samples, we observed three thermal transitions at 67.63 °C, 101.20 °C, and 193.07 °C, respectively (Table 3.14). The melting point of low molecular weight PEO is around 38 °C [140]. Although the melting peak at 38°C is uncertain (Figure 3.65), we believe that the transition at 67 °C may be due to a section of the PSt chain connected to the OEO segments. The melting peak at 193°C shows the formation of PU crystalline domains, which is due to the flexibility offered by OEO chains. This temperature exceeds the melting point of PIB PU's PU domain. This is due to the PU segments being linked to PSt chains with high Tg values instead of an elastomeric structure. The poor mechanical properties and brittleness of OEO-b-PSt-b-OEO PU samples suggest high tensions between plastic and crystalline phases, despite their promising thermal properties.

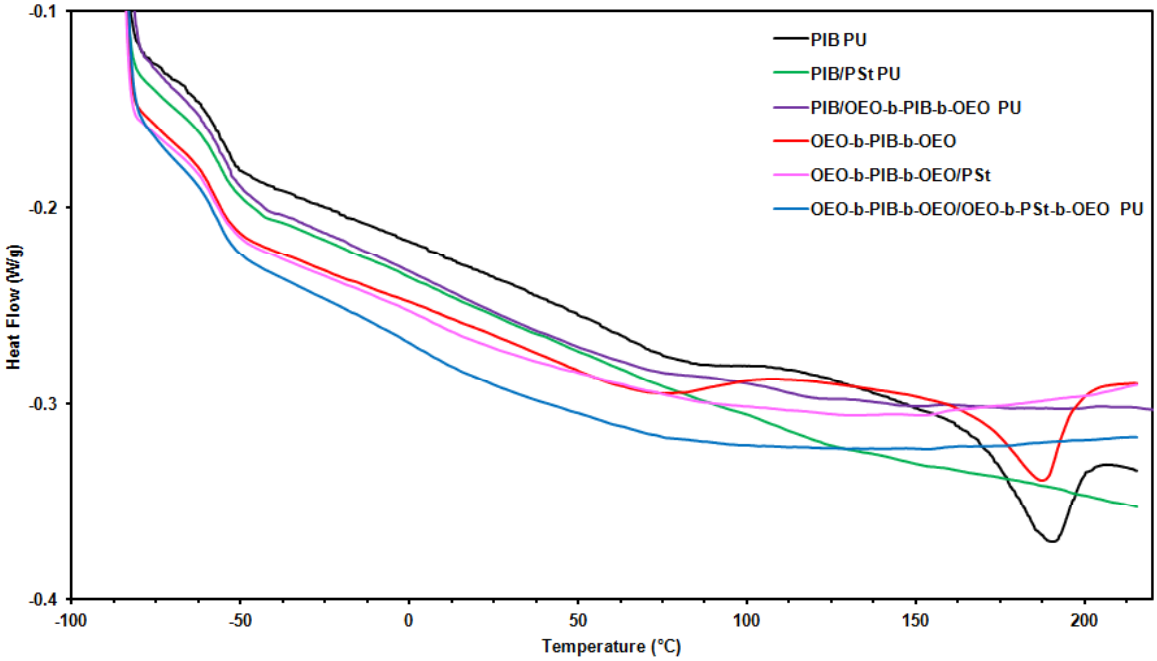

Figure 3.65. DSC thermograms of PIB PU, PIB/PS PU, OEO-b-PIB-b-OEO PU, PIB/OEO-b-PSt-b-OEO PU, OEO-b-PIB-b-OEO/PSt PU and OEO-b-PIB-b-OEO/OEO-b-PSt-b-OEO PU.

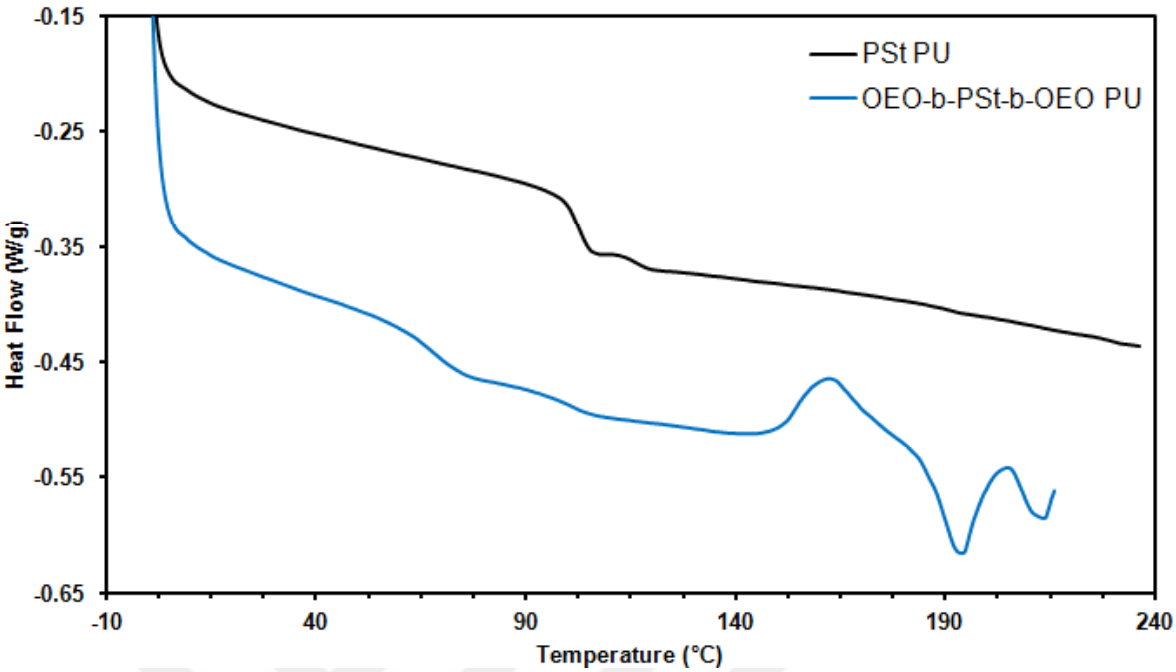

Figure 3.66. DSC thermograms of PSt PU and OEO-b-PSt-b-OEO PU.

Table 3.14. Thermal transition data for PIB/PSt based PUs.

PU	**T_g soft**	**T_g hard**	**T_m**
PIB PU	-53.06	75.39	189.48 5.647J/g
PSt PU		116.75 103.13	-
OEO-b-PSt-b-OEO PU		67.63 101.20	182.66 8.209J/g (max 193.07)
OEO-b-PIB-b-OEO PU	-58.97		187.61 5.892J/g
PIB/PSt PU	-55.81	110.98	-
PIB/OEO-b-PSt-b-OEO PU	-56.58	71.15 110.30	-
OEO-b-PIB-b-OEO/PSt PU	-58.22	80.06 121.59	-
OEO-b-PIBOEO/OEO-b-PSt-b-OEO PU	-58.61	75.85	-

3.3. Conclusions

In the first part of this study, the synthesis of PSt and PIB based PUs was planned to perform. To attain these materials;

i) A-PIB-A was synthesized with a very high allyl functionality (>99%) using the TBDCC/$TiCl_4$ initiating system, followed by quenching the living chain ends with ATMS. Then, regioselective hydroboration of the allyl functional chain ends with 9-BBN followed by alkaline hydrogen peroxide cleavage of carbon-boron bonds yields HO-PIB-OH.

ii) OH-PSt-OH was successfully synthesized with high hydroxyl functionality (>99%) by anionic polymerization of styrene initiated by Li naphthalenide, and followed by quenching of the living chain ends with EO.

iii) To synthesize OEO-b-PIB-b-OEO, the hydroxyl terminals of OH-PIB-OH were converted to corresponding K alkoxides by deprotonation with DPMK. Then, these alkoxides served as a macroinitiator in the anionic ring-opening oligomerization of EO. ^{1}H NMR characterization indicated the addition of an average of 7.4 EO units per chain.

iv) OEO-b-PSt-b-OEO was obtained by the partial deprotonation of HO-PSt-OH with DPMK and successive anionic ring-opening oligomerization of EO. An average of 14 EO units were added per chains according to ^{1}H NMR characterization.

v) By using these starting materials, MDI and 1,4-butanediol in the presence of a catalyst PIB PU, OEO-b-PIB-b-OEO PU, PIB/PS PU, PIB/OEO-b-PSt-b-OEO PU, OEO-b-PIB-b-OEO/PSt PU and OEO-b-PIB-b-OEO/OEO-b-PSt-b-OEO PU were synthesized. The molecular characterization of each product conducted by ^{1}H NMR, FTIR, and SEC demonstrated successful synthesis of them.

vi) The dynamic and static mechanical tests of the abovementioned PIB/PSt PUs revealed that the high strength, tough and creep resistant PIB/PSt PUs can be prepared with oligomeric di-EO telecelicity in both phase. All these results make newly synthesized EO

based PIB/PS PUs quite promising against conventional low strength and low creep resistantancy SIBS.

vii) The soft PIB phase transition in PIB/PSt PU appears around the same temperature, ~-55 °C with PIB-PU. On the other hand, the characteristic hard phase transition arising from amorphous PU segments has shifted from almost 75 °C to a higher temperature of around 110 °C with the additional rigid PSt domains having a Tg of about 100 °C. Besides, disappearence of typical melting endotherm at 189 °C as a signature of highly ordered hard phase in PIB/PSt PU can be attributed to possible destruction of the order in this phase.

4. SYNTHESIS OF SOYBEAN OIL POLYOLS VIA THIOL-ENE CHEMISTRY AND THEIR USAGE IN POLYISOBUTYLENE BASED POLYURETHANE

This chapter is published as: Kurnaz, E., S. Şen, N. Nugay, and T. Nugay, "Biobased Reprocessable Polyisobutylene - Polyurethane Networks", *Journal of Polymer Research*, 30, 327, 2023. This copyrighted article was reproduced with permission from Springer Nature (Figure B.24).

4.1. Introduction

Polyurethanes (PUs) are distinguished from other classes of polymer by their unique segmented block copolymer structure that originated from hard urethane and soft polyol segments [74]. As a result of their distinguished mechanical properties and biocompatibility, PUs are preferred polymers for medical devices. Current biomedical applications of PU are catheters, blood oxygenators, stents, cardiac valves, dialysis devices, dressings, adhesives, drug delivery devices, tissue engineering, pacemaker, and coatings for breast implants [76], [132], [141]. Major handicap of PUs is the lability of inherent urethane linkages to hydrolysis and oxidation. Besides that, the common soft segments like polyethers, polyesters, polycarbonates and polydimethylsiloxanes are also reported to suffer from hydrolytic and oxidative deterioration, and hence these PUs are not able to maintain their superior mechanical properties for long term medical applications [80,81], [142]. It has been reported that although polyurethanes exhibited appropriate mechanical properties for heart valve function, the biological instability of earlier generations put limitations to cardiac applications [142]. Therefore achieving mechanical durability and biostability at the same time is an overarching objective of the researchers.

Polyisobutylene (PIB), on the other hand, is a valuable polymer with outstanding oxidative-hydrolytic-chemical stability, gas impermeability and biocompatibility [75]. PIB is used broadly in areas where environmental and chemical stability, gas impermeability

and high damping characteristics are required, such as tire inner liners (i.e., halogenated butyl rubbers), vibration proof materials and engine mounts, as well as in biomaterial applications e.g., TAXUS coronary stent coating [3], [71]. In this context, PIB based PUs have been realized as unique materials that would embody the superior properties of individual polymers; that is, exceptional inertness, chemical and biostability of PIB and high strength of segmented thermoplastic PUs [75]. Recently, Naficy et al. presented an excellent review on advancements in polyurethane heart valve replacements (HVRs) by addressing the shortcomings of earlier generation of polyurethane HVRs [142]. They pointed out to PIB based polyurethanes in their future perspectives as a potential material having robust performance, calcification resistance, relatively low protein adsorption - particularly the ones with some PTMO co-soft segments and high hydrolytic stability than polyether urethanes and ureas, polycarbonate urethanes and polysiloxane urethanes [142]. Moreover, even only 70 % PIB based PUs without any PTMO co-soft segment with considerably high mechanical strength, hydrolytic-oxidative stability [88], [78,79], calcification resistivity [143], biocompatibility [144] as well as impressive fatigue resistance were recently reported as a superior alternative to conventional TPUs for a synthetic heart valve application [132].

On the other hand, while fossil based starting materials of polyurethanes in biomedical applications are improving, renewable contents seem to be necessary for most of them in order to have a certificate and increase their 0.1% market share [145]. Production of bio-based polyurethanes and their hybrids with petroleum based polyols are thought to be one of the most important issues also for the protection of global environment [146]. Although there has been a considerable research effort on synthesis and characterization of segmented polyurethanes from renewable polyols and diisocyanates [146-148], studies on their hybrids with polyisobutylene based polyol are not included in the literature yet.

In current study it is aimed to develop a synthetic approach for the preparation of a novel bio-based PIB-PU with a soybean oil derivative, X-SBO/PIB-PU. The important milestones of the study are (a) to convert SBO triglycerides to a polyol with primary hydroxyl functionalities via UV activated thiole-ene chemistry, (b) to optimize the grafting efficiency, (c) to synthesize novel X-SBO/PIB-PU. A short strategy were also proposed to

make the resultant networks reprocessable by selective hydrolysis of network moieties which can be resulting in a soyben oil based PIB-PU having valuable polar sites for their further blends and composites forms.

4.2. Experimental

4.2.1. Materials

Hydroxyl telechelic PIB (OHTPIB, $M_{n,NMR}$ = 4418 g/mol) was synthesized as described previously [149]. Dibutyltin dilaurate (DBTDL), 2-mercaptoethanol, diethyl ether (DEE), hydrochloric acid (HCl, 37%), calcium hydride (CaH_2), sodium bicarbonate ($NaHCO_3$) and sodium sulfate (Na_2SO_4) were purchased from Merck and used as received. Dichloromethane (DCM) and tetrahydrofuran (THF) obtained from Merck were refluxed and distilled over CaH_2. 1,4-butanediol (BDO) was purchased from Merck, dried over Na metal, and distilled under reduced pressure. 4,4′-Methylenebis(phenyl isocyanate) (MDI) obtained from Across was distilled under reduced pressure (~150 °C at 10^{-2} mmHg) and stored under N_2 atmosphere in the refrigerator. 2,2-dimethoxy-2-phenylacetophenone (DMPA) purchased from Across was used without further purification.

SBO was purchased from a local grocery shop and used after purification. Following extraction with water, the organic phase was dried over Na_2SO_4, purified by activated carbon, dissolved in toluene, and filtered through a fine-sintered glass. Following the complete removal of water using a Dean-Stark trap, toluene was evaporated on a rotary evaporator, and the oil was dried on the high vacuum line.

4.2.2. Synthesis of SBO Based Polyol

In a typical UV light activated thiol-ene addition reaction, SBO (5.00 g, 5.81 mmol triglyceride), 2-mercaptoethanol (2.75 g, 35.2 mmol, thiol/double bond = 1.44) and DMPA (1.19 g, 4.65 mmol, DMPA/double bond = 0.19) were weighed into a vial and dissolved in 6 ml DCM. The vial was sealed, purged with N_2 and placed into the UV chamber. After irradiation at 11 mW/cm^2 for 4 h at room temperature, the content was dissolved in DEE and extracted with water. The organic phase was dried over Na_2SO_4, filtered through a

sintered glass and the solvent was evaporated on the rotary evaporator. Finally, the modified oil was dried on the high vacuum line to remove any leftover solvent.

Table 4.1. Reaction conditions for the synthesis of SBO based polyol.

Experiment	SBO (mmol)	Thiol (mmol)	DMPA (mmol)	Solvent (DCM) (ml)	DMPA/ene mol ratio	Thiol/ene mol ratio	Reaction time (h)	UV Intensity (mW cm^{-2})
1	0.23	0.99	0.43	0.25	0.48	1.01	1	8
2	0.23	0.99	0.19	0.25	0.19	1.01	2	9
3	0.23	0.99	0.43	0.25	0.48	1.01	2	9
4	0.23	0.99	0.19	0.25	0.19	1.01	4	9
5	0.23	0.99	0.43	0.25	0.48	1.01	4	13
6	5.81	35.2	4.65	6.00	0.19	1.44	4	11
7	0.23	1.40	0.43	0.25	0.48	1.44	4	13

4.2.3. Synthesis of PIB-PU

PIB PU ($M_{n,SEC}$ = 80500 g/mol and MWD = 2.05) was also synthesized according the previous procedure for control purpose [132].

4.2.4. Synthesis of X-SBO/PIB-PU

OHTPIB (0.931 g, 0.211 mmol), SBO polyol (0.118 g, 0.105 mmol) and MDI (0.352 g 1.41 mmol) were weighed into a dried reactor equipped with a condenser. The mixture was degassed on the high vacuum line, charged with N_2, and dissolved in 4 ml dry THF. Prepolymerization reaction was carried out at 65 °C for 1 h upon addition of 0.5 ml of 1.84 mg/ml catalyst solution into the reactor. BDO (0.0982 g, 1.09 mmol) dissolved in 3 ml dry THF was transferred to the reactor via steel capillary under N_2 pressure. Two minutes after

transferring BDO solution, the polymer was cast into a 7 × 7 cm glass mold. THF was evaporated slowly at room temperature for 6 days. The film was further dried in vacuum oven at 60 °C for 20 h and annealed at 80 °C for 1 h.

4.2.5. Acid Catalyzed Hydrolysis of X-SBO/PIB-PU

Acid catalyzed hydrolysis reaction was carried out in a manner similar to that described by Murgasova et al. and Chapman [150,151]. 1.22 g of PU film was refluxed in HCl (0.25 M, 12.2 mmol) in 48.9 ml THF/water mixture (92 % THF by volume) at 70 °C for 48 h. Following the evaporation of the solvent, the hydrolysis product was dissolved in $CHCl_3$, washed with 1% $NaHCO_3$ solution and then with water. The organic phase was then dried over $MgSO_4$ and filtered. The solvent was then evaporated on the rotary evaporator. Finally, the product was solvent cast from THF into a glass mold, air dried for 6 days and vacuum dried for 20 h at 40 °C.

4.2.6. Characterization

UV light-initiated reactions were carried out in a UV chamber equipped with an air circulating fan and low-pressure mercury-vapor fluorescent lamps with an emission maximum at 365 nm. The intensity of light was measured between 8-13 mW/cm^2 by using UVA/B Light Meter.

^1H NMR spectra were obtained using a Varian Gemini 400 MHz in $CDCl_3$ (δ $CDCl_3$: 7.26 ppm) or pyridine (δ pyridine-d5: 7.22, 7.58 and 8.74 ppm).

The molecular weight distributions of the polymers were determined by Size Exclusion Chromatography (SEC) at 30 °C using Waters Isocratic HPLC Pump with Waters 2414 Refractive Index Detector and four Waters 4.6×300 mm Styragel columns HR 3, HR 4, HR 4E and HR 5E. Distilled THF was used as the mobile phase at a flow rate of 0.35 mL/min. PSt standards ranging from 400 to 2.5 × 10^6 g/mol were used for calibration. Samples were injected using 100 μL Hamilton syringe.

FTIR spectra were collected using a Thermo Scientific Nicolet 380 FTIR spectrometer with a smart orbit diamond ATR accessory. 32 scans for each sample with a resolution of 4 cm^{-1} were run in the frequency range of 500-4000 cm^{-1}. Spectral analysis was done using EZ-Omnic software.

Swelling measurement of dried film of the network was performed in THF at room temperature by determining deformations resulting from linear swelling ratio [152]. Lengths of the swollen films were measured using a traveling microscope at regular time intervals until equilibrium swelling was reached. The linear swelling ratio (λ) was calculated as

$$\lambda = \frac{L}{L_0}, \tag{4.1}$$

where L is the length of swollen film and L_0 is the dry length of the film before immersion in THF [152].

Differential Scanning Calorimetric (DSC) measurements were done with a DSC instrument (TA Q200) under N_2 atmosphere. The tests were carried out in a temperature range of -90-230 °C at a heating rate of 10 °C/min.

X-ray diffraction (XRD) analyses of the cast films (1.5×1.5 cm^2) were conducted on Rigaku D/Max-Ultimat diffractometer using CuKα radiation (λ=1.54 Å) as the X-ray source, operating at 40 kV and 40 mA. XRD patterns were recorded from 3° to 70° (2θ) with a scanning rate of 2°/min. Thermogravimetric analyses (TGA) of the samples were performed with a Seiko TG/DTA 6300 instrument in a temperature range of 20-600 °C at 10 °C/min heating rate under N_2.

Stress-strain traces were recorded on a Zwick/Roell Universal Testing Instrument with a 1 kN load cell. Strips (50 × 5 ×0.3 mm) were cut from solvent cast films and tested to failure at a drawing rate of 50 mm/min at room temperature [153].

4.3. Results and Discussion

4.3.1. Synthesis and Characterization of SBO Based Polyol

Considering the polyol is the main constituent of polyurethanes, a great deal of research has been done to functionalize vegetable oil fatty chains with hydroxyl groups in order to increase the bio-content of PUs [91,92], [99,100], [103,104], [154,155]. Commercial ones mostly depend on the epoxidation-ring opening strategy resulting in polyols with secondary hydroxyl groups which do not contribute to urethane formation effectively [103,104]. Hydroformylation and ozonolysis reactions are other strategies focusing on the functionalization of double bonds of fatty acid chains with primary hydroxyl groups via the intermediacy of an aldehyde but particularly the former one requires the use of expensive Rh catalyst for quantitative conversion. In the ozonolysis strategy, on the other hand, lower molecular weight polyol with less than three terminal hydroxyl groups can be achieved for oils with saturated fatty acid chains [103,104]. In spite of this, these methods proceed over two step mechanism. Therefore, radical addition of hydroxyl functional thiols to olefinic unsaturations, has emerged as a prominent alternative to the abovementioned strategies because thiol-ene reaction is one step reaction and allows preparation of polyols with primary hydroxyl functionalities under mild reaction conditions [102], [105-108], [111-115].

SBO polyols by UV induced thiol-ene addition of 2-mercaptoethanol onto triglycerides were synthesized under N_2 using DMPA as the photo initiator in DCM as shown in Figure 4.1. The effects of reaction parameters such as ratios of DMPA to double bond and thiol to double bond as well as irradiation time on the reaction efficiency were studied. For this purpose, 0.48 and 0.19 equiv. DMPA and 1.44 and 1.01 equiv. thiol with respect to double bond were studied at 8-13 mW/cm^2 irradiation intensity for 1-4 h reaction time as summarized in Table 4.1.

Figure 4.2 and 4.3 show ^1H NMR spectra of the purified SBO and the polyol obtained under the reaction conditions of 0.48 equiv. DMPA, 1.44 equiv. thiol at 13 mW/cm^2 for 4h. In the spectrum of SBO, the integral of the peak at 5.33 ppm (–CH=CH–) indicates about 4.2 double bonds per triglyceride and the peak centered at 5.25 ppm is due

to the glycerol unit (–CH_2–CH–CH_2–) [156]. In the spectrum of the SBO polyol, the absence of the peaks at 5.33 (–CH=CH–), 2.03 (–CH_2–CH=) and 2.76 ppm (=CH–CH_2–CH=) belonging to the unsaturations indicated an almost complete conversion of double bonds (~98%). Besides, the appearance of the peak at 2.6 ppm corresponding to the thioether group (–CH–S–) proves addition of 2-mercaptoethanol onto the double bonds and its integral indicates ~92 % grafting efficiency. The peaks at 2.7 (–S–CH_2–) and 3.7 ppm (–CH_2–OH) are due to the protons of the grafted 2-mercaptoethanol.

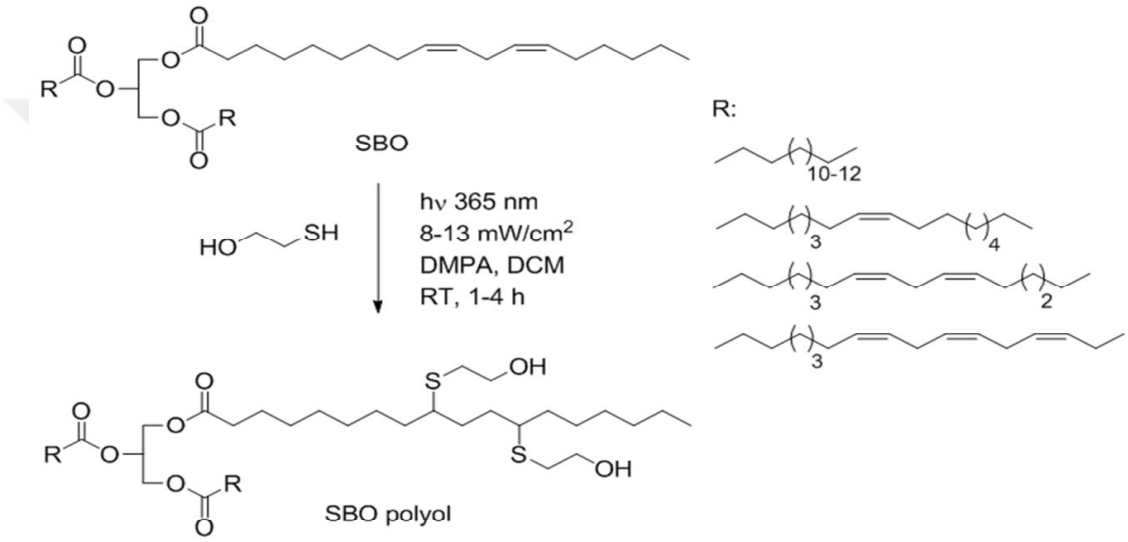

Figure 4.1. UV initiated thiol-ene addition of 2-mercaptoethanol onto triglycerides.

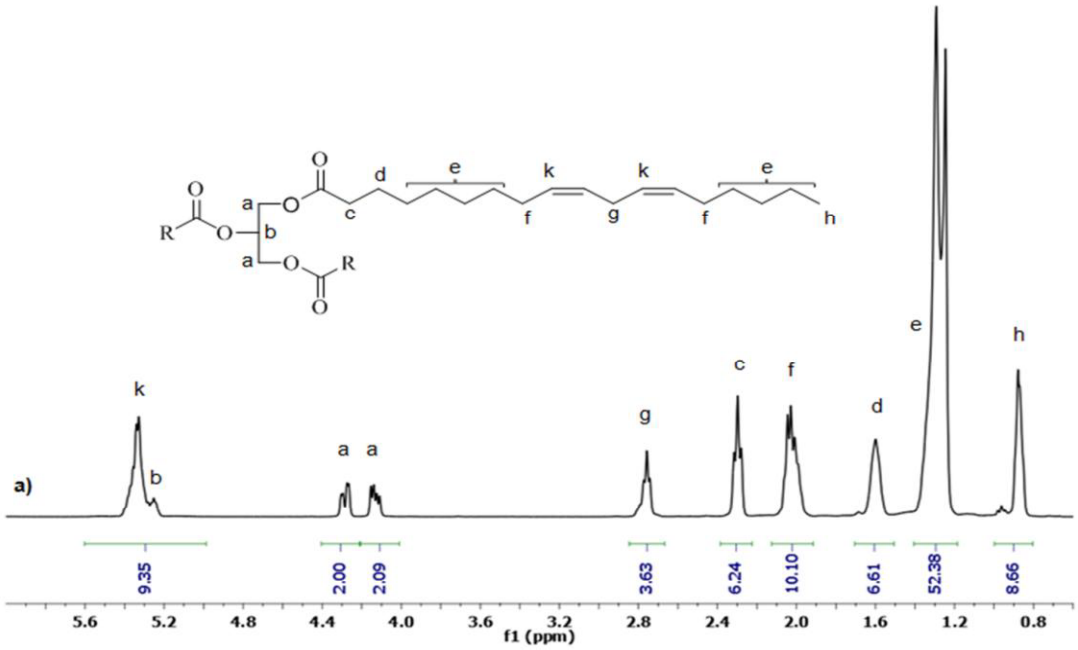

Figure 4.2. ^{1}H NMR spectrum of SBO.

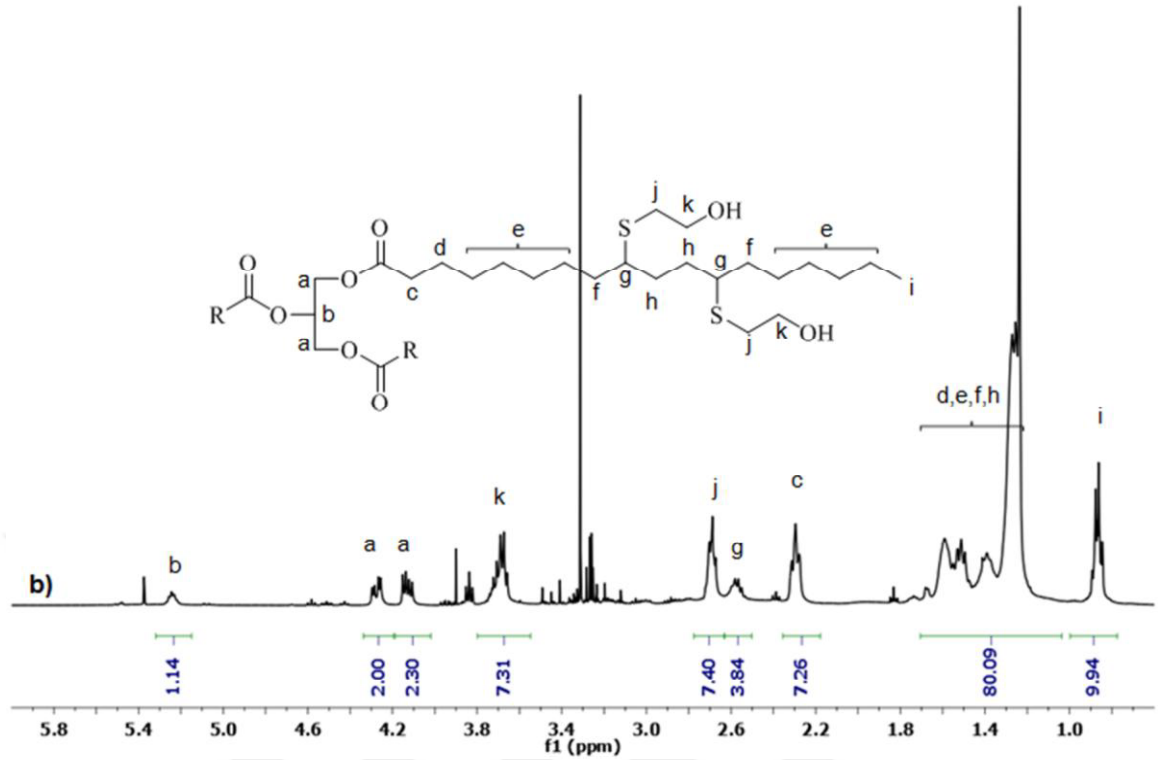

Figure 4.3. [1]HNMR spectrum of SBO polyol (experiment 7 in Table 1)

Figure 4.4 shows the [1]H NMR spectra of the polyols obtained from the set of reactions summarized in Table 4.1. One of the variables having a prominent effect on the reaction efficiency is the irradiation time. The integrals of the peaks at 2.6 ppm representing the proton attached to the carbon adjacent to the newly formed thioether moiety increase with increasing irradiation time, which is followed by a decrease and disappearance of above mentioned peaks at 5.3 ppm and 2.0 ppm. An almost complete consumption of the double bonds (SBO polyol experiment 7) was observed for 4h irradiation. The [1]H NMR spectra with peak integrals are also presented in Supplementary Material File (Figure A.2-A.7).

The conversions of double bonds and the grafting efficiencies were calculated by the ratio of the integrals of the peaks at 5.3 and 2.6 ppm, respectively, to the number of double bonds which is calculated to be 4.2 for the pristine SBO. As shown in Figure 4.5, for the reactions with the same mole ratios of DMPA/double bond, higher percentages of thiol-ene coupling were achieved when their thiol/double bond mole ratios were 1.44 (SBO polyol exp. 6 and 7). Also, among the reactions with the same mole ratios of thiol/double bond, higher percentages of thiol-ene coupling were obtained when their DMPA/double bond

mole ratios were 0.48 (SBO polyol exp. 5 and 7). Under the given reaction conditions, the highest thiol-ene coupling was obtained for the reaction with thiol/DMPA/double bond ratio of 1.44/0.48/1 and at 4 h irradiation.

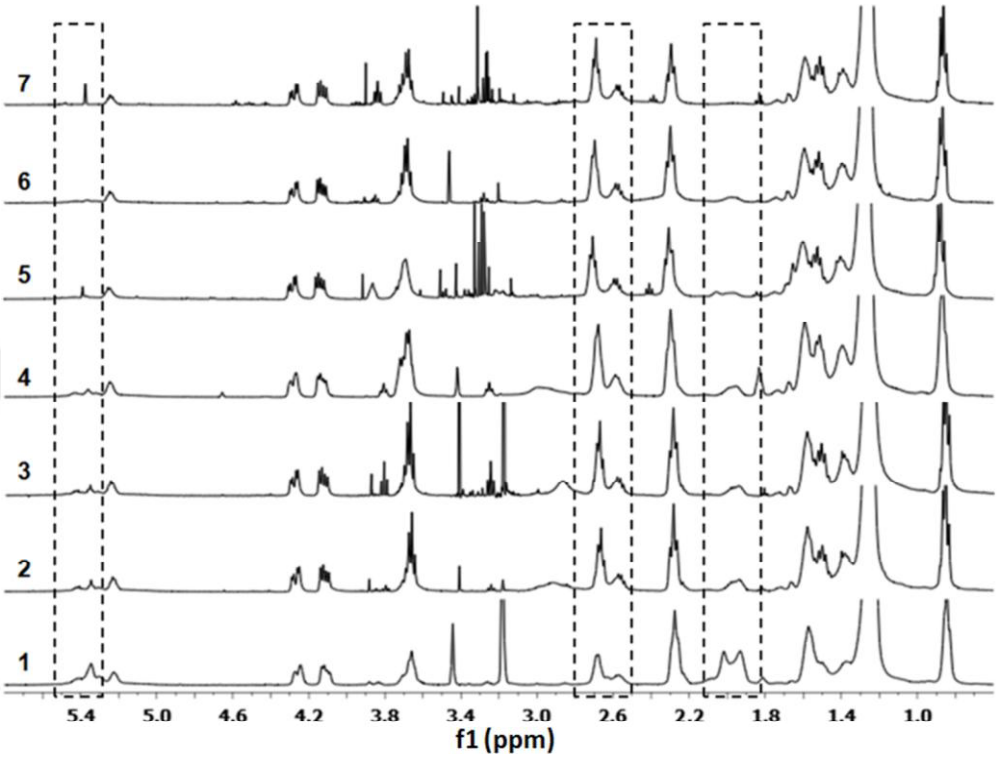

Figure 4.4. ^{1}H NMR spectra of the SBO polyols for different irradiation time and thiol/DMPA/double bond ratios (The numbers (1-7) represent the experiments given in Table 4.1).

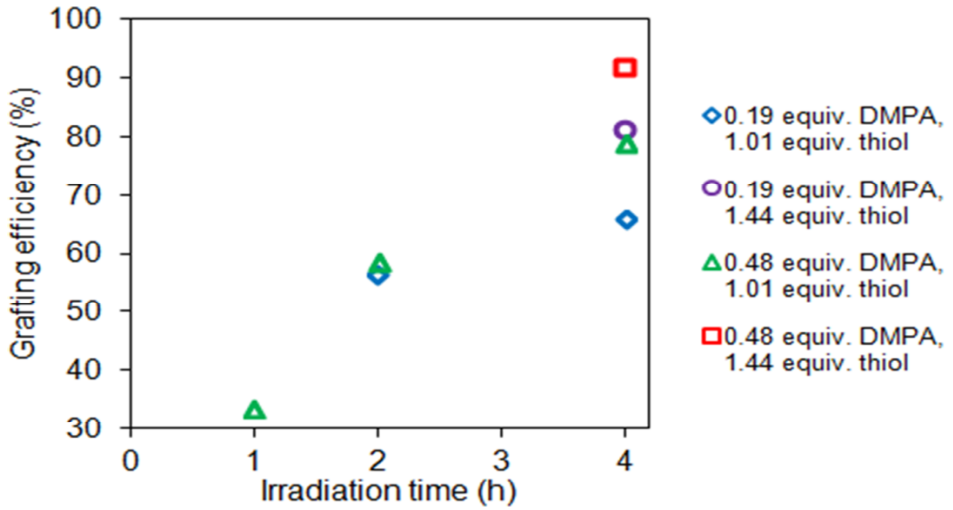

Figure 4.5. Grafting efficiencies for the photoinitiated addition of 2-mercaptoethanol onto SBO for different ratio of DMPA/ene and thiol/ene.

Thiol-ene coupling was also confirmed by FTIR technique. Figure 4.6 shows the spectra of pristine SBO and SBO polyol (thiol/DMPA/double bond=1.44/0.19/1, 4h, 81.3% grafting efficiency, 81.7% double bond conversion). The characteristic absorption bands of inherent functional groups of triglycerides, that is olefinic unsaturations and ester groups, can be easily detected. The bands associated with the internal double bonds appearing at 3008 and 1654 cm^{-1} were due to C—H stretching and weak C=C stretching vibrations of cis H—C=C—H, respectively [157]. C—H bending vibrations of cis double bonds also appeared as weak bands at 1418, 1397 and 913 cm^{-1}, those of trans double bonds appeared at 987 and 967 cm^{-1} [158,159]. Absorptions associated with the ester groups appeared at 1742 cm^{-1} due to strong C=O stretching vibrations and in the region 1300-1000 cm^{-1} due to C—O stretching vibrations [157–159].

After thiol-ene coupling reaction, the appearance of a broad band centered at 3430 cm^{-1} due to hydrogen bonded OH stretching vibrations, and a new distinctive peak observed at 1043 cm^{-1} due to CO stretching of primary alcohol proved the addition of 2-mercaptoethanol.

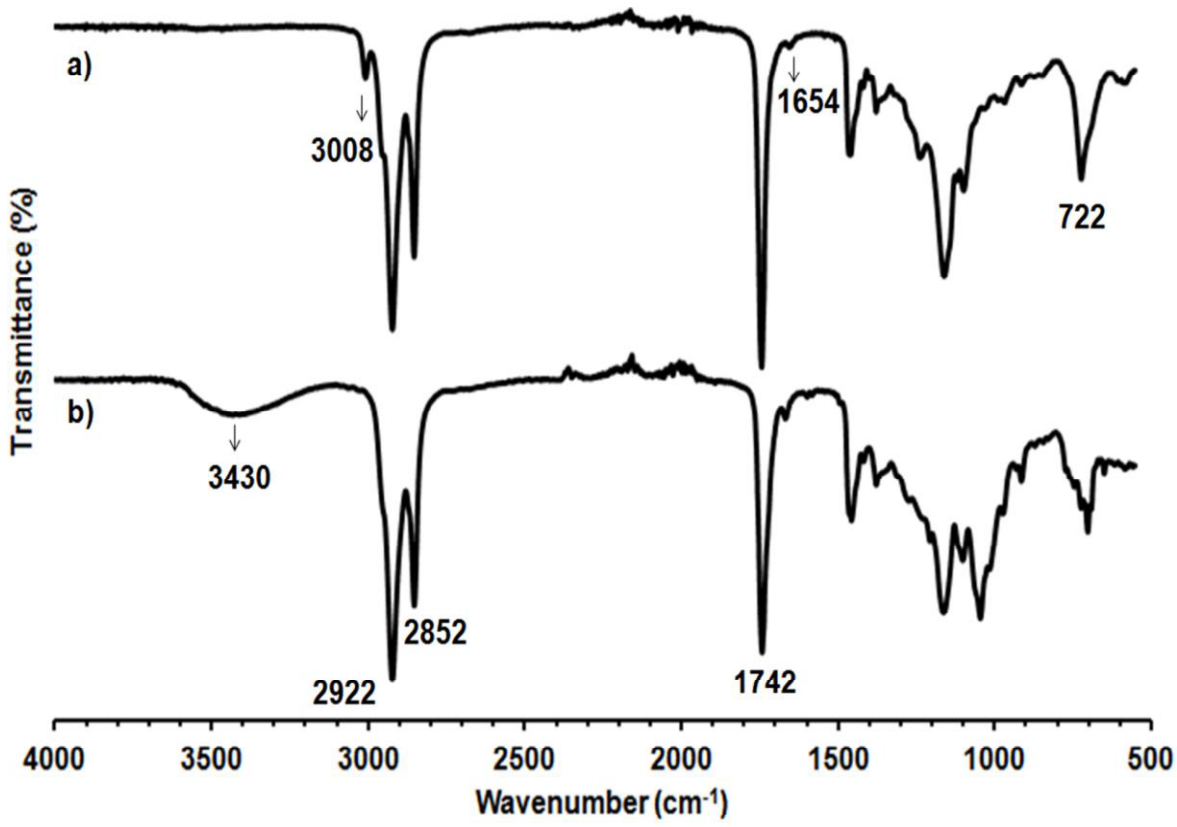

Figure 4.6. FTIR spectra of (a) SBO and (b) SBO polyol.

4.3.2. Synthesis and Characterization of X-SBO/PIB-PU

Figure 4.7 outlines the strategies for the preparation of the PU network by the use of both PIB and SBO polyols, conventional diisocyanate (MDI) and chain extender (BDO) as well as for the acid catalyzed hydrolysis of the products.

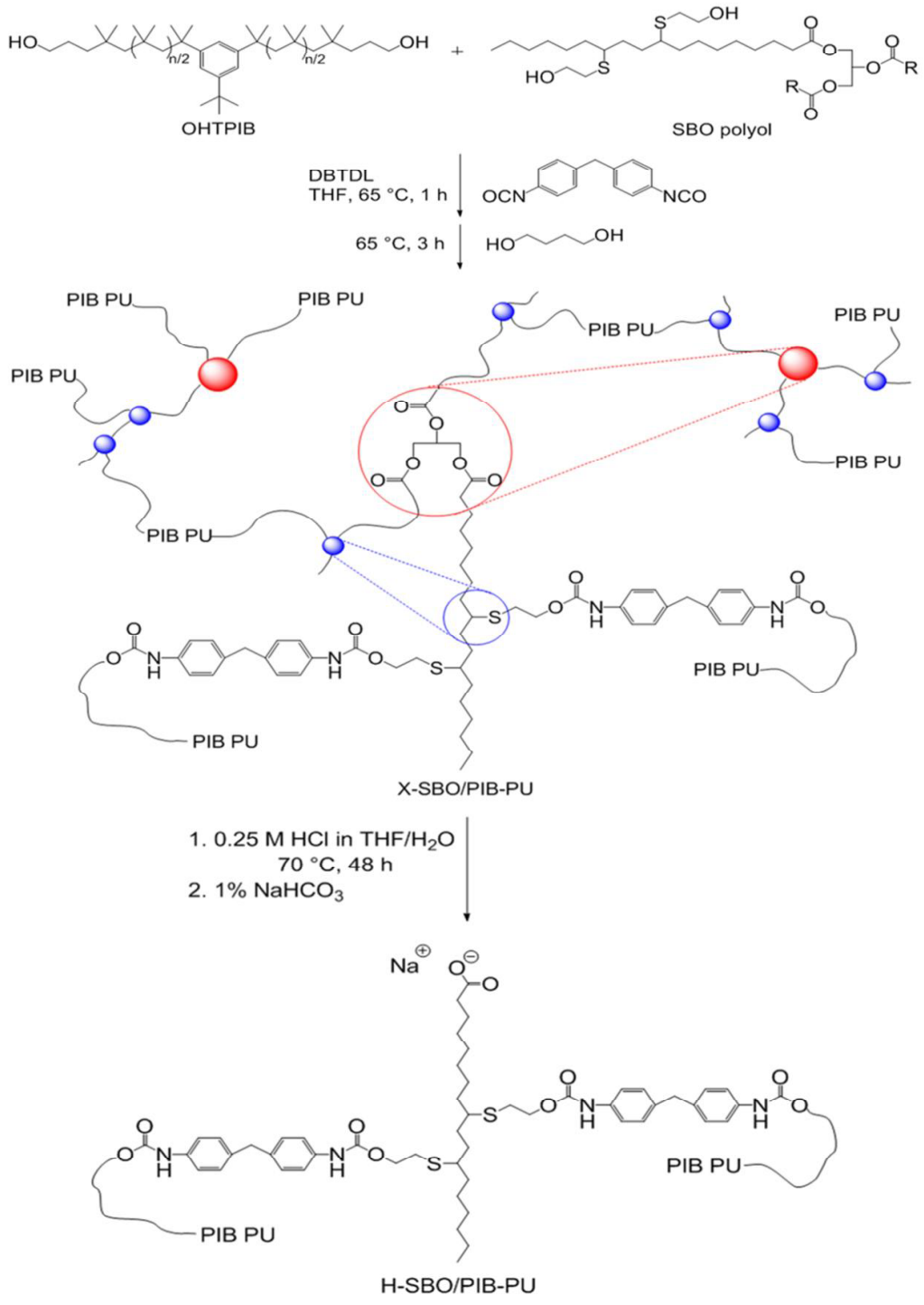

Figure 4.7. Synthesis of X-SBO/PIB-PU followed by acid catalyzed hydrolysis.

Due to multiple primary hydroxides of SBO polyol, the polyurethane formation resulted in a network film. Both insolubility of the network and almost 2.2 equilibrium swelling ratio in good solvent THF (Figure 4.8) confirmed the crosslinked nature of X-SBO/PIB-PU.

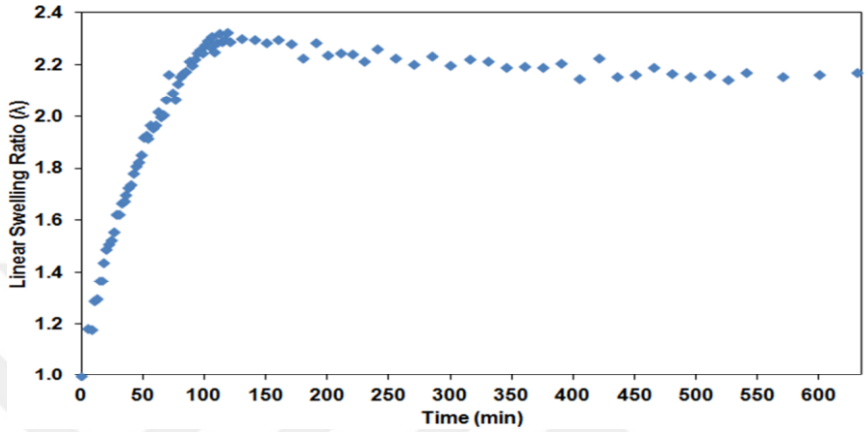

Figure 4.8. Linear swelling ratio vs swelling time for X-SBO/PIB-PU.

The optical clarities of X-SBO/PIB-PU and H-SBO/PIB-PU films are also compared with a typical PIB-PU film in Figure 4.9. As compared with a optically clear PIB based PU (Figure 4.9a), slight scattering dependent haziness in X-SBO/PIB-PU film (Figure 4.9b) can be attributed to the network junction based optical imperfections.

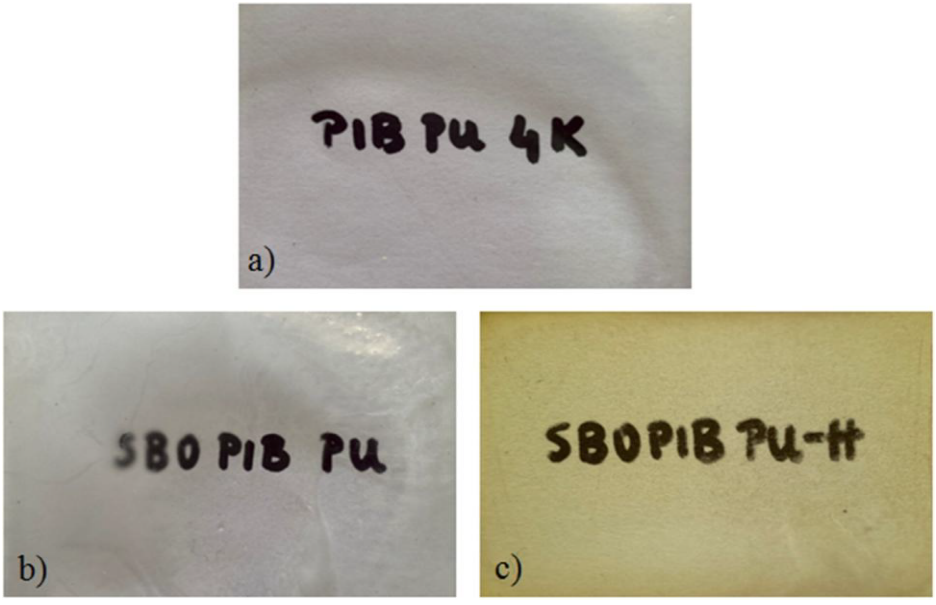

Figure 4.9. Comparisons of optical clarities of the (a) PIB-PU, (b) X-SBO/PIB-PU, and (c) H-SBO/PIB-PU films.

X-SBO/PIB-PU was also characterized by FTIR technique (Figure 4.10). X-SBO/PIB-PU spectrum exhibits all characteristic absorption bands of urethane groups, PIB soft segment, and triglycerides. At 3324 cm^{-1}, hydrogen bonded N—H stretching vibrations of urethane groups appeared as a medium band, whereas a weak shoulder at 3440 cm^{-1} assigned to free N—H groups is barely visible. In the region of 1760-1650 cm^{-1}, the carbonyl stretching peaks of ester and urethane groups combined and appeared as a broad band with a maxima and shoulder at 1700 and 1733 cm^{-1}, respectively, representing the hydrogen bonded and free carbonyl groups [136]. The presence of above mentioned relatively weak stretching bands for both free N—H groups and carbonyl groups indicates that most of the carbonyl groups are apparently hydrogen bonded.

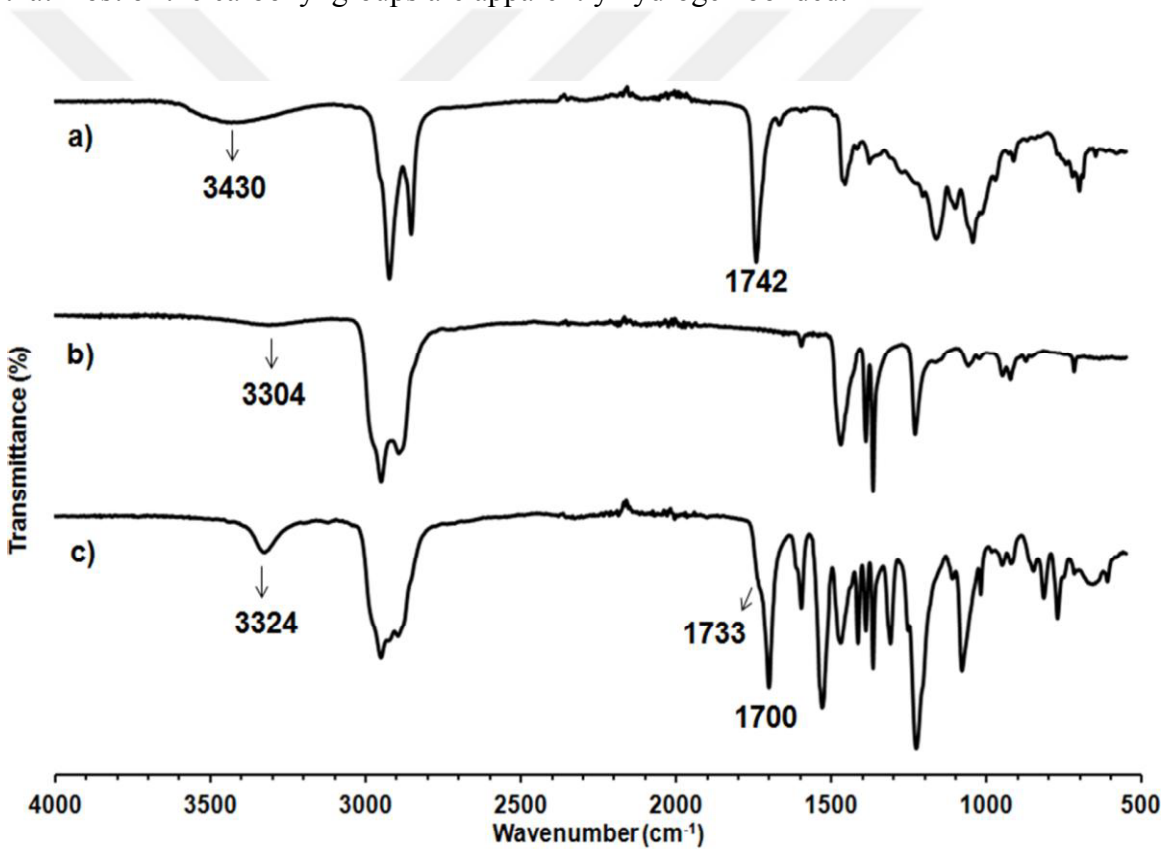

Figure 4.10. FTIR spectra of (a) SBO polyol, (b) OHTPIB, and (c) X-SBO/PIB-PU.

Other peaks of urethane groups were observed at 1596 cm^{-1} due to the C=C stretching vibrations of the aromatic rings and at 1529, 1310 cm^{-1} (Figure 4.10) due to the overlapping N—H bending and C—N stretching vibrations [136]. In the region 1280-1000 cm^{-1}, the strong absorption centered at 1226 cm^{-1} was assigned to the overlapping vibrations of N—H bending and C—N stretching of the urethane groups and C—H bending of the methylene groups of the PIB backbone. The shoulder near 1250 cm^{-1} and

the peak at 1080 cm^{-1} appeared due to C—O—C stretching vibrations of urethanes [136]. The absorption peaks typical of PIB soft segment were observed at 2949 and 2892 cm^{-1} due to strong C—H stretching vibrations. The peak at 1470 cm^{-1} corresponded to C—H bending, and the peaks at1388 and 1365 cm^{-1} were due to CH_3 swing of the methyl groups [125,126].

4.3.3. Acid Catalyzed Hydrolysis of X-SBO/PIB-PU

X-SBO/PIB-PU contains functional groups that have different hydrolytic stabilities, i.e., urethanes and ester moieties coming from the SBO triglycerides (Figure 4.7). In literature, selective hydrolysis has been widely applied to characterize the soft and hard phases of PUs [150,151]. The preferential cleavage of the ester bonds stems from the higher reactivity of the ester bonds when compared to the ether and urethane bonds under acid/alkaline hydrolysis conditions. Chapman *et al* proposed that acid hydrolysis selectively cleaves polyester soft blocks of polyester based PUs and leave the hard blocks unharmed [151]. This methodology allowed study of the hard segment length distribution by MALDI, SEC, and IR analyses [150]. In light of this information, acid catalyzed hydrolysis of the X-SBO/PIB-PU film was conducted for selective cleavage of the ester bonds enabling recovery of PIB polyurethane segments with carboxylic acid functionalities (Figure 4.7).

Figure 4.11 and 4.12 show the ^1H NMR and FTIR spectra of the selective acid catalyzed–hydrolysis product, H-SBO/PIB-PU. The peaks associated with the urethane linkages appeared at 4.23 and 4.35 ppm due to –CH_2–O– protons of BDO (peak c) and OHTPIB (peak b), respectively, and at 10.64 ppm due to –NH protons (peak h) [160]. The peaks related to SBO polyol appeared at 2.81 ppm corresponding to tertiary –CH–S– protons (peak i), at 2.97 ppm due to –S–CH_2– protons (peak k), and 4.54 ppm due to –CH_2–O– protons (peak l) confirming the incorporation of SBO polyol in the PU structure. Meanwhile, the absence of the peaks associated with the glycerol moiety of the triglycerides (peaks a and b in Figure 4.3) proved the preferential cleavage of the more labile ester linkages leaving the urethane bonds intact. The aromatic protons of MDI (peaks d and f) and the cationic initiator (peak e) appeared between 7.90 and 7.30 ppm, while the methylene protons between the aromatic rings of MDI appeared at 3.94 ppm (peak a).

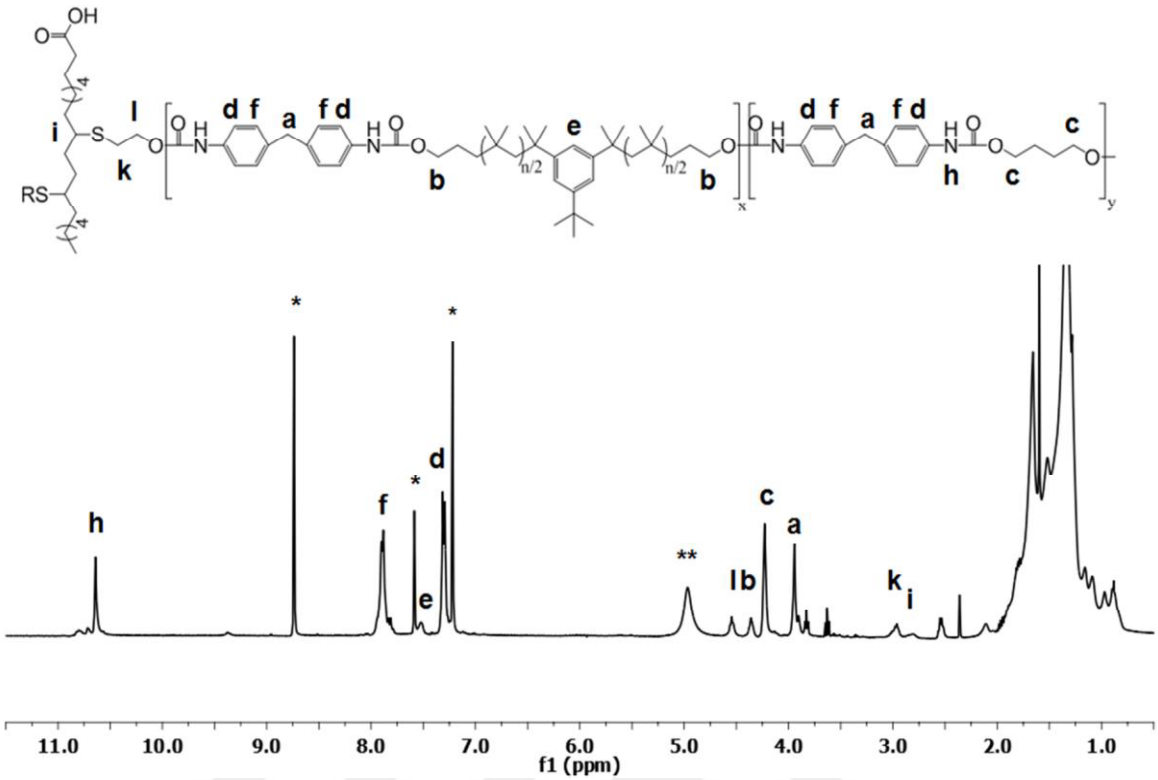

Figure 4.11. ^{1}H NMR spectrum of H-SBO/PIB-PU in pyridine-d5 (*pyridine-d5, ** water).

Table 4.2 depicts the SEC traces of the OHTPIB and H-SBO/PIB-PU. Almost two times higher number average molecular weight (M_n) and broader molecular weight distribution (MWD) than that of OHTPIB for H-SOB/PIB-PU can be accepted as another proof of preservation of the urethane linkages during hydrolysis [150,151].

Table 4.2. Molecular Weight Characterization data for OHTPIB and H-SBO/PIB-PU.

Samples	**$M_{n,SEC}$ (g/mol)**	**MWD (M_w/M_n)**
OHTPIB	4800	1.14
H-SBO/PIB-PU	11500	1.75

FTIR spectra of the network and the hydrolysis product are given in Figure 4.12. SBO related methylene stretching vibrations that can be seen at 2922 and 2852 cm^{-1} in Figure 4.6, shifted slightly and appeared at 2918 and 2850 cm^{-1} in the spectrum of the hydrolysis product. This proves that, after acid hydrolysis, the fatty acyl chains of the SBO

polyol are still present in the structure of the PU through the urethane linkages. Moreover, the soluble and solvent castable hydrolysis product leading to a clear film without haziness (Figure 4.9c) can be accepted as an indication of the successful cleavage of the ester bonds of the SBO polyol at the network junctions. Besides, an increase in breath of hydrogen bonded NH at 3324 cm^{-1} suggests the formation of additional hydrogen bonds between acidic end groups of the fatty acyl chains in hydrolyzed product and urethane moiety [46].

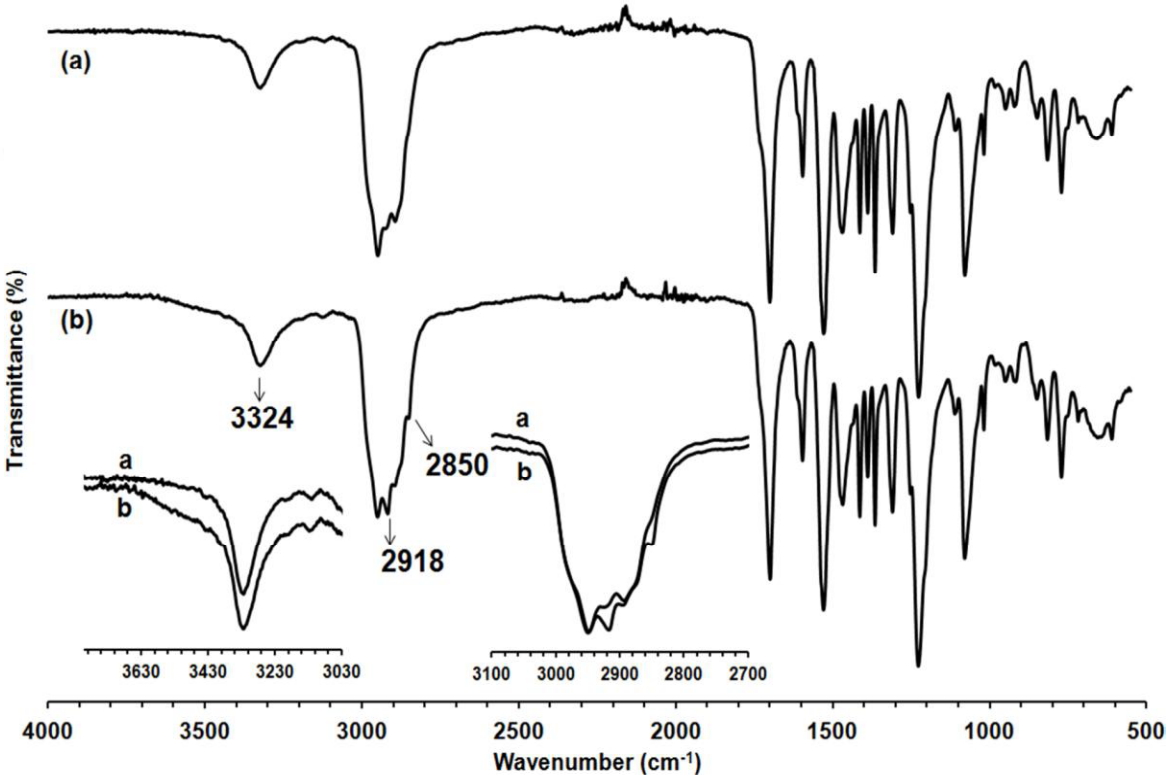

Figure 4.12. FTIR spectra of (a) X-SBO/PIB-PU and (b) H-SBO/PIB-PU. Inserts show the enlarged peak areas from the spectra

Figure 4.13 shows DSC heating traces of PIB-PU and X-SBO/PIB-PU. The thermograms exhibited a prominent glass transition temperature (T_g) of PIB soft phase and a melting endotherm (T_m) due to the crystalline hard phase, indicating microphase separated morphology of the polyurethanes. Both PIB-PU and the network showed an almost similar soft phase related T_g at ~-59 °C. However, the presence of crosslink moieties had a pronounced influence on the higher temperature transitions of the hard phase. Similar results were reported by elsewhere and correlated well with data from dynamic mechanical thermal analysis (DMTA) measurements [161]. The shift of characteristic T_m peak of PIB-PU from 203 °C to 189 °C with much smaller peak area for

the network suggesting the decreasing hard phase crystallinity due to the presence of large network moieties. Multiple endotherms appeared between 30-100 °C may be attributed to presence of different regions relaxing in a broad temperature range. These regions are most probably due to different sized crosslinks and their nonhomogeneous distributions in the network structure [162]. After the acid catalyzed selective hydrolysis reaction, the resulting structure still keeps the characteristic multiple thermal transitions of X-SBO/PIB-PU. The appearance of a melting endotherm at lower temperature (~180 °C), on the other hand, is most probably due to the extra ionic and hydrogen bonding type interactions which may cause to a further disturbance of crystallinity.

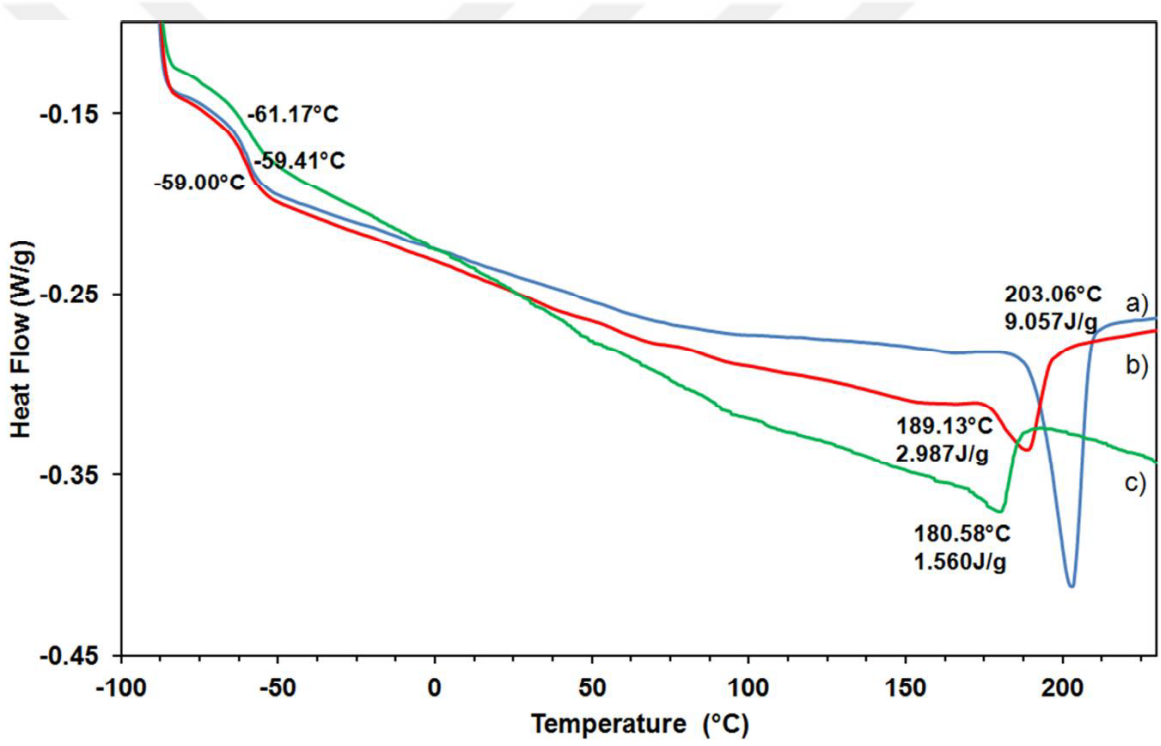

Figure 4.13. DSC thermogram of (a) PIB-PU (blue line), (b) X-SBO/PIB-PU (red line), and (c) H-SBO/PIB-PU (green line).

Figure 4.14 depicts XRD traces of PIB-PU, X-SBO/PIB-PU and H-SBO/PIB-PU and Table 4.3 tabulates the XRD data. XRD analyses yield typical and similar results of polyurethanes having SBO, PIB, MDI, and BDO. It is known that a broader peak at ~14° is due to lateral self-organization of hard domains, the shoulder at ~20° is mainly due to lateral distances between molten aliphatic chains, and the broader low intensity signal in the 30–50° range is due to second-order distances [46]. Gradual decreasing intensity of the peak at ~14° suggests low self-organization of hard and soft domains due to formation of

different sized crosslinks and intense interactions particularly after hydrolysis. Similar trend was also observed by Hu et al. in their studies with carboxylated polyurethanes [163]. In contrast to the broader, less intense peaks of X-SBO/PIB-PU typical of random low periodicity crystals, PIB-PU shows a narrower XRD peak indicating larger crystallites [46]. The disturbance of chain alignment/crystallinity is also in a good agreement with DSC results (Figure 4.13).

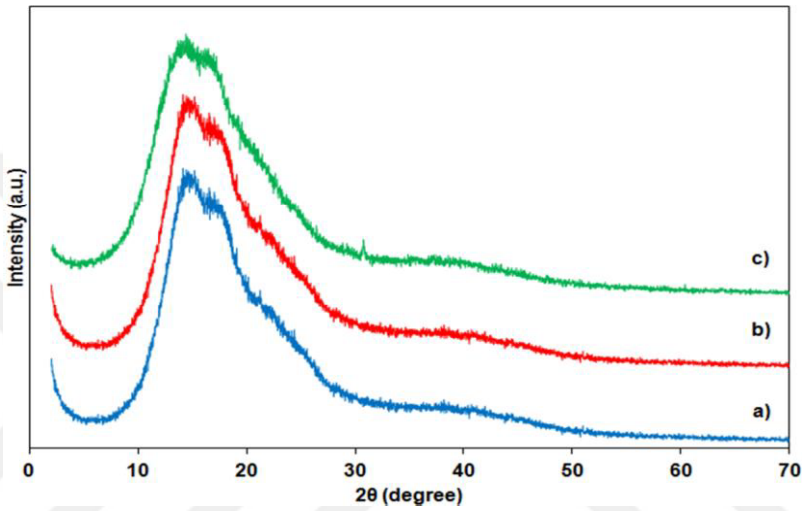

Figure 4.14. XRD traces of (a) PIB-PU (blue line), (b) X-SBO/PIB-PU (red line), and (c) H-SBO/PIB-PU (green line).

Table 4.3. XRD data for PUs.

Samples	2θ (°)	d(Å)	Area	FWHM[1]
PIB-PU	14.63	6.05	8825	0.81
	17.76	4.99	72	0.10
	21.24	4.18	516	0.08
X-SBO/PIB-PU	14.89	5.94	6562	0.69
	18.05	4.90	1945	0.49
	22.61	3.93	2540	0.46
H-SBO/PIB-PU	14.63	6.05	7055	0.67
	15.39	5.75	2689	0.32
	17.44	5.08	4549	0.53
	31.76	2.81	1043	0.15

[1]Full Width Half Maximum as a measure of breath of peak

Figure 4.15 gives both TG and DTG thermograms of the synthesized polyurethanes. The typical peaks at 326 and 418 ^{0}C of PIB-PU are associated with degradation of the hard polyurethane and the soft PIB phase, respectively [46]. Hard phase degradations in X-SBO/PIB-PU and H-SBO/PIB-PU shifted to lower temperatures, 321 and 319 ^{0}C, respectively. This result can be ascribed to the presence of network junctions and intense interactions after their hydrolysis causing a gradual disturbance of the crystallinity which is in consistent with XRD and DSC data. In contrast, soft phase degradation shifted to higher temperatures from 415^{0}C to 430 ^{0}C in network structure by staying almost constant after hydrolysis. Evidently, network formation increases thermal stability of soft phase by almost 15^{0}C as pointed out by Wilkie et al. [164] in their study reporting the correlation between cross linking and thermal stability.

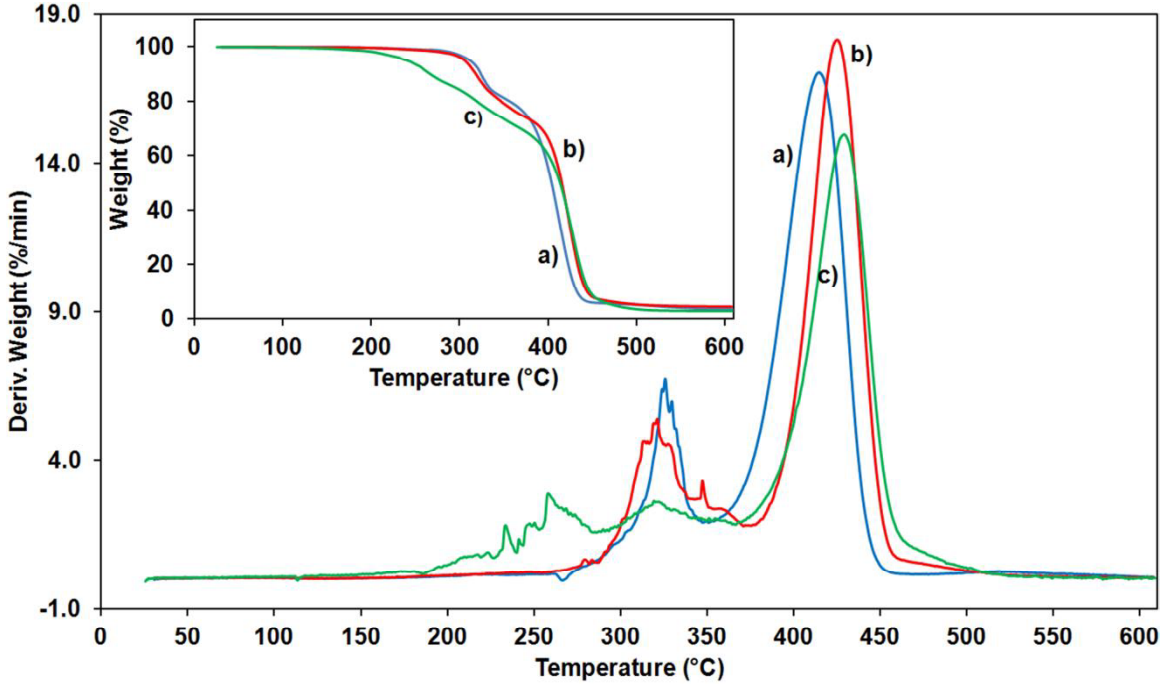

Figure 4.15. TG and DTG curves of (a) PIB-PU (blue line), (b) X-SBO/PIB-PU (red line), and (c) H-SBO/PIB-PU (green line).

Mechanical strengths of the synthesized polyurethanes are given in Figure 4.16. As compared to PIB-PU, higher stiffness (elastic modulus) and lower extension in SBO based PU can be attributed to the high degree of crosslinking. It also seems that hydrolysis resulted in reduced mechanical strength and toughness as well as extensibility in certain amount, this can be driven by decreasing in molecular weight and molecular weight

distributions of PIB-PU as well as lowering in hard domain periodicity and domain size. Almost 30 % increase in elastic modulus for H-SBO/PIB-PU, on the other hand, can be explained by initial resistance to deformation due to the additional ionic and hydrogen bonding type interactions after acid catalyzed hydrolysis [165].

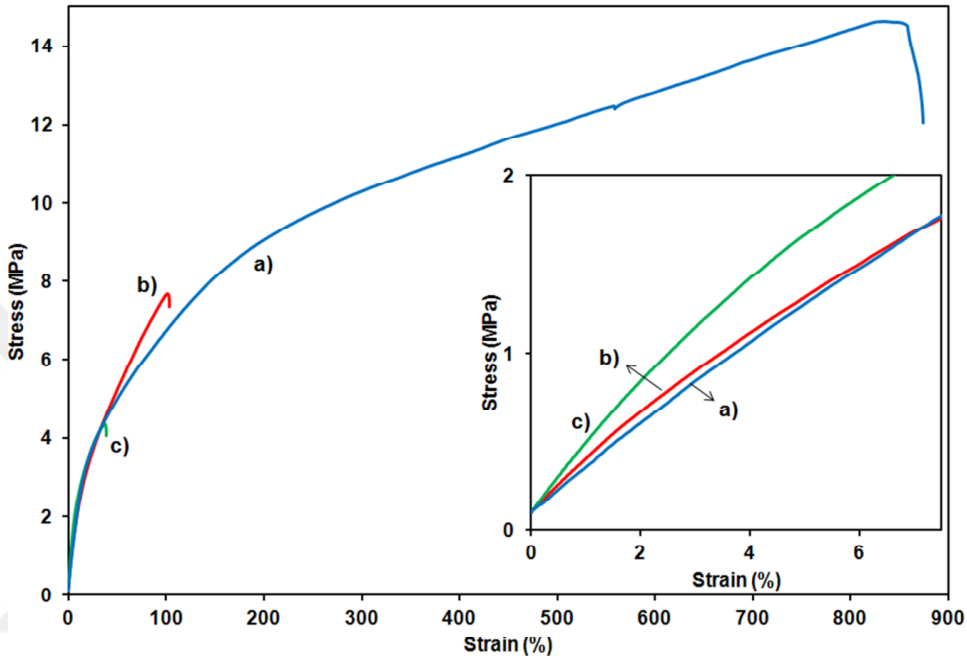

Figure 4.16. Stress-Strain curves of (a) PIB-PU (blue line), (b) X-SBO/PIB-PU (red line), and (c) H-SBO/PIB-PU (green line).

4.4. Conclusions

Novel biobased X-SBO/PIB-PU was successfully prepared with SBO. SBO was first efficiently decorated with primary hydroxyl groups and integrated to PIB based polyurethane formation as a co-polyol. Network characterization data confirmed the crosslinked structure. Subsequent acid catalyzed hydrolysis of resultant X-SBO/PIB-PU film selectively cleaved the ester bonds by enabling the recovery of soluble SBO/PIB based polyurethane segments without disturbing the original polyurethane structure.

It has been suggested that after selective acid hydrolysis of network moieties, carboxylic acid based extra active polar site equipped PIB based polyurethane may then serve as a versatile platform for the synthesis of further novel blend or nanocomposites of biobased PIB-PU materials.

5. CONCLUDING REMARKS

In this study, PIB/PSt/OEO based hybrid PUs and PIB/SBO based PU network were prepared and characterized in terms of structural, thermal and mechanical properties.

The primary aim of the first phase of this study is to enhance the low creep properties of SIBS by integrating hydrogen bonds and crystallizable PU sequences into hybrid PUs (PIB/PSt PUs). These PUs contain both elastomeric and thermoplastic sequences, as well as crystalline segments. Di-hydroxyl telechelic PIB and PSt (HO-PIB-OH and HO-PSt-OH) starting polymers were synthesized for this purpose. Firstly, a di-functional telechelic polyisobutylene (A-PIB-A) was prepared by using TBDCC/$TiCl_4$ to initiate living cationic polymerization of isobutylene (IB), which was then quenched in situ using ATMS. Then, HO-PIB-OH was obtained by regioselectively hydroborating and oxidizing the terminal allyl groups with 9-BBN. HO-PSt-OH was synthesized using living anionic polymerization of styrene (St), followed by quenching the living PStLi chain ends with EO. The functionalization of chain ends for A-PIB-A, HO-PIB-OH, and HO-PSt-OH was confirmed through ^{1}H NMR analysis. Since PIB and PSt macrodiols are incompatible and could possibly separate during PU synthesis, oligo EO blocks were added to both PIB and PSt chain ends to act as compatibilizers. The synthesis process began with the conversion of macrodiols into polymeric potassium alkoxides. This was achieved by deprotonating hydroxyl groups using DPMK. The resulting alkoxides were then used as a macroinitiator in the anionic ring-opening oligomerization of EO. This led to the synthesis of di-OligoEO telechelic PIB and PSt (OEO-b-PIB-b-OEO and OEO-b-PSt-b-OEO). The ^{1}H NMR spectroscopy analysis showed that on average, 7.4 and 14 EO units were added per chain for OEO-b-PIB-b-OEO and OEO-b-PSt-b-OEO, respectively. Several types of PUs and hybrid PUs were synthesized, some with OEO blocks and some without. The types are as follows: PIB PU, OEO-b-PIB-b-OEO PU, PSt PU, OEO-b-PSt-b-OEO PU, PIB/PS PU, PIB/OEO-b-PSt-b-OEO PU, OEO-b-PIB-b-OEO/PSt PU, and OEO-b-PIB-b-OEO/OEO-b-PSt-b-OEO PU. These were created by reacting starting polymers with MDI and BDO, using a catalyst during the process. ^{1}H NMR, FTIR spectroscopy, and SEC confirmed the successful synthesis of PUs. The resulting PUs had M_{nSEC} values in the range of 31800-93000 g/mol. The mechanical and thermal properties of PUs were analyzed using stress-

strain tests, DMA, and DSC techniques. It has been demonstrated that it is possible to prepare high strength, tough and creep resistant PIB/PSt PUs by incorporating OEO segments in both the soft PIB and hard PSt phases. These novel PIB/PSt based hybrid PUs containing OEO exhibit promising potential compared to conventional low strength and low creep resistant SIBS.

The second part of the thesis describes a method for creating a new type of reprocessable PU network that is based on SBO and PIB. This was achieved by first obtaining a polyol derived from SBO using a UV-initiated thiol-ene addition reaction of 2-mercaptoethanol to olefinic double bonds. The optimal reaction conditions, such as photoinitiator/thiol/double bond ratios and irradiation time, were determined. X-SBO/PIB-PU was then synthesized by reacting SBO-derived polyol, PIB macrodiol, BDO, and MDI at specific mole ratios. The formation of a crosslinked polyurethane structure was confirmed through a swelling test. Moreover, the X-SBO/PIB-PU was successfully reprocessed by selectively hydrolyzing the ester bonds originating from modified SBO triglycerides using acid catalysts. This process allowed for the recovery of soluble PIB-based PU segments that possess terminal carboxylic acid functionality. The X-SBO/PIB-PU and the hydrolysis product were studied through thermal, mechanical, and microstructural tests. The results showed that the hydrolysis reaction of this material could be performed without altering the original PU structure. The resulting recycled PIB PU has carboxylic acid terminals, which could be used as a versatile building block for designing PIB-based blends and nanocomposites.

REFERENCES

1. Kennedy, J. P., and E. Marechal, *Carbocationic Polymerization*, John Wiley & Sons, New York, 1982.

2. Matyjaszewski, K., *Cationic Polymerizations: Mechanisms, Synthesis, and Applications*, Marcel Dekker, New York, 1996.

3. Odian, G., *Principles of Polymerization*, Fourth Edition, John Wiley & Sons, New Jersey, 2004.

4. Alves, J. B., M. K. Vasconcelos, L. H. R. Mangia, M. Tatagiba, J. Fidalgo, D. Campos, P. L. Invernici, M. V. Rebouças, M. H. S. Andrade, and J. C. Pinto, "A Bibliometric Survey on Polyisobutylene Manufacture", *Processes*, Vol. 9, No. 8, p. 1315, 2021.

5. Nifant'ev, I. E., S. A. Korchagina, M. S. Chinova, and A. N. Tavtorkin, "Polyisobutylenes with Controlled Molecular Weight and Chain-End Structure: Synthesis and Actual Applications", *Polymers*, Vol. 15, p. 3415, 2023.

6. Higgins, J. J., F. C. Jagisch, and N. E. Stucker, Butyl Rubber and Polyisobutylene. In Skeist, I. (Eds), Handbook of Adhesives, Springer, Boston, 1990.

7. McDonald, M.F., Shaffer, T.D., and Tsou, A.H., Commercial Isobutylene Polymers. In Kirk-Othmer Encyclopedia of Chemical Technology, Third Edition, Wiley: Hoboken, NJ, USA, 2016.

8. Puskas, J. E., and G. Kaszas, Carbocationic Polymerization. In Encyclopedia of Polymer Science and Technology, Wiley-Intersci., 2016.

9. Puskas, J. E., Y. Chen, Y. Dahman, and D. Padavan, "Polyisobutylene-Based Biomaterials", *Journal of Polymer Science Part A: Polymer Chemistry*, Vol. 42, No. 13, pp. 3091–3109, 2004.

10. Kennedy, J. P., "Goodyear Medalist Lecture: Rubber Research in the Service of Mankind", *Rubber Chemistry and Technology*, Vol. 81, No. 2, pp. 169–181, 2008.

11. Pinchuk, L., G. J. Wilson, J. J. Barry, R. T. Schoephoerster, J. M. Parel, and J. P. Kennedy, “Medical Applications of Poly(styrene-block-isobutylene-block-styrene) ("SIBS")”, *Biomaterials*, Vol. 29, No. 4, pp. 448-460, 2008.

12. Gallocher, S. L., A. F. Aguirre, V. Kasyanov, L. Pinchuk, and R. T. Schoephoerster, “A Novel Polymer for Potential Use in a Trileaflet Heart Valve”, *Journal of Biomedical Materials Research Part B: Applied Biomaterials*, Vol. 79, No. 2, pp. 325-334, 2006.

13. Pinchuk, L., I. Riss, J. F. Batlle, Y. P. Kato, J. B. Martin, E. Arrieta, P. Palmberg, R. K. Parrish, B. A. Weber, Y. Kwon, and J. M. Parel, “The Development of a Micro-Shunt Made from Poly(styrene-block-isobutylene-block-styrene) to Treat Glaucoma”, *Journal of Biomedical Materials Research Part B: Applied Biomaterials*, Vol. 105, No. 1, pp. 211–221, 2017.

14. Kennedy, J., and T. Nugay, “Technical Notes: Silicones vs Polyisobutylenes in Medicine, with a Glimpse of Future”, *Rubber News*, 2022.

15. Pinchuk, L., “The Development of a SIBS Shunt to Treat Glaucoma”, *Journal of Ocular Pharmacology and Therapeutics*, Vol. 39, No. 8, pp. 530-540, 2023.

16. Merna, J., P. Vlček, V. Volkis, and J. Michl, “Li+ Catalysis and Other New Methodologies for the Radical Polymerization of Less Activated Olefins”, *Chemical reviews*, Vol. 116, No. 3, pp. 771–785, 2016.

17. Volkis, V., H. Mei, R. K. Shoemaker, and J. Michl, “$LiCB_{11}(CH_3)_{12}$-Catalyzed Radical Polymerization of Isobutylene: Highly Branched Polyisobutylene and an Isobutylene-Ethyl Acrylate Copolymer”, *Journal of the American Chemical Society*, Vol. 131, No. 9, pp. 3132–3133, 2009.

18. Volkis, V., C. Douvris, and J. Michl, “Oxidatively Induced Concurrent Cationic and Radical Polymerization of Isobutylene in the Presence of $LiCB_{11}Me_{12}$. *Journal of the American Chemical Society*, Vol. 133, No. 20, pp. 7801-7809, 2011.

19. Volkis, V., R. K. Shoemaker, and J. Michl, “Highly Branched Polyisobutylene by Radical Polymerization under $Li[CB_{11}Me_{12}]$ Catalysis”, *Macromolecules*, Vol 45, No. 23, pp. 9250−9257, 2012.

20. Kennedy, J. P., “Living Cationic Polymerization of Olefins. How Did the Discovery Come About?”, *Journal of Polymer Science Part A: Polymer Chemistry*, Vol. 37, No. 14, pp. 2285-2293, 1999.

21. Kennedy, J. P., and R. A. Smith, "New Telechelic Polymers and Sequential Copolymers by Polyfunctional Initiator-Transfer Agents (Inifers). II. Synthesis and Characterization of α,ω-di(tert-Chloro)Polyisobutylenes", *Journal of Polymer Science: Polymer Chemistry Edition*, Vol. 18, No. 5, pp. 1523-1537, 1980.

22. Chang, V. S. C., J. P. Kennedy, and B. Iván, “New Telechelic Polymers and Sequential Copolymers by Polyfunctional Initiator-Transfer Agents (Inifers) 8. The Effects of Polymerization Conditions on the Functionality of Telechelic Polyisobutylenes”, *Polymer Bulletin*, Vol. 3, pp. 339-346, 1980.

23. Kennedy, J. P., L. R. Ross, J. E. Lackey, and O. Nuyken, “New Telechelic Polymers and Sequential Copolymers by Polyfunctional Initiator-Transfer Agents (inifers) 10. Three-Arm Star Telechelic Polyisobutylenes Carrying Chlorine, Olefin or Primary Alcohol Endgroups”, *Polymer Bulletin*, Vol. 4, pp. 67–74, 1981.

24. Santos, R., J. P. Kennedy, and M. Walters, “New Telechelic Polymers and Sequential Copolymers by Polyfunctional Initiator-Transfer Agents (INIFERS). 40. Telechelic Polyisobutylenes by Sterically Hindered Binifers”, *Polymer Bulletin*, Vol. 11, pp. 261–267, 1984.

25. Santos, R., A. Fehervari, and J. P. Kennedy, "New Telechelic Polymers and Sequential Copolymers by Polyfunctional Initiator-Transfer Agents (Inifers). XII. Kinetic and Reactivity Studies on Sterically Hindered Inifers", *Journal of Polymer Science: Polymer Chemistry Edition*, Vol. 22, pp. 2685-2697, 1984.

26. Nugay, T., and N. Nugay, Chapter 3 - Multifunctional Initiators for Living Isobutylene Polymerization. In Lubnin, A., and G. Erdodi (Eds), Macromolecular Engineering, Elsevier, 2021.

27. R. Faust, A. Nagy, and J. P. Kennedy, "Living Carbocationic Polymerization. V. Linear Telechelic Polyisobutylenes by Bifunctional Initiators", *Journal of Macromolecular Science: Part A - Chemistry*, Vol. 24, No. 6, pp. 595-609, 1987.

28. Mishra, M. K., and J. P. Kennedy, "Living Carbocationic Polymerization. VIII. Telechelic Polyisobutylenes by the $MeO(CH_3)_2C\text{-}p\text{-}C_6H_4\text{-}C(CH_3)_2OMe/BCl_3$ Initiating System", *Polymer Bulletin*, Vol. 17, No. 1, pp. 7–13, 1987.

29. Wang, B., M. K. Mishra, and J. P. Kennedy, "Living Carbocationic Polymerization XII. Telechelic Polyisobutylenes by a Sterically Hindered Bifunctional Initiator", *Polymer Bulletin*, Vol. 17, No. 3, pp. 205-211, 1987.

30. Kaszás, G., J. Puskás, and J. P. Kennedy, "Living Carbocationic Polymerization XIV. Living Polymerization of Isobutylene with Ester-$TiCl_4$ Complexes" *Makromolekulare Chemie. Macromolecular Symposia*, Vol. 13-14, No. 1, pp. 473-493, 1988.

31. Kaszás, G., J. Puskás, and J. P. Kennedy, "Living Carbocationic Polymerization. XV. Telechelic Polyisobutylenes by the $CH_3O(CH_3)_2C\text{-}pC_6H_4\text{-}C(CH_3)_2OCH_3$ $TiCl_4$ Initiating System", *Polymer Bulletin*, Vol. 18, pp. 123–130, 1987.

32. Kang, J., G. Erdodi, J. P. Kennedy, "Polyisobutylene-based Polyurethanes with Unprecedented Properties and How They Came About", *Journal of Polymer Science Part A: Polymer Chemistry*, Vol. 49, No. 18, pp. 3891-3904, 2011.

33. Ivan, B., J. P. Kennedy, and V. Chang, "New Telechelic Polymers and Sequential Copolymers by Polyfunctional Initiator-Transfer Agents (Inifers). VII. Synthesis and Characterization of α,ω-di(hydroxy)polyisobutylene", *Journal of Polymer Science: Polymer Chemistry Edition*, Vol. 18, No. 11, pp. 3177-3191, 1980.

34. Kéki, S., M. Nagy, G. Deák, A. Lévai, and M. Zsuga, "Dimethyldioxirane as a New and Effective Oxidation Agent for the Epoxidation of α,ω-di(Isobutenyl)polyisobutylene: A Convenient Synthesis of α,ω-di(2-Methyl-3-hydroxypropyl)-Polyisobutylene", *Journal of Polymer Science Part A: Polymer Chemistry*, Vol. 40, No. 22, pp. 3974-3986, 2002.

35. Nielsen, L. V, R. R. Nielsen, B. Gao, J. Kops, and B. Iván, "Synthesis of Isobutenyl-Telechelic Polyisobutylene by Functionalization with Isobutenyltrimethylsilane, *Polymer*, Vol. 38, No. 10, pp. 2529-2534, 1997.

36. Feldthusen, J., B. Iván, and A. H. E. Müller, "The Effect of Reaction Conditions on the Chain End Structure and Functionality During Dehydrochlorination of tert-Chlorine Telechelic Polyisobutylene by Potassium tert-Butoxide", *Macromolecular Rapid Communications*, Vol. 19, No. 12, pp. 661-663, 1998.

37. Iván, B. and J. P. Kennedy, "Living Carbocationic Polymerization. XXX. One-Pot Synthesis of Allyl-Terminated Linear and tri-Arm Star Polyisobutylenes, and Epoxy- and Hydroxy-Telechelics Therefrom", *Journal of Polymer Science: Part A: Polymer Chemistry*, Vol. 28, No. 1, pp. 89-104, 1990.

38. Wilczek, L., and J. P. Kennedy, "Electrophilic Substitution of Organosilicon Compounds. II. Synthesis of Allyl-Terminated Polyisobutylenes by Quantitative Allylation of tert-Chloro-Polyisobutylenes with Allyltrimethylsilane", *Journal of Polymer Science: Part A: Polymer Chemistry*, Vol. 25, No. 12, pp. 3255-3265, 1987.

39. Ummadisetty, S., and J. P. Kennedy, "Quantitative Syntheses of Novel Polyisobutylenes Fitted with Terminal Primary –Br, -OH, -NH_2, and Methacrylate Termini", *Journal of Polymer Science: Part A: Polymer Chemistry*, Vol. 46, No. 12, pp. 4236-4242, 2008.

40. Ojha, U., R. Rajkhowa, S. R. Agnihotra, and R. Faust, "A New General Methodology for the Syntheses of End-Functional Polyisobutylenes by Nucleophilic Substitution Reactions", *Macromolecules*, Vol. 41, No. 11, pp. 3832-3841, 2008.

41. Morgan, D.L., and R. F. Storey, "Primary Hydroxy-Terminated Polyisobutylene via End-Quenching with a Protected N-(ω-Hydroxyalkyl)pyrrole", *Macromolecules,* Vol. 43, No. 3, pp. 1329-1340, 2010.

42. Morgan, D. L., N. Martinez-Castro, and R. F. Storey, "End-Quenching of $TiCl_4$-Catalyzed Quasiliving Polyisobutylene with Alkoxybenzenes for Direct Chain End Functionalization", *Macromolecules*, Vol. 43, No. 21, pp. 8724-8740, 2010.

43. Martinez-Castro, N., A. J. D. Magenau, and R. F. Storey, "Functional Polyisobutylenes via a Click Chemistry Approach", *Journal of Polymer Science: Part A: Polymer Chemistry*, Vol. 48, No. 12, pp. 2533-2545, 2010.

44. Magenau, A. J. D., J. W. Chan, C. E. Hoyle, and R. F. Storey, "Facile Polyisobutylene Functionalization via Thiol-Ene Click Chemistry", *Polymer Chemistry*, Vol. 1, No. 6, pp. 831-833, 2010.

45. Kennedy, J., T. Nugay, and N. Nugay, "Photochemical Preparation of Hydroxyl-Terminated Polyisobutylenes and Related Methods and Uses", US Patent WO 2014/138001 A1, September 12, 2014, https://patents.google.com/patent/WO2014/138001A1/en, Accessed on April 4, 2024.

46. Toth, K., N. C. Kekec, N. Nugay, and J. P. Kennedy, "Polyisobutylene-Based Polyurethanes. VIII. Polyurethanes with -O-S-PIB-S-O- Soft Segments", *Journal of Polymer Science: Part A: Polymer Chemistry*, Vol. 54, No. 8, pp. 1119-1131, 2016.

47. Ntetsikas, K., V. Ladelta, S. Bhaumik, and N. Hadjichristidis, "Quo Vadis Carbanionic Polymerization?" *ACS Polymers Au*, Vol. 3, No. 2, pp. 158–181, 2023.

48. Grady, B. P., S. L. Cooper, and C. G. Robertson, Thermoplastic Elastomers. In Mark, J., B. Erman, M. Roland, (Eds.), The Science and Technology of Rubber, Elsevier, Oxford, 2013.

49. Baskaran, D., and A. H. E. Müller, Anionic Vinyl Polymerization. In Müller A. H. E., and K. Matyjaszewski (Eds), Controlled and Living Polymerizations, WILEY-VCH, Weinheim, 2009.

50. Handlin, D. L., D. R. Hansen, K. J. Wright, and S. R. Trenor, Industrial Applications. In A. H. E. Müller, and K. Matyjaszewski (Eds), Controlled and Living Polymerizations, WILEY-VCH, Weinheim, 2009.

51. T. Kwee, S. C. Taylor, Mauritz K. A., and R.F. Storey, "Morphology and Mechanical and Dynamic Mechanical Properties of Linear and Star Poly(styrene-b-isobutylene-b-styrene) Block Copolymers", *Polymer*, Vol. 46, No. 12, pp. 4480–4491, 2005.

52. Szwarc, M., M. Levy, and R. Milkovich, “Polymerization Initiated by Electron Transfer to Monomer. A New Method of Formation of Block Polymers”, *Journal of the American Chemical Society*, Vol.78, No. 11, pp. 2656-57, 1956.

53. Szwarc, M., ““Living” Polymers”, *Nature*, Vol. 178, No. 4543, pp. 1168-69, 1956.

54. Szwarc, M., “Shelftime of Living Polymers. Some Comments on Living Cationic Polymerization of Vinyl Monomers”, *Die Makromolekulare Chemie Rapid Communications*, Vol. 13, No. 3, pp. 141-145, 1992.

55. Grubbs, R.B., and R.H. Grubbs, “50th Anniversary Perspective: Living Polymerization Emphasizing the Molecule in Macromolecules”, *Macromolecules*, Vol. 50, No. 18, pp. 6979-6997, 2017.

56. Quirk, R., Anionic Polymerization. In E. Saldívar-Guerra, and E. Vivaldo-Lima (Eds), Handbook of Polymer Synthesis, Characterization, and Processing, John Wiley & Sons, 2013.

57. Herzberger, J., K. Niederer, H. Pohlit, J. Seiwert, M. Worm, F. R. Wurm, and H. Frey, “Polymerization of Ethylene Oxide, Propylene Oxide, and Other Alkylene Oxides: Synthesis, Novel Polymer Architectures, and Bioconjugation”, *Chemical reviews*, Vol. 116. No. 4, pp. 2170–2243, 2016.

58. Penczek, S., J. Pretula, and S. Slomkowski, “Ring-Opening polymerization”, *Chemistry Teacher International*, Vol. 3, No. 2, pp. 33-57, 2021.

59. Kazanskii, K. S., A. A. Solovyanov, and S. G. Entelis, “Polymerization of Ethylene Oxide by Alkali Metal Naphthalene Complexes in Tetrahydrofuran, *European Polymer Journal*, Vol. 7, No. 10, pp. 1421-1433, 1971.

60. Cabasso, I., and A. Zilkha, “Observations on the Anionic Polymerization of Ethylene Oxide by Alkali Metal Naphthalene and Anthracene Complexes, *Journal of Macromolecular Science: Part A - Chemistry*, Vol. 8, No. 8, pp. 1313-1324, 1974.

61. Quirk, R. P., and J. J. Ma, "Characterization of the Functionalization Reaction Product of Poly(styryl)lithium with Ethylene Oxide", *Journal of Polymer Science: Part A: Polymer Chemistry*, Vol. 26, pp. 2031-2037, 1988.

62. R. P. Quirk, R. T. Mathers, C. Wesdemiotis, and M. A. Arnould, "Investigation of Ethylene Oxide Oligomerization during Functionalization of Poly(styryl)lithium Using MALDI−TOF MS and NMR", *Macromolecules*, Vol. 35, No. 8, pp. 2912-2918, 2002.

63. Calderara, F., Z. Hruska, G. Hurtrez, J. P. Lerch, T. Nugay, and G. Riess, "Investigation of Polystyrene-Poly(ethylene oxide) Block Copolymer Micelle Formation in Organic and Aqueous Solutions by Nonradiative Energy Transfer Experiments", *Macromolecules*, Vol. 27, No. 5, pp. 1210-1215, 1994.

64. Tonhauser, C., and H. Frey, "A Road Less Traveled to Functional Polymers: Epoxide Termination in Living Carbanionic Polymer Synthesis" *Macromolecular Rapid Communications*, Vol. 31, No. 22, pp. 1938-1947, 2010.

65. Xie, H. Q., and D. Xie, "Molecular Design, Synthesis and Properties of Block and Graft Copolymers Containing Polyoxyethylene Segments", *Progress in Polymer Science*, Vol. 24, No.2, pp. 275–313, 1999.

66. D. H. Richard, and M. Szwarc, "Block Polymers of Ethylene Oxide and Its Analogues with Styrene", *Transanctions of the Faraday Society*, Vol. 55, pp. 1644-1650, 1959.

67. Xie, H., and P. Zhou, "Synthesis of Poly(oxyethylene-styrene-oxyethylene) Triblock Copolymers and Their Phase Behavior", *Polymer Engineering and Science*, Vol. 25, No. 1, pp. 32-36, 1985.

68. Wilhelm, M., C. L. Zhao, Y. Wang, R. Xu, M. A. Winnik, J. L. Mura, G. Riess, M. D. Croucher, "Poly(Styrene-Ethylene Oxide) Block Copolymer Micelle Formation in Water: A Fluorescence Probe Study", *Macromolecules*, Vol. 24, No. 5, pp. 1033–1040, 1991.

69. Zhang, Y., G. Wang, and J. Huang, "Preparation of Amphiphilic Poly(ethylene oxide)-block-polystyrene Macrocycles via Glaser Coupling Reaction under CuBr/pyridine System", *Journal of Polymer Science: Part A: Polymer Chemistry*, Vol. 49, No. 22, pp. 4766–4770, 2011.

70. S. Angot., D. Taton, and Y. Gnanou, “Amphiphilic Stars and Dendrimer-Like Architectures Based on Poly(Ethylene Oxide) and Polystyrene”, *Macromolecules*, Vol. 33 No. 15, pp. 5418-5426, 2000.

71. Pinchuk, L., G. J. Wilson, J. J. Barry, R. T. Schoephoerster, J. M., Parel, and J. P. Kennedy, “Medical applications of poly(styrene-block-isobutylene-block-styrene) ("SIBS")”, *Biomaterials*, Vol. 29, No. 4, pp. 448–460, 2008.

72. Pinchuk, L., I. Riss, J. F. Batlle, Y. P. Kato, J. B. Martin, E. Arrieta, P. Palmberg, R. K. Parrish, B. A. Weber, Y. Kwon, and J. M. Parel, “The Use of Poly(styrene-block-isobutylene-block-styrene) as a Microshunt to Treat Glaucoma”, *Regenerative biomaterials*, Vol. 3, No. 2, pp. 137–142, 2016.

73. Ovcharenko, E, M. Rezvova, P. Nikishau, S. Kostjuk, T. Glushkova, L. Antonova, D. Trebushat, T. Akentieva, D. Shishkova, E. Krivikina, K. Klysnikov, Y. Kudryavtseva, L. Barbarash, “Polyisobutylene-Based Thermoplastic Elastomers for Manufacturing Polymeric Heart Valve Leaflets: In Vitro and In Vivo Results”, *Applied Sciences*, Vol. 9, No. 22, p. 4773, 2019.

74. Prisacariu, C., *Polyurethane Elastomers From Morphology To Mechanical Aspects*, Springer, Vienna, 2011.

75. Kang, J., G. Erdodi, and J.P. Kennedy, “Polyisobutylene-Based Polyurethanes with Unprecedented Properties and How They Came About”, *Journal of Polymer Science, Part A: Polymer Chemistry*, Vol. 49, No. 18, pp. 3891-3904, 2011.

76. Heath, D. E., and S. L. Cooper, Polyurethanes. In Ratner, B. D., A. S. Hoffman, F. J. Schoen, J. E. Lemons (Eds), Biomaterials Science An Introduction to Materials In Meddicine, Academic Press, Oxford, 2013.

77. Vermette, P., H. J. Griesser, G. Laroche, and R. Guidoin, *Biomedical Applications of Polyurethanes*, Landes Bioscience, Georgetown, Texas, 2001.

78. Kang, J., and J. P. Kennedy, “Hydrolytically Stable Polyurethanes”, *Journal of Polymer Science, Part A: Polymer Chemistry*, Vol. 53, No. 1, pp. 1-4, 2015.

79. Toth, K., N. Nugay, and J. P. Kennedy, “Polyisobutylene-Based Polyurethanes: VII. Structure/Property Investigations for Medical Applications”, *Journal of Polymer Science, Part A: Polymer Chemistry*, Vol. 54, No. 4, pp. 532-543, 2016.

80. Chaffin, K.A., A. J. Buckalew, J. L. Schley, X. Chen, M. Jolly, J. A. Alkatout, J. P. Miller, D. F. Untereker, M. A. Hillmyer, and F. S. Bates, “Influence of Water on the Structure and Properties of PDMS Containing Multiblock Polyurethanes”, *Macromolecules*, Vol. 45, No. 22, pp. 9110-9120, 2012.

81. Chaffin, K.A., X. Chen, L. McNamara, F. S. Bates, and M A. Hillmyer, “Polyether Urethane Hydrolytic Stability after Exposure to Deoxygenated Water”, *Macromolecules*, Vol. 47, No. 15, pp. 5220-5226, 2014.

82. Chang, V. S. C., and J. P. Kennedy, “Gas Permeability, Water Absorption, Hydrolytic Stability and Air-Oven Aging of Polyisobutylene-Based Polyurethane Networks”, *Polymer Bulletin*, Vol. 8, pp. 69–74, 1982.

83. Speckhard, T. A., P. E. Gibson, S. L. Cooper, V. S. C. Chang, and J. P. Kennedy, "Properties of Polyisobutylene Polyurethane Block Copolymers: 2. Macroglycols Produced by the ‘Inifer’ Technique”, *Polymer*, Vol. 26, No. 1, pp. 55–69, 1985.

84. Speckhard, T. A., K. K. S. Hwang, S. L. Cooper, V. S. C. Chang, J. P. Kennedy, “Properties of Polyisobutylene Polyurethane Block Copolymers: 3. Hard Segments Based on 4,4′-dicyclohexylmethane Diisocyanate (H_{12}MDI) and Butane Diol”, *Polymer*, Vol. 26, No. 1, pp. 70–78, 1985.

85. Jewrajka, S. K., E. Yılgor, I. Yılgor, and J. P. Kennedy, “Polyisobutylene-Based Segmented Polyureas. I. Synthesis of Hydrolytically and Oxidatively Stable Polyureas”, *Journal of Polymer Science, Part A: Polymer Chemistry*, Vol. 47, No. 1, pp. 38-48, 2009.

86. Jewrajka, S. K., J. Kang, G. Erdodi, J. P. Kennedy, E. Yılgor, and I. Yılgor, “Polyisobutylene-Based Polyurethanes. II. Polyureas Containing Mixed PIB/PTMO Soft Segments”, *Journal of Polymer Science, Part A: Polymer Chemistry*, Vol. 47, No. 11, pp. 2787-2797, 2009.

87. Erdodi, G., J. Kang, J. P. Kennedy, E. Yılgor, and Yılgor, I., "Polyisobutylene Based Polyurethanes. III. Polyurethanes Containing PIB/PTMO Soft Co-Segments", *Journal of Polymer Science, Part A: Polymer Chemistry*, Vol. 47, No. 20, pp. 5278-5290, 2009.

88. Kang, J., G. Erdodi, C. M. Brendel, D. Ely, and J. P. Kennedy, "Polyisobutylene Based Polyurethanes. V. Oxidative-Hydrolytic Stability and Biocompatibility", *Journal of Polymer Science, Part A: Polymer Chemistry*, Vol. 48, No. 10, pp. 2194-2203, 2010.

89. Kang, J., G. Erdodi, J. P. Kennedy, E. Yılgor, and I. Yılgor, "PIB-Based Polyurethanes. IV. The Morphology of Polyurethanes Containing Soft Co-Segments", *Journal of Polymer Science, Part A: Polymer Chemistry*, Vol. 47, No. 22, pp. 6180-6190, 2009.

90. Erdodi, K., J. Kang, and J. P. Kennedy, "Polyisobutylene-Based Polyurethanes. VI. Unprecedented Combination of Mechanical Properties and Oxidative/Hydrolytic Stability by H-Bond Acceptor Chain Extenders", *Journal of Polymer Science, Part A: Polymer Chemistry*, Vol. 48, No. 11, pp. 2361-237, 2010.

91. Meier, M. A. R., J. O. Metzger, and U. S. Schubert, "Plant Oil Renewable Resources as Green Alternatives in Polymer Science", *Chemical Society Reviews*, Vol. 36, No 11, pp. 1788-1802, 2007.

92. Lligadas, G., J. C. Ronda, M. Galia, and V. Cadiz, "Plant Oils as Platform Chemicals for Polyurethane Synthesis: Current State-of-the-Art", *Biomacromolecules*, Vol. 11, No. 11, pp. 2825-2835, 2010.

93. Guner, F.S., Y. Yagcı, A. T. Erciyes, "Polymers from Triglyceride Oils", *Progress in Polymer Science*, Vol. 31, No. 7, pp. 633-670, 2006.

94. Zlatanıc, A., C. Lava, W. Zhang, and Z. S. Petrovıc, "Effect of Structure on Properties of Polyols and Polyurethanes Based on Different Vegetable Oils", *Journal of Polymer Science, Part B: Polymer Physics,* Vol. 42, No. 5, pp. 809-819, 2004.

95. Maisonneuve, L., G. Chollet, E. Grau, and H. Cramail, "Vegetable Oils: a Source of Polyols for Polyurethane Materials", *Oilseeds and Fats, Crops and Lipids*, Vol. 23, No. 5, p. 508, 2016.

96. Ionescu, M., and S. Z. Petrović, Polymerization of Soybean Oil with Superacids. In Tzi-Bun Ng (Ed), Soybean - Applications and Technology, 2011.

97. Biermann, U., W. Friedt, S. Lang, W. Lühs, G. Machmüller, J. O. Metzger, M. R. Klaas, H. J. Schafer, and M. P. Schneider, "New Syntheses with Oils and Fats as Renewable Raw Materials for the Chemical Industry", *Angewandte Chemie, International Edition*, Vol. 39, No. 13, pp. 2206–2224, 2000.

98. L., Yongshang, and R. Larock, "Novel Polymeric Materials from Vegetable Oils and Vinyl Monomers: Preparation, Properties, and Applications", *ChemSusChem*, Vol. 2, No. 2, pp. 136 – 147, 2009.

99. Xia, Y., and R. C. Larock, "Vegetable Oil-Based Polymeric Materials: Synthesis, Properties, and Applications", *Green Chemistry*, Vol. 12, pp. 1893–1909, 2010.

100. Pfister, D. P., Y. Xia, and R. C. Larock, "Recent Advances in Vegetable Oil-Based Polyurethanes", *ChemSusChem*, Vol. 4, No. 6, pp. 703–717, 2011.

101. Ionescu, M., D. Radojčić, X. Wan, Z. S. Petrović, and T. A. Upshaw, "Functionalized Vegetable Oils as Precursors for Polymers by Thiol-Ene Reaction", *European Polymer Journal*, Vol. 67, pp. 439–448, 2015.

102. Alagi, P., R. Ghorpade, J. H. Jang, C. Patil, H. Jirimali, V. Gite, and S. C. Hong, "Functional Soybean Oil-Based Polyols as Sustainable Feedstocks for Polyurethane coatings", *Industrial Crops and Products*, Vol. 113, pp. 249–258, 2018.

103. Desroches, M., M. Escouvois, R. Auvergne, S. Caillol, and B. Boutevin "From Vegetable Oils to Polyurethanes: Synthetic Routes to Polyols and Main Industrial Products", *Polymer Reviews*, Vol. 52, No. 1, pp. 38-79, 2012.

104. Petrovich, Z. S., "Polyurethanes from Vegetable Oils", *Polymer Reviews*, Vol. 48, pp. 109-155, 2008.

105. Desroches, M., S. Caillol, V. Lapinte, R. Auvergne, and B. Boutevin, "Synthesis of Biobased Polyols by ThiolEne Coupling from Vegetable Oils", *Macromolecules*, Vol. 44, No. 8, pp. 2489-2500, 2011.

106. Caillol, S., M. Desroches, S. Carlotti, R. Auvergne, B. Boutevin, "Synthesis of New Polyurethanes from Vegetable Oil by Thiol-Ene Coupling", *Green Materials*, Vol. 1, No.1, pp. 16-26, 2013.

107. Alagi, P., Y. J. Choi, J. Seog, and S. C. Hong, "Efficient and Quantitative Chemical Transformation of Vegetable Oils Topolyols through a Thiol-Ene Reaction for Thermoplastic Polyurethanes", *Industrial Crops and Products*, Vol. 87, pp. 78–88, 2016.

108. Alagi, P., Y. J. Choi, and S. C. Hong "Preparation of Vegetable Oil-Based Polyols with Controlled Hydroxyl Functionalities for Thermoplastic Polyurethane", *European Polymer Journal*, Vol. 78, pp. 46–60, 2016.

109. Derboven, P., D. R. D'hooge, M. M. Stamenovic, P. Espeel, G. B. Marin, F. E. Du Prez, and M. F. Reyniers, "Kinetic Modeling of Radical Thiol−Ene Chemistry for Macromolecular Design: Importance of Side Reactions and Diffusional Limitations", *Macromolecules*, Vol. 46, No. 5, pp. 1732-1742, 2013.

110. Lowe, A. B., "Thiol–Ene "Click" Reactions and Recent Applications in Polymer and Materials Synthesis: a First Update", *Polymer Chemistry*, Vol. 5, No. 17, pp. 4820-4870, 2014.

111. Samuelsson, J., M. Jonsson, T. Brinck, and M. Johansson, "Thiol–Ene Coupling Reaction of Fatty Acid Monomers", *Journal of Polymer Science: Part A: Polymer Chemistry*, Vol. 42, No. 24, pp. 6346–6352, 2004.

112. Turunc, O., and M. A. R. Meier, "Fatty Acid Derived Monomers and Related Polymers via Thiol-ene (Click) Additions", *Macromolecular Rapid Commununications*, Vol. 31, No. 20, pp. 1822–1826, 2010.

113. Lluch, C., J. C. Ronda, M. Galia, G. Lligadas, and V. Cadiz, "Rapid Approach to Biobased Telechelics through Two One-Pot Thiol-Ene Click Reactions", *Biomacromolecules*, Vol. 11, No. 6, pp. 1646–1653, 2010.

114. Desroches, M., S. Caillol, R. Auvergne, B. Boutevin, and G. David "Biobased Cross-linked Polyurethanes Obtained from Ester/Amide Pseudo-Diols of Fatty Acid Derivatives

Synthesized by Thiol–Ene Coupling", *Polymer Chemistry*, Vol. 3, No. 2, pp. 450–457, 2012.

115. Pham, P. D., V. Lapinte, Y. Raoul, and J. J. Robin "Lipidic Polyols Using Thiol-ene/yne Strategy for Crosslinked Polyurethanes", *Journal Of Polymer Science, Part A: Polymer Chemistry*, Vol. 52, No. 11, pp. 1597–1606, 2014.

116. Freeman, P. K., and L. L. Hutchinson, "Alkyllithium Reagents from Alkyl Halides and Lithium Radical Anions", *Journal of Organic Chemistry*, Vol. 45, No. 10, pp. 1924-1930, 1980.

117. Storey, R. S., and Y. Lee, "Living Carbocationic Polymerization of Isobutylene Using Blocked Dicumyl chloride or Tricumyl Chloride/$TiCl_4$/Pyridine Initiating system", *Journal of Macromolecular Science, Part A: Pure and Applied Chemistry*, Vol. 29, No. 11, pp. 1017-1030, 1992.

118. Groenewolt, M., T. Brezesinski, H. Schlaad, M. Antonietti, P. W. Groh, and B. Ivan, "Polyisobutylene-block-Poly(ethylene oxide) for Robust Templating of Highly Ordered Mesoporous Materials, *Advanced Materials*, Vol. 17, No. 9, pp. 1158-1162, 2005.

119. Pasztoi, B., T. B. Trötschler, A. Szabo, G. Szarka, B. Kerscher, R. Mülhaupt, and B. Ivan, "Synthesis of Tosyl-and Nosyl-Ended Polyisobutylenes with High Extent of Functionalities: The Effect of Reaction Conditions", *Polymer*, Vol. 12, No. 11, p. 2504, 2020.

120. Francis, R., D. Taton, J. L. Logan, P. Masse, Y. Gnanou, and R. S. Duran, "Synthesis and Surface Properties of Amphiphilic Star-Shaped and Dendrimer-Like Copolymers Based on Polystyrene Core and Poly(ethylene oxide) Corona", *Macromolecules*, Vol. 36, No. 22, pp. 8253–8259, 2003.

121. Brown, H. C., and G. Zweifel, "Hydroboration. VII. Directive Effects in the Hydroboration of Olefins", *Journal of American Chemical Society*, Vol. 82, No. 17, pp. 4708–4712, 1960.

122. Snyder, H. R., J. A. Kuck, and J. R. Johnson, "Organoboron Compounds, and the Study of Reaction Mechanisms. Primary Aliphatic Boronic Acids", *Journal of American Chemical Society*, Vol. 60, No. 1, pp. 105–111, 1938.

123. T. C. Chung, M. Raate, E. Berluche, and D. N. Schulz, "Synthesis of Functional Hydrocarbon Polymers with Well-Defined Molecular Structures", *Macromolecules*, Vol. 21, No. 7, pp. 1903-1907, 1988.

124. Mao, G., J. Wang, S. R. Clingman, and C. K. Ober, "Molecular Design, Synthesis, and Characterization of Liquid Crystal-Coil Diblock Copolymers with Azobenzene Side Groups", *Macromolecules,* Vol. 30, No. 9, pp. 2556-2567, 1997.

125. Walch, E, R. J. Gaymans, "Telechelic Polyisobutylene with Unsaturated End Groups and with Anhydride End Groups", *Polymer*, Vol. 35, No. 8, pp. 1774-1778, 1994.

126. Socrates, G., *Infrared and Raman characteristic group frequencies tables and charts*, Third Edition, Wiley, Chichester, 2001.

127. Tuzar, Z., and P. Kratochvíl, "Block and Graft Copolymer Micelles in Solution", *Advances in Colloid and Interface Science*, Vol. 6, No. 3, pp. 201-232, 1976.

128. Hruska, Z., G. Hurtrez, S. Walter, and G. Riess, "An Improved Technique of the Cumylpotassium Preparation: Application in the Synthesis of Spectroscopically Pure Polystyrene-Poly(ethylene oxide) Diblock Copolymers", *Polymer*, Vol. 33, No. 11, pp. 2447-2449, 1992.

129. Roovers, J. E. L., and S. Bywater, "Effect of Counter-ion in the Anionic Polymerization of Styrene in Cyclohexane", *Canadian Journal of Chemistry*, Vol. 46, pp. 2711-2713, 1968.

130. Richards, D. H., and M. Szwarc, "Block Polymers of Ethylene Oxide and Its Analogues with Styrene", *Transactions of the Faraday Society*, Vol. 55, pp. 1644-1650, 1959.

131. Taton, D., E. Cloutet, and Y. Gnanou, "Novel Amphiphilic Branched Copolymers Based on Polystyrene and Poly(ethy1ene oxide)", Macromolecular Chemistry and Physics, Vol. 199, No. 11, pp. 2501-2510, 1998.

132. Deodhar, T., N. Nugay, T. Nugay, R. Patel, G. Moggridge, and J. P. Kennedy, Synthesis of High-Molecular-Weight and Strength Polyisobutylene-Based Polyurethane and Its Use for the Development of a Synthetic Heart Valve", *Macromolecular Rapid Communications*, Vol. 44, No. 1, p. e2200147, 2023.

133. YíIgör, I, K. Ahmad, W. P. Steckle, D. Tyagi, G. L. Wilkes, J. E. McGrath, "Segmented Organosiloxane Copolymers. 1. Synthesis of Siloxane—Urea Copolymers, *Polymer*, Vol. 25, No. 12, pp. 1800-1806, 1984.

134. Gallu, R., F. Méchin, F. Dalmas, J. F. Gérard, R. Perrin, and F. Loup, "On the Use of Solubility Parameters to Investigate Phase Separation-Morphology-Mechanical Behavior Relationships of TPU", *Polymer*, Vol. 207, p. 122882, 2020.

135. Toth, K., N. Nugay, and J. P. Kennedy, "Polyisobutylene-Based Polyurethanes. IX. Synthesis, Characterization, and Properties of Polyisobutylene-Based Poly(urethane-ureas)", *Journal of Polymer Science, Part A: Polymer Chemistry,* Vol. 54, No. 15, pp. 2361-2369, 2016.

136. Srichatrapimuk, V. W., and S. L. Cooper, "Infrared thermal analysis of polyurethane block polymers", *Journal of Macromolecular Science, Part B: Physics*, Vol. 15, No. 2, pp. 267-311, 1978.

137. Bertoldi, S., S. Fare, S. Montagna, and M. C. Tanzi, "Innovative polymers for TMD rehabilitation devices", *Journal of Dental Applications*, Vol. 1, No. 6, pp. 119-123, 2014.

138. Makarevich, M. I., P. A. Nikishau, I. A. Berezianko, T. V. Glushkova, M. A. Rezvova, E. A. Ovcharenko, G. E. Bekmukhamedov, D. G.Yakhvarov, and S. V. Kostjuk, "Aspects of the Synthesis of Poly(styrene-block-isobutylene-block-styrene) by $TiCl_4$-Co-initiated Cationic Polymerization in Open Conditions", *Macromol*, Vol. 1, No. 4, pp. 243-255, 2021.

139. Rudin, A., and D. Burgin, “Effects of Molecular Weight and Chain Ends on Glass Transition of Polystyrene”, *Polymer*, Vol. 16, No. 4, pp. 291-297, 1975

140. Booth, C., J. M. Bruce, and M. Buggy, “Effect of End Groups on the Melting Temperatures of Low Molecular Weight Poly(ethylene oxide), *Polymer*, Vol. 13, No. 10, pp. 475-478, 1972

141. Venkateshaiah, A., V. V. T. Padil, M. Nagalakshmaiah, S. Waclawek, M. Cernik, and R. S. Varma, “Microscopic Techniques for the Analysis of Micro and Nanostructures of Biopolymers and Their Derivatives”, *Polymers*, Vol. 12, No. 3, p. 512, 2020.

142. Crago, M., A. Lee, S. Farajikhah, F. Oveissi, D. F. Fletcher, F Dehghani, D. S. Winlaw, and S. Naficy, “The Evolution of Polyurethane Heart Valve Replacements: How Chemistry Translates to the Clinic”, *Materials Today Communications*, Vol. 33, p. 104916, 2022.

143. Kekec, N. C., M. B. Akolpoglu, U. Bozuyuk, S. Kizilel, N. Nugay, T. Nugay, and J. P. Kennedy, “Calcification Resistance of Polyisobutylene and Polyisobutylene-Based Materials”, *Polymers Advnced Technologies*, Vol. 30, No. 7, pp. 1836-1846, 2019.

144. Kekec Senel, N. C., *High Strength Polyisobutylene Based Structures: Synthesis, Characterizaton and Suitability for Biomedical Applications*, Ph.D. Thesis, Bogazici University, 2023.

145. Weldels, S., and L. Averous, “Biobased Polyurethanes for Biomedical Applications”, *Bioactive Materials*, Vol. 6, No. 4, pp. 1083-1106, 2021.

146. Pechar, T. W., S. Sohn, G. L. Wilkes, S. Ghosh, C. E. Frazier, A. Fornof, and T. E. Long, “Characterization and Comparison of Polyurethane Networks Prepared Using Soybean-Based Polyols with Varying Hydroxyl Content and Their Blends with Petroleum-Based Polyols”, *Journal of Applied Polymer Science*, Vol. 101, No. 3, pp. 1432-1443, 2006.

147. Robertson, M. L., M. A. Hillmyer, A. C. Mortamet, and A. J. Ryan, “Biorenewable Multiphase Polymers”, *MRS Bulletin*, Vol. 35, No. 3, pp. 194-200, 2010.

148. Morales-Cerrada, R., R. Tavernier, and S. Caillol, “Fully Bio-Based Thermosetting Polyurethanes from Bio-Based Polyols and Isocyanates”, *Polymers*, Vol. 13, No. 8, p. 1255, 2021.

149. Kennedy, J. P, G. Erdodi and S. Jewrajka, “Polymers Having Both Hard and Soft Segments, and Process for Making Same”, US Patent WO 2010039986 A1, April 8, 2010. https://patentscope.wipo.int/search/en/detail.jsf?docId=WO2010039986, Accessed on April 4, 2024.

150. Murgasova, R., E. L. Brantley, D. M. Hercules, and H. Nefzger, “Characterization of Polyester-Polyurethane Soft and Hard Blocks by a Combination of MALDI, SEC, and Chemical Degradation”, *Macromolecules*, Vol. 35, No. 22, pp. 8338-8345, 2002.

151. Chapman, T. M., “Models for Polyurethane Hydrolysis Under Moderately Acidic Conditions: a Comparative Study of Hydrolysis Rates of Urethanes, Ureas, and Amides”, *Journal of Polymer Sciene Part A Polymer Chemistry*, Vol. 27, No. 6, pp. 1993-2005, 1989.

152. Erman, B., B. M. Baysal, “Temperature Dependence of Swelling of Polystyrene Networks”, *Macromolecules*, Vol. 18, No. 9, pp. 1696-1700, 1985.

153. Sugiyama, F., A. T. Kleinschmidt, L. V. Kayser, D. Rodriquez, M. Finn, M. A. Alkhadra, J. M. H. Wan, J. Ramírez, A. S. C. Chiang, S. E., Root, S. Savagatrupa, and D. J. Lipomi, “Effects of Flexibility and Branching of Side Chains on the Mechanical Properties of Low-Bandgap Conjugated Polymer”, *Polymer Chemistry*, Vol. 9, No. 33, pp. 4354-4363, 2018.

154. Sawpan, A. M., “Polyurethanes from Vegetable Oils and Applications: a Review”, *Journal of Polymer Research*, Vol. 25, p. 184, 2018.

155. Rahman, M. Z., M. Rahman, T. Mahbub, M. Ashiquzzaman, S. Sagadevan, and M. E. Hoque, “Advanced Biopolymers for Automobile and Aviation Engineering Applications”, *Journal of Polymer Research*, Vol. 30, p. 106, 2023.

156. Barison, A., C. W. da Silva, F. R. Campos, F. Simonelli, C. A. Lenz, and A. G. Ferreira, “A Simple Methodology for the Determination of Fatty Acid Composition in

Edible Oils through ^{1}H NMR Spectroscopy", *Magnetic Resonance in Chemistry*, Vol. 48, No. 8, pp. 642-650, 2010.

157. Vlachos, N., Y. Skopelitis, M. Psaroudaki, V. Konstantinidou, A. Chatzilazarou, and E. Tegou, "Applications of Fourier Transform-Infrared Spectroscopy to Edible Oils", *Analytica Chimica Acta*, Vol. 573–574, pp. 459-465, 2006.

158. Zhang, Q., A. S. M. Saleh, and Q. Shen, "Monitoring of Changes in Composition of Soybean Oil During Deep-Fat Frying with Different Food Types", *Journal of the American Oil Chemist's Society*, Vol. 93, No. 1, pp.69-81, 2016.

159. Poiana, M. A., E. Alexa, M. F. Munteanu, R. Gligor, D. Moigradean, and C. Mateescu, "Use of ATR-FTIR Spectroscopy to Detect the Changes in Extra Virgin Olive Oil by Adulteration with Soybean Oil and High Temperature Heat Treatment", *Open Chemistry*, Vol. 13, No. 1, pp. 689-698, 2015.

160. Lu, Q. W., T. R. Hoye, and C. W. Macosko, "Reactivity of Common Functional Groups with Urethanes: Models for Reactive Compatibilization of Thermoplastic Polyurethane Blends", *Journal of Polymer Science Part A Polymer Chemistry*, Vol. 40, No. 14, pp. 2310-2328, 2002.

161. Lligadas, G., J. C. Ronda, M. Galià, U. Biermann, and J. O. Metzger, "Synthesis and Characterization of Polyurethanes from Epoxidized Methyl Oleate Based Polyether Polyols as Renewable Resources", *Journal of Polymer Science Part A Polymer Chemistry*, Vol. 44, No. 1, pp. 634-645, 2006.

162. Nugay, N., T. Nugay, T. Deodhar, B. L. Keszler, J. P. Kennedy "Low Cost Bifunctional Initiators for Bidirectional Living Cationic Polymerization of Olefins. II. Hyperbranched Styrene–Isobutylene–Styrene Triblocks with Superior Combination of Properties", *Journal of Polymer Science Part A Polymer Chemistry*, Vol. 56, pp. 705-713, 2018.

163. Hu, L., Z. Pu, Y. Zhong, L. Liu, J. Cheng, and J. Zhong, "Effect of Different Carboxylic Acid Group Contents on Microstructure and Properties of Waterborne Polyurethane Dispersions", *Journal of Polymer Research*, Vol. 27, p. 129, 2020.

164. Levchik, G. F., K. Si, S. V. Levchik, G. Camino, and C. A. Wilkie, “The Correlation between Cross-linking and Thermal Stability: Cross-Linked Polystyrenes and Polymethacrylates*”, Polymer Degradation Stability*, Vol. 65, No. 3, pp. 395-403, 1999.

165. Mittal, N., T. Benselfelt, F. Ansari, K. Gordeyeva, S. V. Roth, L. Wagberg, and L. D. Söderberg, “Ion-Specific Assembly of Strong, Tough, and Stiff Biofibers”, *Angew Chem Int* Vol. 58, No.51, pp. 18562-18569, 2019.

APPENDIX A: SUPPLEMENTARY MATERIAL

Supporting figures associated with this thesis can be found here.

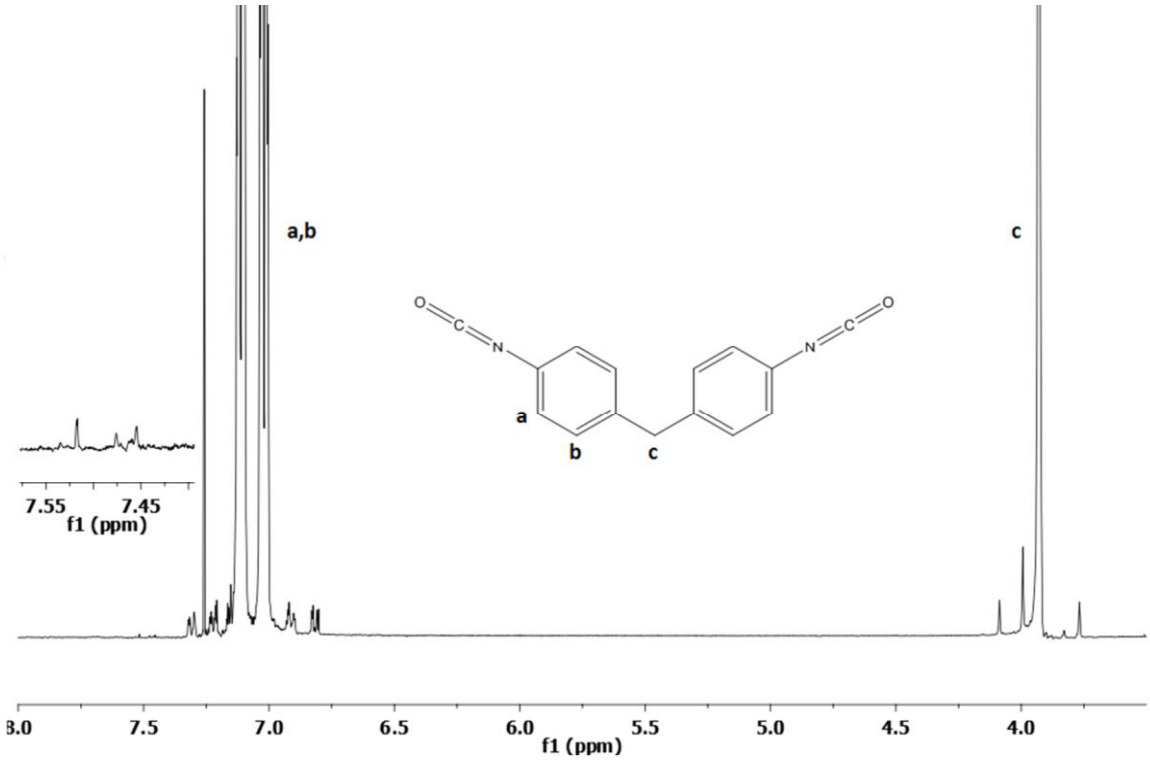

Figure A.1. ^{1}H NMR spectrum of distilled MDI.

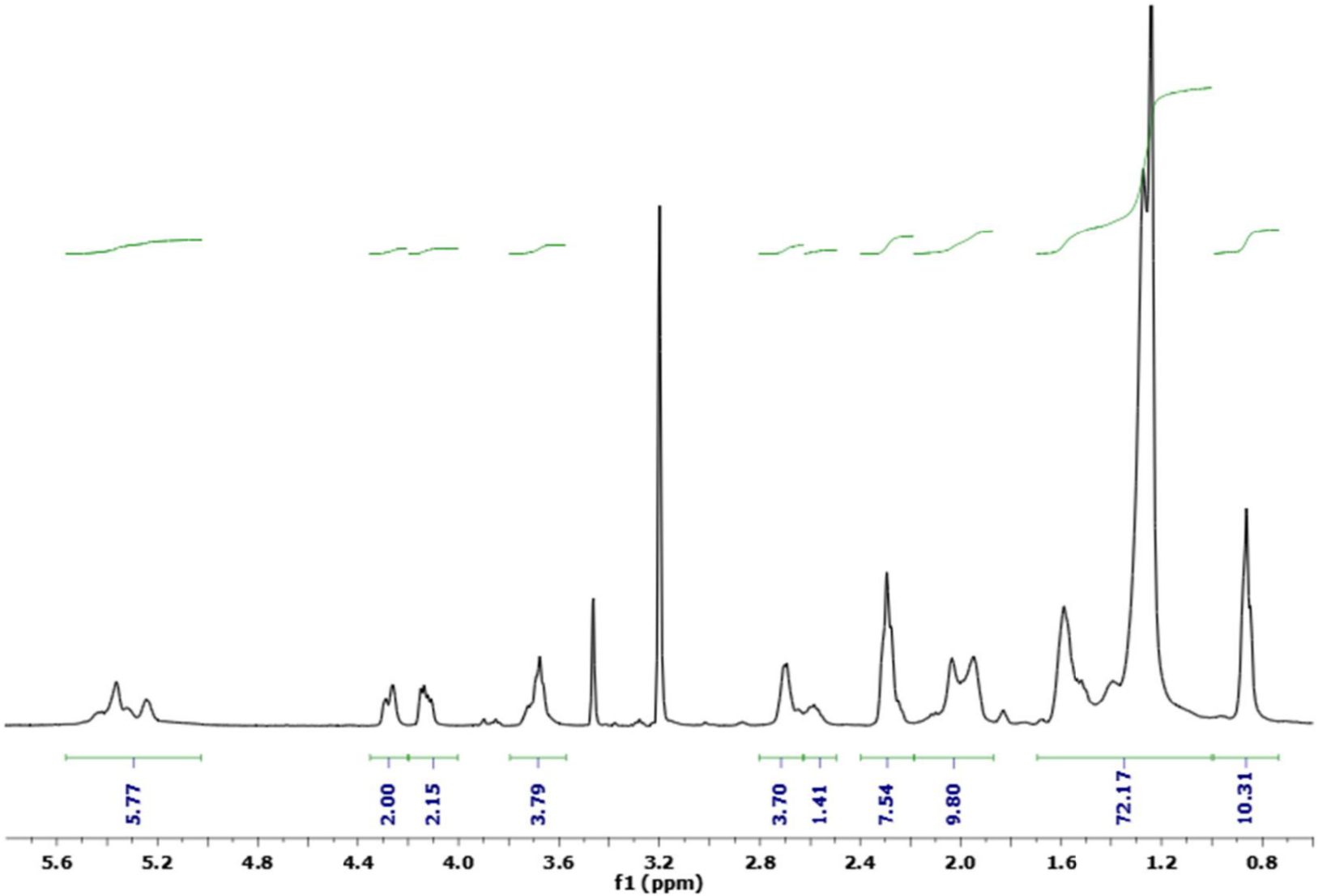

Figure A.2. ^{1}H NMR spectrum of SBO polyol experiment 1.

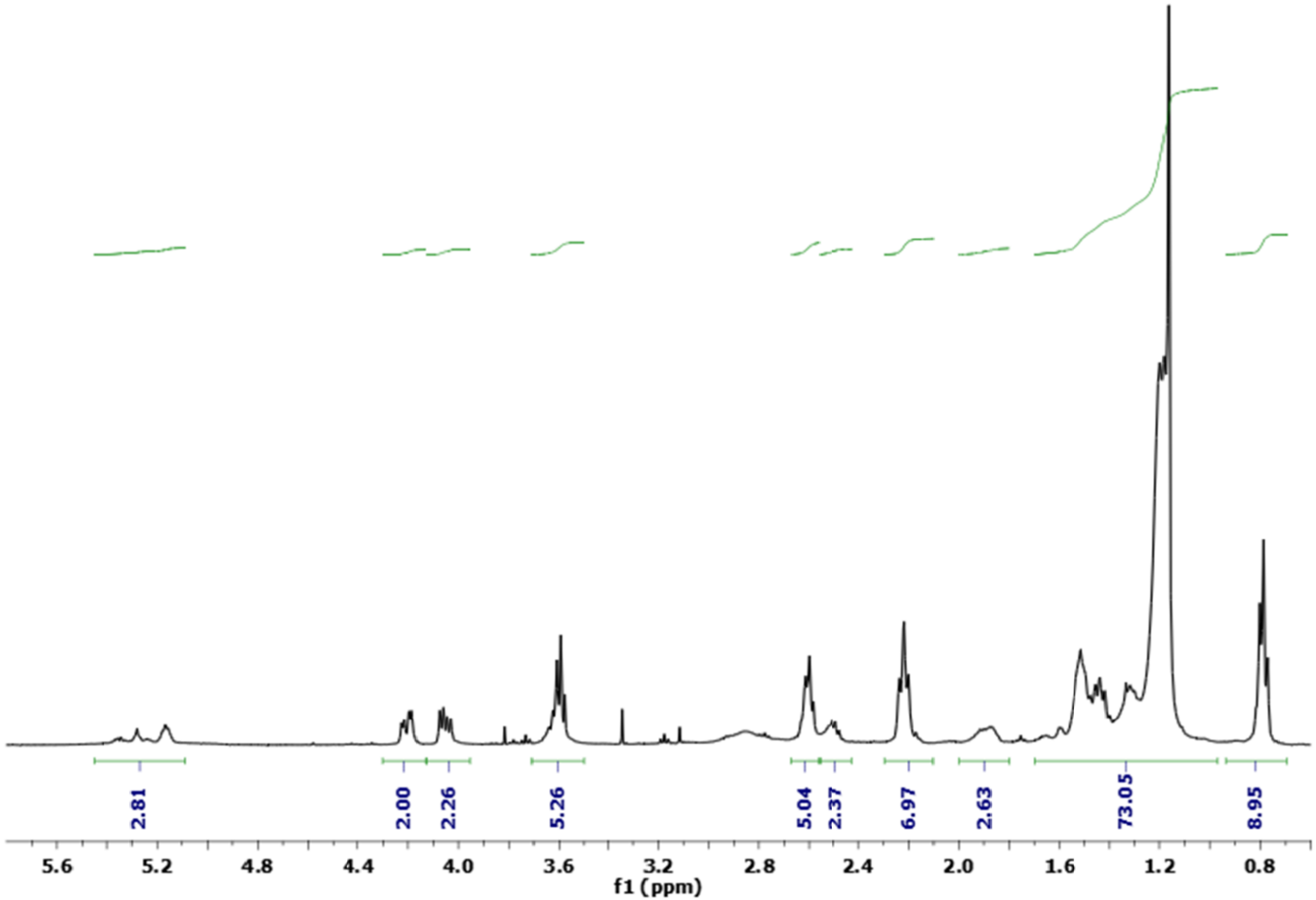

Figure A.3. ^{1}H NMR spectrum of SBO polyol experiment 2.

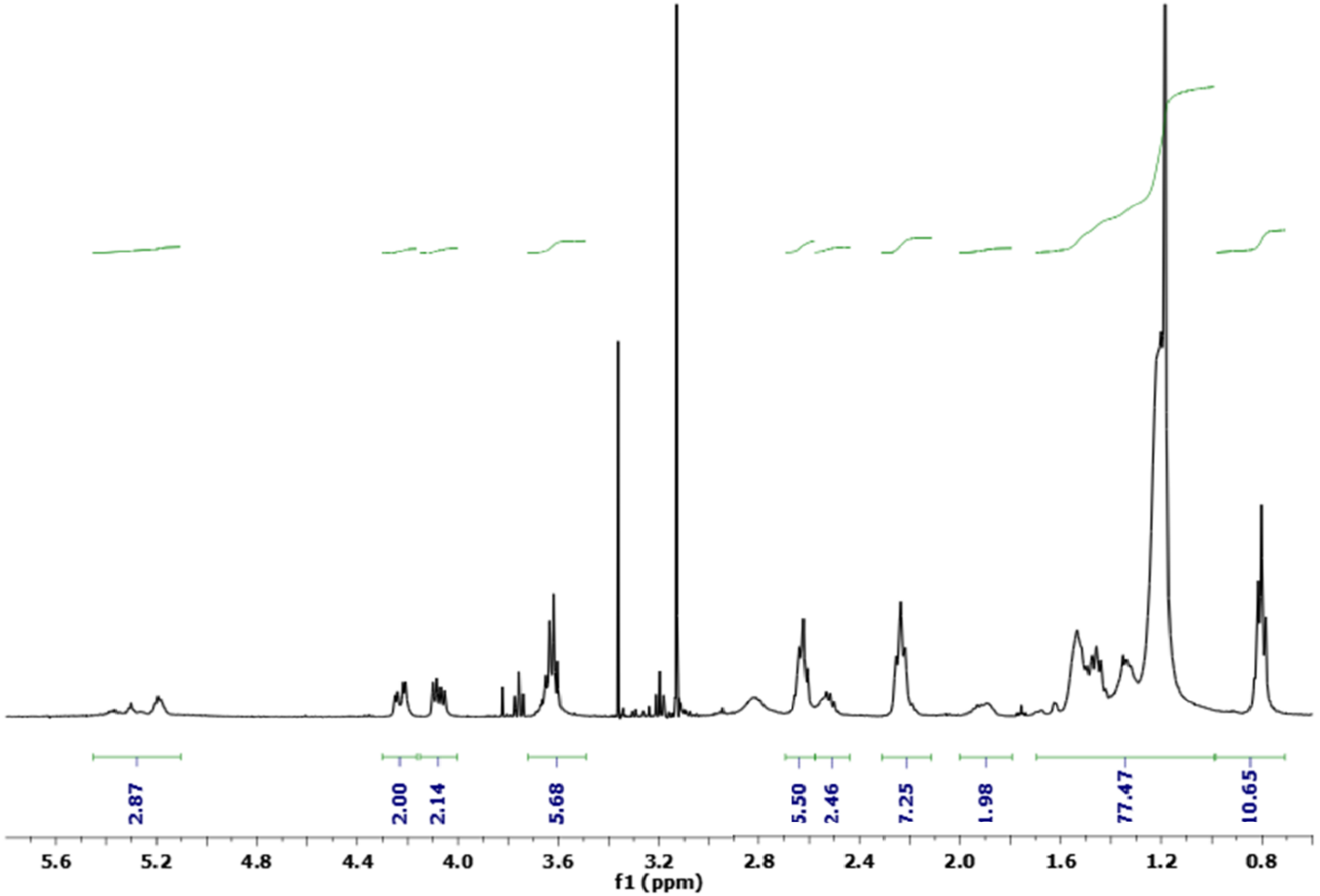

Figure A.4.[1]H NMR spectrum of SBO polyol experiment 3.

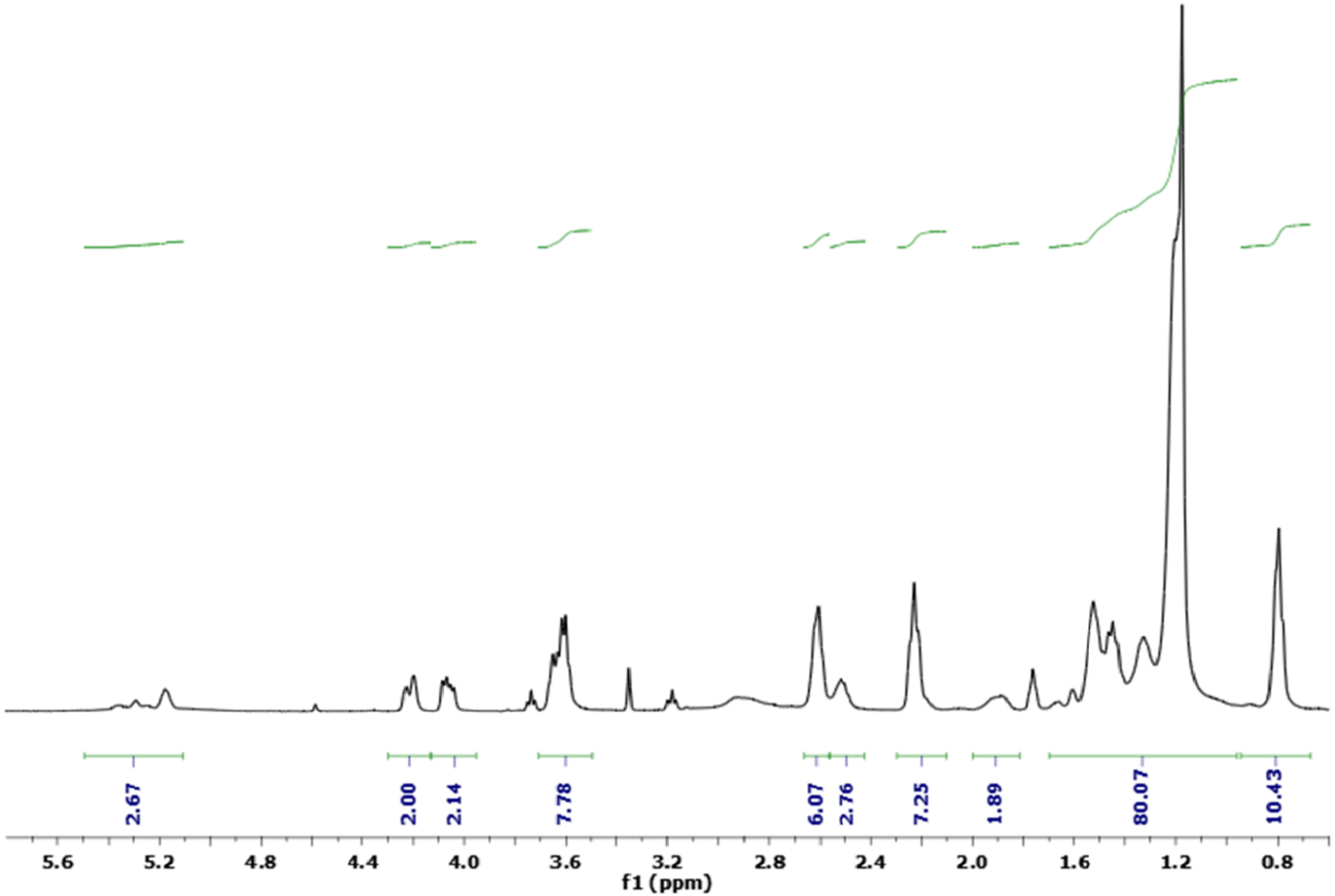

Figure A.5. ^{1}H NMR spectrum of SBO polyol experiment 4.

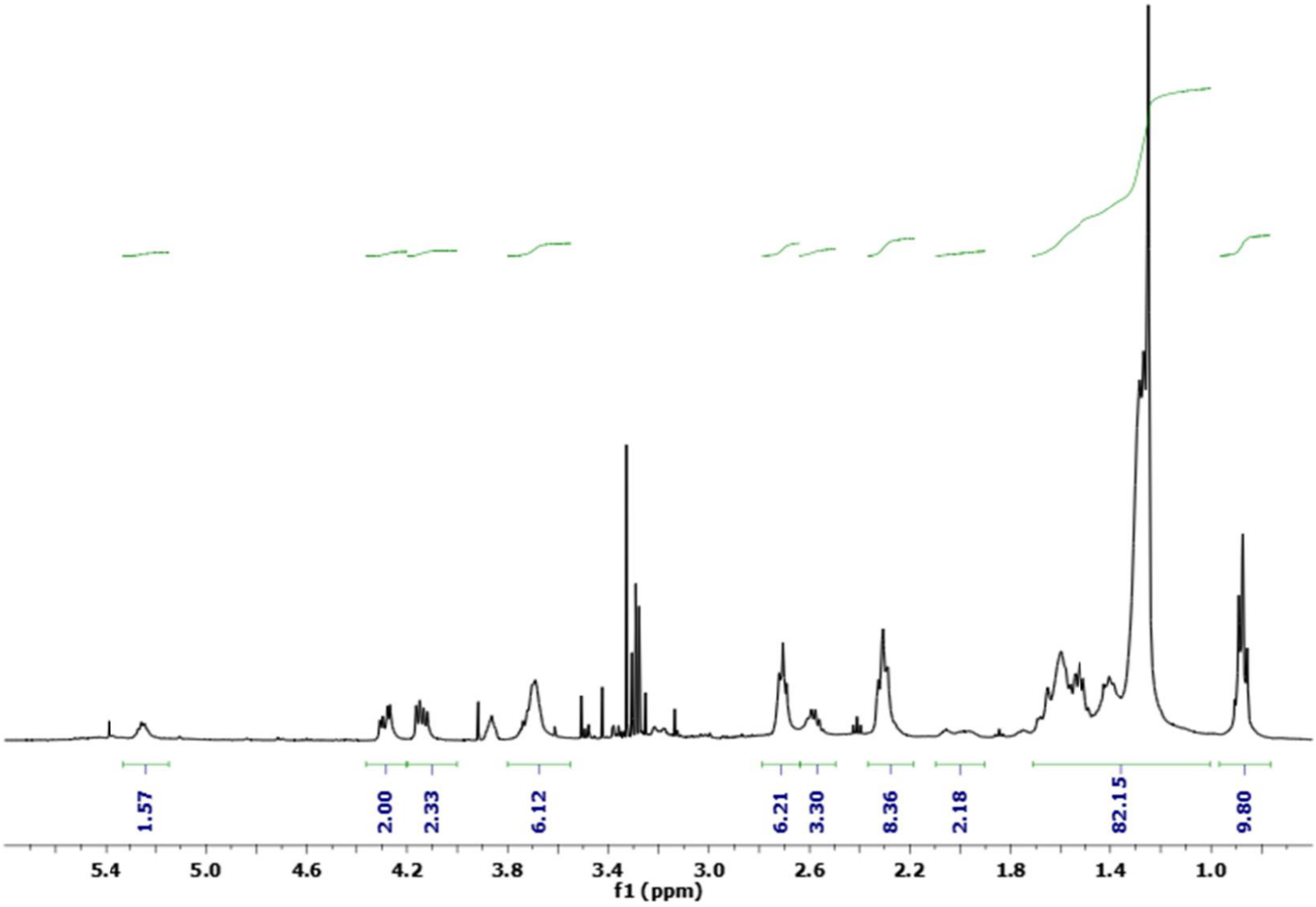

Figure A.6. ^{1}H NMR spectrum of SBO polyol experiment 5.

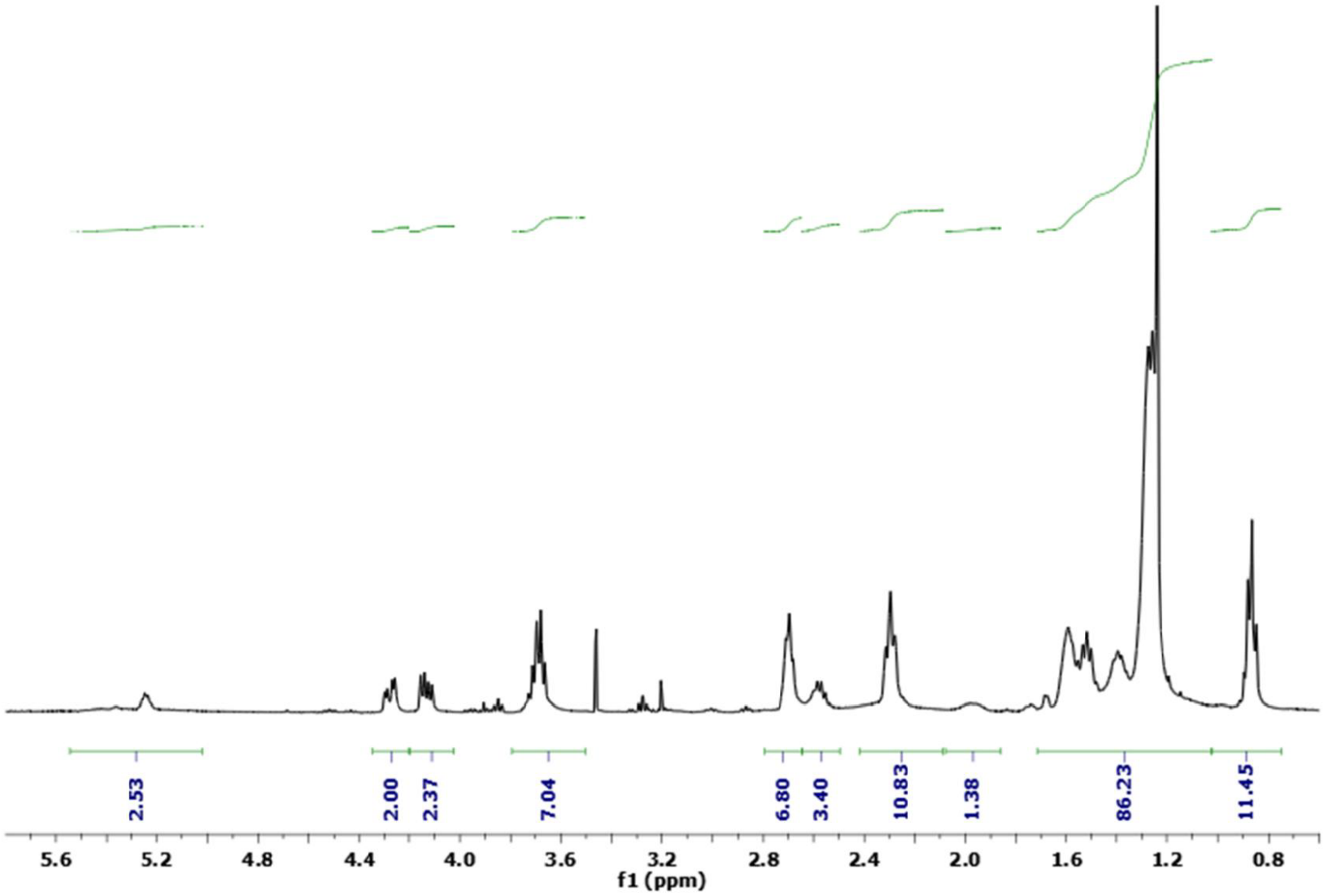

Figure A.7. ^{1}H NMR spectrum of SBO polyol experiment 6.

APPENDIX B: COPYRIGHT LICENCES

The copyrights for figures taken from journal articles or books can be found here.

License Details

This Agreement between Bogazici University -- Elif Kurnaz ("You") and Springer Nature ("Springer Nature") consists of your license details and the terms and conditions provided by Springer Nature and Copyright Clearance Center.

Print Copy

License Number	5753720424928
License date	Mar 21, 2024
Licensed Content Publisher	Springer Nature
Licensed Content Publication	Polymer Bulletin
Licensed Content Title	New telechelic polymers and sequential copolymers by polyfunctional initiator-transfer agents (inifers)
Licensed Content Author	Victor S. C. Chang et al
Licensed Content Date	Dec 31, 1969
Type of Use	Thesis/Dissertation
Requestor type	academic/university or research institute
Format	print and electronic
Portion	figures/tables/illustrations
Number of figures/tables/illustrations	1
Will you be translating?	no
Circulation/distribution	1 - 29
Author of this Springer Nature content	no
Title of new work	SYNTHESIS OF NOVEL POLYISOBUTYLENE/POLYSTYRENE AND POLYISOBUTYLENE/MODIFIED SOYBEAN OIL BASED POLYURETHANES AND THEIR CHARACTERIZATIONS
Institution name	Bogazici University
Expected presentation date	Mar 2024
Portions	Image on page 340
Requestor Location	Bogazici University General Delivery

Figure B.1. Permission for Figure 1.2 from [22], Springer Nature, Copyright (1969).

License Details

This Agreement between Bogazici University -- Elif Kurnaz ("You") and John Wiley and Sons ("John Wiley and Sons") consists of your license details and the terms and conditions provided by John Wiley and Sons and Copyright Clearance Center.

Print Copy

License Number	5753740218259
License date	Mar 21, 2024
Licensed Content Publisher	John Wiley and Sons
Licensed Content Publication	Journal of Polymer Science Part A: Polymer Chemistry
Licensed Content Title	Living carbocationic polymerization. XXX. One-pot synthesis of allyl-terminated linear and tri-arm star polyisobutylenes, and epoxy- and hydroxy-telechelics therefrom
Licensed Content Author	Joseph P. Kennedy, Béla Iván
Licensed Content Date	Mar 10, 2003
Licensed Content Volume	28
Licensed Content Issue	1
Licensed Content Pages	16
Type of Use	Dissertation/Thesis
Requestor type	University/Academic
Format	Print and electronic
Portion	Figure/table
Number of figures/tables	1
Will you be translating?	No
Title of new work	SYNTHESIS OF NOVEL POLYISOBUTYLENE/POLYSTYRENE AND POLYISOBUTYLENE/MODIFIED SOYBEAN OIL BASED POLYURETHANES AND THEIR CHARACTERIZATIONS
Institution name	Bogazici University
Expected presentation date	Mar 2024
Portions	Image on page 100
Requestor Location	Bogazici University General Delivery

Figure B.2. Permission for Figure 1.3 from [37], Springer Nature, Copyright (2003).

License Details

This Agreement between Bogazici University -- Elif Kurnaz ("You") and John Wiley and Sons ("John Wiley and Sons") consists of your license details and the terms and conditions provided by John Wiley and Sons and Copyright Clearance Center.

Print Copy

License Number	5753740782625
License date	Mar 21, 2024
Licensed Content Publisher	John Wiley and Sons
Licensed Content Publication	Journal of Polymer Science Part A: Polymer Chemistry
Licensed Content Title	Quantitative syntheses of novel polyisobutylenes fitted with terminal primary ⊐Br, ⊐OH, ⊐NH2, and methacrylate termini
Licensed Content Author	Joseph P. Kennedy, Subramanyam Ummadisetty
Licensed Content Date	May 15, 2008
Licensed Content Volume	46
Licensed Content Issue	12
Licensed Content Pages	7
Type of Use	Dissertation/Thesis
Requestor type	University/Academic
Format	Print and electronic
Portion	Figure/table
Number of figures/tables	1
Will you be translating?	No
Title of new work	SYNTHESIS OF NOVEL POLYISOBUTYLENE/POLYSTYRENE AND POLYISOBUTYLENE/MODIFIED SOYBEAN OIL BASED POLYURETHANES AND THEIR CHARACTERIZATIONS
Institution name	Bogazici University
Expected presentation date	Mar 2024
Portions	Image on page 4238
Requestor Location	Bogazici University General Delivery

Figure B.3. Permission for Figure 1.4 from [39], John Wiley and Sons, Copyright (2008).

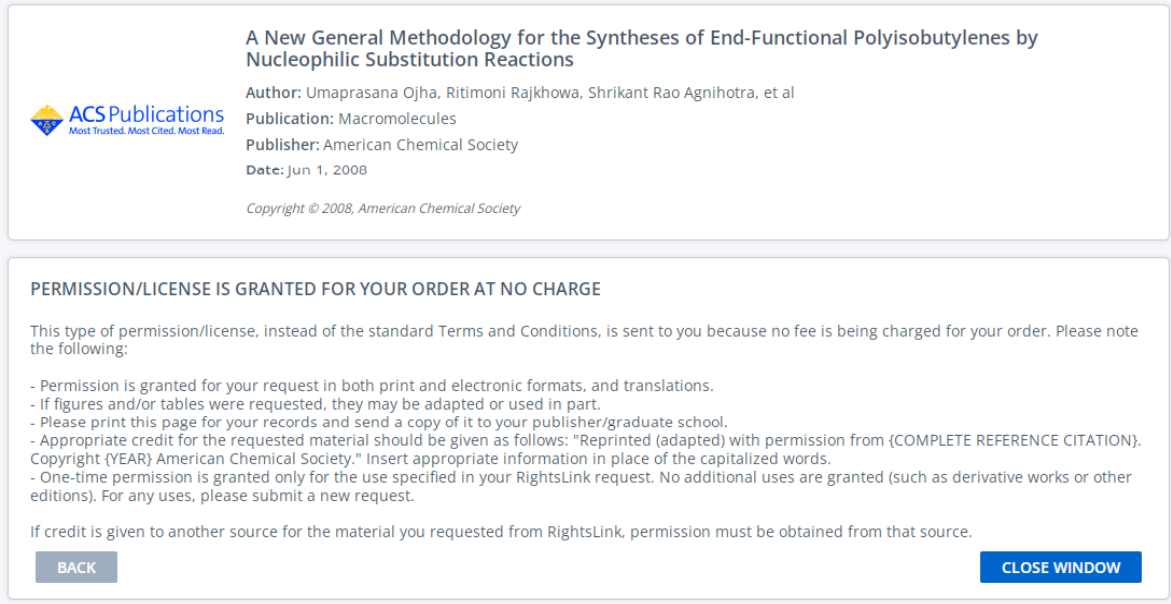

Figure B.4. Permission for Figure 1.5 from [40], American Chemical Society, Copyright (2008).

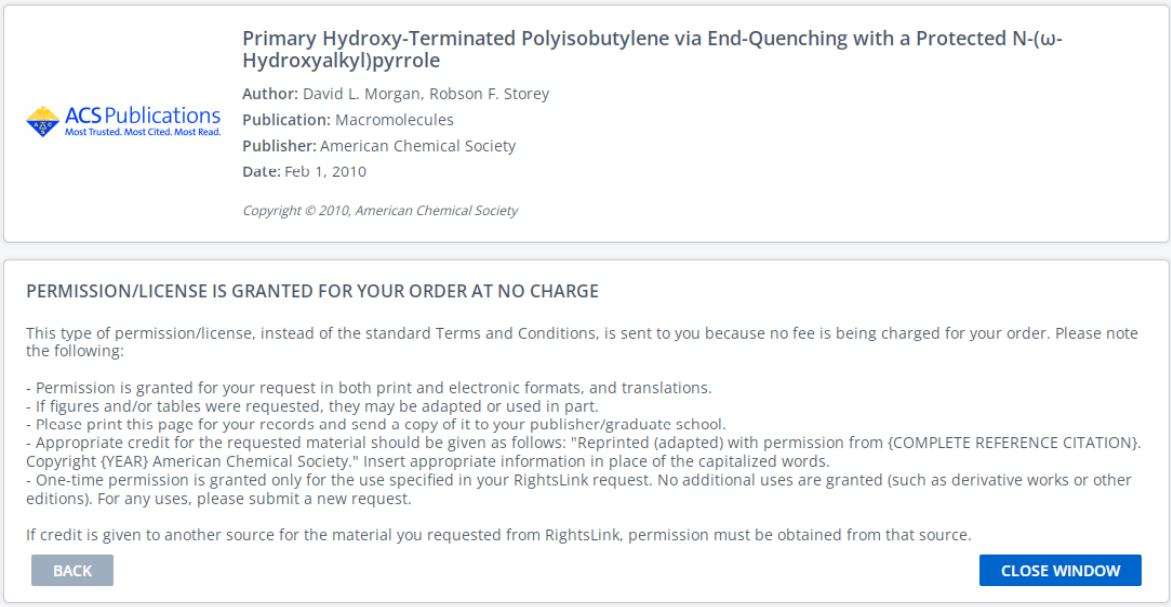

Figure B.5. Permission for Figure 1.6 from [41], American Chemical Society, Copyright (2010).

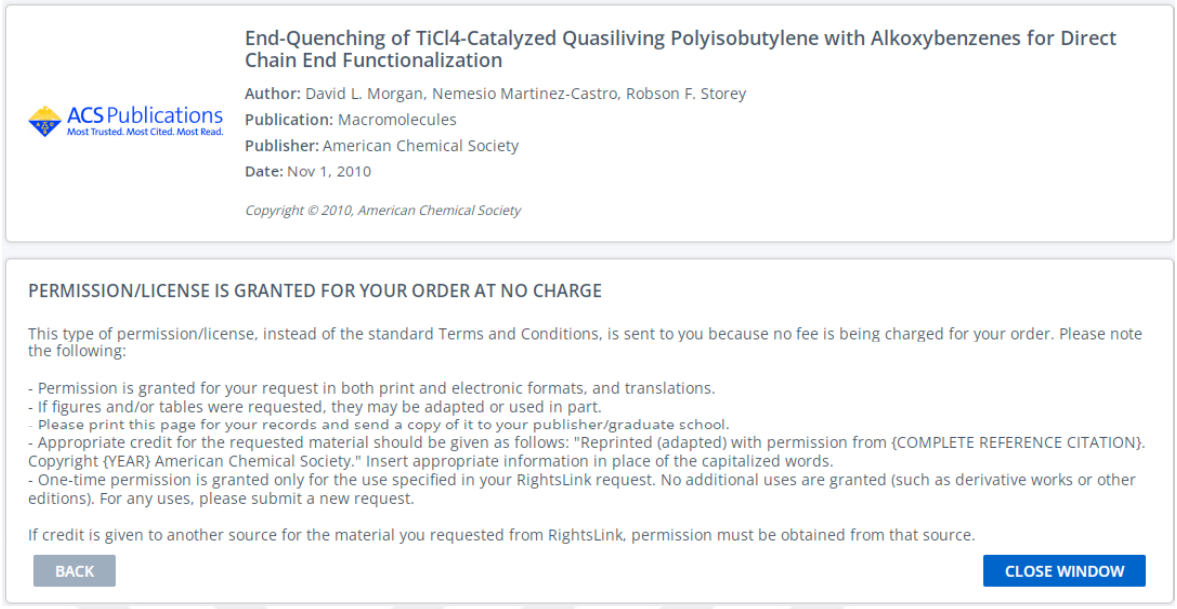

End-Quenching of TiCl4-Catalyzed Quasiliving Polyisobutylene with Alkoxybenzenes for Direct Chain End Functionalization

Author: David L. Morgan, Nemesio Martinez-Castro, Robson F. Storey
Publication: Macromolecules
Publisher: American Chemical Society
Date: Nov 1, 2010

Copyright © 2010, American Chemical Society

PERMISSION/LICENSE IS GRANTED FOR YOUR ORDER AT NO CHARGE

This type of permission/license, instead of the standard Terms and Conditions, is sent to you because no fee is being charged for your order. Please note the following:

- Permission is granted for your request in both print and electronic formats, and translations.
- If figures and/or tables were requested, they may be adapted or used in part.
- Please print this page for your records and send a copy of it to your publisher/graduate school.
- Appropriate credit for the requested material should be given as follows: "Reprinted (adapted) with permission from {COMPLETE REFERENCE CITATION}. Copyright {YEAR} American Chemical Society." Insert appropriate information in place of the capitalized words.
- One-time permission is granted only for the use specified in your RightsLink request. No additional uses are granted (such as derivative works or other editions). For any uses, please submit a new request.

If credit is given to another source for the material you requested from RightsLink, permission must be obtained from that source.

BACK CLOSE WINDOW

Figure B. 6. Permission for Figure 1.6 from [42], American Chemical Society, Copyright (2010).

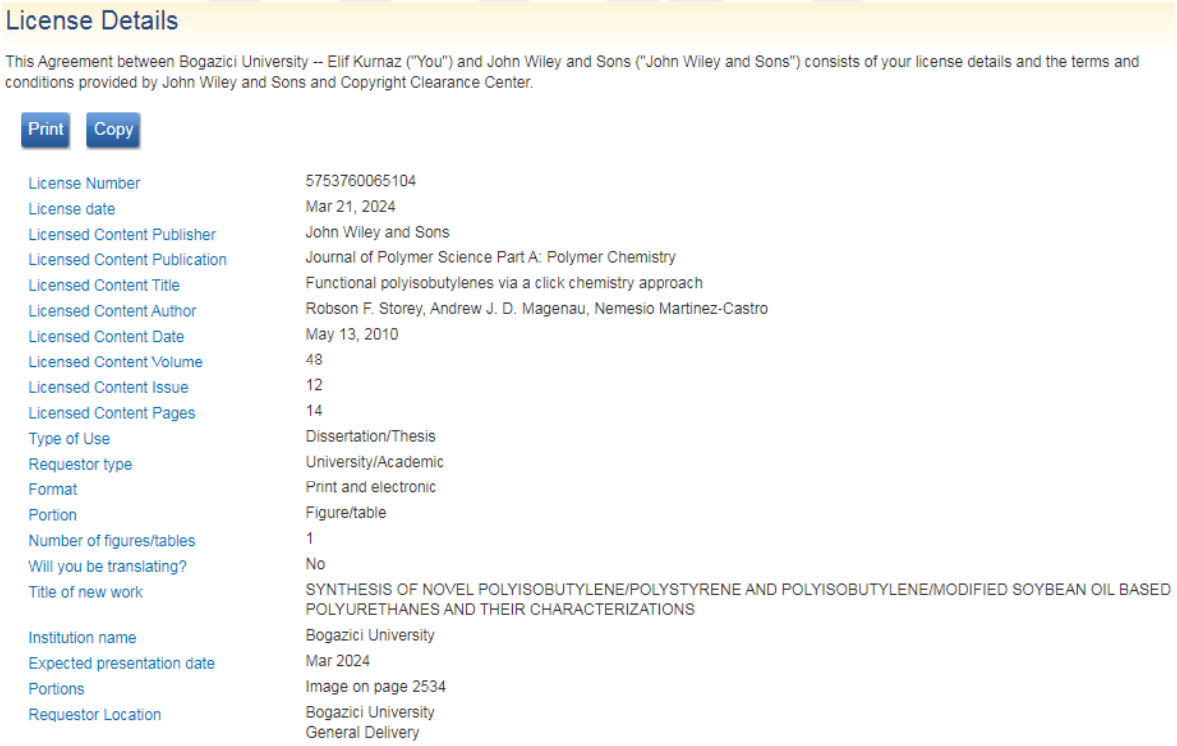

License Details

This Agreement between Bogazici University -- Elif Kurnaz ("You") and John Wiley and Sons ("John Wiley and Sons") consists of your license details and the terms and conditions provided by John Wiley and Sons and Copyright Clearance Center.

Print Copy

License Number	5753760065104
License date	Mar 21, 2024
Licensed Content Publisher	John Wiley and Sons
Licensed Content Publication	Journal of Polymer Science Part A: Polymer Chemistry
Licensed Content Title	Functional polyisobutylenes via a click chemistry approach
Licensed Content Author	Robson F. Storey, Andrew J. D. Magenau, Nemesio Martinez-Castro
Licensed Content Date	May 13, 2010
Licensed Content Volume	48
Licensed Content Issue	12
Licensed Content Pages	14
Type of Use	Dissertation/Thesis
Requestor type	University/Academic
Format	Print and electronic
Portion	Figure/table
Number of figures/tables	1
Will you be translating?	No
Title of new work	SYNTHESIS OF NOVEL POLYISOBUTYLENE/POLYSTYRENE AND POLYISOBUTYLENE/MODIFIED SOYBEAN OIL BASED POLYURETHANES AND THEIR CHARACTERIZATIONS
Institution name	Bogazici University
Expected presentation date	Mar 2024
Portions	Image on page 2534
Requestor Location	Bogazici University General Delivery

Figure B.7. Permission for Figure 1.7 from [43], John Wiley and Sons, Copyright (2010).

CCC Marketplace

This is a License Agreement between Elif Kurnaz ("User") and Copyright Clearance Center, Inc. ("CCC") on behalf of the Rightsholder identified in the order details below. The license consists of the order details, the Marketplace Permissions General Terms and Conditions below, and any Rightsholder Terms and Conditions which are included below.

All payments must be made in full to CCC in accordance with the Marketplace Permissions General Terms and Conditions below.

Order Date	21-Mar-2024	Type of Use	Republish in a thesis/dissertation
Order License ID	1464692-1	Publisher	Royal Society of Chemistry
ISSN	1759-9962	Portion	Image/photo/illustration

LICENSED CONTENT

Publication Title	Polymer chemistry	Rightsholder	Royal Society of Chemistry
Article Title	Facile polyisobutylene functionalization viathiol–ene click chemistry	Publication Type	e-Journal
		Start Page	831
Author/Editor	Royal Society of Chemistry (Great Britain)	Issue	6
Date	01/01/2010	Volume	1
Language	English	URL	http://www.rsc.org/Publishing/Journals/PY...
Country	United Kingdom of Great Britain and Northern Ireland		

REQUEST DETAILS

Portion Type	Image/photo/illustration	Distribution	Worldwide
Number of Images / Photos / Illustrations	1	Translation	Original language of publication
Format (select all that apply)	Print, Electronic	Copies for the Disabled?	No
Who Will Republish the Content?	Publisher, not-for-profit	Minor Editing Privileges?	Yes
Duration of Use	Life of current edition	Incidental Promotional Use?	No
Lifetime Unit Quantity	Up to 499	Currency	USD
Rights Requested	Main product, any product related to main product, and other compilations/derivative products		

NEW WORK DETAILS

Title	SYNTHESIS OF NOVEL POLYISOBUTYLENE/POLYSTYRENE AND POLYISOBUTYLENE/MODIFIED SOYBEAN OIL BASED POLYURETHANES AND THEIR CHARACTERIZATIONS	Institution Name	Bogazici University
		Expected Presentation Date	2024-03-21
Instructor Name	Elif Kurnaz		

ADDITIONAL DETAILS

Order Reference Number	N/A	The Requesting Person / Organization to Appear on the License	Elif Kurnaz

REQUESTED CONTENT DETAILS

Title, Description or Numeric Reference of the Portion(s)	Scheme 1	Title of the Article / Chapter the Portion Is From	Facile polyisobutylene functionalization viathiol–ene click chemistry
Editor of Portion(s)	Magenau, Andrew J. D.; Chan, Justin W.; Hoyle, Charles E.; Storey, Robson F.	Author of Portion(s)	Magenau, Andrew J. D.; Chan, Justin W.; Hoyle, Charles E.; Storey, Robson F.
Volume / Edition	1	Issue, if Republishing an Article From a Serial	6
Page or Page Range of Portion	831	Publication Date of Portion	2010-07-13

Figure B.8. Permission for Figure 1.7 from [44], Royal Society of Chemistry, Copyright (2010).

License Details

This Agreement between Bogazici University -- Elif Kurnaz ("You") and John Wiley and Sons ("John Wiley and Sons") consists of your license details and the terms and conditions provided by John Wiley and Sons and Copyright Clearance Center.

Print Copy

License Number	5753790333322
License date	Mar 21, 2024
Licensed Content Publisher	John Wiley and Sons
Licensed Content Publication	Journal of Polymer Science Part A: Polymer Chemistry
Licensed Content Title	Polyisobutylene-based polyurethanes. VIII. Polyurethanes with -O-S-PIB-S-O- soft segments
Licensed Content Author	Joseph. P. Kennedy, Nihan Nugay, Nur Cicek Kekec, et al
Licensed Content Date	Oct 28, 2015
Licensed Content Volume	54
Licensed Content Issue	8
Licensed Content Pages	13
Type of Use	Dissertation/Thesis
Requestor type	University/Academic
Format	Print and electronic
Portion	Figure/table
Number of figures/tables	1
Will you be translating?	No
Title of new work	SYNTHESIS OF NOVEL POLYISOBUTYLENE/POLYSTYRENE AND POLYISOBUTYLENE/MODIFIED SOYBEAN OIL BASED POLYURETHANES AND THEIR CHARACTERIZATIONS
Institution name	Bogazici University
Expected presentation date	Mar 2024
Portions	Image on page 1120
Requestor Location	Bogazici University General Delivery

Figure B.9. Permission for Figure 1.8 from [46], John Wiley and Sons, Copyright (2015).

License Details

This Agreement between Bogazici University -- Elif Kurnaz ("You") and John Wiley and Sons ("John Wiley and Sons") consists of your license details and the terms and conditions provided by John Wiley and Sons and Copyright Clearance Center.

Print Copy

License Number	5753790757821
License date	Mar 21, 2024
Licensed Content Publisher	John Wiley and Sons
Licensed Content Publication	Wiley Books
Licensed Content Title	Anionic Vinyl Polymerization
Licensed Content Author	Axel H. E. Müller, Durairaj Baskaran
Licensed Content Date	Jan 7, 2010
Licensed Content Pages	56
Type of Use	Dissertation/Thesis
Requestor type	University/Academic
Format	Print and electronic
Portion	Figure/table
Number of figures/tables	1
Will you be translating?	No
Title of new work	SYNTHESIS OF NOVEL POLYISOBUTYLENE/POLYSTYRENE AND POLYISOBUTYLENE/MODIFIED SOYBEAN OIL BASED POLYURETHANES AND THEIR CHARACTERIZATIONS
Institution name	Bogazici University
Expected presentation date	Mar 2024
Portions	Scheme 1.1 on page 2
Requestor Location	Bogazici University General Delivery

Figure B.10. Permission for Figure 1.9 from [49], John Wiley and Sons, Copyright (2010).

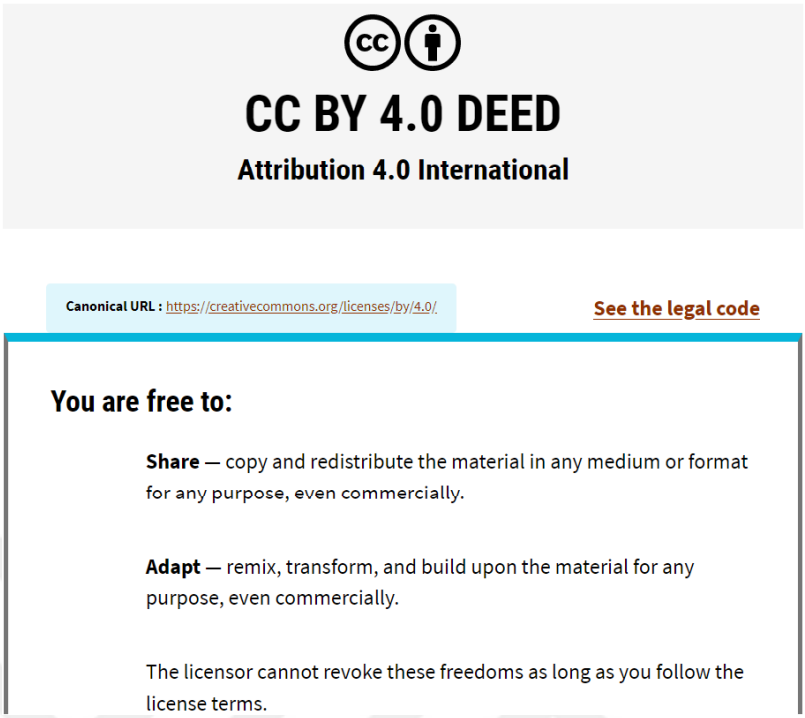

Figure B.11. Permission for Figure 1.10 from [58] https://www.degruyter.com/document/doi/10.1515/cti-2020-0028/html, licensed under CC BY 4.0 https://creativecommons.org/licenses/by/4.0/

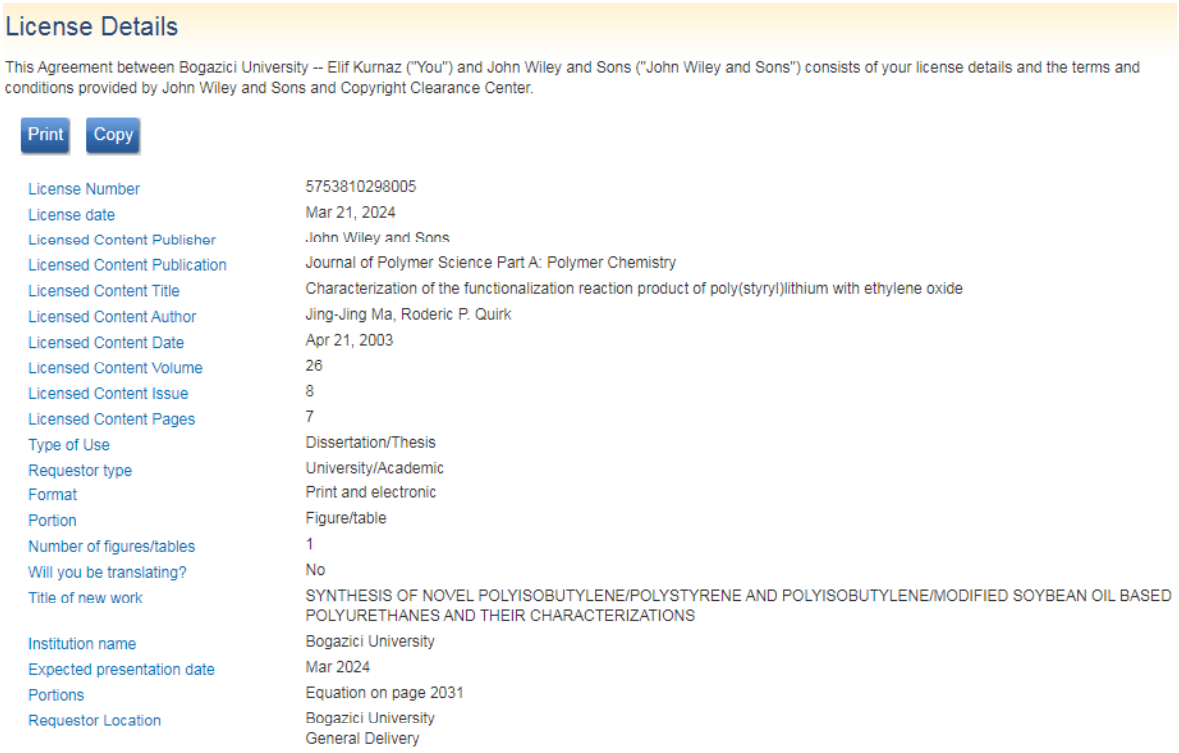

Figure B.12. Permission for Figure 1.11 from [61], John Wiley and Sons, Copyright (2003).

License Details

This Agreement between Bogazici University -- Elif Kurnaz ("You") and John Wiley and Sons ("John Wiley and Sons") consists of your license details and the terms and conditions provided by John Wiley and Sons and Copyright Clearance Center.

Print Copy

License Number	5753810770389
License date	Mar 21, 2024
Licensed Content Publisher	John Wiley and Sons
Licensed Content Publication	Journal of Polymer Science Part A: Polymer Chemistry
Licensed Content Title	Preparation of amphiphilic poly(ethylene oxide)-block-polystyrene macrocycles via glaser coupling reaction under CuBr/pyridine system
Licensed Content Author	Junlian Huang, Guowei Wang, Yannan Zhang
Licensed Content Date	Aug 23, 2011
Licensed Content Volume	49
Licensed Content Issue	22
Licensed Content Pages	5
Type of Use	Dissertation/Thesis
Requestor type	University/Academic
Format	Print and electronic
Portion	Figure/table
Number of figures/tables	1
Will you be translating?	No
Title of new work	SYNTHESIS OF NOVEL POLYISOBUTYLENE/POLYSTYRENE AND POLYISOBUTYLENE/MODIFIED SOYBEAN OIL BASED POLYURETHANES AND THEIR CHARACTERIZATIONS
Institution name	Bogazici University
Expected presentation date	Mar 2024
Portions	Scheme on page 4768
Requestor Location	Bogazici University General Delivery

Figure B.13. Permission for Figure 1.12 from [69], John Wiley and Sons, Copyright (2011).

License Details

This Agreement between Bogazici University -- Elif Kurnaz ("You") and Elsevier ("Elsevier") consists of your license details and the terms and conditions provided by Elsevier and Copyright Clearance Center.

Print Copy

License Number	5753811179829
License date	Mar 21, 2024
Licensed Content Publisher	Elsevier
Licensed Content Publication	Biomaterials
Licensed Content Title	Medical applications of poly(styrene-block-isobutylene-block-styrene) ("SIBS")
Licensed Content Author	Leonard Pinchuk,Gregory J. Wilson,James J. Barry,Richard T. Schoephoerster,Jean-Marie Parel,Joseph P. Kennedy
Licensed Content Date	Feb 1, 2008
Licensed Content Volume	29
Licensed Content Issue	4
Licensed Content Pages	13
Type of Use	reuse in a thesis/dissertation
Portion	figures/tables/illustrations
Number of figures/tables/illustrations	1
Format	both print and electronic
Are you the author of this Elsevier article?	No
Will you be translating?	No
Title of new work	SYNTHESIS OF NOVEL POLYISOBUTYLENE/POLYSTYRENE AND POLYISOBUTYLENE/MODIFIED SOYBEAN OIL BASED POLYURETHANES AND THEIR CHARACTERIZATIONS
Institution name	Bogazici University
Expected presentation date	Mar 2024
Portions	Figure 7 on page 453
Requestor Location	Bogazici University General Delivery

Figure B.14. Permission for Figure 1.13 from [71], Elsevier, Copyright (2008).

License Details

This Agreement between Bogazici University -- Elif Kurnaz ("You") and Springer Nature ("Springer Nature") consists of your license details and the terms and conditions provided by Springer Nature and Copyright Clearance Center.

Print Copy

License Number	5753820525303
License date	Mar 21, 2024
Licensed Content Publisher	Springer Nature
Licensed Content Publication	Springer eBook
Licensed Content Title	Chemistry of polyurethane elastomers
Licensed Content Author	Dr. Cristina Prisacariu
Licensed Content Date	Jan 1, 2011
Type of Use	Thesis/Dissertation
Requestor type	academic/university or research institute
Format	print and electronic
Portion	figures/tables/illustrations
Number of figures/tables/illustrations	2
Will you be translating?	no
Circulation/distribution	1 - 29
Author of this Springer Nature content	no
Title of new work	SYNTHESIS OF NOVEL POLYISOBUTYLENE/POLYSTYRENE AND POLYISOBUTYLENE/MODIFIED SOYBEAN OIL BASED POLYURETHANES AND THEIR CHARACTERIZATIONS
Institution name	Bogazici University
Expected presentation date	Mar 2024
Portions	Figure 1.5 and Figure 1.6
Requestor Location	Bogazici University General Delivery

Figure B.15. Permission for Figure 1.14 and Figure 1.15 from [74], Springer Nature, Copyright (2011).

License Details

This Agreement between Bogazici University -- Elif Kurnaz ("You") and John Wiley and Sons ("John Wiley and Sons") consists of your license details and the terms and conditions provided by John Wiley and Sons and Copyright Clearance Center.

Print Copy

License Number	5745900536434
License date	Mar 11, 2024
Licensed Content Publisher	John Wiley and Sons
Licensed Content Publication	Journal of Polymer Science Part A: Polymer Chemistry
Licensed Content Title	Polyisobutylene-based polyurethanes. V. Oxidative-hydrolytic stability and biocompatibility
Licensed Content Author	Joseph P. Kennedy, Daniel Ely, Christopher M. Brendel, et al
Licensed Content Date	Apr 8, 2010
Licensed Content Volume	48
Licensed Content Issue	10
Licensed Content Pages	10
Type of Use	Dissertation/Thesis
Requestor type	University/Academic
Format	Print and electronic
Portion	Figure/table
Number of figures/tables	1
Will you be translating?	No
Title of new work	SYNTHESIS OF NOVEL POLYISOBUTYLENE/POLYSTYRENE AND POLYISOBUTYLENE/MODIFIED SOYBEAN OIL BASED POLYURETHANES AND THEIR CHARACTERIZATIONS
Institution name	Bogazici University
Expected presentation date	Mar 2024
Portions	Scheme 1 on page 2196
Requestor Location	Bogazici University General Delivery

Figure B.16. Permission for Figure 1.16 from [88], John Wiley and Sons, Copyright (2010).

License Details

This Agreement between Bogazici University -- Elif Kurnaz ("You") and John Wiley and Sons ("John Wiley and Sons") consists of your license details and the terms and conditions provided by John Wiley and Sons and Copyright Clearance Center.

Print Copy

License Number	5745920705763
License date	Mar 11, 2024
Licensed Content Publisher	John Wiley and Sons
Licensed Content Publication	Journal of Polymer Science Part A: Polymer Chemistry
Licensed Content Title	PIB-based polyurethanes. IV. The morphology of polyurethanes containing soft co-segments*
Licensed Content Author	Iskender Yilgor, Emel Yilgor, Joseph P. Kennedy, et al
Licensed Content Date	Oct 8, 2009
Licensed Content Volume	47
Licensed Content Issue	22
Licensed Content Pages	12
Type of Use	Dissertation/Thesis
Requestor type	University/Academic
Format	Print and electronic
Portion	Figure/table
Number of figures/tables	1
Will you be translating?	No
Title of new work	SYNTHESIS OF NOVEL POLYISOBUTYLENE/POLYSTYRENE AND POLYISOBUTYLENE/MODIFIED SOYBEAN OIL BASED POLYURETHANES AND THEIR CHARACTERIZATIONS
Institution name	Bogazici University
Expected presentation date	Mar 2024
Portions	Figure 1 on page 6182
Requestor Location	Bogazici University General Delivery

Figure B.17. Permission for Figure 1.17 from [89], John Wiley and Sons, Copyright (2009).

License Details

This Agreement between Bogazici University -- Elif Kurnaz ("You") and John Wiley and Sons ("John Wiley and Sons") consists of your license details and the terms and conditions provided by John Wiley and Sons and Copyright Clearance Center.

Print Copy

License Number	5753830702496
License date	Mar 21, 2024
Licensed Content Publisher	John Wiley and Sons
Licensed Content Publication	Journal of Polymer Science Part A: Polymer Chemistry
Licensed Content Title	Polyisobutylene-based polyurethanes. VI. Unprecedented combination of mechanical properties and oxidative/hydrolytic stability by H-bond acceptor chain extenders
Licensed Content Author	Joseph P. Kennedy, Jungmee Kang, Gabor Erdodi
Licensed Content Date	Apr 26, 2010
Licensed Content Volume	48
Licensed Content Issue	11
Licensed Content Pages	11
Type of Use	Dissertation/Thesis
Requestor type	University/Academic
Format	Print and electronic
Portion	Figure/table
Number of figures/tables	2
Will you be translating?	No
Title of new work	SYNTHESIS OF NOVEL POLYISOBUTYLENE/POLYSTYRENE AND POLYISOBUTYLENE/MODIFIED SOYBEAN OIL BASED POLYURETHANES AND THEIR CHARACTERIZATIONS
Institution name	Bogazici University
Expected presentation date	Mar 2024
Portions	Scheme 1 and Figure 7
Requestor Location	Bogazici University General Delivery

Figure B.18. Permission for Figure 1.18 and Figure 1.19 from [90], John Wiley and Sons, Copyright (2010).

License Details

This Agreement between Bogazici University -- Elif Kurnaz ("You") and John Wiley and Sons ("John Wiley and Sons") consists of your license details and the terms and conditions provided by John Wiley and Sons and Copyright Clearance Center.

Print Copy

License Number	5745941466167
License date	Mar 11, 2024
Licensed Content Publisher	John Wiley and Sons
Licensed Content Publication	Journal of Polymer Science Part A: Polymer Chemistry
Licensed Content Title	Polyisobutylene-based polyurethanes. VI. Unprecedented combination of mechanical properties and oxidative/hydrolytic stability by H-bond acceptor chain extenders
Licensed Content Author	Joseph P. Kennedy, Jungmee Kang, Gabor Erdodi
Licensed Content Date	Apr 26, 2010
Licensed Content Volume	48
Licensed Content Issue	11
Licensed Content Pages	11
Type of Use	Dissertation/Thesis
Requestor type	University/Academic
Format	Print and electronic
Portion	Figure/table
Number of figures/tables	1
Will you be translating?	No
Title of new work	SYNTHESIS OF NOVEL POLYISOBUTYLENE/POLYSTYRENE AND POLYISOBUTYLENE/MODIFIED SOYBEAN OIL BASED POLYURETHANES AND THEIR CHARACTERIZATIONS
Institution name	Bogazici University
Expected presentation date	Mar 2024
Portions	Figure 8 on page 2370
Requestor Location	Bogazici University General Delivery

Figure B.19. Permission for Figure 1.20 from [90], John Wiley and Sons, Copyright (2010).

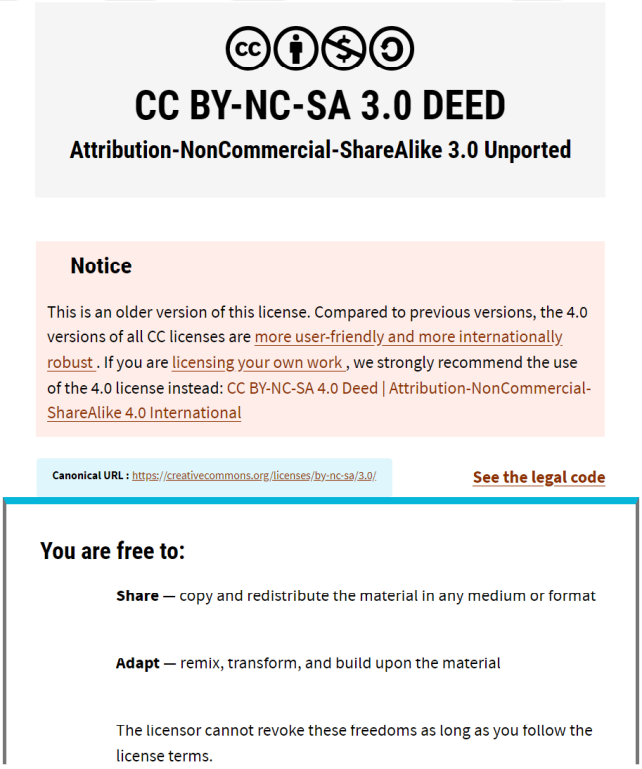

Figure B.20. Permission for Figure 1.21 and Table 1.1 from [96] (https://www.intechopen.com/chapters/15795), licensed under CC BY-NC-SA 3.0 (https://creativecommons.org/licenses/by-nc-sa/3.0/)

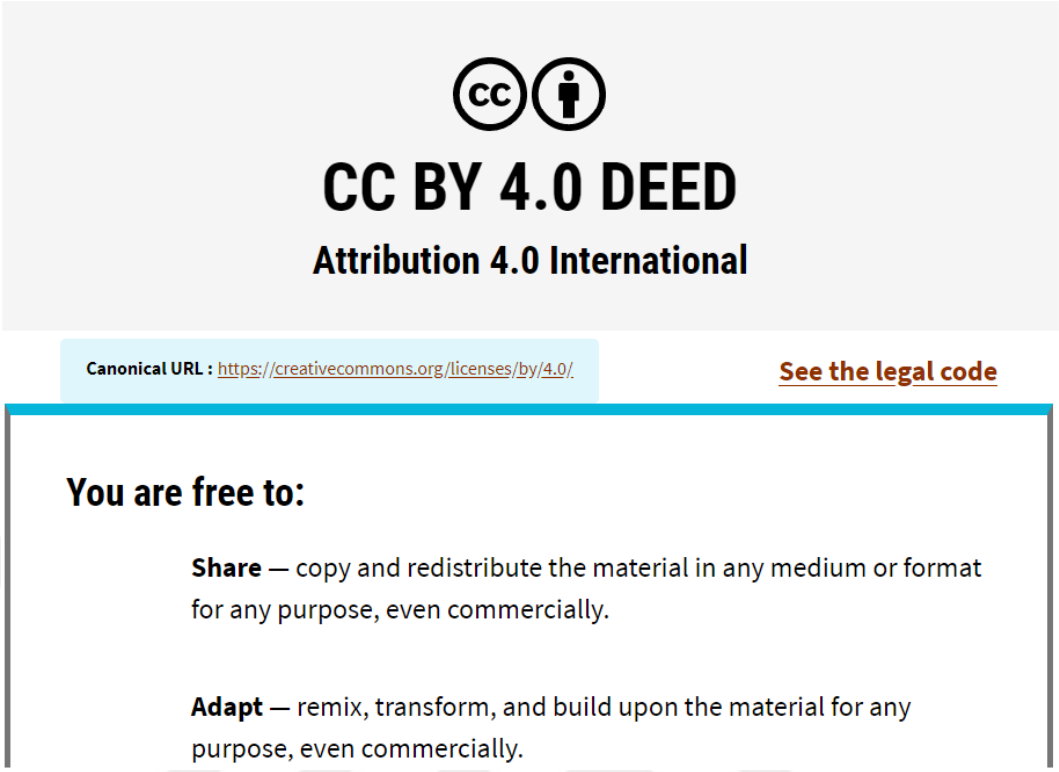

Figure B.21. Permission for Figure 1.22 from [95] (https://www.ocl-journal.org/articles/ocl/full_html/2016/05/ocl160031-s/ocl160031-s.html), licensed under CC BY 4.0 (https://creativecommons.org/licenses/by/4.0/)

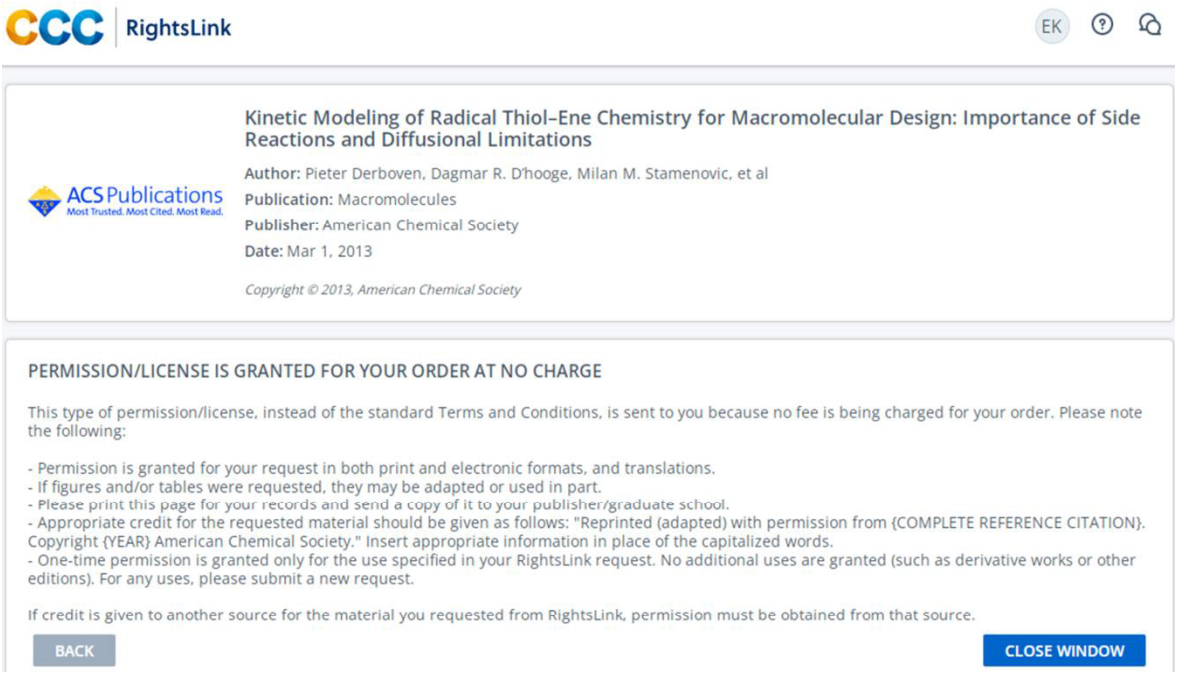

Figure B.22. Permission for Figure 1.23 from [109], American Chemical Society, Copyright (2013).

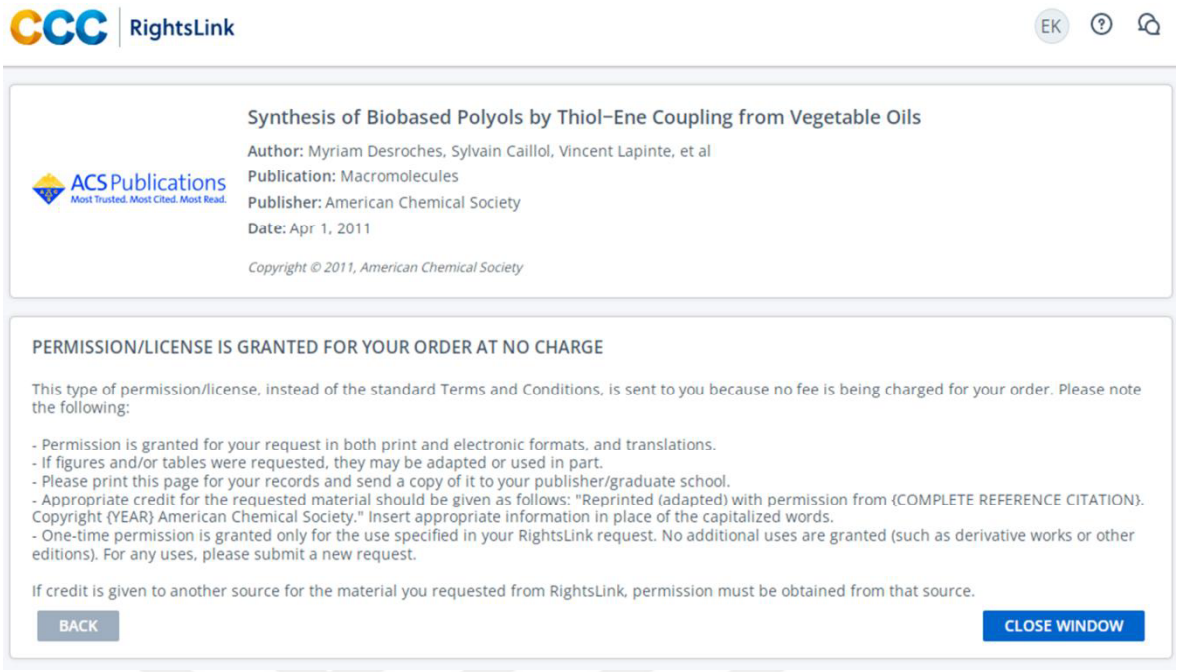

Figure B.23. Permission for Figure 1.24 from [105], American Chemical Society, Copyright (2011).

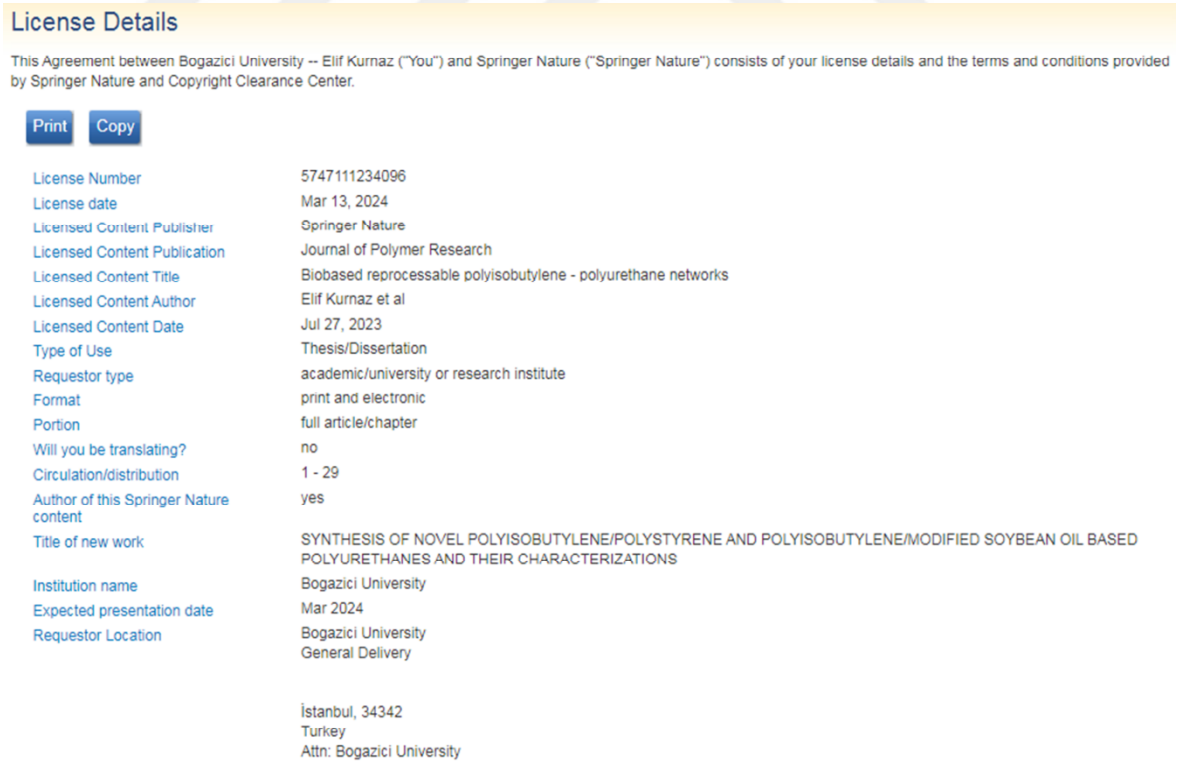

Figure B.24. Permission for Chapter 4 from "Biobased Reprocessable Polyisobutylene - Polyurethane Networks", Springer Nature, Copyright (2023).